TRIUMF

ANNUAL REPORT
SCIENTIFIC ACTIVITIES
1979

MESON FACILITY OF:

UNIVERSITY OF ALBERTA
SIMON FRASER UNIVERSITY
UNIVERSITY OF VICTORIA
UNIVERSITY OF BRITISH COLUMBIA

DECEMBER 1980

TRIUMF

ANNUAL REPORT
SCIENTIFIC ACTIVITIES
1979

TRIUMF
4004 WESBROOK MALL
VANCOUVER, B.C.
CANADA V6T 2A3

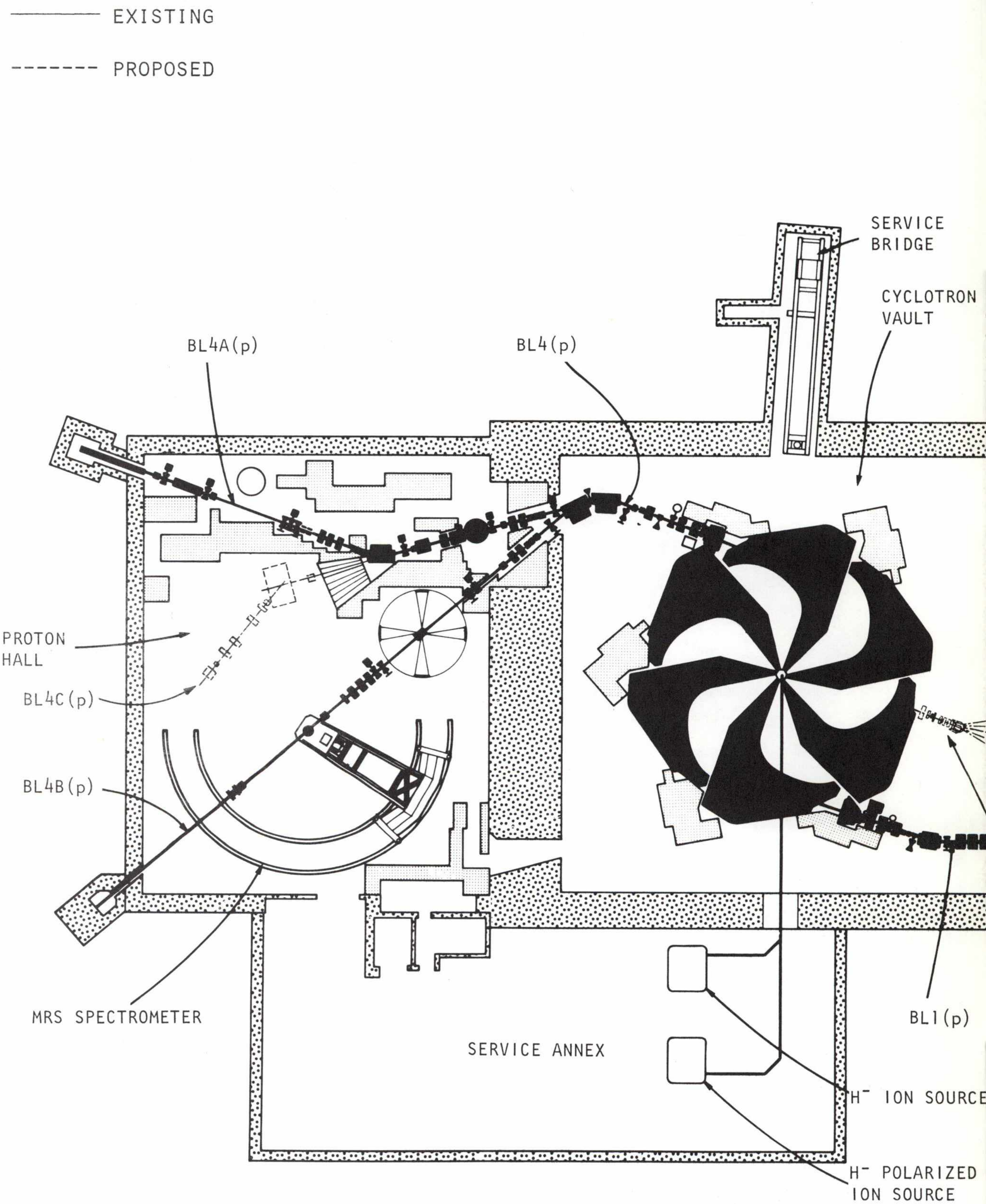
EXISTING
PROPOSED
SERVICE BRIDGE
CYCLOTRON VAULT
BL4A(p)
BL4(p)
PROTON HALL
BL4C(p)
BL4B(p)
MRS SPECTROMETER
SERVICE ANNEX
BL1(p)
H⁻ ION SOURCE
H⁻ POLARIZED ION SOURCE

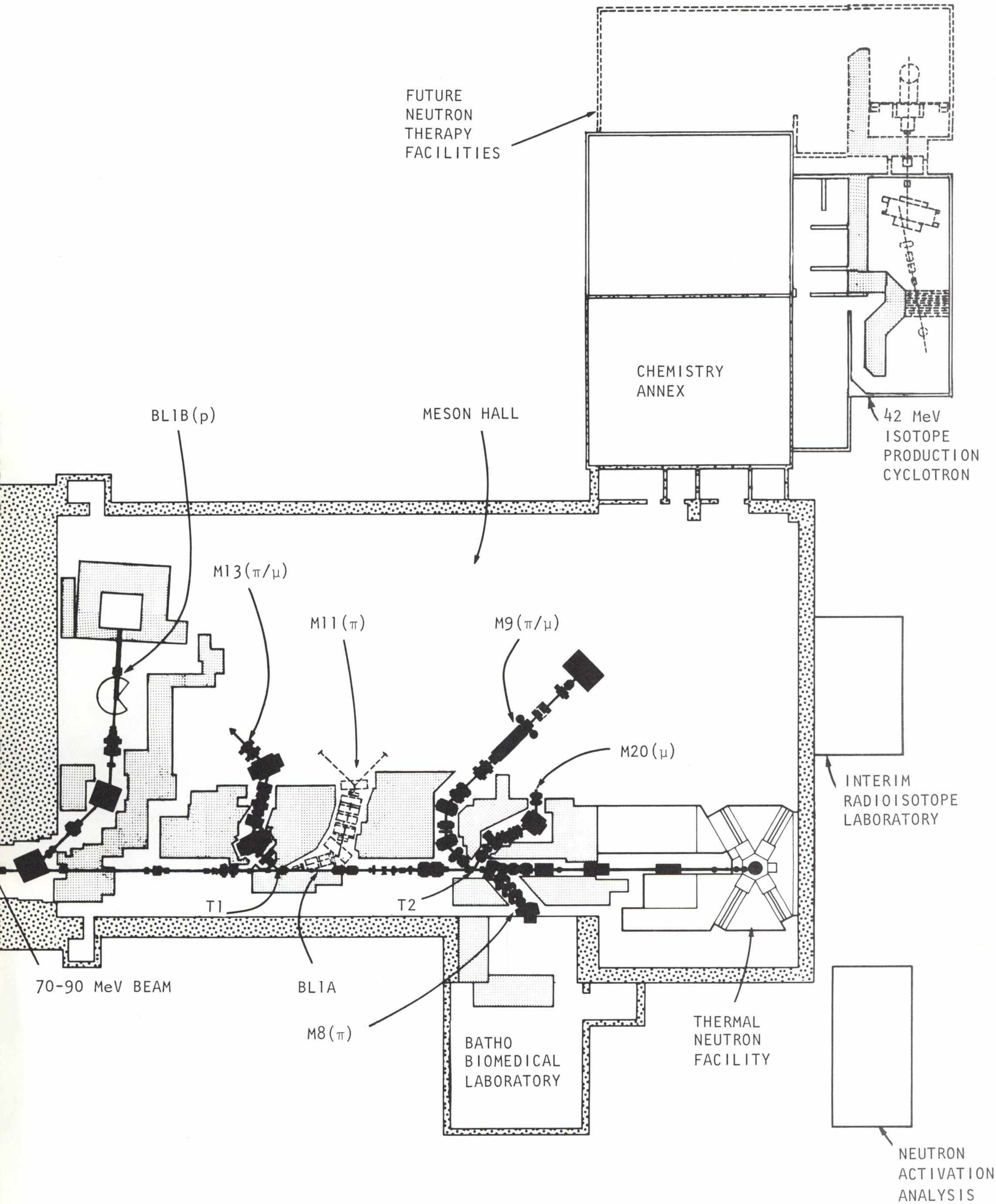
FUTURE NEUTRON THERAPY FACILITIES
CHEMISTRY ANNEX
42 MeV ISOTOPE PRODUCTION CYCLOTRON
BL1B(p)
MESON HALL
M13(π/μ)
M11(π)
M9(π/μ)
M20(μ)
INTERIM RADIOISOTOPE LABORATORY
T1
T2
70-90 MeV BEAM
BL1A
M8(π)
BATHO BIOMEDICAL LABORATORY
THERMAL NEUTRON FACILITY
NEUTRON ACTIVATION ANALYSIS

This Annual Report is dedicated to our much loved colleague Mike Pearce (1926-1980) in appreciation of his many contributions to TRIUMF. As a scientist and as an administrator his devotion to our project was a source of inspiration to us all.

FOREWORD

The threefold increase in TRIUMF's beam (integrated over the whole year) from 1978 to 1979 has led to a corresponding increase in the research program. Both the applied program and the fundamental research program have seen some important experiments completed, some promising experiments begun, and many other interesting experiments with great progress.

It was a year in which there was considerable international focus on TRIUMF. The project served as the host of the major biennial international conference pertaining to the research fields of the meson factories—the Eighth International Conference on High Energy Physics and Nuclear Structure—with more than 500 participants from around the world.

TRIUMF continues to attract researchers from around the world. In November the citizens of Vancouver funded the Gordon M. Shrum Scientist Exchange Fund whose endowment will annually provide more than $50,000 to enable exchange of scientists between TRIUMF and the Weizmann Institute in Israel.

TRIUMF was conceived and built for first-rate people and ideas, and it is providing just that.

Erich Vogt

E.W. Vogt
Chairman of the Board of Management

TRIUMF was established in 1968 as a laboratory operated and to be used jointly by the University of Alberta, Simon Fraser University, the University of Victoria and the University of British Columbia. The facility is also open to other Canadian as well as foreign users.

The experimental program is based on a cyclotron capable of producing three simultaneous beams of protons, two of which are individually variable in energy, from 180-520 MeV, and the third fixed at 70 MeV. The potential for high beam currents—100 μA at 500 MeV to 300 μA at 400 MeV—qualified this machine as a 'meson factory'.

Fields of research include basic science, such as medium-energy nuclear physics and chemistry, as well as applied research, such as isotope research and production and nuclear fuel research. There is also a biomedical research facility which uses mesons in cancer research and treatment.

The ground for the main facility, located on the UBC campus, was broken in 1970. Assembly of the cyclotron started in 1971. The machine produced its first full-energy beam in 1974 and its full current in 1977.

The laboratory employs approximately 230 staff at the main site in Vancouver and 14 based at the four universities. The number of university scientists, graduate students, and support staff associated with the present scientific program is about 215.

CONTENTS

INTRODUCTION

New developments at TRIUMF during 1979 accompanied improvements of existing facilities and services with a continuation of the "exponential" increase in delivered beam and a cyclotron availability approaching 88%. During a trial run a current of 150 μA was delivered to beam line 1, and 100 μA operation has become routine. In a series of careful measurements and minor alterations the Beam Development group has demonstrated that a beam energy resolution of 10^{-3} is attainable.

The increase in integrated current delivered during the year by a factor of more than three was made possible by several improvements in systems and procedures to reduce beam spill (and therefore induced radioactivity of machine components) on the one hand and reduced exposure time of maintenance crews on the other. Vacuum improvement and the use of "shadow shields" are two items in a long list. Polarized beam was delivered for 21% of the 5100 h of operation with increased stability and reliability. There were no requests for operation at maximum polarized beam output during the year, unlike the demand for high intensity to produce polarized neutrons during 1978.

Several new facilities have been developed, some to the point of commissioning. Two primary beam lines, 1B and 2C, have received beam. Beam line 1B, a low intensity branch of beam line 1, is available for experiments during polarized beam operation, thus doubling productivity in this mode. Although beam line 2C has yet to be designed and built, the feasibility of extraction of a 70-100 MeV beam has been demonstrated. A new secondary beam line, M13, provides a new source of low energy pions and muons to relieve some of the pressure on M9. A new target, 1AT1, serves M13 as well as the projected M11. M9 has been improved by the addition of an electrostatic separator which will make possible "pure" muon beams for experiments such as those to be carried out with the time projection chamber which has shown great progress in development, with spatial and time resolution approaching design specifications.

Experimental programs in particle and nuclear physics have continued from those begun in previous years. The nucleon-nucleon scattering program reached a milestone in that measurements are complete for determination of Wolfenstein parameters between 200-500 MeV. Measurements of the neutron radius of some nuclei by the scattering of negative pions have been shown to be a valuable means of determining a nuclear parameter not easily measured by other methods. The demand for muons has continued to increase with applications to solid state physics and chemistry outstripping those of particle and nuclear physics. This trend may reverse when the time projection chamber is completed and commissioned.

The applied science program has shown great progress, the highlight being the beginning of the clinical experiment in negative pion cancer therapy: the first patients were exposed during 1979. The production and delivery of high quality ^{123}I to several hospitals was continued pending commercial production by Atomic Energy of Canada Ltd. with the facilities being developed for them at TRIUMF. Trial production runs of several other isotopes were conducted for the AECL program.

TRIUMF and the University of British Columbia were hosts to the Eighth International Conference on High Energy Physics and Nuclear Structure during August. The approximately 600 attendees contributed to a scientific program which equalled or exceeded the quality and quantity of the preceding conferences in the series. A highlight of the conference was the boat trip to Nanaimo at which city the participants met a picketing anti-nuclear group which professed to believe that we were there to select a site for a nuclear power station. During the conference a very successful Kaon Factory Workshop confirmed that there is much exciting physics to be done with such a facility.

The TRIUMF Board of Management, the governing body of the joint venture called TRIUMF by the four founding partners (the University of Alberta, Simon Fraser University, the University of Victoria and the University of British Columbia), elected Dr. E.W. Vogt for a further term as Chairman. The University of Alberta has changed its representation on the Board: Dr. G.C. Neilson, Director, Nuclear Research Centre, University of Alberta has replaced Mr. W.A.B. Saunders, whose long service on the Board of Management was extremely valuable to TRIUMF. The

University of Alberta nominated a replacement for Dr. G. Roy on the Operating Committee. Dr. J.M. Cameron will serve as senior member and Dr. G.A. Moss will act as alternate. The Experiments Evaluation Committee met twice during 1979 to consider new proposals and review progress on previously approved experiments. The scientists and management at TRIUMF wish to thank retiring members Dr. R. Engfer and Dr. G.T. Ewan for providing their expertise to the committee. We welcome Drs. G. Beer, R.L. Burman, J. Domingo, A. Turkevich and M. Walker as new members of the EEC.

In spite of budget cuts by the Federal Government in many areas, support for TRIUMF increased for fiscal 1979/80 as shown in the following table:

Funding	1978/79	1979/80
Operating	$7,176,000	$8,340,000
Capital	1,519,000	1,201,000
Research grants	1,818,000	1,663,040

The National Research Council and the Natural Sciences and Engineering Research Council were able to provide increased funds to a growing organization even though their overall budget increase was slight.

J.T. Sample
Director

OPERATION AND DEVELOPMENT OF CYCLOTRON

CYCLOTRON OPERATION

Beam operation commenced in the first days of 1979 and continued until the end of May, when the facility was shut down for maintenance and expansion. During the five months beam was delivered for a total of 2511 h, of which 16% was polarized operation. Following the mid-year shutdown the target station 1AT1 was commissioned with graphite targets (1 mm or 10 mm thick) for the M13 channel, increasing the number of simultaneously operating meson channels to four.

Beam operation resumed on July 10 and continued uninterrupted until the Christmas shutdown. The second operating period was the most productive in TRIUMF history with 2584 h of beam available (25.5% of it polarized) at an average beam intensity of 30 μA. The corresponding average for the whole of 1979 is 27.6 μA at the meson production targets, an increase by a factor of almost three over 1978.

Operation in the proton hall continued much the same as in the previous year when beam intensity in beam line 4A varied from several nanoamperes to 10 μA at energies from 187 to 520 MeV. Experiments using polarized beam (21% of yearly total) were using the low-intensity beam lines 1B and 4B, and were receiving beams of polarized protons typically from 0.5 nA to 50 nA.

The overall operational record is shown in Fig. 1 and in detail in Table I. It should be clarified that the overhead in Fig. 1 represents times when beam is available but not used, mainly for procedural or safety reasons. Based on operational decisions associated usually with simultaneous extraction of two proton beams, the beam injection is interrupted to allow for energy changes in one beam line while the extraction conditions must remain unchanged for other users, or to permit a quick inspection of experimental apparatus in the proton beam lines without de-energizing the beam line components and retracting the stripping foil to satisfy the safety interlock system. Beam injection is then interrupted and entry is permitted at the expense of beam loss for other users.

Hours of beam operation per week are shown in Fig. 2 and cyclotron downtime in Fig. 1. The four major systems, i.e. the ion source and injection system, the RF, the vacuum and the magnet (including trim and harmonic coils) contribute to almost 60% of the downtime, with ISIS being the major single contributor (26%). This is a change in comparison with previous years when RF always led the table.

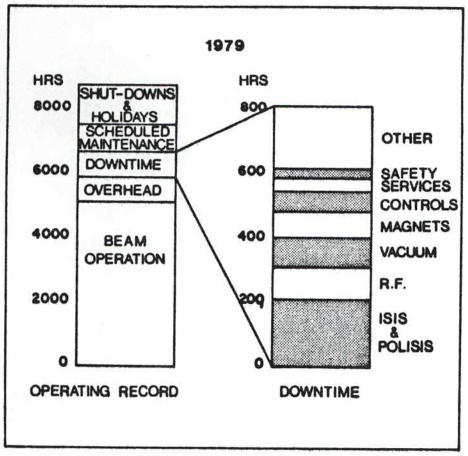

Fig. 1. Operating record for 1979.

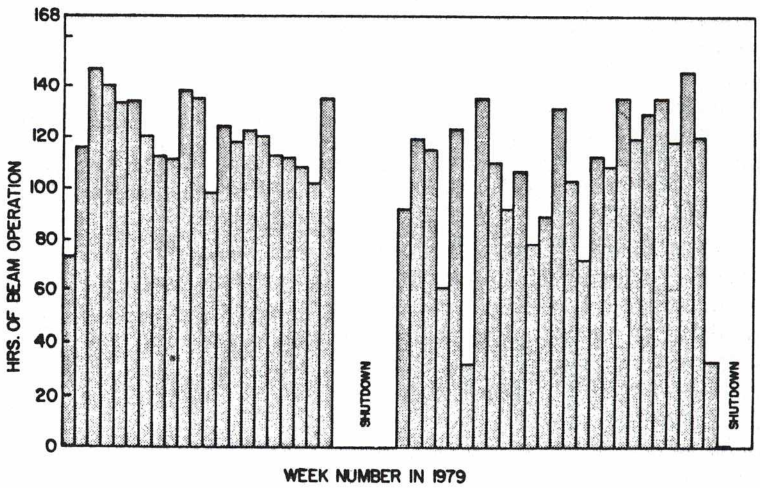

Fig. 2. Hours of beam operation per week.

Table I. Summary of machine performance 1979.

	hours
Scheduled operating time	7480.50
Scheduled maintenance	876.55
Beam available	5122.55
Unpolarized	4060.85
Polarized	1061.65
Cyclotron	
Development	567.45
Tuning	343.65
Operator training	56.25
Beam line 1A	
Tuning and development	75.75
Experiment	2904.15
μA hours	80 298.00
Beam line 1B	
Tuning and development	266.70
Experiment	512.70
Beam line 4A	
Tuning	203.40
Experiment	1871.05
μA hours	2714.92
Beam line 4B	
Tuning and development	173.45
Experiment	1587.45
Downtime	807.45
Controls	63.55
Safety	31.25
ISIS + POLISIS	208.45
Magnets	82.65
RF	97.18
Vacuum	94.50
Probes	4.15
Services	33.52
Other	192.22

Figures 3 to 5 indicate the trend toward improving TRIUMF's performance over the last five years. The scheduled 75,000 μA h were slightly exceeded, and a total of 83,000 μA h were extracted into the high-intensity proton beam lines.

Two curves in Fig. 4 reflect the increase in utilization of the facility. While curve 1 (hours of operation per year) is somewhat misleading, since there was only one major shutdown scheduled in 1979, curve 2 (system failures per hours of operation) shows a desirable trend for a facility five years in operation. The average availability of the cyclotron was 87.8% in 1979, the highest so far achieved.

The curves in Fig. 5 reflect the effort of the Development and Operations groups towards

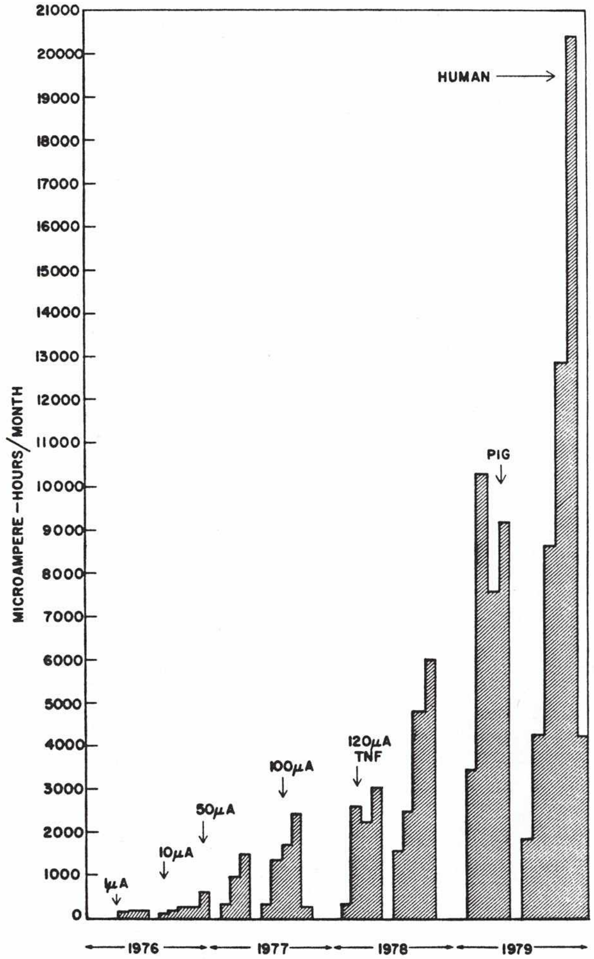

Fig. 3. Charge delivered per month over past four years. Peak current intensities and experimental achievements are highlighted (inscripts refer to milestones in cancer treatment program).

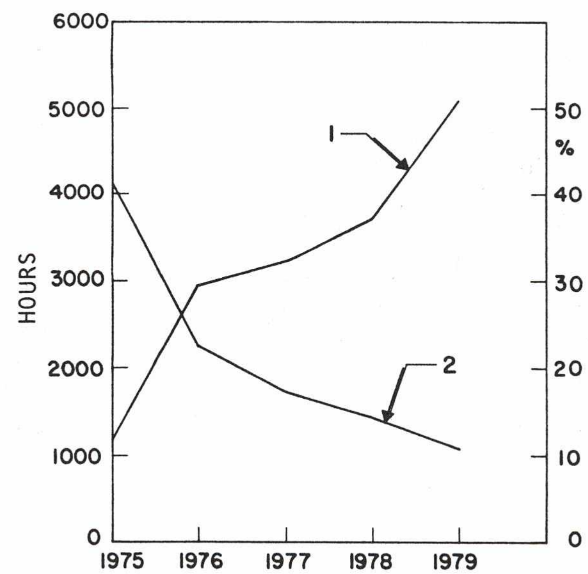

Fig. 4. Cyclotron utilization.

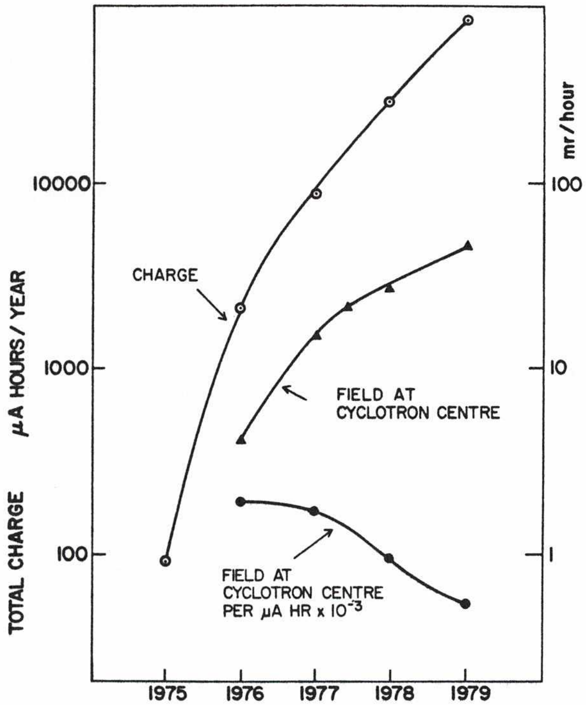

Fig. 5. Microampere-hours per year and residual activity in the cyclotron since first beam.

reducing the residual activity in the cyclotron to minimize radiation exposures to personnel working on the cyclotron during major shutdowns. The trend is again favourable, as seen from the bottom curve.

Approximately 56 h or 1% of beam time was used for training the Operations staff, and partly as a result of this the facility is operated routinely by operators only. This led to abolishing the requirement of a duty beam physicist later in the year. Beam physicists act only as advisors during cyclotron tuning for 100 μA operation or during tuning for beam with high energy resolution.

Beam time to experiments

The number of 12 h beam shifts scheduled to experiments in 1979 is shown in Table II. The actual beam time received was 77.6% of scheduled, averaged for all experiments.

CYCLOTRON DEVELOPMENT

The cyclotron development effort was oriented towards the traditional goals of improved beam energy resolution, higher average intensity, higher peak intensity, improved reliability and stability, new extracted beams, and improved polarized and non-polarized ion sources. A considerable effort also went into establishing reproducible and quick procedures for setting up new, recently demonstrated, production modes like the 100 μA operation and the 1:5 selector operation.

The amount of progress along the above lines was partially conditioned at the beginning of the year by budget restrictions which limited the funding and the manpower resources for development. In this situation special emphasis was given towards design effort and studies for those long-term projects where an initial delay would have caused a substantial delay in our long-term goals. Included are the design and the partial installation of a 70-100 MeV extraction system for beam line 2C, a conceptual design for a high-intensity 400-500 MeV extraction line for beam line 2A, model studies for a new, high brightness H^- source in a laboratory test stand, and the design of an improved, more reliable, RF resonator system to replace wholly or partly the original system should this prove inadequate for long-term reliability or for third harmonic RF flat-topping of the fundamental wave form. Tests to assess performance in these areas are in progress. A study of the long-term man-dose requirements in the vault region for maintenance and development jobs was also initiated, with the purpose of determining priorities for mechanical improvements to the cyclotron systems and to the remote handling equipment with a view towards minimizing future dose requirements.

At the same time, intermediate goals, which were deemed to be achievable within the available resources, were set as a milestone for the year and demonstrated. Included are the extraction of beams with an improved or 'medium' energy resolution ($\Delta E/E \simeq 1/1000$), the achievement of a peak beam intensity of 150 μA dc and the demonstration of '100 μA

Table II. Beam time to experiments 1979.

Area/ Beam Line	Experiment	Short Title	Spokesman	Number of 12-hour shifts scheduled
				P polarized beam
CYCLOTRON	-	Development	M.K. Craddock G. Dutto	74 + 6P
BEAM LINE 1A	-	Development	M.K. Craddock	3
BEAM LINE 1B	-	Development	M.K. Craddock	12
M8	61	Biomedical	L.D. Skarsgard	44 @ 100 μA 5 100 μA fraction 212 @ low or medium current 53 with Cu target 311.5 total
	110	Microdosimetry	Y. Ito	10P
M9	-	Development	J.A. Macdonald	47.5
	1,53,54	π scattering	R.R. Johnson	60
	41a	π capture	M. Salomon	16
	41b	Charge exchange	M.D. Hasinoff	11
	47,83	Bound μ decay	M.D. Hasinoff	10
	52	π → eγ	D.A. Bryman	5
	71	μSR	T. Yamazaki	53
	78,91	μSR in solids	J. Brewer	22
	80	Pionic X-rays	R.M. Pearce	25
	89	μ fission	S. Kaplan	10
	104	TPC	D.A. Bryman C.K. Hargrove	20
	127	Pionic deuterium	G.A. Beer	10
	128	X-ray intensities	R.M. Pearce	10
	141	Muonic hydrogen	J. Brewer	2
M13	-	Commissioning	J. Doornbos C. Oram	20
	1,54	π scattering	R.R. Johnson	27.5 + 51
	60	Muonium in insulators	J.B. Warren	44.5
	91	μSR in semiconductors	J. Brewer	8
	111	π^- absorption	C. Cernigoi	16
	140	Stopping π^- in H_2/D_2	D.F. Measday	8
M20	-	Development	J. Doornbos C. Oram	1
	35	μSR chemistry	D.G. Fleming	116.5
	60	Muonium in insulators	J.B. Warren	21
	71,78	μSR	T. Yamazaki	18.5 + 34
	78,91	μSR in solids	J. Brewer	9
	88	μ capture	T. Yamazaki	75
	104	TPC	D.A. Bryman C.K. Hargrove	9
	122	μSR in cobalt	B.D. Patterson	9
BEAM LINE 1B	10	π production	G. Jones	71.5P
	87	Proton radiography	E.W. Blackmore	11P
BEAM LINE 4A	3	Fragments	R.G. Korteling	20
	6	Fission	B.D. Pate	1
	11	Gas jet	J.M. D'Auria	9
	26	np scattering	L.P. Robertson	150.5
	48	FERFICON	I.M. Thorson	11
	77	^{123}I production	J.S. Vincent	31.5
	115	Pion production from Bi	J.M. D'Auria	10
	120	^{11}Be production	K.P. Jackson	5
	-	Isotope production	B.D. Pate	5
BEAM LINE 4B	-	MRS development	J.G. Rogers	6
	14	p elastic scattering	J.M. Cameron	12.5P
	59	(p,2p)	W.T.H. van Oers	9P
	86	p elastic scattering	D.A. Hutcheon	12 + 41.5P
	99	(p,d) reactions	J. Kallne	14 + 18P
	103	Spin dependence	G. Roy	6 + 11P
	113	(p,p)^{3}He at backward ang	W.T.H. van Oers	11P
	114	(p,2p) on He	W.T.H. van Oers	8
	121	(n,p) charge symmetry	W.T.H. van Oers	11P
	124	Giant resonances	F.E. Bertrand	23
	131	$(\vec{p},\gamma)$ on ^{3}He and ^{6}Li	J.M. Cameron	17
	132	p,p → $d\pi^+$	P. Walden	8
	144	Polarized p,d reactions	J.M. Cameron	8P
		Dibaryons	R. Abegg	4P

routine operation', where the term 'routine' signifies that the operators did not require beam physicist assistance, and that controls, diagnostic and machine safety were adequate.

All cyclotron groups were extremely busy with design work, model studies, beam calculations and tests, which were performed in parallel with the effort constantly dedicated to maintaining the machine in good operating condition.

The demonstration of the medium energy resolution performance was mainly due to the effort of the Beam Development group. A system of one radial flag and three slits in the central region is used to define the phase interval and the radial amplitude of a well-centred beam. At 200 MeV the turns are actually separated, but at higher energies they overlap due to magnetic field instabilities and to the sinusoidal shape (in absence of third harmonic flat-topping) of the RF wave form. It was calculated that in these conditions the lower limit to the achievable energy spread would be around 1/1000 of the extracted energy. This was actually observed experimentally for five energies (see Fig. 6) by measuring the size of the beam dispersion at a special location down beam line 4B, after setting up a purely dispersive tune and calibrating the dispersion through cyclotron techniques; more details are provided in the Beam Research and Development section of this report. Measurements with the medium

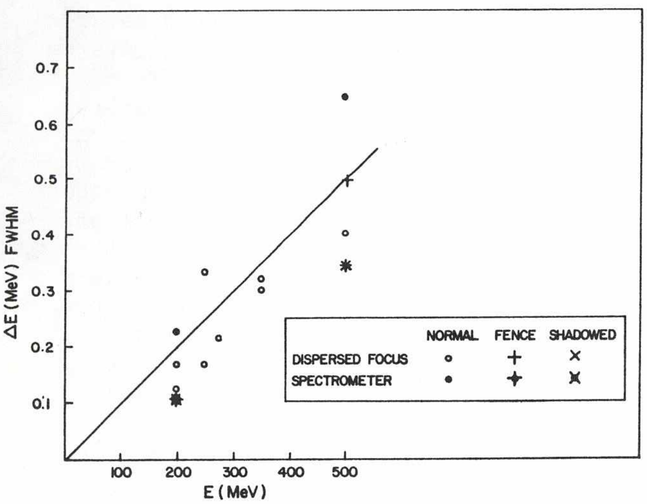

Fig. 6. Measurements made with a profile monitor at a dispersed focus and by a spectrometer show energy spreads close to the aim of $\Delta E/E \sim 10^{-3}$ (line). The beam was prepared by using central slits and harmonic coils (normal), picket fence, shadowing techniques or by a combination of these.

resolution spectrometer confirmed the results. The extracted beams were reasonably stable and reproducible. Currents up to 5-10 μA of unpolarized beam and up to 10-20 nA of polarized beam are expected to become available. The establishment of a simplified setting-up procedure for routine beam production is in progress. A technique for counting the number of overlapping turns being actually extracted, based on the detection of the time of arrival of the particles with respect to an RF reference signal, was also developed and will represent a powerful diagnostic tool for operational purposes.

For the energy spread of the extracted beam to be improved to values of ~100 keV at 500 MeV, the beam phase is required to be stable to within ±2° (from the present ±~6°), and a suitable third harmonic component has to be added to the fundamental component of the RF frequency. In these conditions, particles within a small but practical phase interval will have, at extraction, almost equal energy and almost equal radial position, with the consequence that the turns are radially separated from each other. The phase instability is mainly due to the residual instability of the main magnet. A few attempts at improving the stabilization circuit of the 20,000 A power supply were, so far, unsuccessful. However, work has proceeded toward a special digital feedback unit, which was designed to accept either the extracted beam phase signal or an NMR magnet signal, or the emf signal induced on one of the outer trim coils. A microprocessor elaborates the correction to the RF frequency required to keep the extracted beam phase constant. This system was ready to be tested by the end of the year. An NMR probe had been installed in the magnet and a signal had been obtained with the required sensitivity. However, radiation damage occurred a few months after the installation and prevented its utilization for feedback purposes. In case it should be confirmed that the NMR cannot be operated reliably with the required accuracy, a combination of extracted beam phase signal and induced trim coil emf will be used for the feedback.

The problems encountered in tuning the RF cavity to the third harmonic resonance are described in the RF section of this report. The 100 kW amplifier was at an advanced stage of construction at the end of the year; power tests are expected to take place in the coming year.

The achievement of the milestone of 150 μA extracted at 500 MeV was mainly due to the efforts of the Cyclotron Development group. Of the three lines of action being pursued towards higher intensity, i.e. better ion source, better acceptance of the cyclotron and injection line systems, and better bunching efficiency, the latter was the one which gave the first significant gain, with an increase of about 50% in the extracted beam current. 150 μA could be delivered to the 1AT2 Be target for several minutes. Temperature trip levels on the collimator downstream of 1AT2 and on the 1AT2 primary water cooling return prevented tests of longer duration. 140 μA could be maintained on the target indefinitely. In a pulsed 66% mode a maximum peak current of 170 μA could be observed. The improvement in bunching efficiency was obtained by inserting a second harmonic double gap sinusoidal buncher along the injection line, 5 m downstream of the existing first harmonic buncher. The effect of this second harmonic buncher, as illustrated in Fig. 7, is that of better approximating the desired longitudinal sawtooth distribution of the ion velocity at the buncher location. The acceptance of the cyclotron to energy variations in the injected beam was measured; the velocity limits which correspond to only 50% of the beam being accepted are shown in the figure. The improvement in bunching efficiency, calculated neglecting space charge effects, agrees well with the measured efficiencies for injected beam currents of the order of 500 μA.

The work aimed at improving the H^- source continued in the development laboratory. A new PIG source with a self-heated cathode and no filament was developed and is being tested. The geometry of the new source is extremely simplified and will be used to study the H^- output as a function of the basic geometrical source parameters. The systematic investigation of the source details was started and should allow a substantial improvement to be in hand very soon. Reproducibility studies for the operational source have also been initiated. A new, more adequate, arc power supply and a 20 kV extractor power supply have been ordered. The goal is to raise the source output by a factor 4 to 10 to a level compatible with a 400 μA extracted beam, say down beam line 1A, with other high-intensity beams being simultaneously extracted on other extraction ports (Beam lines 2A and 2C).

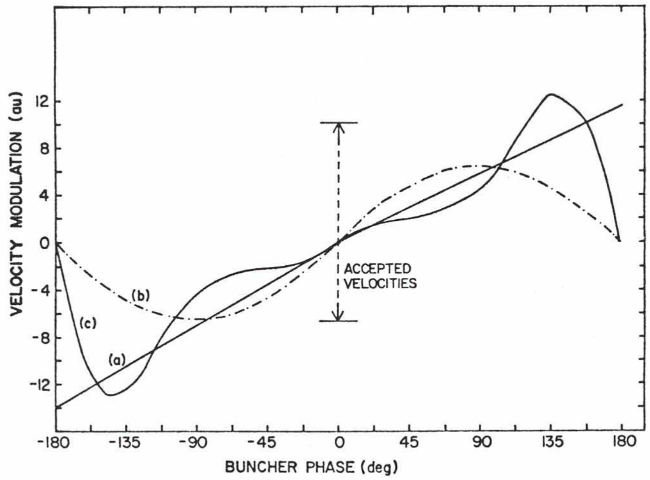

Fig. 7. Effect of the second harmonic buncher phase on the velocity distribution of the beam at the buncher location.

A demonstration of the achievement of 100 μA 'routine' conditions was given in November-December, when 31 or 32 daily periods were scheduled for the irradiation of human patients. The successful completion of this series of irradiations was the result of tight collaboration between Operations and the Development groups. In addition to the available higher maximum beam intensity, which made the 100 μA production less marginal, several improvements in the software and hardware interlocks gave greater confidence in the machine protection system and allowed on-line tuning at the high-intensity levels. The cooled collimators and protection diagnostics in the electrostatic injection line proved quite useful and adequate, preventing any major voltage breakdown on the electrodes. The software interlocks on the transmission and on the vertical losses of the beam in the cyclotron helped reduce the tank activation per unit current and prevented any thermal damage. The protection monitors for beam position and density at the targets 1AT1 and 1AT2 and at the thermal neutron facility prevented any beam power damage on the target systems and down the beam line.

Several improvements were introduced for reliability and easier operation. Along the injection line a system of several sublimation pumps, which were becoming obsolete and were marginal for high-current operation, were substituted by cryopumps adequate for hydrogen and capable of producing a vacuum around 10^{-7} Torr almost everywhere. In the cyclotron tank a straightening operation of the sagging resonators and modifications to prevent further sagging were prepared and ready for the January 1980 shutdown. A high-energy probe was substituted by a more reliable one, and more reliable slits for medium and high resolution operation were constructed and ready to be installed. Extraction mechanisms for low-energy beams at four discrete energies between 70 and 100 MeV were installed and commissioned, with successful beam extraction. An internal non-intercepting beam phase probe was tested with a special electronic circuit developed at KVI in Groningen. The system was found adequate for beam phase detection at currents as low as 4 μA peak in the cyclotron, with a typical RF background noise of a few volts. On the external beam line, where the RF noise is substantially lower, a similar circuit was used to detect the output of a special capacitive probe for beam currents as low as 10 nA. The importance of good phase measurements for low extracted beam currents is related to the requirements for phase stability feedbacks. Other improvements for reliability and easier operations were introduced in the control system, such as the expansion of the REMCON system, the implementation of an automatic polarized spin flipper, and several console and diagnostic improvements. These improvements are described in the Control section of this report.

The improved reliability in the tank allowed the total integrated current to be increased to about 83,000 μA h for 1979. An increase to 120,000 μA h is planned for 1980. To plan further increases in harmony with the remaining development installations and the recurring maintenance in the cyclotron tank and in the vault, it was decided to evaluate short- and long-term man-dose requirements with the above-mentioned dose study. As a policy, exposures to personnel are kept, at TRIUMF, five times below the national permissible levels; therefore, careful planning of the work in areas with appreciable residual activity becomes important. In the dose study all maintenance and development jobs are listed, the procedures analysed and optimized, and dose predictions are made using the extrapolated levels of residual activity. If certain jobs are too dose consuming, new procedures are investigated, if necessary with more remote handling involvement.

The remote handling equipment, including service bridge, trolleys and radio-positioning devices, was improved in reliability and functionality. At present a large amount of tank work is still being done hand-on due to the very reasonable levels of residual activity (10-20 mrem/h at the tank centre during a shutdown). However, it is expected that remote handling will have to be progressively more and more utilized in the future when levels will rise by as much as a factor of five to ten. Also the reliability of the systems will have to be improved in order to require less maintenance and, therefore, less dose to personnel.

At the same time the effort to reduce the avoidable beam spill inside the tank has to continue. A liquid He cryopump, designed to pump a large fraction of the residual hydrogen in the tank, was partially commissioned. However, a nitrogen leak requiring a shutdown repair prevented the system becoming operational during the year. Tests will resume after the coming shutdown. The Beam Development group continued the work on better beam centring through several measurements in the central region. New power supplies were ordered in order to power more central region harmonic coils. It is expected that the vertical beam losses, presently around 3% of the accelerated beam can be avoided with better centring for all phases within the 40° wide acceptance phase interval.

BEAM RESEARCH AND DEVELOPMENT

INTRODUCTION

Major accomplishments this year have been the demonstration of 0.1% energy resolution proton beams, the successful running of a high-intensity test at 150 μA, the commissioning of five new beam lines and the design of six more.

Medium energy resolution operation (MERO) was first demonstrated in the spring at 200 MeV, when single turns were extracted into beam line 4B with a measured energy spread of 166 ± 20 keV, rather than the regular 500-600 keV. The cyclotron stability is at present insufficient to maintain separate turns above 250 MeV. Nevertheless the energy-radius correlation has been good enough to permit beams of ⩽0.1% energy resolution to be extracted at 200, 250, 275, 350 and 500 MeV for periods of half an hour or more. Beam intensities of 4 μA have been obtained and 10 μA should be possible.

The emphasis on beam tuning during the 100 μA runs has resulted in improved overall beam transmission. At lower beam currents (<20 μA) where space charge effects are not important, and with the aid of the second harmonic buncher, a record 54% of the dc beam at the fast target was accelerated and extracted at 500 MeV. The transmission without the second buncher reached a record 38%. At high intensities the Cyclotron Development group co-ordinated successful test runs at 150 μA cw and at 170 μA peak with a 66% duty cycle.

Two new beams were commissioned at the beginning of the year. Beam line 1B (the 'Peanuts' line), designed for the utilization of low-intensity (polarized or high resolution) beams in beam line 1, performed as expected between 200 and 350 MeV; higher-energy beams await power supply improvements. The M13 slow pion/muon channel also operated successfully, providing surface muon beams at 4 MeV and useful pion beams down to 15 MeV; the channel runs up to 130 MeV/c, as designed, but consideration is being given to upgrading some components in order to extend the momentum range.

In the fall the M9 extension and beam lines 2C and 4C were brought into operation. The extension to M9, incorporating a crossed-field dc separator, was commissioned with both 77 MeV/c and surface muons; the beam flux, contamination and spot size were as expected. The first section of beam line 2C, to provide 65-100 MeV protons for isotope production in the vault, was installed and 70 and 90 MeV beams delivered on target at the microampere level. Beam line 4C has been designed and partially installed and commissioned this year to provide low-intensity beams (10^5 p/sec) to the polarized target. Initial runs confirm that these low intensities can be achieved through partial stripping (a factor 10^{-5}) and the use of a 1 mm diam collimator (a factor 10^{-3}).

New designs which have not yet been installed include two primary and four secondary beams. An extended version of beam line 1B has been designed to provide an additional target station capable of accommodating the 'Discovery' pion spectrometer, the beam stop being moved outside the building. Beam line 2A would take 400-500 MeV protons north of the cyclotron vault for production of high flux pion or muon beams, or injection into a post-accelerator. The effect of installing an RF separator in the M9 extension has been studied and shown to be favourable; a doubling of the 77 MeV/c muon flux is predicted. A major upgrading of the M20 muon channel is proposed to give larger acceptance and cleaner beams; a decay section would be included and there would be two alternative final legs, one incorporating the dc separator. Two high flux (~1 sr) annular channels have been studied. One, designed for muons, would utilize three toroidal magnets. The other, to provide π^- for radiation therapy, would employ two coaxial superconducting coils.

Finally, spectrometer studies should be mentioned. A ray-tracing study of the optics of the MRS was initiated and is being pursued in parallel with experimental work; and design studies have begun on the HRS and the 'Discovery' pion spectrometer.

CYCLOTRON

Medium energy resolution

Principles

At the present time the stability of the cyclotron magnet system and the absence of a flat-topping third harmonic RF do not permit the acceleration of separated turns much above 200 MeV; however, the energy spread at all energies can be improved to a level ($\Delta E/E \sim 10^{-3}$) which will match the present resolution of spectrometers in beam line 4B and 1B. This has been done by eliminating any coherent radial betatron oscillations and reducing the amplitude of the incoherent oscillations so that the beam energy is closely correlated with radius. A narrow stripper foil (typically 0.75 mm wide) is then used to extract. These conditions give an improved energy spread even though the RF phase width may be such that the turns overlap and the cyclotron stability may cause the number of turns taken to reach a given energy to vary.

The slit system described in last year's report is used:

a) To make the appropriate selection in r-p_r space to limit the betatron amplitude (the transmitted beam intensity is estimated to vary roughly inversely as the square of the slit aperture): the amplitude is restricted to 0.6 mm for good resolution at high energies or to, say, 1.5 mm for moderate resolution with higher intensity, or for low energies (dE/dR varies from 0.9 to 2.5 MeV/cm from 200 to 500 MeV).

b) To restrict the phase width of the transmitted beam sufficiently to provide separated turns near 70 MeV: this facilitates adjustment of the inner harmonic coils to centre the beam and eliminate coherent oscillations at this energy, which is outside the $\nu_r \approx 1$ region where they may be produced by first harmonic imperfections in the magnetic field.

With careful adjustment of isochronism individual turn structure has been observed out to 200 MeV, but the cyclotron stability is such that it is lost soon thereafter; nevertheless resolutions of $\Delta E/E \sim 10^{-3}$ have been achieved up to and including 500 MeV (Fig. 6, p. 7).

The beam current transmitted through the slits is typically 3% of that presented to the entrance of the inflector, 4 μA having been extracted using the unpolarized ion source; these figures have approached 10% and 30 μA for the polarized source. About half the rejected beam is stopped at 0.5 MeV by the radial flag on the first turn. This phase selection is followed by a second phase selection and restriction of the vertical amplitude at 4 MeV using slit H2 and the vertical flag. The final radial amplitude selection is made by the outer slits H1, H3 and H4, positioned somewhere between 15 and 35 MeV depending on the final extraction energy and resolution desired. The phase reduction made by the various apertures is illustrated in Fig. 8, which shows timing spectra obtained with a time-to-pulse height converter started by extracted beam scattered into a counter and stopped by the next RF pulse. The result includes instrumental resolution and cyclotron drift.

Techniques and equipment

The coherent oscillations are eliminated by compensating a residual first harmonic field of about 0.3 G to a precision of 0.02 G using inner harmonic coils. This is done empirically by observing changes in the turn pattern produced on a chart recorder by a differential probe scanning near 70 MeV. The initial rate of convergence can be improved using a computer program which takes as input the minimum and maximum turn spacing at three harmonic coil settings and predicts a fourth (improved) setting. Experimental precision limits the accuracy of the prediction as the centring improves; however, it is hoped to modify the program to produce a prediction based on all previously measured data rather than the last three points.

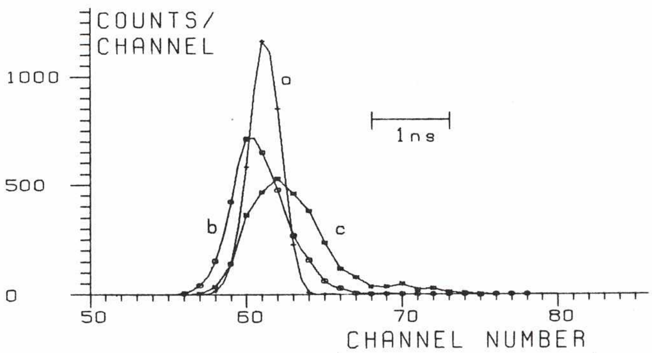

Fig. 8. Time width of beam. a) All slits and flags in use, b) outer slits H1, H3 and H4 retracted, c) all slits H1-H4 retracted but flags still inserted.

The restriction in phase space is made by positioning two slits at the same azimuth separated in radius by a quarter of a precession cycle. Phase-dependent coherent oscillations, which lead to particles of several energies overlapping at the radius of one of the slits, can be eliminated by a third slit on the opposite side of the machine or half a precession cycle away.

This philosophy can be extended to larger radius, for example where $\nu_r \approx 1.25$ near 200 MeV, and the slits combined into a single 'picket fence' structure with two or three apertures separated by the radius gain per turn, since the radial phase precesses through one quarter cycle per turn. Such a structure was assembled on a stripper foil mounted in the beam line 1A cartridge and located at 185 MeV. The dee voltage or isochronism was adjusted so that the turn separation matched the slit spacing, while an inner harmonic coil was adjusted to maximize transmission. This produced a stable beam of good resolution (see below). A permanent, pneumatically operated picket fence slit is therefore planned. The advantages are that no careful slit settings are necessary and inner harmonic coil adjustments are a matter of optimizing transmission rather than interpreting turn patterns. Also it may be possible to combine a fence with the beam line 1A extraction foil to run 20 μA in beam line 1A while having improved beam quality at higher energy in beam line 4. The disadvantages are first that the beam not transmitted by the fence is stripped and hits the tank wall; the resulting activation restricts the current to 1 μA. Secondly, certain non-zero betatron amplitudes can have a precessional radius gain per turn equal to that due to the dee voltage and thus pass through the slits. This is especially true at integral values of $1/(\nu_r-1)$; elsewhere the chance of tuning into this off-centred beam can be reduced by increasing the number of apertures. Set-up is easier if the beam is approximately centred to start with and the extracted quality can be observed at a dispersed focus. Thirdly, since the fence aperture is fixed and chosen for 500 MeV the fraction of beam transmitted at 200 MeV is less than the normal slits and operating conditions would permit.

A useful development has been the identification of the relative turn numbers of the extracted beam. The arrangement of Fig. 9(a) measures the flight time between the injection line 1 kHz macropulser and a particle detector adjacent to the extracted beam line. The beam pulses extend over many RF acceptance buckets and have a rise time less than 15 nsec compared with the bucket spacing of 43 nsec. The particles providing the stop signal can rise anywhere in the macropulse, and sufficient events must be accumulated to provide a description of the leading edge. The leading edge is rectangular if the beam extracted comes from a single turn. If several turns are extracted simultaneously the display consists of several macropulses superimposed, the leading edge of each displaced by a time corresponding to one turn (215 nsec). The number of steps observed corresponds to the number of turns simultaneously extracted.
A digital delay operating in units of RF frequency is used to provide a jitter-free signal. This allows us to identify the turns in a turn pattern [Fig. 9(b)], an important factor at large values of ν_r where the precessional radius gain per turn can be larger than that due to the dee voltage, resulting in overlapping turns and a lack of radial variation in beam intensity.

The energy spread of the extracted beam may be measured independent of spectrometers by setting up a dispersed focus in beam line 4B. The quadrupole fields must be set within rather tight tolerances, e.g. 0.5% of maximum, to ensure a true focus (i.e. that the horizontal spot width is independent of the divergence at the stripper foil). This is done by using an outer harmonic coil in the neighbourhood of the foil to displace the beam radially in the cyclotron. The motion is adiabatic, and as the phase of the first harmonic field component is rotated around the cyclotron the beam energy extracted by the foil varies sinusoidally. Figure 10 compares the change in beam energy caused by powering the harmonic coil at various phase angles with that predicted from a knowledge of the magnetic field; no normalization has been made. The change in direction of beam leaving the foil is expected to follow a similar sinusoidal variation with harmonic coil angle but shifted by $\pi/2$. Dispersed tunes have been set up at 200, 250, 275, 350 and 500 MeV with typical magnification $R_{11} \simeq 1$, dispersion $R_{16} \simeq 10$ cm/% $\Delta p/p$ and $R_{12} \leqslant 0.1$ cm/mrad.

Results and future developments

Figure 11 shows beam profiles at a dispersed focus as the extracted energy is varied by

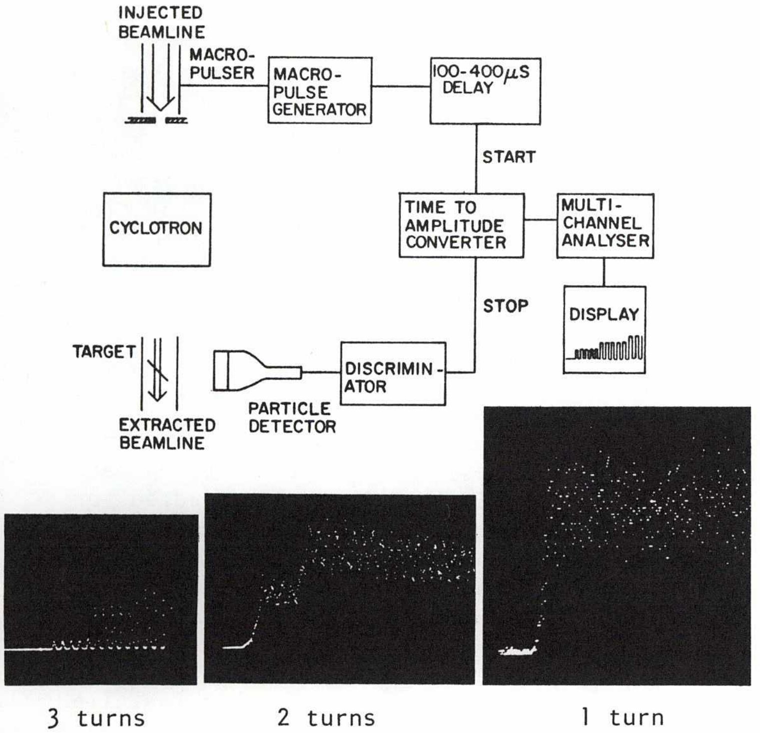

Fig. 9(a). Technique to measure the transit time through the cyclotron.

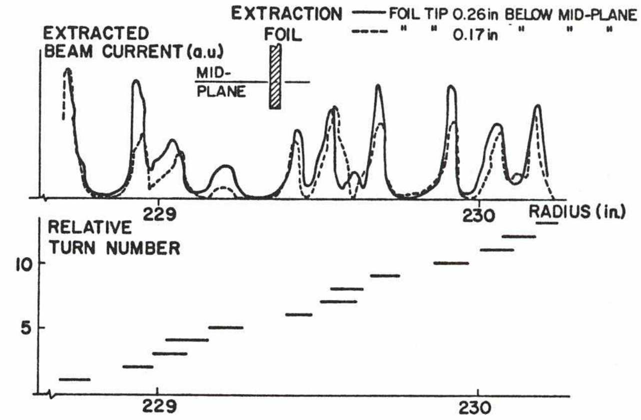

Fig. 9(b). A differential turn pattern using a narrow foil with the turns identified using the equipment of 9(a).

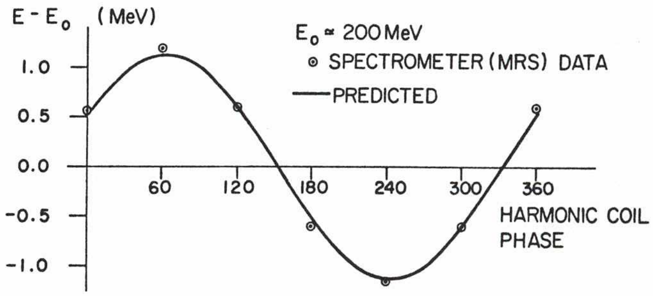

Fig. 10. Change in central energy produced by a controlled first harmonic magnetic field bump in the adiabatic region.

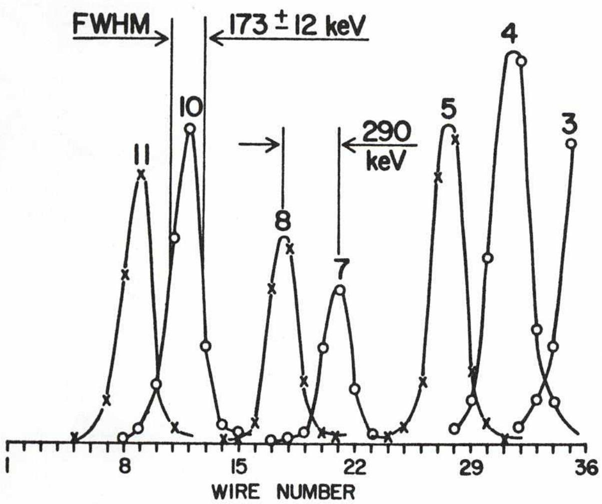

Fig. 11. Beam profiles measured at a dispersed focus as the relative turn number to extraction is varied.

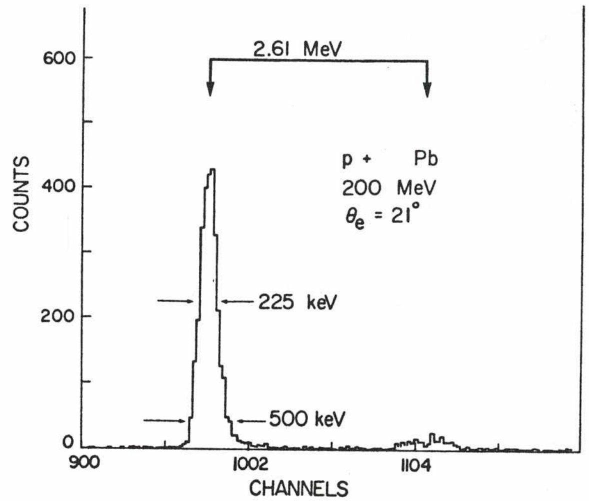

Fig. 12. Spectrometer resolution including beam energy spread, target and other instrumental contributions.

increasing the current in a harmonic coil. (The relative turn number from an arbitrary zero is shown over the peaks.) The dispersion of 83 keV/wire implies an energy gain of 273 keV/turn, close to that expected.

Figure 6 (p. 7) shows the FWHM energy spread measured with a profile monitor and dispersed tune. The beam line 4B medium resolution spectrometer with a windowless vacuum system, no detector to define the incident ray and a high resolution delay line readout position detector in the focal plane has measured a combined beam and spectrometer resolution of 0.25 MeV at 200 MeV and 0.65 MeV at 500 MeV using a lead target (Fig. 12). These figures can sometimes be improved by intercepting part of the beam incident on the foil by a probe inserted from the opposite side of the machine.

The medium resolution beam is stable in energy spread and central energy once set up. Figure 13 shows a stability to ±15 keV over 45 min for both picket fence and slit-selected beam. Most cyclotron parameters can be adjusted to optimize the transmitted intensity without affecting the resolution. Experiments have taken data using a medium resolution beam over a two-day period with no major retuning required.

The slits have transmitted 4 μA from the regular ion source and 30 nA from the polarized source. The latter figure is acceptable to many experiments on beam lines 4A, 4B and 1B, but it would be useful to increase the unpolarized beam to 20 or 30 μA so that some meson experiments may be run on beam line 1A in parallel with improved resolution in beam line 4B. It should be possible to obtain 10 μA with the existing cyclotron, while third harmonic flat-topping would help towards reaching 30 μA.

ISIS: Improved bunching

A second harmonic buncher was installed in ISIS this year and has been shown to operate successfully. The possibilities studied for adding a second harmonic to the existing 'fundamental' double-gap buncher included its replacement by a triple-gap buncher and the addition of a second harmonic buncher at various locations. For reasons concerned mainly with ease of manufacture and installation, a second harmonic buncher was installed at a less than optimum position 4.6 m downstream of the fundamental buncher. The acceptance of the cyclotron to energy variations in ISIS was measured and folded into the calculations. These showed that 36% of the dc beam could be expected within the 35° phase interval accepted by the cyclotron with only the fundamental buncher, whereas 57% could be expected with the additional second harmonic buncher (Fig. 14). This prediction has been verified by the observed increase in transmission (dc injection to 500 MeV extraction) from ~35% to ~55%.

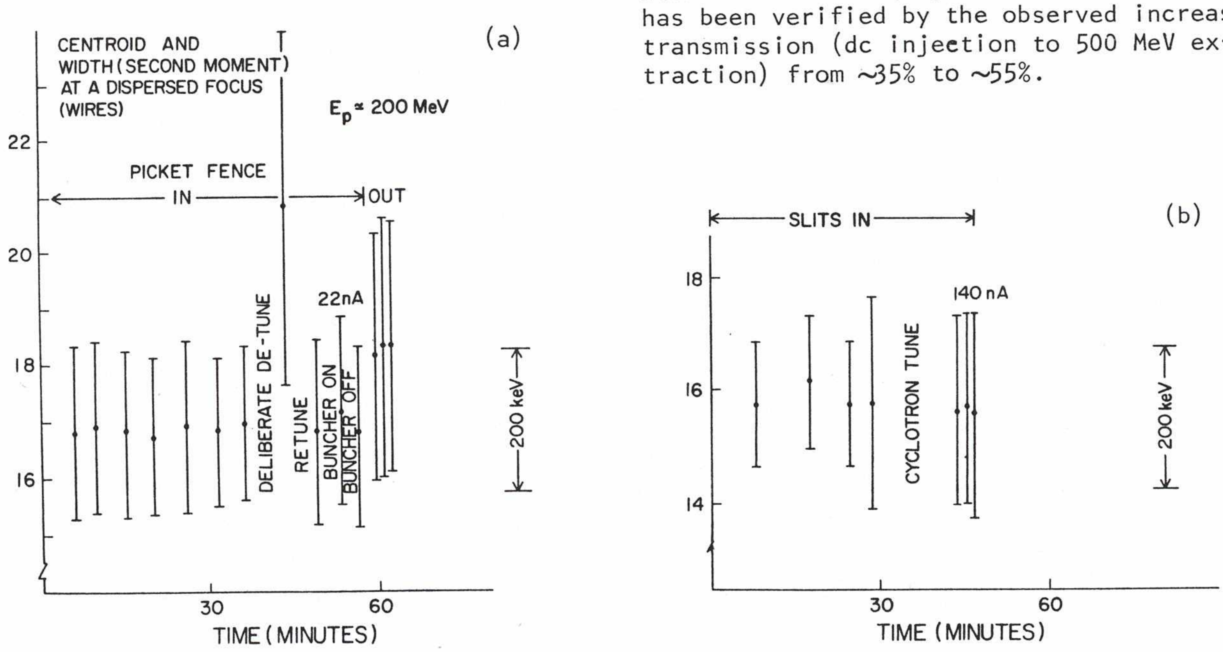

Fig. 13. Once established the energy and energy spread are stable and the tune is reproducible for both a) picket fence and b) slit-selected beams.

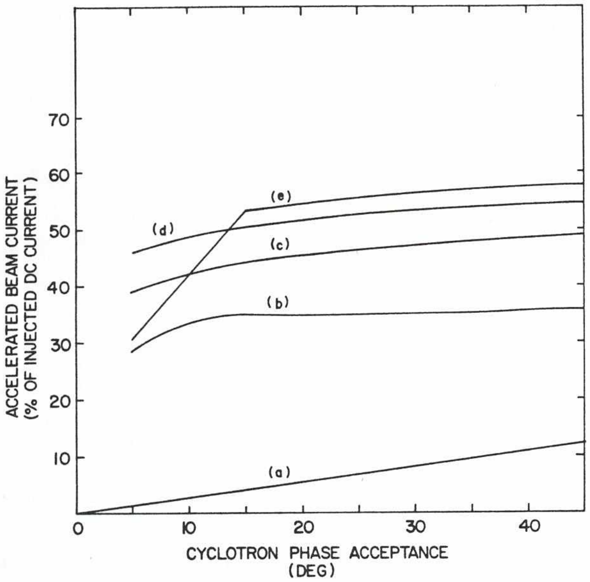

Fig. 14. a) No buncher, b) double-gap buncher (fundamental only), c) triple-gap buncher (fundamental + 2nd harmonic), d) double buncher (fundamental + 2nd harmonic 3.1 m downstream, e) double buncher (fundamental + 2nd harmonic 4.6 m downstream).

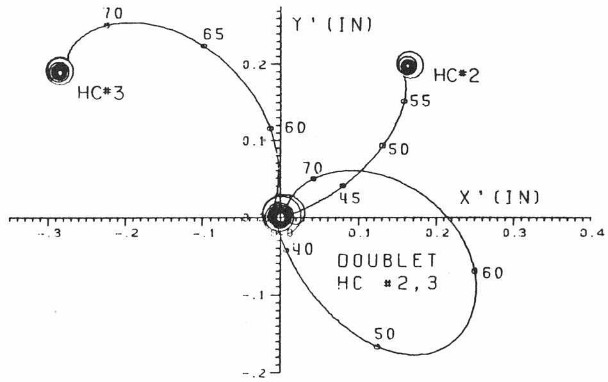

Fig. 15. Off-centredness in the precessing coordinate system caused by 100 At in harmonic coils 2 and 3 individually and by the two coils suitably powered together. The labelled points indicate the radius.

Beam centring

Further improvements have been made to the beam centring with the help of additional probes and harmonic coils. Reduced RF lea age into the beam gap allowed a number of successful runs to be made with the low-energy probes LE1 and LE2 (10.5-143.5 in.). For the first time it was possible to record digitized data from these probes (every 0.1 in.) and transmit them to the Computing Centre. It was thus possible to measure, and later correct, the vertical centring of the beam over the entire inner half of the cyclotron.

The broad radial range of the LE probes has also enabled the radial centring perpendicular to the dee gap to be determined outside the range of the slits (i.e. inside 72 in. and outside 113 in.) for the first time. With power supplies specially wired up to harmonic coil No. 4 (in addition to HC's 2, 3 and 5) the inner region of good centring was extended in radius from 70 in. to 128 in.—unfortunately at the expense of some worsening in the centring at larger radii. This occurred because the coils were adjusted individually and purely with regard to their local effects, without any allowance for long-range effects, which are quite strong for the inner coils. To overcome this problem in the future, a new control mode is proposed in which two harmonic coil sets (fed by six power supplies) are run together at suitable relative amplitudes and phase to cancel out any effects at larger radii (see Fig. 15). A similar technique, using three trim coils, has been used successfully for phase adjustments for several years.

Beam polarization

The polarizations of 200-500 MeV beams in beam line 4A have been measured, the results being normalized by means of the (p,π) polarimeter in beam line 1B, run at a fixed energy of 199 MeV. Some checks were made for fluctuations in polarization. Spin-off runs in beam line 1B showed small but significant variations in instrumental asymmetry, giving a standard deviation of 0.5% in polarization. This is most likely a steering effect due to small energy fluctuations associated with instability of the cyclotron magnet. Spin-up and -down runs also showed variations outside statistics; correcting for instrumental asymmetry using the nearest spin-off run reduced the error from 1.1% to 0.8% for spin-up.

The energy variation of the polarization, measured with the BASQUE polarimeter, was similar to that observed in 1977 but was explored in more detail (Fig. 16). The accelerating beam showed a broad 3-5% drop in polarization between 280 and 308 MeV and a sharp 6-9% drop between 460 and 470 MeV. The polarization of the decelerating beam also

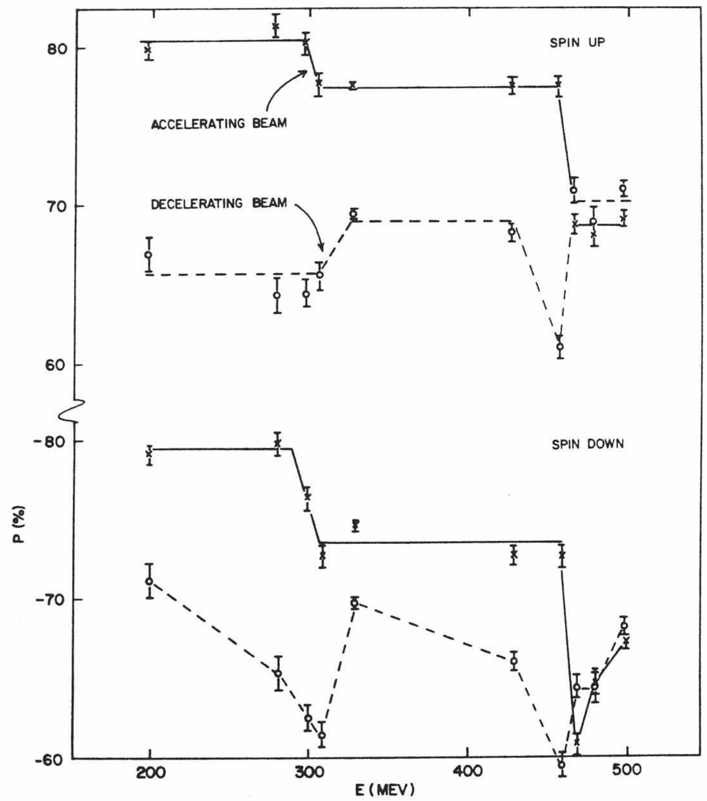

Fig. 16. Measured polarization of the accelerating and decelerating beams. The lines are to guide the eye.

changed at these energies but in a more complicated way.

The strongest depolarizing resonance predicted to occur in the TRIUMF cyclotron is the $6 - \nu_z = 3.79\gamma$ resonance at 467 MeV (Fig. 17). This is intrinsic to the machine in that it stems from the inescapable sixth harmonic of the magnetic field. Its

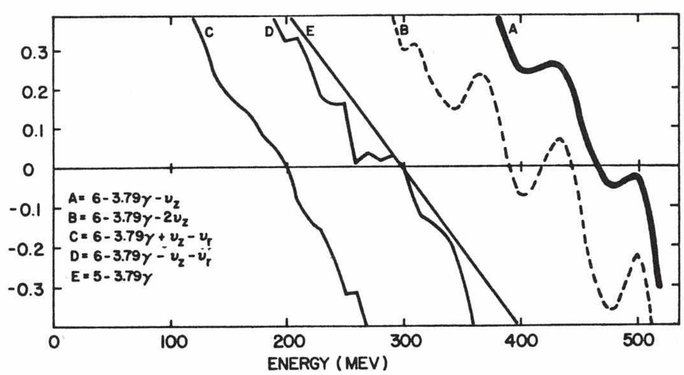

Fig. 17. Deviations from various depolarizing resonances. Relative strengths are indicated by line thicknesses.

strength also depends on the amplitude A_Z of the vertical betatron oscillations. A rough calculation assuming $A_Z = 0.3$ in. predicts about 7% depolarization, as observed. The next most serious resonances ($6 - \nu_z - \nu_r = 3.79\gamma$ and $5 = 3.79\gamma$) are predicted to occur at 300 MeV; again consistent with an energy at which polarization loss is observed.

PRIMARY BEAM LINES

Beam line 1A

The installation of the thin pion production target (1AT1) at the beginning of the year required some recommissioning work. The beam spot normally used is approximately 1 × 8 mm^2 at 1AT1, compatible with the heat-dissipating capabilities of the water-cooled targets that have been used up to now. Settings have been determined for the four quadrupoles between 1AT1 and 1AT2 to provide a focus-to-focus condition at 500 MeV. This keeps the 1AT2 spot size the same, independent of 1AT1 target thickness. Unfortunately one quadrupole suffers from cooling problems and cannot, at the moment, be run at the desired setting.

The effects of the steering of the proton beam at 1AT1 on the secondary particle fluxes are shown in Fig. 18. The 30 MeV/c surface μ^+ flux seen in M13 is about 50% larger when a 1 mm wide beam is steered to the left (M13) side of a carbon target than when it is centred. The electron contamination is also much lower when the beam is to the left. The 91 MeV/c μ^+ rate is much less sensitive to beam position. (In later measurements the π^+ profile became flat-topped when a larger target paddle was used.)

The advent of new radiation-cooled carbon targets for pion production makes it possible to use small (1-2 mm diam) circular beam spots instead of the relatively large asymmetric beam shapes used on the existing water-cooled targets. When a small beam spot is steered to the top left corner of a target, it is hoped that the electron contamination of the M8 π^- beam (and other beams) will decrease and that the flux of surface muons will increase (as in Fig. 18). In addition, use of these small beam spots would improve the optics of the secondary channels and considerably simplify the operation of the primary beam line. Therefore, beam line 1A optics is being redesigned to have a 1 mm spot at 1AT1 and 2 mm spot at 1AT2. Calculations and some preliminary experimental

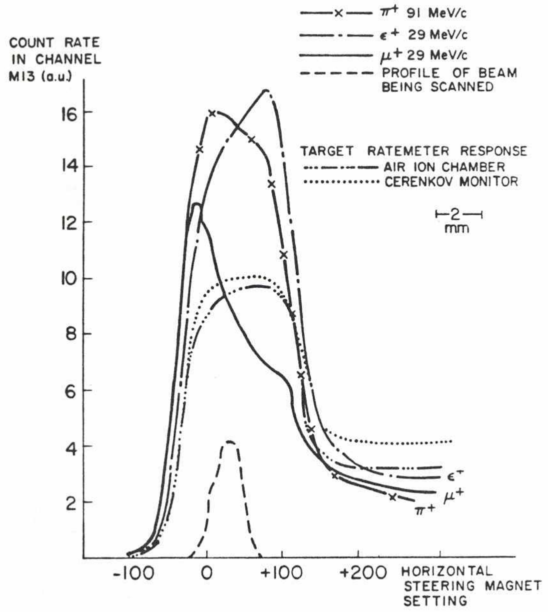

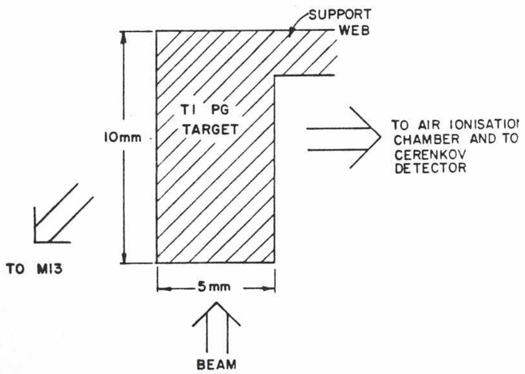

Fig. 18. The control room ratemeters and the M13 π^+ flux have a flat-topped response when a narrow beam is steered across a pyrolytic graphite target. The μ^+ rate, and particularly the (μ^+/e^+ contamination) ratio, peaks when the beam grazes the target edge facing M13.

work have demonstrated that a 1 × 1.5 mm^2 spot at 1AT1 and a 1 × 2 mm^2 spot at 1AT2 are readily achievable. Further work is necessary to improve this tune, in particular to get a suitable spot at the thermal neutron facility and to check the spills at high currents. It is hoped that the new targets will be compatible with currents of 200 μA or more.

Beam line 1B

Beam line 1B was installed to provide an additional location at which polarized beam could be utilized. At the present time the (p,π) spectrometer occupies the experimental position.

Early in the year the line was commissioned at beam energies of 200, 250, 300 and 350 MeV. Nominally 10 mm horizontally by 2 mm vertically, the beam spot at the (p,π) target location was observed to be 2 wires by 1 wire on a wire chamber with 5 mm wire spacings. Attempts to commission the line at and above 400 MeV were unsuccessful. This was because of instabilities in the dipole power supplies at the required current levels.

Later in the year experimenters found problems around 250 MeV in achieving zero asymmetry in the polarimeter (located between the two 43° dipoles) and, at the same time, small beam spill at the beam dump. Similar difficulties were not encountered at other energies. A study of this effect is planned in the new year.

As initially conceived, beam line 1B has two experimental target locations, with the beam stop inside the meson hall. Figure 19 indicates a possible reconfiguration of the beam line to accommodate the 'Discovery' pion spectrometer. The first target location (1BT1) would provide a beam spot 3 mm in diameter. Experiments performed here would be similar to those performed at the 4BT1 position on beam line 4B. A beam spot 1 cm horizontally and 0.1 cm vertically would be provided at the second experimental location (1BT2). This would be a suitable site for the proposed pion spectrometer. The beam dump would be buried outside the north wall of the meson hall.

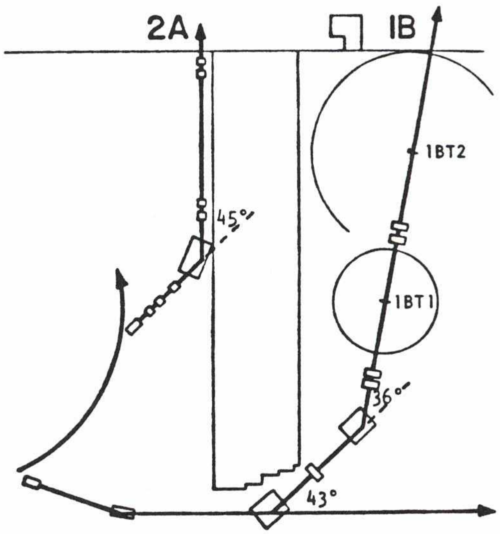

Fig. 19. Layout for the proposed beam line 2A and for beam line 1B with its beam dump buried outside the meson hall.

Beam line 2A

A proposal has been made to construct a line to carry beams of energies ≳400 MeV. This line would be extracted from port No. 2 and would run northwards parallel to the east wall of the vault, exiting from the vault in the northeast corner.

Studies of the optics for this line began late this year. A possible layout is shown in Fig. 19. In the configuration shown, the bend angle of the combination magnet has been increased by 5° from that currently used on beam lines 1 and 4. (That is, at 400 MeV, for example, the combination magnet bends the beam ≃19° compared with the present combination magnet bend of ≃14°.) Further studies are under way.

Beam line 4C

A stable polarized proton beam of 10^5-10^6 particles/sec within an area of 3 × 3 mm^2 and an angular emittance of 5 × 5 $mrad^2$ is required for experiments using the polarized hydrogen target. A design study for a special beam line to deliver the low-intensity beam to the new experimental station was initiated at the beginning of the year. After considering various possible locations it was decided to install the new facility in the experimental area downstream of the neutron collimator positioned behind the LD_2 target on beam line 4A. The layout of beam line 4A with the new branch known as beam line 4C is shown in Fig. 20.

The elements required along beam line 4A or on beam line 4C to monitor the polarization and control the direction of polarization of the beam included: (i) a relatively thick CH_2 polarimeter, (ii) a superconducting solenoid to rotate the spin by 90°, and (iii) a 35° bending magnet to precess the spin horizontally to form a longitudinally polarized beam. It was decided to keep the polarimeter in the present location, immediately downstream of the SFU scattering chamber on beam line 4A, where it was installed for polarized beam experiments. Similarly the superconducting solenoid was maintained in its position upstream of the LD_2 target. The 35° magnet was placed a short distance from the neutron collimator exit to bend the beam south into the experimental area available between beam line 4A and beam line 4B.

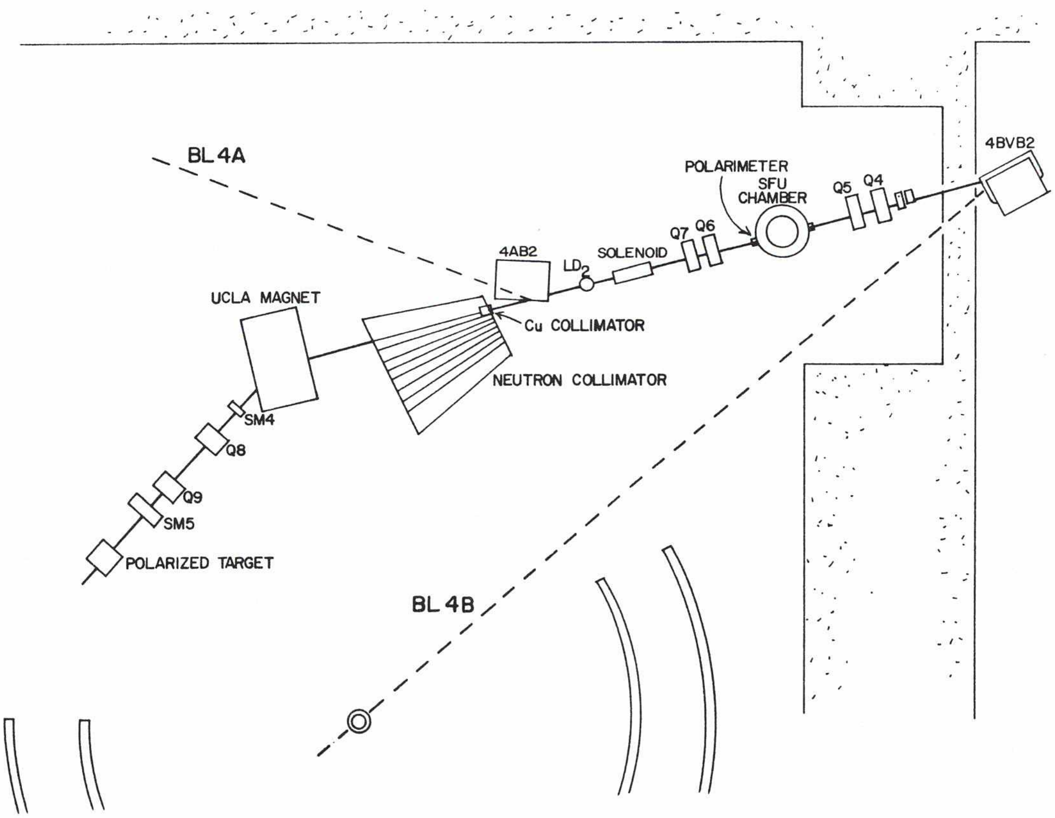

Fig. 20. Layout of beam line 4C.

In order to focus and centre the beam on target two quadrupoles and two steering magnets were placed in optimized positions downstream of the 35° bender. The positions of the upstream quadrupoles and steering elements along beam line 4A were not altered, in accordance with the criterion of not interfering with the other modes of beam line 4A operation. The liquid deuterium target and the neutron collimator were left in their present positions, and adequate space was left for a monitor between the neutron collimator exit and the 35° bender, to maintain compatibility with neutron beam experiments. Elements which would interfere with the neutron beam mode of operation were designed to be easily removable.

A 3 mm diam, 20 cm long copper collimator was placed at the entrance of the neutron collimator. This collimator serves two purposes. On the one hand it allows a reduction factor of up to 1,000 to be achieved thus allowing the primary proton beam to be sufficiently intense (10^8-10^9 particles/sec) for an on-line measurement of the polarization to take place with a standard polarimeter of reasonable thickness (~0.1 in.). On the other hand it has the essential function of reducing the beam emittance, which is substantially enlarged by multiple scattering at the polarimeter, to a small value compatible with the required beam size at the polarized target. Reducing the beam intensity down beam line 4C makes the requirements of a high split ratio between the two beams, simultaneously extracted from the cyclotron, less severe. With a split ratio of 10^4, which has been shown to be achievable with good stability, a beam of 10^{12}-10^{13} particles can be extracted down beam line 1A, more than presently available during polarized beam acceleration.

A typical calculated beam envelope along beam lines 4A-4C is shown in Fig. 21. A waist is produced at the polarimeter location in order to minimize the distorting effects of multiple scattering on the emittance. The beam then diverges towards the 3 mm collimator both horizontally and vertically. The quadrupoles between polarimeter and collimator can be used to control the beam size at the collimator entrance, which determines the reduction in intensity and emittance. Downstream of the collimator the pencil beam diverges only slightly; the quadrupoles downstream of the 35° bender are mainly used to focus the beam horizontally to counteract the dispersing effect of the magnet. The energy spread of the beam (90% of the particle) is of the order of ±1 MeV, including the original energy spread at extraction and the contribution from the polarimeter and the collimator.

The beam calculations were performed initially with program TRANSPORT, based on an rms Gaussian scattering approximation at the polarimeter and on a geometric defining action at the collimator. For the optimized tunes the calculations were repeated with the REVMOC program, based on more accurate formulas in a Monte Carlo routine. The

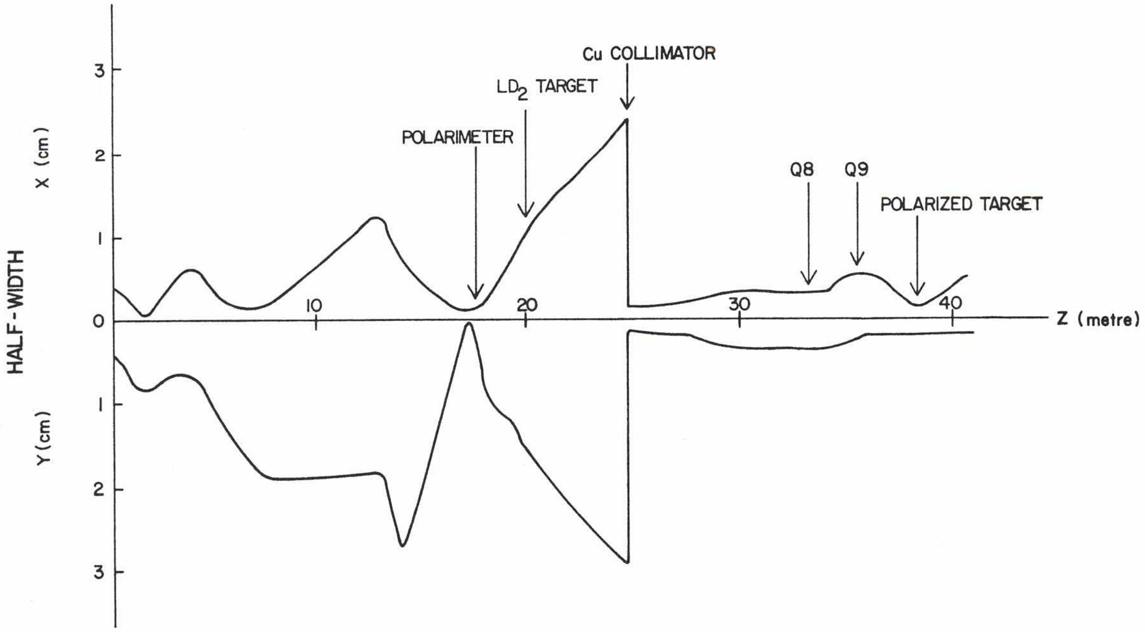

Fig. 21. Beam envelopes (500 MeV) along beam line 4C as calculated by TRANSPORT.

results in terms of beam size and angular spread were in good agreement.

Preliminary measurements on the beam size and beam alignment properties downstream of the collimator were performed before the end of the year. For the first tests a 1 mm diam collimator was used. The behaviour of the pencil beam and the intensity reduction factor were as expected.

SECONDARY CHANNELS AND SPECTROMETERS

M9 extension with dc separator

The design of this extension was described last year. The line was first tuned with 30 MeV/c surface μ^+ to the waist W3. The flux was optimized by changing the quadrupole settings from their theoretical values one by one, starting with Q1 and iterating. The optimum values agreed with theory within 10%. The beam spot is enlarged a factor three or four by the 0.001 in. kapton windows on either side of the separator, but these could be replaced by 0.00025 in. windows.

The tune to the waist W4 (the TPC position) was first obtained with 77 MeV/c muons. Again, the theoretical and experimental quadrupole settings agreed. The negative muon flux is about 450 k/sec for 100 μA protons, a 10 cm Be production target and 10% Δp/p. Sufficient beam purity has not yet been obtained because of the present limit on the voltage (340 kV) over the 10 cm separator gap. The next step is to raise this limit by running the separator in an argon atmosphere.

M9 extension with RF separator

In the present M9 extension a dc crossed-field separator is used to obtain clean muon beams. Since the phase space of this separator is poorly matched to that of the M9 channel a severe flux loss occurs. It is therefore intended to replace the dc separator with a 1 m long RF separator, presently under development. This separator will be centred at the same spot as the dc separator, 12 m from the production target. The beam will be steered into it by the quadrupole doublet Q4/Q5 and the doublet Q4'/Q5', which will be placed right in front of it. The rest of the extension will remain unchanged.

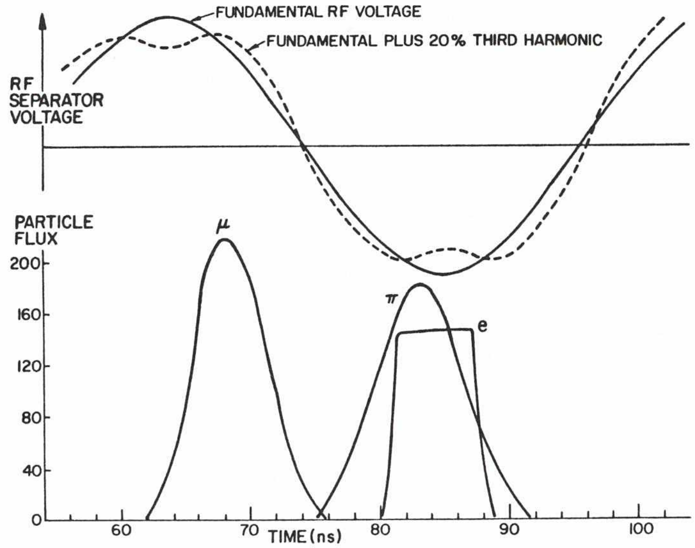

Fig. 22. Time-of-flight spectrum expected at the centre of the RF separator (below) compared to the time variation of the RF separator voltage (above).

The separator will be used for a narrow range of momenta around 77 MeV/c; it operates in the following way. A high RF voltage (360 kV) is generated over the 15 cm vertical gap with a period of 43 nsec, the time between two consecutive cyclotron bursts. A crossed static magnetic field B is also applied to cancel out the effect of the RF electric field E for muons so that there is no net deflection. The pions and electrons arrive 125° (15 nsec) later at a time when the electric and magnetic fields work in the same direction. The electrons are 360° (43 nsec) out of phase with the pions. Since the angular separation is proportional to $(300B + E/\beta)/p$ the separation is better for pions than for electrons.

Figure 22 illustrates the time of arrival at the centre of the separator for muons, pions and electrons with respect to the RF wave. These results have been obtained with a Monte Carlo program. The proton burst was assumed to have a 5 nsec square distribution, and the momentum slits in M9 were closed to give a momentum acceptance of 10% FWHM. The electron distribution is also square with the 5 nsec width of the proton burst because, of course, $\beta \simeq 1$ for the electrons, independent of momentum.

Adding 20% third harmonic to give a flatter RF wave improves the pion contamination slightly, but it also results in a lower effective electric field and therefore makes the electron contamination worse. Furthermore, it was found that the muon transmission is barely influenced by the presence of a third harmonic. Therefore, no third harmonic component will be added.

The following results have been obtained with a Monte Carlo program in which the peak voltage across the 15 cm gap was 300 kV and the magnetic field 94 G. The pion contamination was 0.2% and the electron contamination 4%. The muon flux at 77 MeV/c was 9×10^5/sec for a 100 μA proton beam on a 10 cm long Be production target and with 75% of the muon beam within a 10% momentum bite.

M11 channel

Optical design of the M11 pion channel was finalized during the past year. A small downstream shift was made in the position of the 'mid-plane' focus. As is indicated in Fig. 108 (p.110), this had no effect on the overall layout of the channel. Recalculated parameters of the channel are listed in Table III.

Sextupole strengths required for second-order corrections were calculated for the new configuration. Solutions were found which allow the use of sextupoles of current design. Contributions of second-order terms to the (horizontal) spot size at the target locations are ±0.08 cm in the achromatic mode, ±0.36 cm (= ±0.11% $\Delta p/p$) in the 'normal dispersed' mode and ±0.78 cm (= ±0.061% $\Delta p/p$) in the 'reverse dispersed' mode. All numbers correspond to particles having coordinates at the target of ($\pm x$, $\pm\theta$, $\pm y$, $\pm\phi$) = (±0.1 cm, ±20 mr, ±0.25 cm, ±130 mr) and a momentum variance as listed in Table III.

M13 channel

The optics design and the hardware of this beam line were described in last year's annual report. The line was started in January and extensive measurements have been made. The magnet settings were determined by a procedure involving the use of a movable ^{244}Cm α-source (equivalent to pions of momentum 91 MeV/c) at the position of the production target 1AT2. A movable solid state detector was placed at the F1, F2 and F3 foci in turn, and the dispersion, magnification and solid angle were determined. The results were in good agreement with the theoretical predictions and are presented below in Table IV.

Next the channel was tested with pions. Only very minor changes in magnet settings were necessary to obtain the best tune. A variety of measurements was made of flux, beam composition and beam spot size for 91 and 55 MeV/c and Be, V, Cu and C production targets. A remarkable result is that the negative pion flux per g/cm^2 for V is 1.5 times higher than for Cu, whereas the positive pion fluxes are the same.

The momentum dependence of the flux was measured for a 1.45 mm carbon production target. The results are shown in Figs. 23(a) and 23(b). The flux for positive pions and muons is about five times that for their negative counterparts. The positron and electron flux are the same above 55 MeV/c where the momentum dependence is flat. Later measurements with the 1 cm carbon production target which is presently being used confirmed the expectation that pion and muon fluxes can be scaled with target thickness. The positive pion flux for the 7 cm C target and 8% $\Delta p/p$ FWHM (all slits open) is 2×10^5/sec/μA at 100 MeV/c and 4×10^5/sec/μA at the present maximum

Table III. M11 fast pion channel.

	Operating mode		
	Achromatic	'Normal dispersed'	'Reverse dispersed'
R_{11}	1.4645	0.9893	2.1308
R_{16} (cm/%)	0.0	-3.3000	12.7319
R_{33}	-1.9875	-2.0000	1.8821
$\Delta\Omega\Delta p$ (msr-MeV/c)	247.4	180.1	85.7
Δp (MeV/c)	24.9	24.5	9.5
$\Delta\Omega$ (msr)	9.9	7.4	9.0

Table IV. Comparison of design and measured beam line parameters.

	Experiment		Design specification
	F1	F2	F1 and F2
Solid angle	33	29	38 msr
Dispersion	1.22	1.18	1.26 cm/% $\Delta p/p$
Horizontal magnification	0.84	0.81	0.90
Vertical magnification	5.1	4.3	4.4

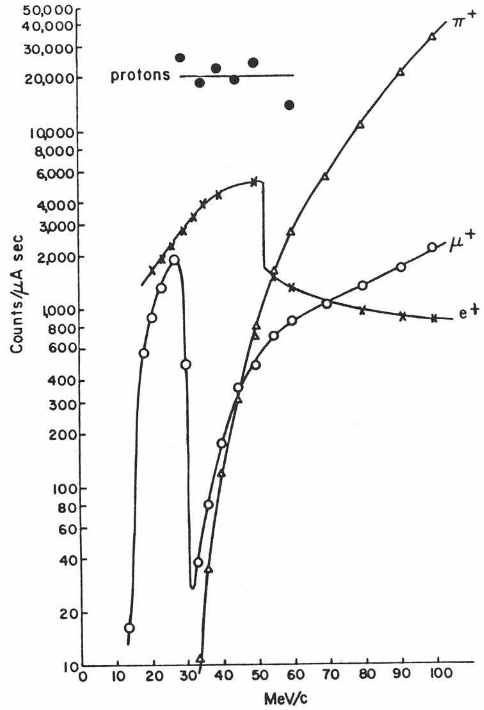

Fig. 23(a). Positive particle fluxes from 1.45 mm carbon target (18-100 MeV/c).

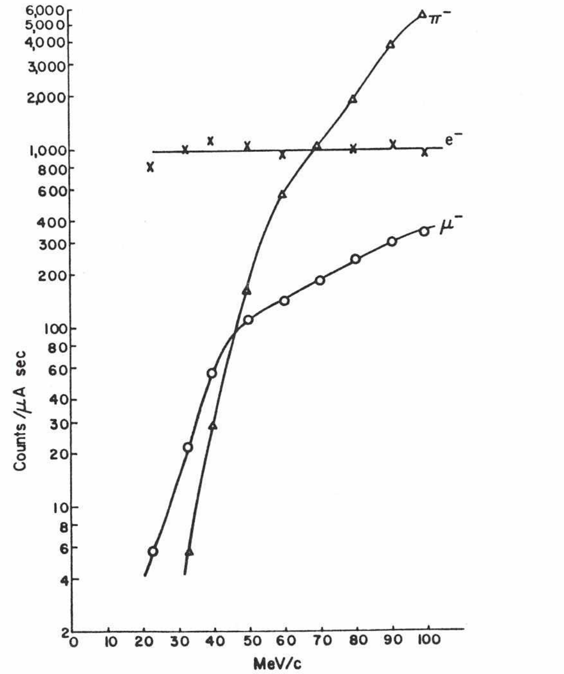

Fig. 23(b). Negative particle fluxes from 1.45 mm carbon target (18-100 MeV/c).

momentum of 130 MeV/c. Recent investigations indicate that with appropriate changes in the power supplies and magnet cooling the maximum momentum can be raised to 155 MeV/c, where the π^+ flux would be 3.5×10^5/sec/μA.

The flux of 29 MeV/c positive (surface) muons for 1 cm C is 1.2×10^4/sec/μA. The effect of the steering of the proton beam on the target has been investigated and found to be considerable, not only with respect to the flux, but also with respect to the positron contamination. There are between one and two times as many positrons as muons (see Fig. 23).

The size of the horizontal pion beam spot 1.20 m downstream of the last quadrupole as a function of the apertures of the horizontal jaws in front of B1 and the horizontal slits of the first dispersed focus F1 is given in Fig. 24. The vertical beam size is 2 cm FWHM and 3 cm FW(quarter)M. Finally we remark that the electron, surface muon and pion beam spots were the same size, but that the cloud muon beam spot was much larger.

The momentum acceptance of the channel as a function of the horizontal slit aperture at F1 was measured with a completely new method. A large (4 cm diam) SiLi detector was placed at the final focus. The horizontal jaws in front of B1 were closed, thus eliminating second-order effects and ensuring that the beam spot was confined to the sensitive area of the detector. The widths of the proton and ^{3}He peaks in the observed energy spectrum were then measured for a 2 mm long C target and a 60 nA primary proton beam. The results for a 55 MeV/c tune are given in Fig. 25. The agreement between theory and experiment is good, although the observed momentum acceptance for

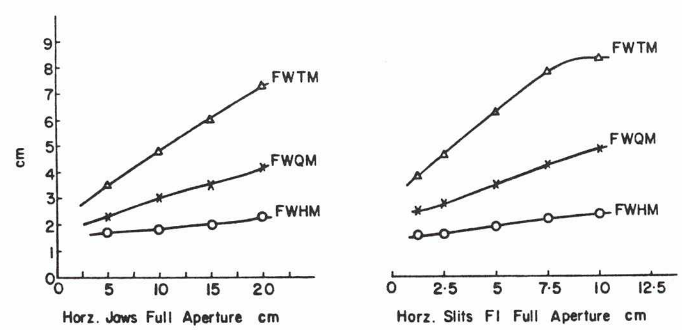

Fig. 24. Effect of jaws and F1 slits (horizontal) on horizontal beam spot at F3 + 33 cm.

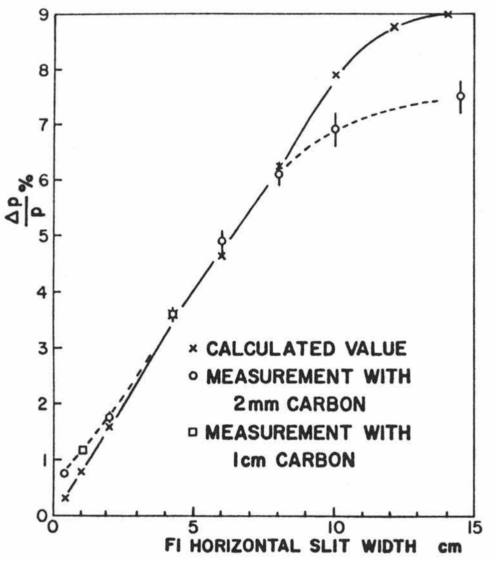

Fig. 25. Momentum acceptance of beam line (horizontal jaws opening 4 cm).

open slits is somewhat smaller than predicted. More care needs to be taken to measure the resolution for small slit apertures.

M20 channel

The plan for the redesign of M20 is to keep the present Q1 and B1 (40° bender) but to replace the rest of the line (Fig. 26). The present Q2 would be replaced by a 12 in. quadrupole. After B1 the next elements are two quadrupoles to inject pions of at most 165 MeV/c into a decay section of 6 to 10 quadrupoles; this is followed by two quadrupoles for the extraction of highly polarized forward or backward muons. B2 which follows bends counterclockwise and has two exit ports for beams bent through 37.5° and 75°, respectively. The 75° leg has two quadrupoles and gives:

1) Clean backward muon beams for momenta $\leqslant$ 90 MeV/c
2) Clean forward muon beams for momenta $\leqslant$ 100 MeV/c
3) Heavily contaminated forward muon beams for momenta $\leqslant$ 175 MeV/c

The 37.5° leg consists of a drift space, two quadrupoles, a dc separator and a further two quadrupoles. This leg gives:

1) A clean surface muon beam with the possibility of precessing the spin through 90°
2) A heavily contaminated forward muon beam of 175 MeV/c
3) Possibly clean forward muon beams for momenta $\leqslant$ 140 MeV/c
4) Clean unpolarized cloud muon beams for momenta $\leqslant$ 120 MeV/c

The luminosities for forward and backward muon beams would be five times higher than for M20 in its present state. The channel can, of course, also be used to obtain clean pion beams. The transmitted momentum bite is 8%. The resolution for a 10 cm long production target is also 8%. In that case no momentum slits are needed.

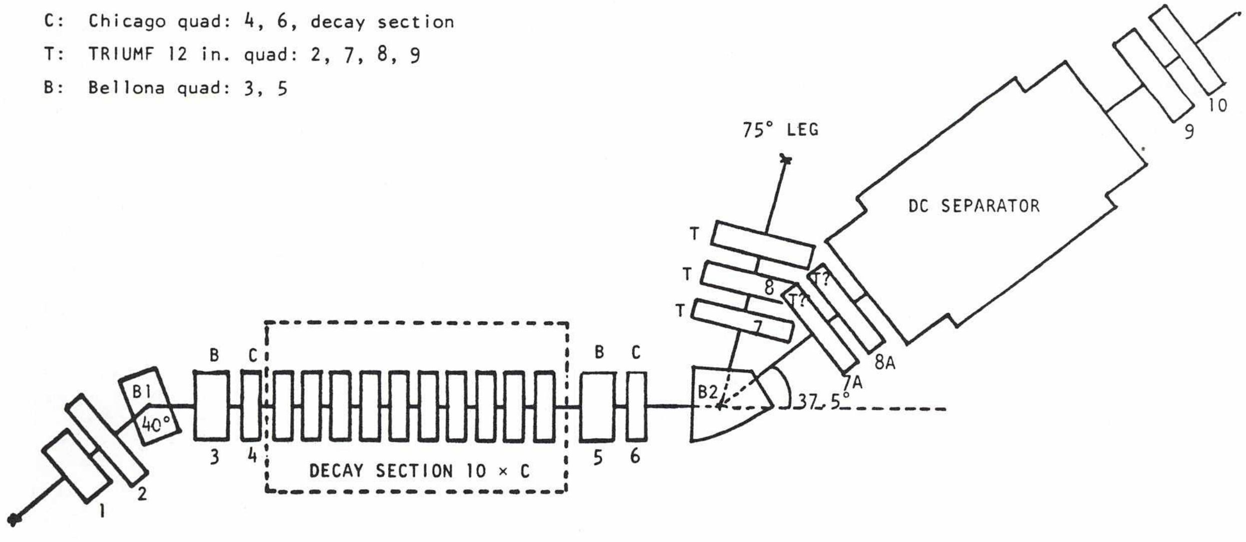

Fig. 26. General layout of M20 channel.

A study is under way:

1) To investigate the best positions for the various elements in the two legs to optimize performance taking into account the fact that floor space is limited. Shuffling quadrupoles between the two modes seems the best solution.
2) To determine the size of quadrupoles.
3) To find the positions where jaws (before B1?) and slits (when using a small production target) should be placed.
4) To determine the optimum number of quadrupoles between B1 and B2.
5) To find out if two legs are necessary at all because the 75° leg seems to have a limited use.

High flux muon channel

A preliminary study has been made of an axisymmetric muon channel utilizing three toroidal magnets. The first torus followed by an axial aperture defines the momentum bite, the second torus and aperture separate pions and muons, and the third torus produces the final muon beam spot. The acceptance and cost are roughly estimated to be 0.5 sr and \$3 million, compared to 1.0 sr and \$1.5 million for the iron-free three-coil channel; however, the three-torus system has the advantage that both the production target and muon focus would be in magnetic field-free regions.

High flux pion channel for radiation therapy

The properties of an axisymmetric system composed of two coaxial coils are under investigation to determine if such a channel would produce a beam suitable for radiation therapy. Such a channel could have a peak solid angle of acceptance ~1 sr with a momentum acceptance ~4% for $\Omega \geqslant 0.5$ sr. The properties of the beam produced by a fairly long axial line source (~4 cm) are of great interest. For each accepted momentum there is a range of axial positions for which the number of trajectories per unit transverse area is a maximum on the symmetry axis. This maximum is produced by those trajectories which are converging to intersect the axis at the location of interest.

Medium resolution spectrometer

Early in the year it appeared that the experimental resolution of the MRS was considerably larger than had been anticipated. Ray-tracing studies of the MRS were therefore initiated using the measured quadrupole and dipole fields. General agreement was obtained between calculated and experimentally determined values of parameters in the bend plane; the observed values of focal plane angle, dispersion, θ^2 aberration and correlation between momentum and focal plane position were reproduced within a few per cent. Calculations indicated, however, that correlations between bend-plane and non-bend-plane parameters should be seen; experimentally these were not observed.

In December, the resolution measurement was repeated with all scattering material removed from the beam line and front end of the MRS. At 200 MeV a resolution of 225 keV FWHM was observed, in agreement with both design and ray-tracing predictions. Further investigations are planned to resolve the apparent discrepancy between experimental results and analytical calculations in the non-bend plane.

COMPUTING SERVICES

A major event this year has been the movement of the public terminal to a new, dedicated room on the mezzanine of the CRC Lab. In accordance with our agreement with the UBC Computing Centre this move was accompanied by their provision of conversational terminals and the replacement of the Data 100 (Comterm) terminal by a Printronix dot-matrix printer. Two Ann Arbor terminals have been delivered so far, and two more are promised later. The Printronix is relatively slow (300 lpm) but will be replaced by a 600 lpm version next spring; a significant advantage is its ability to produce good resolution printer-plots. A similar conversion is under consideration for the service annex terminal, but a card reader would continue to be maintained there.

The asynchronous communication system has continued to expand. There are five more stations active this year (making 17 in all) and the Computing Centre has provided two more ports and three more lines. In addition, a second graphics terminal is being commissioned so that one will be available in each terminal room. A major improvement occurred in the fall, when the Computing Centre switched 13 lines from a 'line concentrator' feeding into only 7 computer ports and gave them each a dedicated port. The major restriction now is that the 14 multiplexed lines are limited to 1200 (rather than 9600) baud. This limitation will disappear when TRIUMF is provided with more telephone circuits (promised for 1979 but not yet in evidence); to allow for future expansion 50 additional circuits have been requested for computer use. The following summarizes the situation:

	Nov. 1977	Nov. 1978	Dec. 1979
Telephone circuits	7	8	9
Asynchronous facilities			
UBC CC ports	6	9	18
UBC CC lines	9	15	18
TRIUMF stations	8	12	18
Multiplexed lines	1	2	2
9600 bd lines	0	2	2
Synchronous lines	3	3	2

Synchronous communications are already in operation between the Computing Centre and UBC Electrical Engineering. With the recent addition of a programmer to Computing Group II, work is expected to begin imminently on software support for TRIUMF. For very high speed (megabaud) communication TRIUMF has agreed to pay for a Physical Plant feasibility study on laying a fibre optics line to TRIUMF.

RESEARCH PROGRAM

INTRODUCTION

The diversity of research at TRIUMF continued to increase in 1979. In part this was made possible by the increase in delivered beam from 27,000 μAh in 1978 to 83,000 μAh in 1979. Perhaps more important for the future was the addition of two new major facilities. One of these facilities, beam line 1B, is primarily designed for a polarized beam to be used simultaneously with the polarized beam in the proton hall. The availability of this new facility has become increasingly important as the importance of polarized beam experiments has become obvious to the TRIUMF research groups, and by late 1979 there were almost always two experiments making use of the polarized beam whenever it was available. The commissioning of M13, a new low-energy π-μ beam line, was also completed in 1979. This line essentially duplicates in performance the over-subscribed M9 line and will greatly increase the research potential in the meson hall.

In terms of the future, perhaps one should mention first some feasibility studies which have been made in order to convince the Experiments Evaluation Committee to recommend the granting of large blocks of beam time. One of these studies concerned a test of charge symmetry in neutron-proton scattering. This experiment depends on the accuracy with which the cross-over in n-p analysing power can be determined, and the test involved a similar measurement for the p-p case. The effect of the background on the position of the cross-over was investigated and found to be <0.005°. The results of the test appear to be favourable for the n-p experiment. Another feasibility study was oriented to the possibility of an experiment on the reaction $p + p \to \pi^+ + d$ in which both the pion and the deuteron are detected and measured over a wide kinematical angular range. The test showed that the pulse height of a deuteron scintillation detector with the time-of-flight signal from the pion gave a signal for the $pp \to d\pi^+$ reaction clearly separated from background. Another series of tests which bode well for the future was carried out on the components of the time projection chamber (TPC). This chamber will be used to pursue the limits of lepton number conservation in the form of $\mu \to e$ conversion in the field of a nucleus as in $\mu^- + Z \to e^- + Z$. In another area, preliminary measurements were carried out which indicated a clean separation of the desired reaction $^2H(\vec{p},\gamma)$ (polarized protons) from the background gammas of the $(\vec{p},\pi^0)$ reaction.

In 1979 the BASQUE group completed a five-year experimental program concerned with the precise determination of the neutron-proton phases in the energy range 200-500 MeV. The analysing power P and D_t were measured in 1977, and in 1978 the transfer spin parameters A_t and D_t were determined. Finally in 1979 the most difficult measurements of all, those of the absolute n-p differential cross section, were completed. The spin correlation measurements have substantially improved the spin-orbit and tensor combinations of phase shifts, but the cross-section data were required to improve the determination of the central combination of phase shifts.

1979 has seen the successful culmination of the effort of several years in the determination of the total lifetime of muons captured in various materials. Elimination of troubles caused by counter inefficiencies, double counting, etc., together with the use of the low contamination backward muon beam of M20, has made possible the routine measurement of total lifetimes to an accuracy of 1 nsec. An intriguing result of this experiment is the possibility of determining the fractional amounts of two-component mixtures with a much higher precision than can be achieved with X-rays. On the other hand, it appears that the rare decay modes of pionic atoms, e.g. $^{12}C(\pi^-,2\gamma)^{12}B$ cannot be used to discover a possible pion condensation effect, as suggested by Ericson and Wilkin. In particular, it is found experimentally that the residual nucleus in the above reaction (^{12}B) is usually left in its ground or low excited state. Therefore, it appears that the bremsstrahlung process is dominant in pion capture from a P-state, and this prevents a direct exploration of the pionic field in the nucleus.

Because of its long mean free path in nuclear matter the low-energy π^- makes an excellent probe of the neutron density in the nucleus. This characteristic has been used by the low-energy π-nuclear scattering group at TRIUMF to determine the effective radius of the neutron density in nuclei. In particular the neutron radius of ^{13}C was determined relative to that of ^{12}C by measuring the ratio of the π^- elastic differential scattering cross sections on the two isotopes. The proton radii of ^{12}C and ^{13}C were taken from electron scattering data, and the neutron radius of ^{12}C was set equal to its proton radius. An extensive χ^2 search yielded the result $\langle r_n^2 \rangle^{13}C = 2.35 \pm 0.03$ fm and similarly $\langle r_n^2 \rangle^{18}O = 2.81 \pm 0.03$ fm was obtained. The section of this report on the theoretical program discusses some implications of these results. Preliminary π^- scattering data on ^3He have been obtained which should be of interest to theorists, in view of the relative simplicity of the target.

Two experiments involving fission obtained results in 1979. In the first, a study was made of the intensities of particles evaporated pre- and post-fission. The absence of spectral shifts from Doppler or Coulomb barrier effects is evidence for fission occurring predominantly after evaporation. The second experiment was concerned with μ^- capture in fissile nuclides. The time distribution of fission following a μ^- stop indicates a single mean life of 71.5 ± 0.9 nsec for ^{235}U whereas for ^{238}U there is clear evidence for a short-lived component involving 8% of the delayed fissions with a mean life of 18 ± 5 nsec, in addition to the dominant mean life of 76 ± 1.3 nsec. The short component was not seen in π^--induced fission.

The availability at TRIUMF of a 200-500 nA polarized (80%) beam has made possible the exploration of a new and fertile field of research. It now appears that measurement on the asymmetries in the nuclear reactions produced by polarized protons give data which form a severe test for the accepted theories for predicting such reactions, and in fact most tests end in failure. It is clear that much more experimental data are needed in order that reliable theories can be developed. Several groups at TRIUMF are trying to satisfy this need. The subjects of the experiments are: the elastic $\vec{p}$-^4He scattering, elastic $\vec{p}$ scattering from Ca and Pb, the $(\vec{p},d)$ reaction (two experiments), $\vec{p}$-^4He inclusive scattering, and asymmetries in the reactions $^2H(\vec{p},\gamma)^3He$ and $^3H(p,\gamma)^4He$. A glance at the theoretical curves for the asymmetries will show the magnitude of the failure of the present theories.

The groups exploring the applications of muons and muon decay to the study of chemistry and solid-state physics pursued their goals in 1979 in their usual lively manner. Two major improvements in technology are important for the future and have been combined in a new experimental tool. One is the use of the muons coming from pions decaying near the surface of the proton target. These muons, with a 4.1 MeV energy, can be focused to give a very high stopping density. The other technique is the use of longitudinal and zero magnetic fields. A 'surface muon' beam 10,000/sec can be delivered to a 1 cm diam target with a stopping range of 140 mg/cm^2 and a range spread of 20 mg/cm^2. This flux is normalized to 20 μA of protons on the primary target. The research is much too multifaceted to describe or even summarize. As an example one might mention the measurements on the paramagnetic shift of μ^+ in MnO in a magnetic field. As a function of the temperature, the shift changes abruptly at 230°K and is not linearly related to the susceptibility, but changes with the length of time since the muon entered the crystal, suggesting a slow trapping of the muon at Mn^{++} vacancies. The experiment provides the first measurement of the contact hyperfine field at the μ^+ in a magnetic insulator. The result is unexpectedly negative and presents a challenging theoretical problem. The fashionable subject of 'spin glasses' has provided a rewarding application of the zero magnetic field longitudinal relaxation method. The mean local field distribution is extracted, and also its average fluctuation time. Continuing the measurements of the Mu spin system in quartz, the experiment was performed at 77°K and zero field, and completely different 'quadrupole oscillations' were observed from those at room temperature. In contrast to the previous experiment where the Mu site is symmetric about the $\hat{c}$ axis, the lower temperature results indicate the Mu atom is trapped in a site without axial symmetry.

Research has continued on muonium chemistry; in particular the formation of muonium in various gases still has some puzzling features. Also studies of the 'spin-exchange' process $Mu(\uparrow) + NO(\downarrow) \rightarrow Mu(\downarrow) + NO(\uparrow)$ have confirmed the bimolecular nature of the reaction mechanism. Studies of the formation and reactions of muonium with matter in the liquid phase have proceeded, with research in kinetic isotope effects, the reactivity of muonium with biologically significant systems, and residual muon polarization in aqueous solutions of K_2CrO_4. For the solid state an extensive program was carried out concerning the formation and subsequent motion of muonium in various oxide powders (SiO_2, M_3O, $A\ell_2O_3$, CaO, etc.).

It should be pointed out that the TRIUMF theoretical program is described in a separate section of this report and that many of the items discussed there concern the experimental program of TRIUMF. These items include radiative muon capture, nuclear sizes from low-energy pion scattering, proton-induced inclusive reactions, a unified theory for the reaction $^4He(p,d)^3He$, the (p,γ) reaction, proton-proton bremsstrahlung, and bound muon decay. The close collaboration between theory and experiment is an important feature of TRIUMF.

Experiment 26
np differential cross section

The BASQUE group completed the measurements of the neutron proton elastic differential cross section over the angular range 10° to 180° in the laboratory system at four energies, 220, 330, 430 and 500 MeV, to a statistical accuracy of better than 2%. This measurement is the last in a series of experiments that previously measured neutron-proton spin correlation parameters, in progress since 1974. The spin correlation measurements have substantially improved the determination of the spin-orbit and tensor combinations of phase shifts. The differential cross-section (spin-averaged) data were essentially required to improve the determination of the central (spin-independent) combination of the phase shifts. Analysis of the differential cross-section data is still in progress.

For the forward part of the angular distribution the carbon polarimeter employed in previous experiments was converted into a neutron detector. The carbon polarization analyser was used as a neutron converter with a veto counter and veto multiwire proportional chamber (MWPC) upstream of the carbon block, and a counter telescope plus MWPC array downstream. The efficiency of this detector was found to be inversely proportional to the kinetic energy of the incident neutron, as shown in Fig. 27.

For the charge exchange region of the angular distribution, the neutron detector was converted into a spectrometer. The veto counter and carbon block were removed and a small magnet was positioned between forward and rear MWPC arrays. The same monitor of incident neutron flux was used for both regions of the angular distribution. Preliminary results at 420 MeV are shown in Fig. 28.

The cross section in the forward region was measured by determining the number of neutrons scattered at a fixed angle to the number of neutrons incident at zero degrees. The number of neutrons incident at zero degrees was measured in a transmission configuration corresponding to a measurement of the total cross section. Additional total cross-section data were obtained using a standard fixed counter geometry. Preliminary results are shown in Fig. 29. The established accuracy is of the order 1-3%.

Further checks on beam normalization were made by measuring the rate for the reaction $np \rightarrow d\pi^0$ by observing recoil deuterons in the spectrometer. The rate for this reaction can be related to the measured rate for the

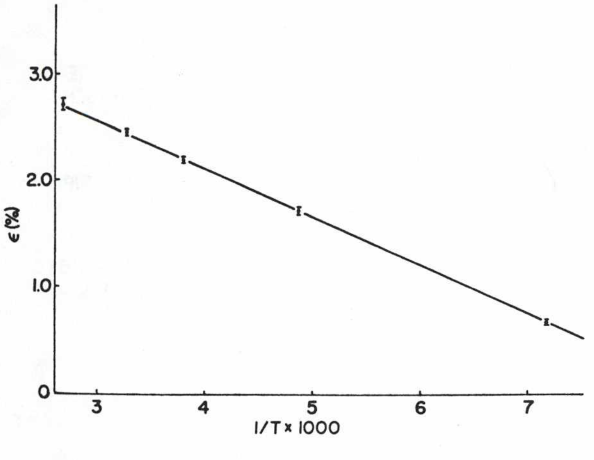

Fig. 27. Neutron detector efficiency.

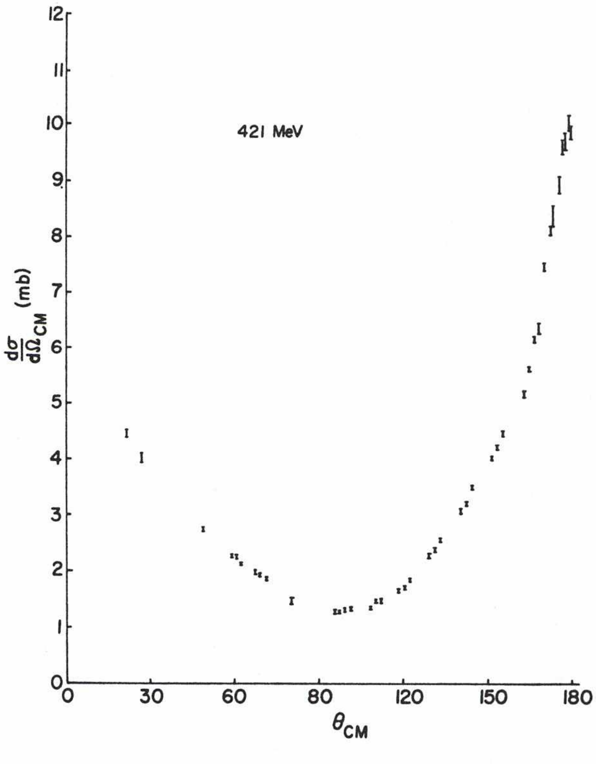

Fig. 28. Preliminary np differential cross-section data at 430 MeV.

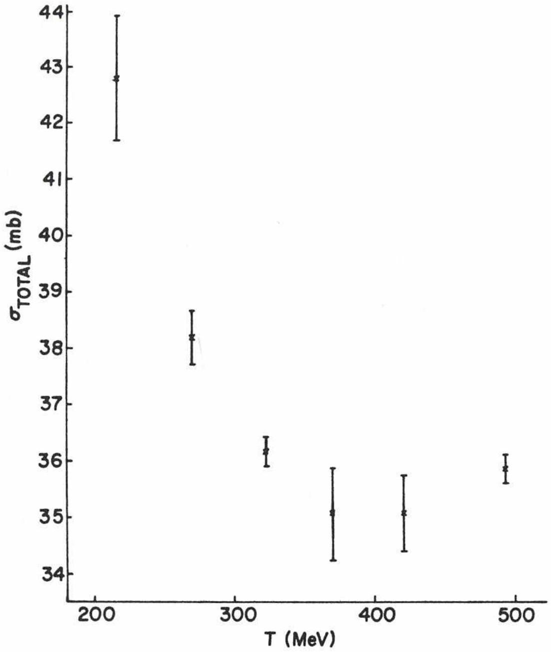

Fig. 29. np total cross section.

charged particle reaction $pp \to d\pi^+$ assuming isotopic spin invariance. The $np \to d\pi^0$ rate was measured at 380, 430 and 500 MeV.

Finally, the π^+-to-π^- ratio in the two inelastic reactions $np \to nn\pi^+$ and $np \to pp\pi^-$ was measured at 380, 430 and 500 MeV. The amplitude for these reactions can be written as a linear combination of isospin = 1 and isospin = 0 amplitudes, the sign being different in the two cases. In the previous analysis of np spin correlation data the I=0 inelastic amplitude was assumed to be zero with the prediction that the π^+/π^- ratio is unity. This assumption will be checked with the analysis of these data.

Upon completion of these experiments the experimental area is being reconfigured for installation of beam line 4C and a polarized proton target.

Experiment 83
Bound muon decay in nuclei

The energy spectrum of electrons produced when an orbiting negative muon decays has been predicted to differ from that of a free μ^+ because of several effects:

- reduction of the phase space available due to the μ^- binding energy
- time dilation produced by the orbital motion
- attractive Coulomb interaction between the e^- and the nucleus
- finite size of the nucleus

The goal of this experiment is to measure the energy spectrum and the energy dependence of the asymmetry of the decay electrons from μ^- decay in ^{12}C and other targets (Ti, Cu, Pb).

We have devised a time differential analysis method using μSR techniques to eliminate backgrounds having lifetimes different from that of the target element. We have obtained the energy spectrum in ^{12}C, Ti and Pb, which shows the predicted behaviour (a shift towards lower energies as the atomic number of the nucleus is increased), but our measurements for heavy targets are not background free below 20 MeV and must await the separated muon beam being completed.

Using an improved set-up (Fig. 30) we have measured the asymmetry in C, Ti and Pb. The differential asymmetry curves show the beginning of a reduction of the asymmetry at the highest energy in Ti (Fig. 31), which seems to confirm the prediction of Glinsky and Mathews [Phys. Rev. 120, 1450 (1960)]. Unfortunately, the quality of the Pb data is very poor due to the large electron contamination of the beam, and the experiment will be repeated with a separated μ^- beam.

Using the same time differential technique we have measured the polarization of the "cloud" μ^+ beam in M9. We stopped the μ^+ beam in a 1.0 cm thick graphite target maintained in a 250 G transverse magnetic

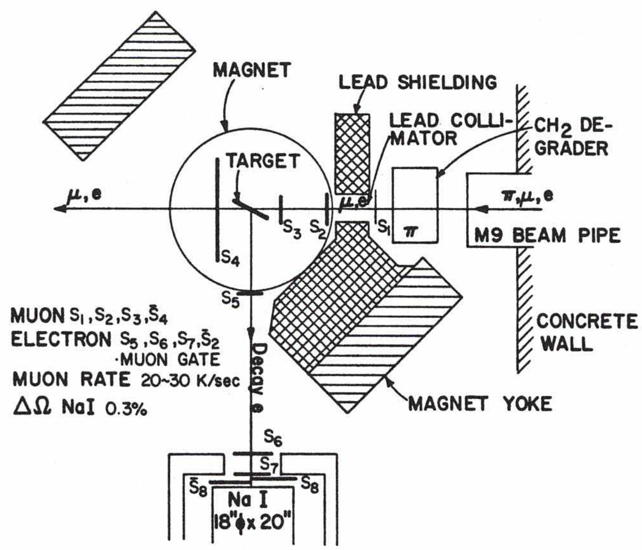

Fig. 30. Bound muon decay geometry, spring 1979.

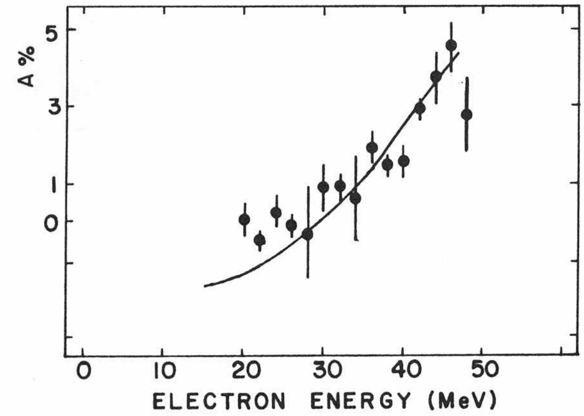

Fig. 31. μ^- decay asymmetry versus electron energy in titanium.

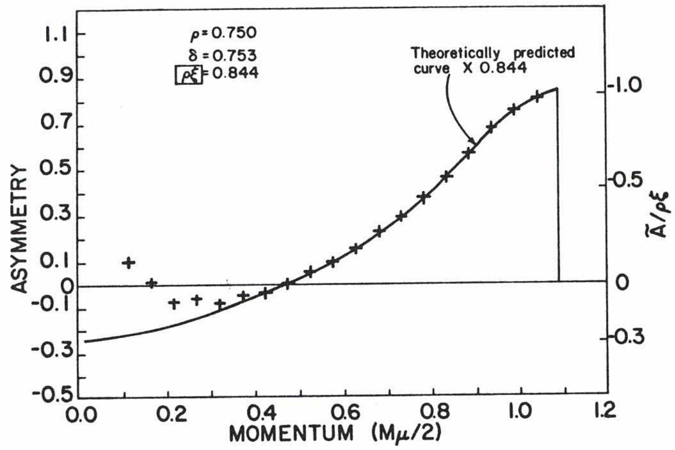

Fig. 32. The electron asymmetry for μ^+ stopping in carbon.

field. TINA, our large sodium iodide detector (46 cm diam × 51 cm long), was used as an electron detector preceded by a conventional plastic scintillator telescope.

The polarization of the beam was obtained from the measured asymmetry at the high energy end of the Michel spectrum. It was derived from a fit to the ratio of the asymmetric part of the measured spectrum to the isotropic part in the energy range 30-50 MeV. The results are summarized in Table V.

Measurements on free μ^+ decay were conducted as a check of the experimental technique; μ^+ were stopped in a 1 cm thick graphite target, and $\sim 2 \times 10^6$ positron decays were recorded. Because of the large number of events observed our sensititivy to the ρ and δ parameters in the Michel spectrum is greatly improved over earlier measurements. A least squares fit analysis of the energy spectrum has been carried out to obtain the value of ρ. The analysis is sensitive to the response function of TINA and to the energy losses of the positron in the target and the telescope. A Monte Carlo simulation has been carried out to reproduce the experimental resolution and is in agreement with the resolution inferred from the χ^2 analysis (8.6 ± 0.2%). The preliminary value of ρ obtained is 0.749 ± 0.002, compared with the V-A prediction of 0.750. (These results are corrected for the radiative contribution to the Michel spectrum.)

A similar analysis can be carried out for the asymmetry measurement from which the δ parameter can be deduced (Fig. 32). The present experiment indicates a value of δ = 0.753 ± 0.009 (ρ fixed at 0.75 and resolution giving the minimum χ^2 for the fit to the energy spectrum), again in agreement with the standard V-A prediction.

At present our measurement shows a contamination at low energy which could be removed by using a separated μ^+ beam now available on M9.

Table V. Measured μ-polarization $\overline{P}$.

	P_μ (MeV/c)	$\overline{P}$ (%)	Midplane X-slits (cm)
Cloud	77	31.8 ± 3.0	30
	96	47.3 ± 3.0	30
	120	57.3 ± 3.0	30
		57.5 ± 4.0	5
	135	77.4 ± 3.0	10
Forward	135	93.0 ± 3.6	10
Cloud and forward	135	84.4 ± 0.5	10
Surface	29	>80	

Experiment 88
Muon capture

This experiment has been several years in development, but in 1979 it has reaped the rewards. After a great deal of effort the problems of minute distortions in muon decay time spectra (due to counter inefficiencies more than one muon in the target at once, accidental electron triggers, and the biases created by attempts to eliminate these primary sources of error using electronic logic) have finally been conquered. Combined with the low-contamination 'backward muon' beam of M20, this has allowed routine measurement of total lifetimes to accuracies of about 1 nsec. Although more impressive accuracy has been achieved for (e.g.) positive muon lifetime measurements, this accuracy is a considerable improvement upon earlier surveys of muon capture rates and has allowed a systematic investigation of higher precision than ever before.

Table VI shows a tabulation of preliminary results.

Several of these results are particularly interesting. In the case of ^{12}C and ^{13}C the isotope effect is not significant. A. Fujii pointed out that this was due to the same Q values of ^{12}C and ^{13}C.

The lifetime of ^{93}Nb, a proton-odd nucleus, is very short compared with its neighbours Zr and Mo. This may reflect the effect of tremendous magnetic fields upon the Cabbibo angle [Salam and Strathdee, Nature 252, 569 (1974)]. Inside the proton-odd nucleus the magnetic field is effectively $\sim 10^{16}$ G, which could cause the Cabbibo angle to vanish locally [Watson, Phys. Lett. 58B, 431 (1975); Kirzhnits and Linde, Phys. Lett. 42B, 471 (1972)]. The hyperfine effect is about 3% on Nb; if we add to this the effect of the vanishing Cabbibo angle (as much as $1/(\cos \theta_C)^2$ the small muon lifetime (large capture rate) in Nb can be explained.

Table VI. Negative muon lifetimes.

Z	Element	Mean lifetime TRIUMF (nsec)	Mean lifetime Past result[a] (nsec)
3	separated ^{6}Li	2177.0 ± 2.2	2175.8 ± 0.4[a]
	separated ^{7}Li	2188.3 ± 1.0	2186.2 ± 0.4[a]
4	Be	2162.1 ± 1.8	2153 ± 9
5	separated ^{10}B	2070.7 ± 2.0	2082 ± 6
	separated ^{11}B	2096.1 ± 2.0	2102 ± 6
6	^{12}C	2026.3 ± 2.0	2034 ± 4
	separated ^{13}C	2028.1 ± 3.0	-
7	N	1906.8 ± 1.3	1927 ± 13
8	^{16}O	1795.4 ± 1.3	1812 ± 10
	separated ^{18}O	1860.6 ± 3.0	-
11	Na	1204.0 ± 2.0	1190 ± 20
17	Cℓ	560.8 ± 1.0	540 ± 20
19	K	437.0 ± 1.0	410 ± 20
20	Ca	332.7 ± 1.5	343 ± 3
22	Ti	329.3 ± 1.4	328 ± 4
35	Br	133.3 ± 1.0	-
66	Dy	78.8 ± 1.1	-
68	Er	74.4 ± 1.5	-

[a]All past results except Li are cited from M. Eckhause *et al.* [Nucl. Phys. 81, 575 (1966)2; for Li, G. Barain *et al.* [Phys. Lett. 79B, 52 (1978)].

In the course of measuring the muon capture rates in the more reactive elements (where it was usually necessary to use an oxide sample and separate the lifetime components for oxygen and the element of interest) it was noticed that the fits returned not only the lifetimes but also the fractions of the muon ensemble orbitally captured on the different elements, with very high precision. Since considerable effort has been invested in extracting the same information from muonic X-ray intensities, the 'lifetime-component technique' was tested on a variety of metal oxides, resulting in the data shown in Fig. 33.

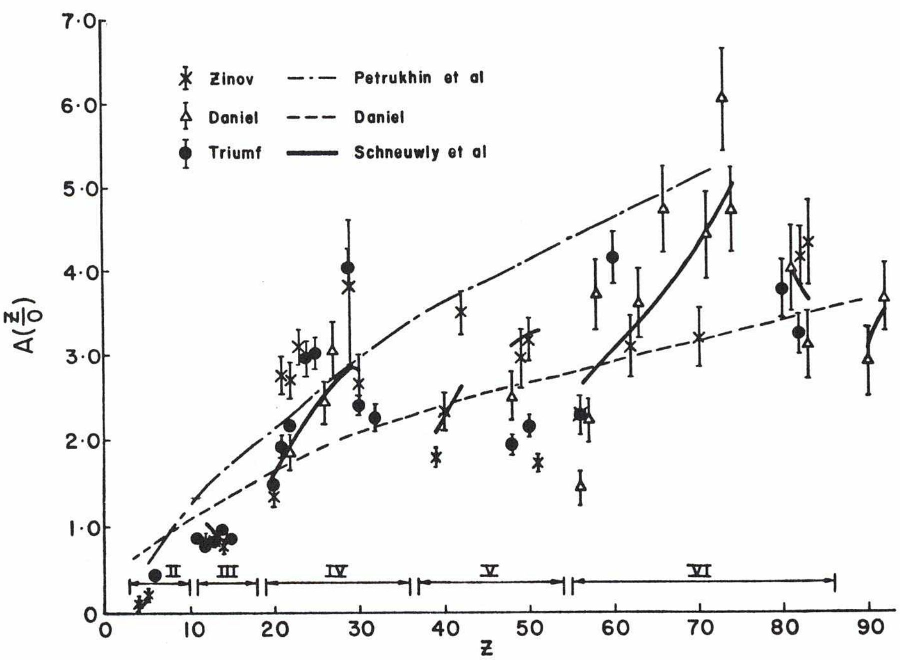

Fig. 33. The periodic dependence of the relative atomic capture probability $A(Z/O) = [m\Lambda(Z)]/[K\Lambda(O)]$ in the metallic oxides Z_KO_m.

The new data follow the X-ray data closely but are much more precise. This method appears to be much more accurate for compounds with only two elements; in all probability the X-ray method will still be superior for studies of multi-element compounds, but the state of the art has not yet reached such complexity. It is to be hoped that some sense can be made of these trends now that more precise data are readily available. Three theoretical curves are shown in Fig. 33; only that of Schneuwly *et al.* shows any of the structure of the data.

Experiment 97
Rare electromagnetic decays of pionic atoms *ic atoms*

The desire to learn more about the nuclear pionic field has prompted several experimental groups to search for the $(\pi^-,2\gamma)$ process in nuclei. Following a suggestion by Ericson and Wilkin [Phys. Lett. 57B, 345 (1975)] that virtual pions could be detected using the annihilation process $\pi^- + \pi^+ \rightarrow 2\gamma$ and that a possible pion condensation effect could be seen in that reaction, a study of the $^{12}C(\pi^-,2\gamma)^{12}B$ was undertaken at TRIUMF using two large NaI detectors, TINA and MINA, and two lead glass Čerenkov counters. The experimental set-up has been described previously [Annual Report 1978].

Although data were recorded simultaneously on the two reactions $(\pi^-,2\gamma)$ and $(\pi^-,2e)$ the complete analysis has been dealing mainly with the first case up to now. The experiment was carried out on the M9 low-energy π/μ channel by stopping a 20 MeV π^- beam in a 2.3 g/cm^2 carbon target at a rate of $\sim 7 \times 10^5$/sec. The low-energy beam was essential to reduce in-flight charge exchange production of real π^0. Pile-up of several π^- in the target was reduced by measuring the energy loss of the beam in the beam-defining counter. By using two NaI detectors good energy resolution was achieved (8% and 10% FWHM) as well as good neutron-gamma separation over a 1 m flight-path. The energy resolution of the lead glass counter was worse, but these counters provided neutron-background-free spectra. From the NaI coincidence, for the first time an energy-sharing distribution of the 2γ events was obtained and by combining all detectors covered an angular distribution over the range 50°-170° laboratory angles.

About 200 γ-γ events were obtained with good energy resolution. The energy-sharing distribution presented in Fig. 34 suggests a preferable emission of the two photons with unequal energies (this implies a strong threshold dependence of the total branching ratio for this process).

The sum energy spectra in Fig. 35 indicate that the $^{12}C(\pi^-,2\gamma)$ reaction does not leave a very large excitation of the residual nucleus as the sum energy peaks near 120-140 MeV (FWHM $\sim$ 40 MeV). By comparing this spectrum with the spectrum of the single radiative capture process, one is forced to the conclusion that the residual nucleus in the $^{12}C(\pi^-,2\gamma)$ reaction is most likely ^{12}B in its ground or low excited state.

The angular distribution (Fig. 36) is very similar to the one obtained previously by

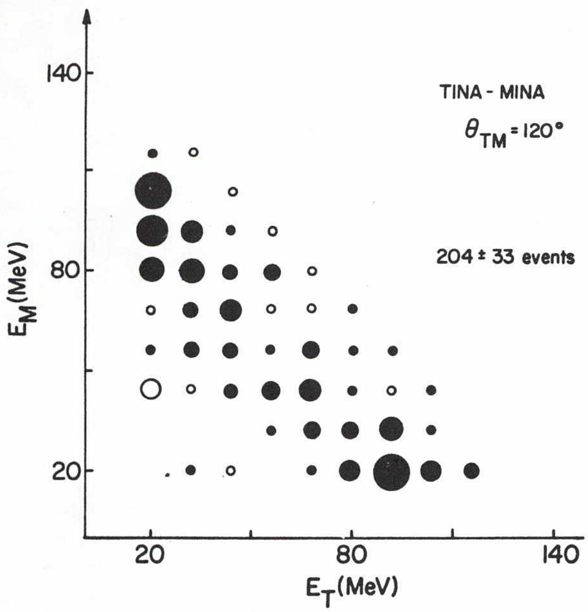

Fig. 34. Energy-sharing between the two photons $(\theta_{TM} = 120°)$.

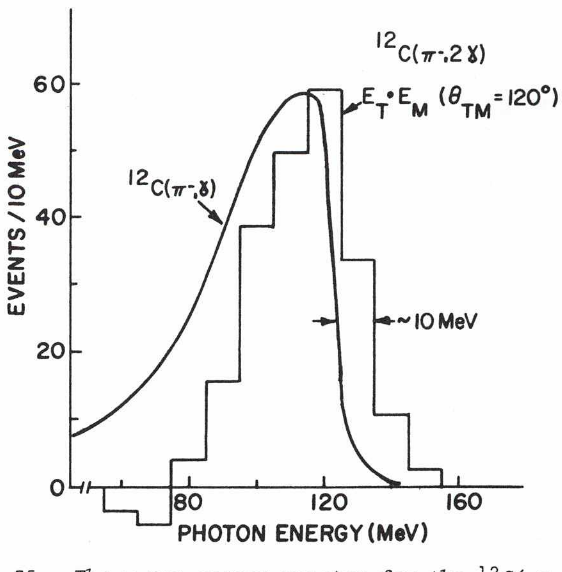

Fig. 35. The γ-ray energy spectra for the $^{12}C(\pi^-,\gamma)$ *and* $^{12}C(\pi^-,2\gamma)$ *reactions. The solid line is the normalized radiative photon energy spectrum as measured with the NaI crystals.*

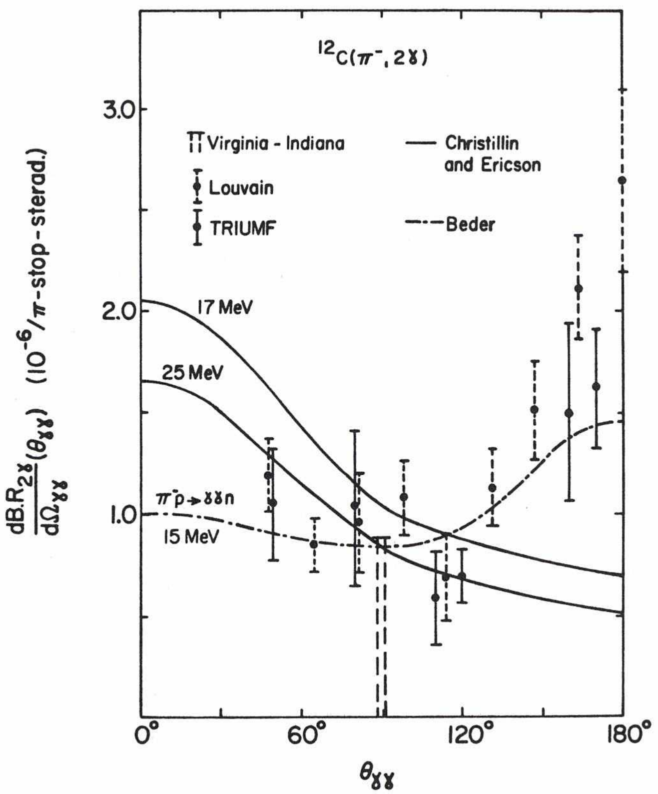

Fig. 36. Angular distribution of the 2γ events. The experimental results of Deutsch et al. and the upper limit obtained by Roberson et al. are compared to our observed angular distribution. The solid lines are the calculations of Christillin and Ericson for cut-offs of 17 and 25 MeV. The dash-dotted line is the calculation made by Beder (15 MeV cut-off) for the nucleonic process.

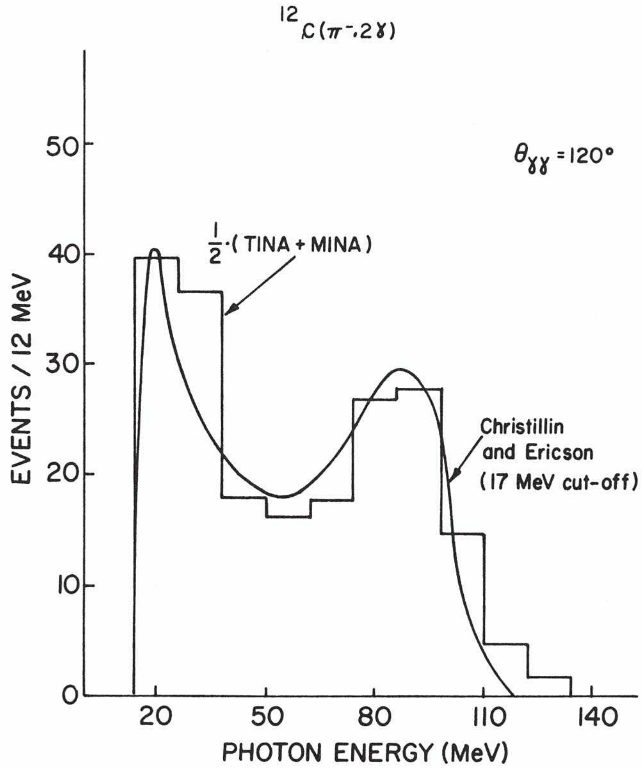

Fig. 37. Photon energy distribution at $\theta_{\gamma\gamma}$ = 120°. The solid curve is the normalized energy distribution calculated by Christillin and Ericson assuming a 17 MeV cut-off. The histogram is the average γ-ray energy spectrum of TINA and MINA.

the Louvain group at CERN [Deutsch *et al.*, Phys. Lett. 79B, 347 (1979)], but the integrated total branching ratios are not in agreement if one takes into account the different energy thresholds used. The rise at large opening angle is probably due to a small hydrogen contamination in the ^{12}C target.

Following the pioneering work of Ericson and Wilkin, both experiment and theory have made good progress in recent years. Work performed by Beder [Nucl. Phys. B156, 482 (1979) and contributed paper to EICOHEPANS] and by Christillin and Ericson [CERN preprint TH2694 (1969) and contributed paper to EICOHEPANS] has shown the importance of the π-capture schedule in the process. It is now clear that bremsstrahlung diagrams dominate when pions are captured from a P state (90% probability in ^{12}C) and will not allow a direct investigation of the pionic field as originally intended. The branching ratio predicted is within 30% of our experimental result. The shape of the photon energy distribution calculated by Christillin and Ericson agrees well with our experimental distribution (Fig. 37).

Except for the rise at large opening angle, angular distributions are also qualitatively reproduced by recent calculations.

Experiment 121
Test of charge symmetry in n-p scattering

During the summer a test measurement was made of the p-p analysing power and cross-over. This test was undertaken to provide some firm evidence that a precision comparable to the desired n-p experiment could be obtained, and to yield quantitative estimates of potential background. A polarized proton beam was incident on scattering targets of differing composition: 1) 73 mg/cm^2 CH_2/484 mg/cm^2 C dummy, 2) 1.92 g/cm^2 CH_2/ 2.00 g/cm^2 C dummy, and 3) thin vertical nylon wire for calibration purposes. Protons were detected in coincidence in symmetric multiwire proportional chamber (MWPC) counter telescopes having central lab angles of 41.65°. The MWPCs allowed track reconstruction to be performed. The NaI detectors employed were sufficiently thick to stop p-p elastic protons which entered them. Detected events were of three types:

1) Both tracks reconstructed; energy information unused or unavailable; time-of-flig information available.

2) Both tracks reconstructed; one proton energy determined in the NaI detectors; TOF information available.

3) Both tracks reconstructed; both proton energies determined; TOF measured.

In the test run approximately 2×10^6 good p-p elastic scattering events of type 1) were obtained for each of the thick and thin CH_2 targets. An appropriate number of events were also obtained for each of the dummy targets.

At present the data tapes have not been fully analysed and only preliminary results obtained on line for a subset of the data (25%) are available. However, they yield useful information on 1) the effectiveness of angular kinematic correlations in eliminating background, 2) the energy distribution of background events, 3) the fraction of C(p,2p) background remaining after cuts, 4) the magnitude of the background asymmetry, and 5) the ability to determine the crossover point from statistical fitting. Results are summarized in Table VII.

Experiment 132
Measurement of the pp → dπ cross section

Experiment 132 was allocated ten 12 h shifts of beam time in 1979 to demonstrate the feasibility of doing the experiment put forth in the proposal. Of this allocated time the group received seven shifts.

The feasibility study was carried out in two 5-shift runs, March 13-16 and May 2-5. The equipment used was that provided by the University of Alberta experimental effort at 4BT1, consisting of rotatable arms holding multiwire proportional chambers (for the trajectory definition) followed by thin

Table VII. Results from a simulation of the n-p charge symmetry experiment, employing p-p scattering in CH_2.

Parameter	p-p experiment at 500 MeV	n-p experiment
Quasi-elastic scattering background	<< 1%	Probably < 1%
Background asymmetry	Small and similar to free p-p	Probably as favourable as the p-p case
Effect of background on crossover	$\Delta\theta_0 \leqslant 0.005°$ pessimistically	Probably similar to the p-p case
Crossover determination for 5-run sample	$\theta_0 = 41.64° \pm 0.09°$ $\chi^2 = 85.74$ for 79 d.f. $dP(\theta)/d\theta_{lab} = -0.024$	

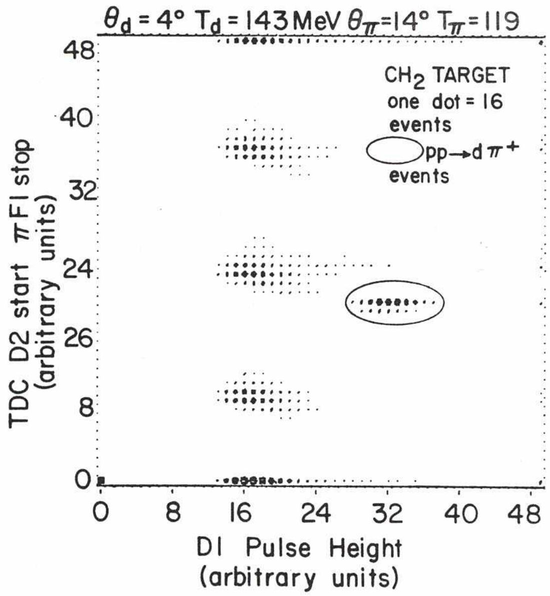

Fig. 38. Elastic pp → dπ⁺ events are uniquely identified in this correlation plot of time of flight vs. pulse height recorded at 400 MeV.

scintillation counters. Both particles in the final state, the π^+ and the deuteron, were detected in coincidence, one in each of the movable arms. A 100 mg/cm^2 CH_2 sheet provided the target protons.

The run was very successful, with the $pp \rightarrow d\pi^+$ signature standing out clearly from background even with deuterons detected as close as 3° to the incident proton beam. A typical example of how clearly the event signal was tagged is shown on the scatter plot in Fig. 38. The plot shows the pulse height of a deuteron scintillation detector D1 versus the timing difference between counters D2 and πF1 of the two detection arms. The signal, $pp \rightarrow d\pi^+$, is clearly separated from the background which consists of random triggers by scattered protons.

On presentation of the results of the feasibility study before the Experiments Evaluation Committee, permission to proceed with the complete Expt. 132 proposal was granted. A new vacuum scattering chamber will be constructed in order to allow detection of the π and deuteron over a large kinematical angular range. The restrictions of this range, imposed by the existing chamber available at TRIUMF, make it inadequate for anything more than a feasibility study.

Experiment 1
Low-energy π-nuclear scattering

During 1979 the results of 29 MeV π^- elastic scattering from ^{208}Pb were published [Johnson *et al.*, Can. J. Phys. 57, 775 (1979)]. Figure 39 shows the experimental results presented in that publication.

Also published in 1979 were the results for the neutron radii of ^{13}C and ^{18}O as measured with π^- elastic scattering [Johnson *et al.*, Phys. Rev. Lett. 43, 844 (1979)]. The fact that the ratio of the scattering amplitude for π^- on neutrons to that for protons is ~3/1 at low pion energies (≤50 MeV), coupled with the long mean free path of low-energy pions in nuclear matter, makes the negative pion an excellent probe of neutron matter. This property has been employed to determine neutron radii of nuclei, a parameter that has long been the focus of theoretical and experimental study. The neutron radii of ^{13}C and ^{18}O were determined relative to those of ^{12}C and ^{16}O, respectively, by measuring the ratio of the π^- elastic differential scattering cross sections on neighbouring isotopes. A fit to the ratios was made using various optical model codes. In the calculations the neutron and proton radii of the N=Z isotope were set equal to the proton radius of that nucleus as determined from electron scattering. Similarly the proton radius of the N>Z isotope was set equal to the value from electron scattering. The neutron radius of the neutron-rich isotope was treated as a parameter in order to minimize a χ^2 formed from the calculated and measured cross-section ratios. The results appear to be model independent. Figures 40, 41 and 42 show the results for $\sigma(^{13}C)/\sigma(^{12}C)$ and $\sigma(^{18}O)/\sigma(^{16}O)$ at 30 MeV and $\sigma(^{13}C)/\sigma(^{12}C)$ at 50 MeV, respectively. Figure 43 shows χ^2 contours for the 30 MeV $\sigma(^{18}O)/\sigma(^{16}O)$ data as a function of r_n and r_p for ^{13}C. These data are very sensitive to the values of r_n used but insensitive to the value of r_p. Our resulting neutron radii are

$$\langle r_n^2 \rangle^{1/2}_{^{13}C} = 2.35 \pm 0.03 \text{ fm} ,$$

$$\langle r_n^2 \rangle^{1/2}_{^{18}O} = 2.81 \pm 0.03 \text{ fm} .$$

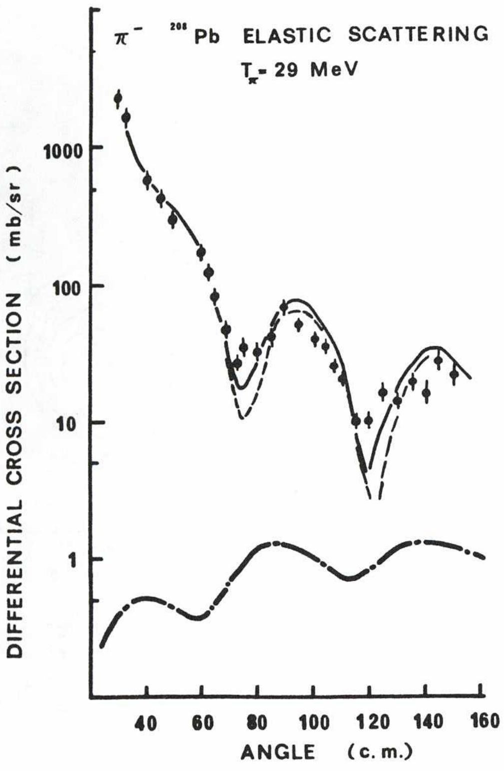

Fig. 39: Angular distribution for π^- elastic scattering from ^{208}Pb. The curves are optical model calculations for elastic and inelastic scattering.

To further demonstrate that the ratio of π^- elastic differential scattering cross sections is in fact a measure of the radii of neutron distributions in nuclei, the ratio for π^+ scattering from ^{11}B and ^{12}C at 40 and 50 MeV has been measured. The resulting data are shown in Figs. 44 and 45, respectively. Employing the same fitting procedure as used for the π^- ratios, but in this case allowing the proton radius of ^{11}B to vary, a preliminary value for the radius of ^{11}B was determined. This preliminary value is

$$\langle r_p^2 \rangle^{1/2}_{^{11}B} = 2.37 \pm 0.04 \text{ fm} .$$

Further studies of the model dependence of this result are presently under way.

In collaboration with the Tel-Aviv group the absorption cross sections for $\pi^\pm$ at 50 MeV as a function of nuclear mass number A were measured. Experimentally $\sigma_{(total)}$ was measured using a transmission technique and the $\sigma_{(elastic\ and\ inelastic)}$ angular distribution. Using the fact that $\sigma_{(charge\ exchange)}$ is a small correction

$$\sigma_{(abs)} + \sigma_{(xch)} = \sigma_{(total)} - \sigma_{(el+inel)} .$$

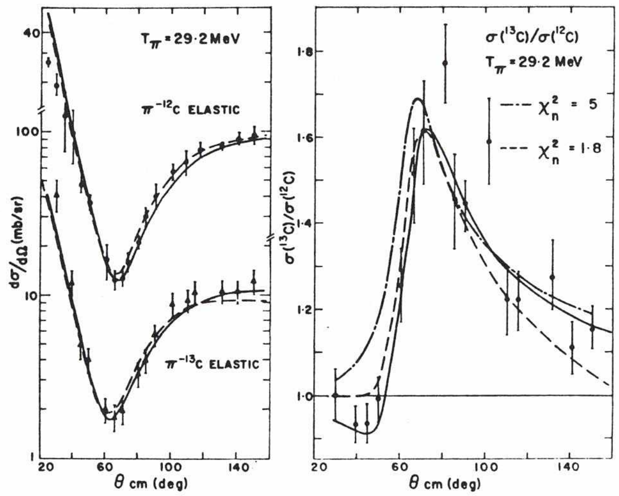

Fig. 40. Angular distributions for the elastic scattering of π^- from ^{12}C and ^{13}C (on the left) at 29.2 MeV. The ratio of the ^{13}C to the ^{12}C cross sections are shown on the right. The curves are the best-fit calculations with the DRRS code (solid line) and SMC code (dashed line). The dot-dashed curve is for SMC with $r_n(^{13}C) = r_p(^{12}C)$.

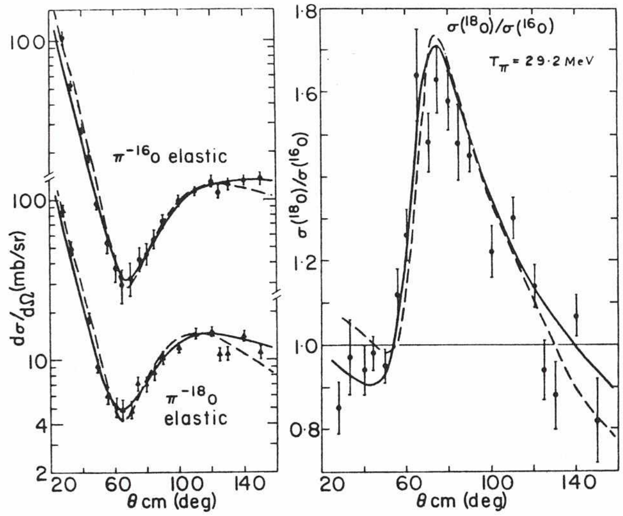

Fig. 41. Angular distributions and ratio for the elastic scattering of π^- from ^{16}O and ^{18}O at 29.2 MeV. The curves are as described in Fig. 40.

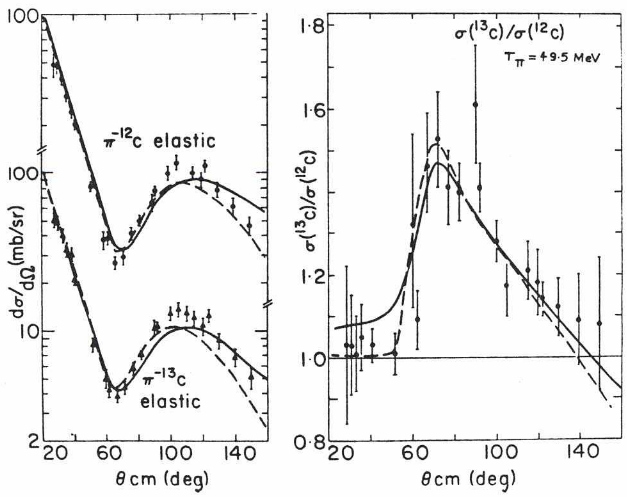

Fig. 42. Angular distributions and ratio for $^{12,13}C$ at 49.5 MeV. The curves are as described in Fig. 40.

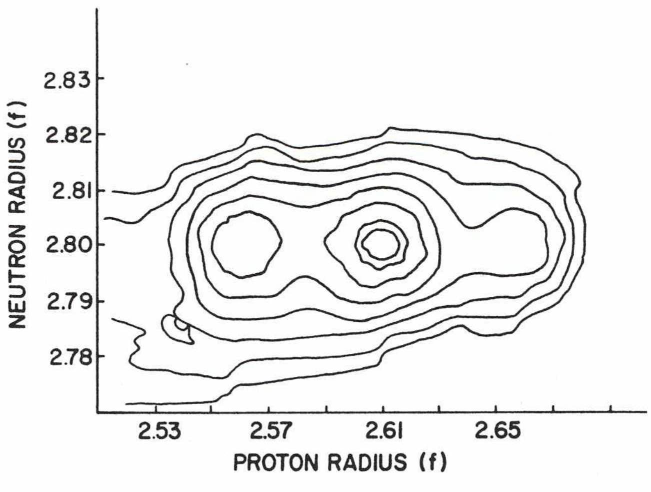

Fig. 43. χ^2 contours from fits to 29.2 MeV π^- on $^{18}O/^{16}O$ cross section ratios. Note the relative insensitivity to the value chosen for the proton radius (in fermi) compared to the sensitivity to the neutron radius.

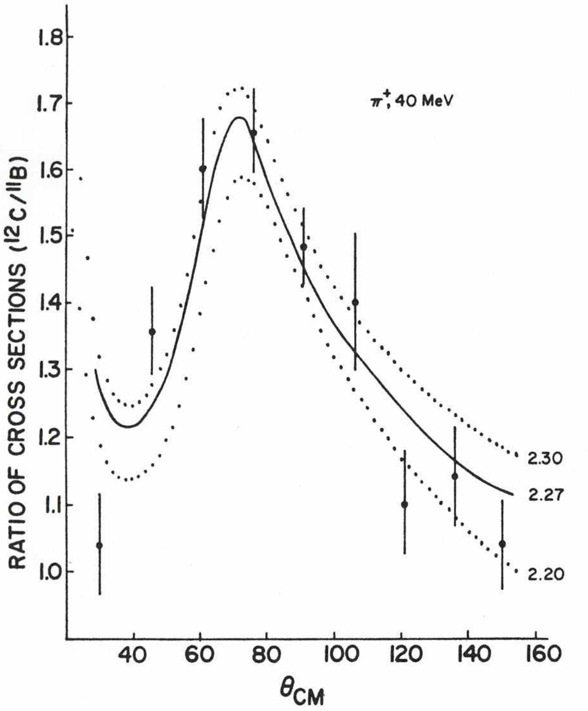

Fig. 44. Ratio of cross sections for 40 MeV π^+ elastic scattering from ^{12}C and ^{11}B. The curves which are optical model calculations show the sensitivity to the proton radius of ^{11}B.

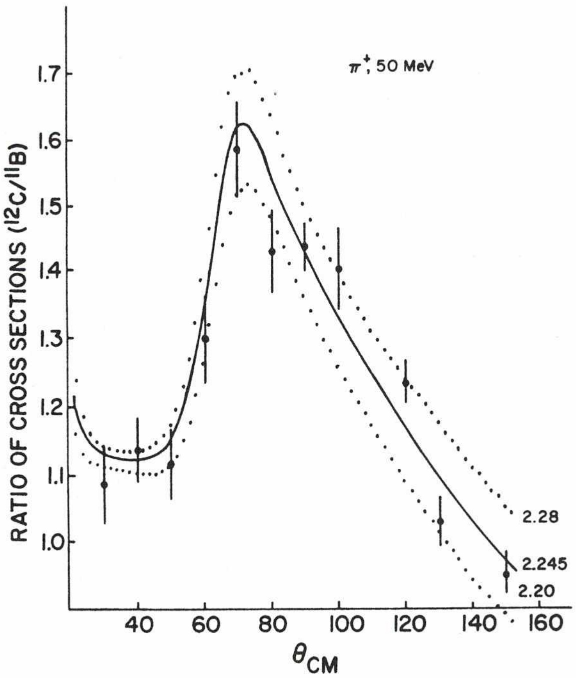

Fig. 45. Same as Fig. 44 for 50 MeV π^+.

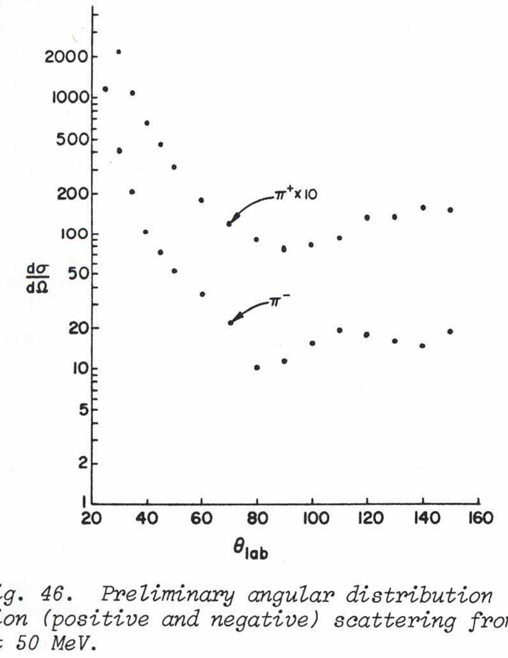

Fig. 46. Preliminary angular distribution for pion (positive and negative) scattering from Fe at 50 MeV.

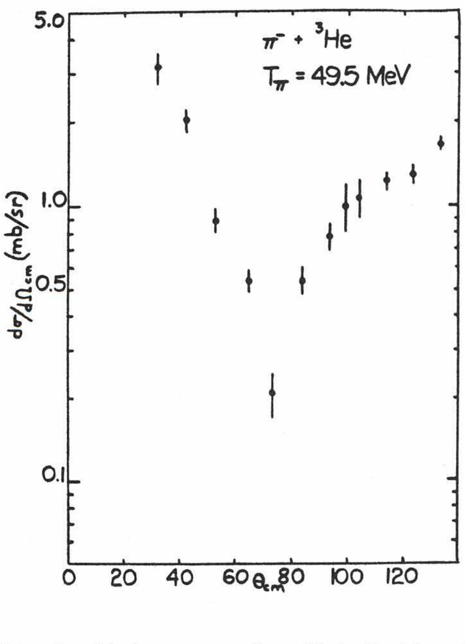

Fig. 47. Preliminary angular distribution for π^- elastically scattered from ^3He.

Figure 46 shows $\sigma_{(el+inel)}$ for Fe.

Pion scattering from the helium isotopes has long been a testing ground for our understanding of the pion-nucleus interaction and has offered a major challenge to theoreticians to calculate observed cross sections from 'fundamental' pion-nucleon amplitudes. Low-energy π^--^{3}He measurements are particularly interesting because the π^- interacts strongly with the single neutron, and several theoretical investigations have been undertaken recently [see for example Gibson in *Meson-Nuclear Physics—1976* (AIP, New York, 1976), p.418]. Elastic scattering of negative pions from a liquid ^{3}He target has been measured [Vincent and Smith, Nucl. Instrum. Methods 116, 551 (1974)]. Both target-in and target-out measurements were made. Scattering pions were detected in two range telescopes described previously [Johnson *et al.*, Can. J. Phys. 57, 775 (1979)]. The preliminary measured angular distribution is shown in Fig. 47. The errors are statistical only. Several 90° and 100° runs had to be excluded because the target casing obstructed the pion path from target to detector. A power failure caused the experiment to be foreshortened, so that several tests still have to be completed. Another run is planned which should have a smaller beam spot on target, thinner windows and more accurate absolute flux measurements. It may also be possible to employ a magnetic spectrometer.

Experiments 3, 117, 142
Studies of fragments emitted from proton interactions with complex nuclei

The ΔE,E data of the general survey portion of Expt. 3 was consolidated into a concise final form [Green and Korteling, submitted to Phys. Rev. C] describing the experimental results and some of the conclusions from the data (summarized in last year's Annual Report). A second article, describing the analysis of the evaporative component in the measured spectra, was also completed during the year.

Analysis of the non-evaporative components of the spectra in terms of a direct knockout model was attempted, with encouraging results [Boal and Woloshyn, Phys. Rev. C 20, 1878 (1979)]. Additional data on ^{9}Be(p,α)X and ^{27}Aℓ(p,α)X reactions were collected and analysed during the year to provide supplemental input for this direct knockout analysis. In turn, results from the calculations were used to aid in planning the initial phases of the coincidence measurements of Expt. 142. In this experiment an emitted high-energy proton, assumed to be the scattered incident proton, will be measured in coincidence with emitted light fragments to test the various proposed models for the description of the non-evaporative component.

The remainder of the data for the detailed time-of-flight portion of Expt. 3 was taken during 1979. The reduction of this data to final form is proceeding and includes corrections for multiple scattering by comparison of TOF data summed over isotopes of a given element to thin target ΔE,E elementally resolved data unaffected by multiple scattering. The previous analysis of evaporation components in the spectra is being extended to this data and should result in a better understanding of the nature of the equilibrated systems formed after energetic reactions. While it is clear that this detailed data also add considerably to the experimental description of the non-evaporative components, it is not yet clear what form the analysis of such components should take for these heavier fragments. This problem is under active consideration.

The remainder of the activity during 1979 centred on detailing systems and new equipment to be used in Expts. 117, the measurement of light fragment spectra to kinematic limits, and 142, the measurement of protons coincident with light fragments. Most of the required HP Ge detector system has been designed and relevant components ordered. The detectors for the NaI proton telescope have been ordered on the basis of a complete conceptual design of the system. Detailed design of the system has been postponed until the detectors have been obtained and their compatibility with the rest of the system can be ensured.

Experiment 6
Intermediate-energy fission

Analysis of data taken in 1978 continued this year, both at the Weizmann Institute (via codes to extract the intensities of particles evaporated pre- and post-fission from angular distributions) and at Vancouver (on the energy spectra of evaporated particles measured at various angles to the fission axis). Figure 48 shows evaporated helium-4

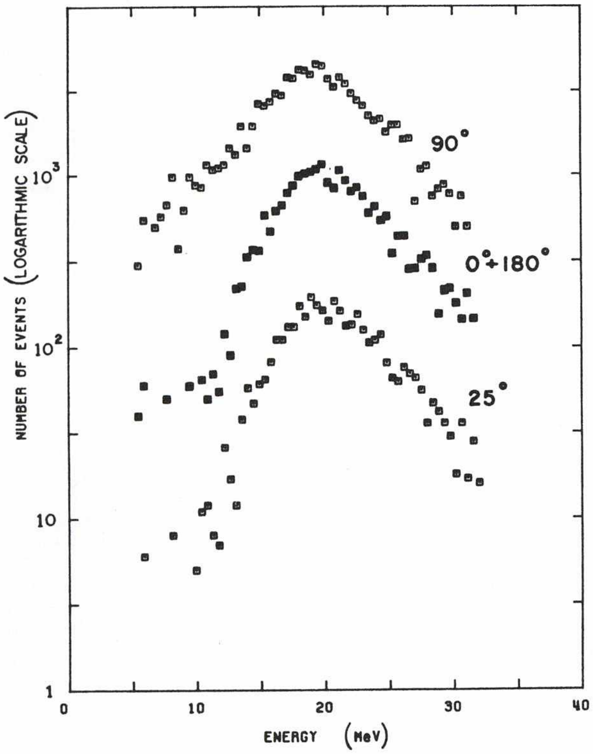

Fig. 48. ⁴*He spectrum from U + 480 MeV protons, measured at various angles to the fission axis. (Zero on the ordinate displaced to display spectra.)*

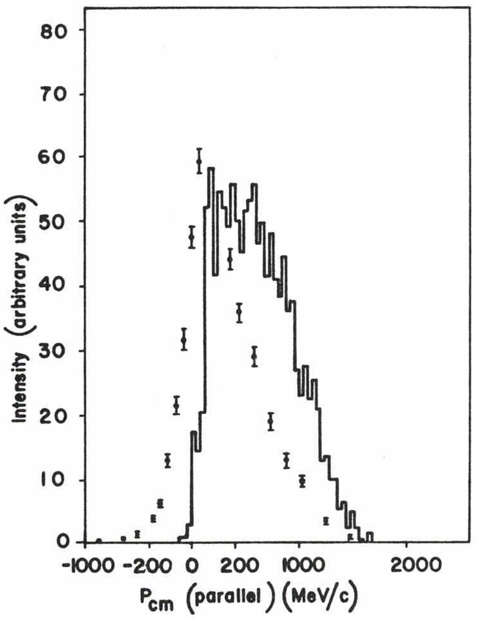

Fig. 49. Centre-of-mass momentum distribution for fission in the system U + 480 MeV protons, deduced from fragment energies and the fragment-fragment angular correlation (points) compared with calculations via the ISOBAR code (histogram).

spectra for a uranium target measured at 25°, 90° and 0° plus 180° to the axis. The absence of spectrum shifts, expected from Doppler or Coulomb barrier effects for particles emitted after fission, is further evidence for fission occurring predominantly after evaporation. A paper has been prepared for publication.

Data on the energy and angular distribution of single and coincident fission fragments from the proton- and pion-induced fission of U, Th, Bi, Au and Ag have been reduced to extract data on angular, mass and energy distributions of the fragments and centre-of-mass momenta. Figures 49 and 50 show some of the results; a Ph.D thesis at Simon Fraser University is advanced in preparation.

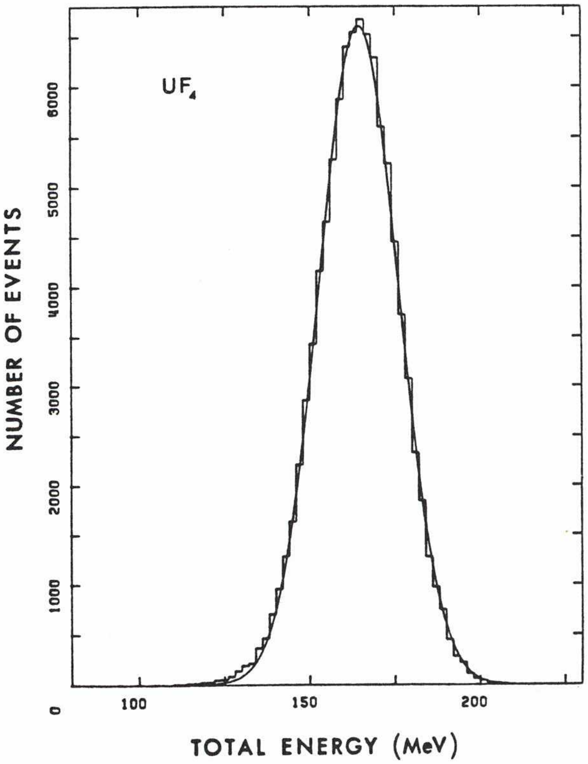

Fig. 50. Measurement via Si(Li) detectors of the total fission fragment kinetic energy from the system U + 480 MeV protons.

Experiment 10
Pion production by proton bombardment of hydrogen and other light nuclei

In 1979 the experimental set-up on beam line 1B was assembled and commissioned. One or two improvements to the target chamber have to be made, but essentially the system is ready to take data.

The spectrometer (a 65 cm Browne-Buechner spectrograph renamed the Captain Cook Bicentennial spectrometer 'Resolution') for analysing pion reaction product momentum uses a simple 3-counter trigger for event definition and 3 helically wound proportional chambers to define the pion trajectory. The spatial resolution of the chambers is better than 1 mm, and the overall energy resolution of the spectrometer should be better than 300 keV. The laboratory angular range of Resolution is from 40° to 140°, and the acceptance is 3 msr.

The present target arrangement is an evacuated container with a simple Geneva wheel-changing mechanism. A more precise target ladder will be installed early in 1980 that will allow a wire beam profile monitor to be inserted at the target location. To fully exploit the improved resolution a beam spot with a vertical size ~1 mm is required; this monitor will help achieve that.

It has been confirmed that the beam line tune satisfies most of the experimental requirements up to a proton energy of 350 MeV. Power supply limitations on the final two dipoles in the line have not allowed operation above 350 MeV. A PDP 11/34 computer is being used in conjunction with the MULTI data acquisition program. As a result we have a significantly more powerful diagnostic program at our disposal than the previous program which ran on a NOVA computer.

Some data have been taken during the commissioning effort: 1) The $D(p,\pi)T$ reaction was used to do line sweeps with the magnet to check the acceptance, dispersion and resolution of the spectrometer. 2) The $^{9}Be(p,\pi^{+})^{10}Be$ and $^{12}C(p,\pi^{+})^{13}C$ reactions have been studied at 250 MeV incident proton energy and at a limited number of angles to complete further resolution studies with the cyclotron tuned to give the best possible beam energy resolution and to begin measurements of the energy dependence of the analysing power in the $(\vec{p},\pi)$ reaction. Results of these runs were summarized at the Experiments Evaluation Committee meeting in November. Since the spectrometer is inherently capable of much better resolution than is achievable with the raw proton beam from the cyclotron, work has been initiated with the Beam Development group towards operation of the cyclotron in a 'single-turn' extraction mode to improve the beam energy resolution. The best resolution obtained to date is shown in Fig. 51, where we have just resolved the 3.09 MeV ^{13}C state from two ^{13}C states at 3.68 and 3.85 MeV.

Figure 52 summarizes the analysing (A_{π}) power measurements compiled during the commissioning phase. Many of these measurements are of a preliminary nature, as an insufficient number of events were collected to reduce the statistical errors to reasonable values. However, it is already clear there is a significant departure from the more or less universally negative value of A_{π} measured for the ^{9}Be and ^{12}C $(\vec{p},\pi)$ reactions at 250 MeV.

The group is looking forward to an exciting year of data-taking.

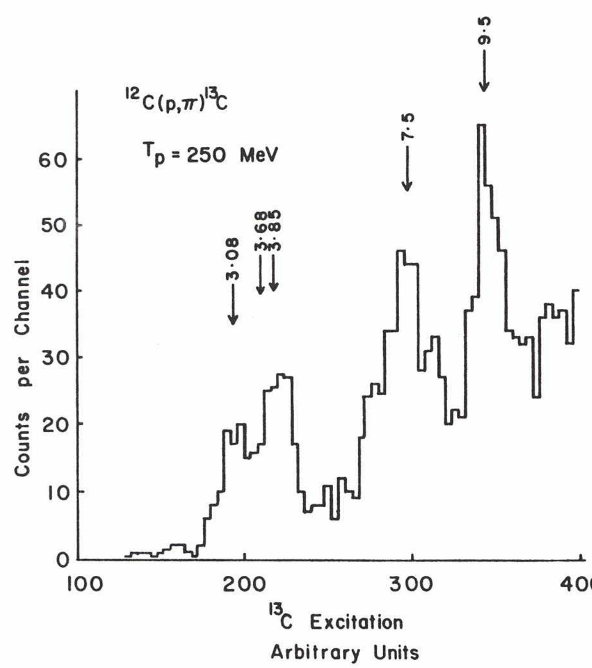

Fig. 51. Energy spectrum of pions in the $^{12}C(p,\pi^{+})^{13}C$ reaction at θ = 65°. Transition to the ^{13}C ground state is suppressed. Cyclotron extracting a 'separated turn' beam.

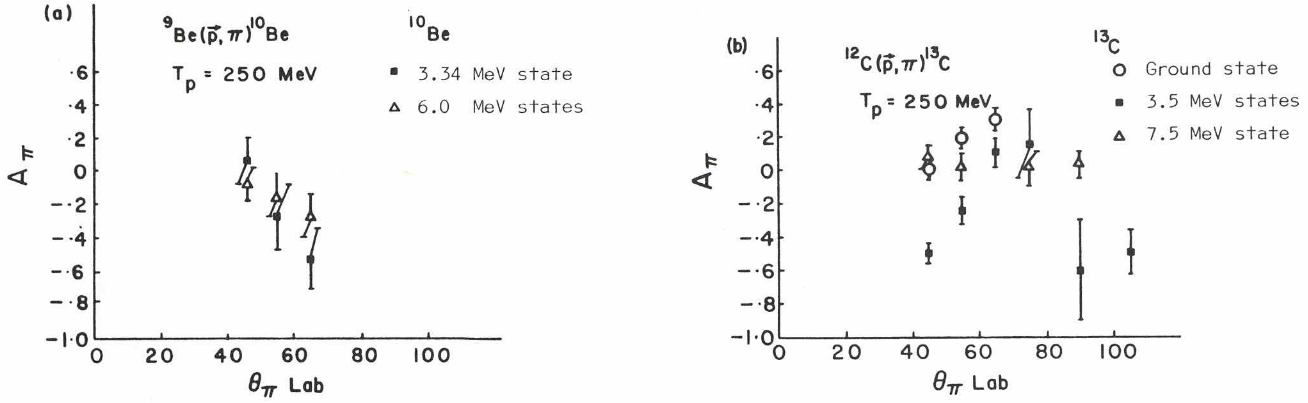

Fig. 52. Analysing power for the $(\vec{p},\pi)$ reaction versus pion laboratory angle. (a) Transitions to ^{10}Be: 3.34 MeV state and two unresolved states at 6.0 MeV. (b) Transitions to ^{13}C: ground state, three unresolved states at approximately 3.5 MeV and the 7.5 MeV state.

Experiment 14
Proton-^{4}He elastic scattering at intermediate energies

Proton-nucleus scattering at intermediate energies has received considerable attention with the advent of accelerators capable of producing high-intensity, variable-energy polarized beams having good energy resolution. Extensive data for differential cross sections and analysing powers have been obtained, which should provide a stimulus to the search for a successful microscopic description of the processes involved.

The elastic scattering of protons from ^{4}He is an unusually good case to investigate thoroughly for several reasons: the initial and final states are well defined theoretically; the target nucleus has spin zero, minimizing the complications that arise in some spin-dependent calculations; and inelastic processes are easily distinguishable, which reduces experimental demands on energy resolution.

It has become apparent that analysing power (polarization) angular distributions are very important in the evaluation of the validity of theoretical models. In the energy range of the present experiment, 200 to 500 MeV, the analysing power exhibits a rich and variable structure. Although a proper description of the differential cross section has established the need for spin-dependent terms, far more stringent demands are established when analysing power data are to be explained as well.

The present experiment represents the last phase of a three-part study of p-^{4}He elastic scattering at TRIUMF. The first part [Stetz *et al.*, Nucl. Phys. A290, 285 (1977)] examined $d\sigma(\theta)/d\Omega$ and $A_y(\theta)$ in the small angle region (4°-16° in the laboratory). This measurement was made with a gas target having a well-defined density and thickness. The cross-section results of this first phase have been used as a normalization benchmark for the remaining two parts of the study.

The second part of the investigation [McCamis *et al.*, Nucl. Phys. A302, 388 (1978)] involved measurement of $d\sigma(\theta)/d\Omega$ and $A_y(\theta)$ at backward angles (144°-168° in the laboratory) for several incident proton energies between 185 and 500 MeV. One of the goals of the experiment was a careful search for energy-dependent backward peaking of the differential cross section. The analysing power measurements made at the same time were intended to aid in a more complete understanding of the reaction process.

In the present experiment we have completed the cross section and analysing power angular distributions at 200, 350 and 500 MeV with measurements in the intermediate-angle region. At these three energies, data sets spanning the laboratory angle range from 4° to 168° are now available.

The results of the experiments are summarized in Figs. 53 and 54 showing $d\sigma(t)/dt$ and $A_y(\theta_{c.m.})$. Further work measuring the spin rotation parameter R in p-^{4}He elastic scattering is under way (Expt. 152).

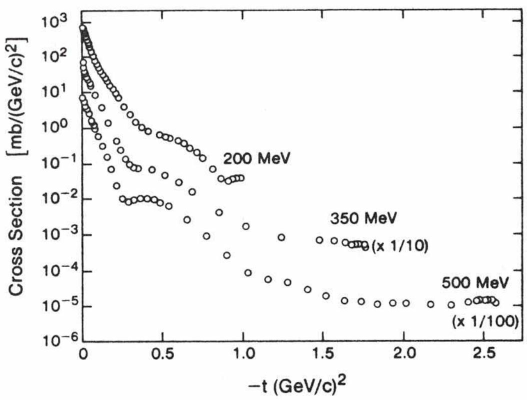

Fig. 53. The differential cross section at 200, 350 and 500 MeV as a function of the four-momentum transfer -t. The data from Stetz et al. and McCamis et al. are included here. The normalization uncertainty is about 5% at all energies.

Experiment 41a
Radiative capture of pions in deuterium

This experiment intends to measure the ratio:

$$S = \frac{w(\pi^- d \rightarrow nn)}{w(\pi^- d \rightarrow \gamma nn)} .$$

The two conflicting values (3.16 ± 0.12 and 2.89 ± 0.09) previously obtained disagree and have large errors.

We have remeasured S by using a high pressure target and the large NaI crystal TINA to observe the gamma rays.

The gas target consists of two scintillators (CsI and NE102) in the flask viewed by one photomultiplier. The signals of both scintillators are recognized by their light decay time, thereby defining the entry and exit of the pions. In this way it is possible to identify pions stopping in the gas. The maximum operating pressure of the target is 100 atm.

The value of S can then be obtained either by comparing runs of hydrogen and deuterium under equal conditions (the fraction of gammas per stopped pion is accurately known in hydrogen), or by counting the absolute number of pions stopped in deuterium. Both methods have been used and the data are presently being analysed. We hope to obtain a value of S with a relative error of better than 2%.

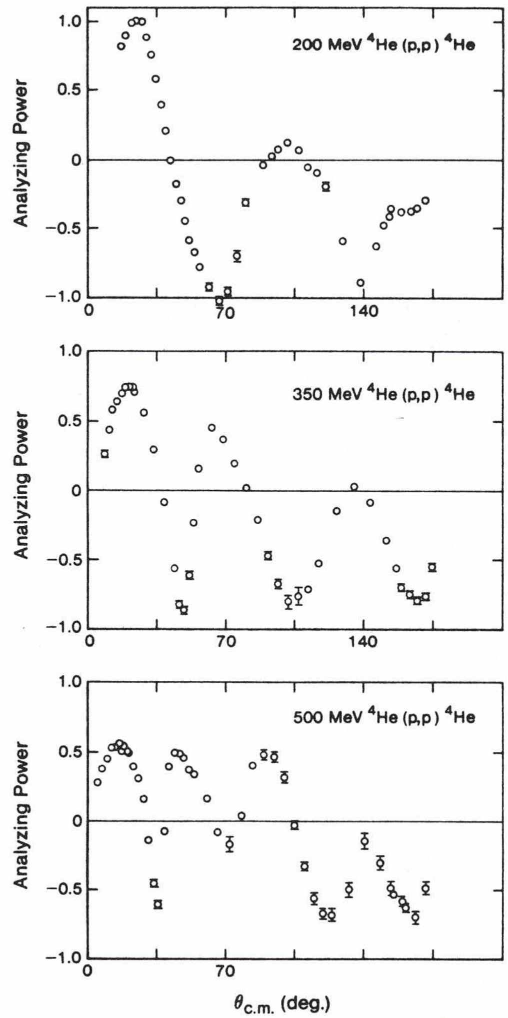

Fig. 54. The p-^{4}He analysing power as a function of $\theta_{c.m.}$ at 200, 350 and 500 MeV. The scale uncertainty is about 1-1.5% at all energies.

Experiment 59
Investigation of the (p,2p) reaction on ^{4}He

The ^{4}He(p,2p)^{3}H reaction was studied in a coplanar symmetric geometry at 200, 350 and 500 MeV. At all three energies measurements were made of the energy-sharing spectrum at the quasifree equal angles (~41°-41°). Measurements of the symmetric angular distributions were made at 350 and 500 MeV. The angular distributions were mapped out for recoil directions parallel and antiparallel to the incident proton momentum. The data resolve the discrepancy between the zero-recoil cross sections at 460 MeV and at 590 MeV in favour of the 590 MeV SREL result [Frascaria *et al.*, Phys. Rev. C 12, 243 (1975); Perdrisat *et al.*, Phys. Rev. 187, 1201 (1969); and Tyren *et al.*, Nucl. Phys. 79, 321 (1966)]. The 500 MeV symmetric angular distribution extends to recoil momenta in the 500 MeV/c range, which is appreciably further into the tail of the momentum distribution than in previous $^4He(p,2p)^3H$ experiments (Fig. 55). The angular distribution data confirm the excess of high-momentum components as compared to distorted wave impulse approximation (DWIA) calculations already indicated by the 590 MeV SREL results. A detailed account for the results obtained has been submitted for publication [Epstein *et al.*, Phys. Rev. Lett., in press]. Further measurements of the symmetric angular distributions at 250 and 500 MeV using polarized protons have been made to test the factorization of the differential cross section in the DWIA. Data analysis is in progress. The DWIA calculations will be made using a code that includes a spin-orbit term in the distorting optical potentials for the ingoing and outgoing channels. In preparation for these calculations the existing $^3He(p,p)^3He$, $^3H(p,p)^3H$ and $^4He(p,p)^4He$ data above 100 MeV incident energy have been analysed using an optical model which includes exchange and relativistic corrections.

Experiment 86
Proton elastic scattering

This was the first experiment to measure an angular distribution on the medium resolution spectrometer (MRS), following installation of overhead shielding late in 1978. After two commissioning runs with unpolarized beam, data were taken with polarized beam in runs during May, October and

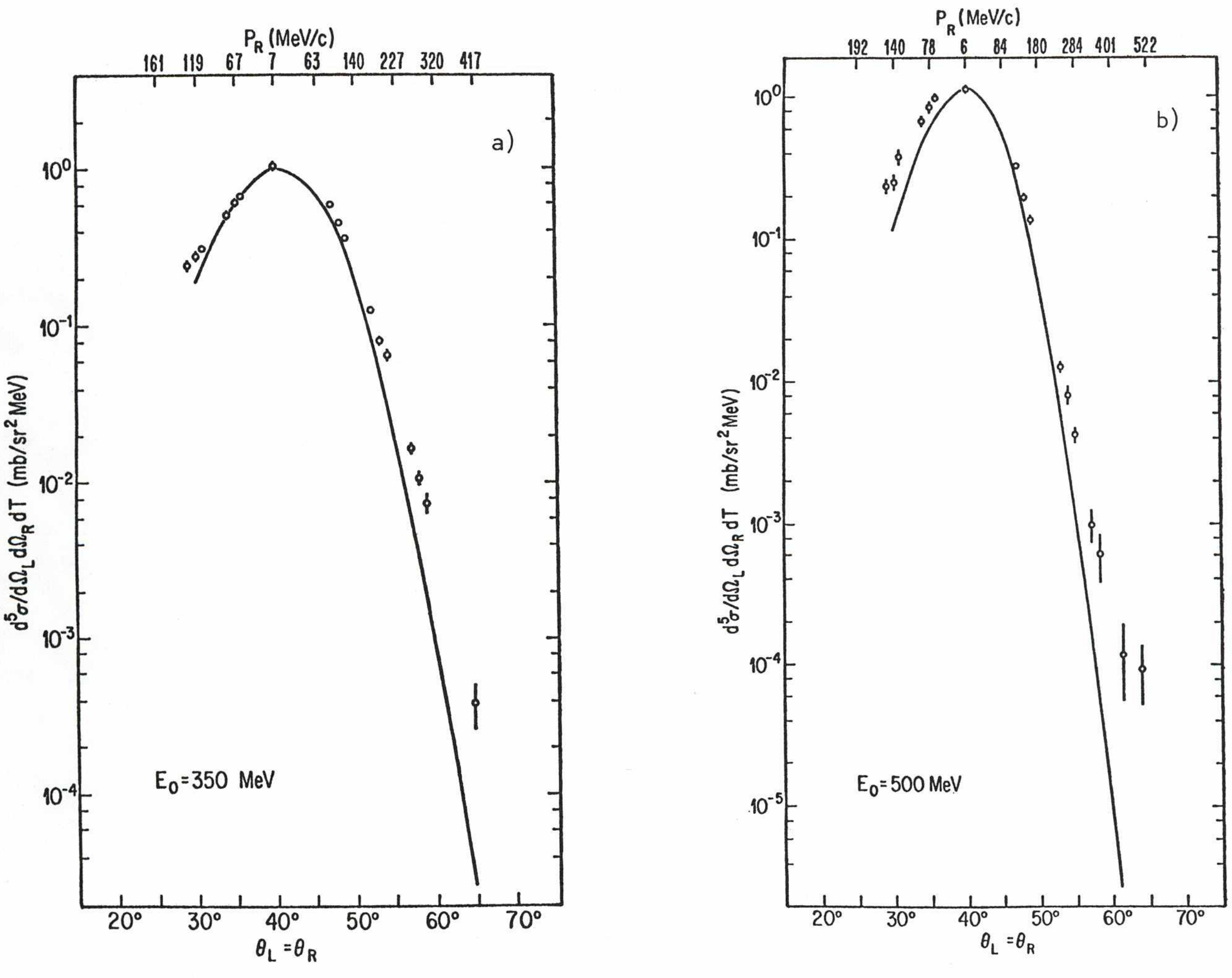

Fig. 55. $^4He(p,2p)^3H$ angular distributions.

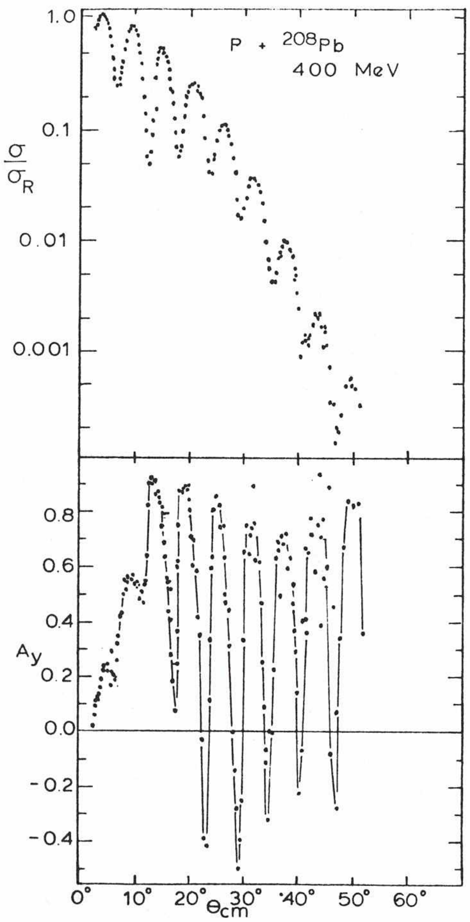

Fig. 56. Cross section and analysing powers for elastic p-Pb scattering.

December. Angular distributions of cross section and analysing power were measured for elastic scattering from Ca and ^{208}Pb targets at 200, 400 and 500 MeV from 3° to approximately 50°.

The data acquisition system was not sufficiently powerful to produce final results on line. Consequently, data were recorded on magnetic tape and replayed off line. Slightly more than half the data were reduced to final form by year's end.

^{208}Pb results at 400 MeV are shown in Fig. 56 where the cross sections have been normalized to the Rutherford cross section; cross sections change by almost eight orders of magnitude over the angular range 2.8° to 52°. The ^{208}Pb data have been fitted using an optical model (SNOOPY 6), and the optical potentials compared with results at lower and higher energies. Figure 57 shows volume integrals of the real and imaginary parts of the central term and of the spin-orbit term in the optical potential. It shows that the imaginary spin-orbit strength K_I^{SO} changes abruptly between 200 and 400 MeV, that the real central potential is still attractive at 400 MeV, and that the imaginary central term

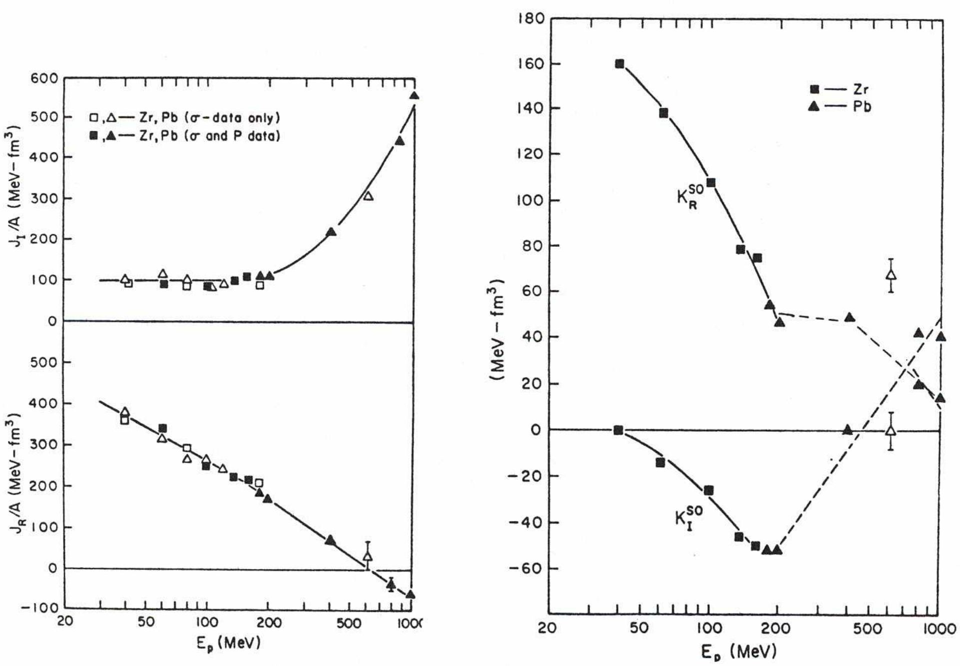

Fig. 57. Volume integrals of the real and imaginary parts of the optical potential.

doubles between 200 and 400 MeV, in keeping with change in mean free paths deduced from σ_R data.

Experiment 80
Measurement of pionic 2p-1s X-rays

Exotic atoms are formed when any negative particles, other than ordinary electrons, are captured into hydrogen-like orbits in the Coulomb field of the nucleus. Muonic atoms, together with elastic electron scattering, are used to investigate the nuclear charge distribution. Pionic atoms and pion elastic scattering provide a tool for studying the nuclear matter distribution. Much of the model dependence in determining nuclear matter distributions is removed by selecting isotope pairs. Our investigations have concentrated on light nuclei, where the shift in the energy of the 1s level depends mainly on the s-wave pion-nuclear interaction. The X-ray linewidth gives a direct measure of the absorptive part of the interaction.

During the past year we have taken pionic and muonic data on ^{12,13}C and ^{16,18}O. These isotopes were chosen to complement the TRIUMF low-energy pion scattering measurements (Expt. 54). Preliminary results were reported at the Vancouver meeting. Figure 58 shows pionic X-rays observed during these runs. Two shifts were used for an investigation of the backgrounds involved in measuring the very broad ^{24}Mg 2p-1s transition.

The sensitivity of our πB measurements to the nuclear matter distribution has been investigated in an attempt to estimate the model dependence of the procedure. Results have been encouraging, and a similar analysis of the ^{12,13}C and ^{16,18}O data is in progress.

An accurate measurement of the πNe strong interaction shift and width is of interest in connection with anomalous behaviour of the πNa width [Olin *et al.*, Nucl. Phys. A312, 361 (1978)]. A cryogenic Ne target has been prepared, and data-taking is scheduled for early 1980.

Experiment 89
μ^- capture in fissile nuclides

Our aim has been to study the interaction of muons with fissile nuclides. Muons were used as a probe to study the fission barrier, in particular the double humped fission barrier which produces shape isomeric states. The primary goals of the present experimental program are: 1) to measure the delayed fission yields in coincidence with μ^- uranium K_α X-rays and to determine the absolute fission yield (both prompt and delayed) per muon stop in ^{235}U and ^{238}U; 2) to measure the fission lifetime and to check for the presence of a short lifetime component in the time distributions of fissions in μ^- ^{235}U and μ^- ^{238}U; and 3) to attempt to identify the gamma rays from back decay of the isomeric state and to measure the decay time with respect to the muon stop time in $\sim$2 g/cm^2 targets of ^{235}U and ^{238}U.

In contrast to previous measurements, absolute fission yields following μ capture in ^{235}U and in ^{238}U calibrated multiplate fission chambers have been obtained using the μ^- uranium K_α X-ray to define unambiguously the stop of a μ^- in uranium. Data were collected on all fissions following a coincidence between a beam telescope stop signal and an X-ray as measured using a Ge(Li) detector. Off-line analysis was used to restrict the X-rays to μ^- uranium K_α on the basis of energy cuts. Following efficiency calibrations of the two chambers using thermal neutrons from the University of California Berkeley reactor, these measurements gave directly the absolute yield of fissions due to muon capture from the muonic K-shell.

Concurrently the time distributions of fission following a μ^- stop signal were obtained for both chambers. For ^{235}U the distribution is well fitted with a single mean life of 71.5 ± 0.9 nsec, whereas in our present ^{238}U time distribution there is clear evidence for a short-lived component corresponding to (8±2)% of the delayed fissions and having a mean life of 18 ± 5 nsec, in addition to the dominant mean lifetime of 76 ± 1.3 nsec. This short component was found to be independent of the fission pulse amplitude and was not seen in π^--induced fission spectrum. Although our observation [Ahmad *et al.*, Abstracts of contributed papers, EICOHEPANS, Vancouver, 1979, p. 129] of a short lifetime component is qualitatively consistent with that of Ganzorig *et al.* [Phys. Lett. 78B, 41 (1978)], the relative yield is somewhat higher: a further run is planned to clarify the ^{238}U time spectrum. The absolute yield appears to be much too large to be explained by fission isomer excitation. The measured

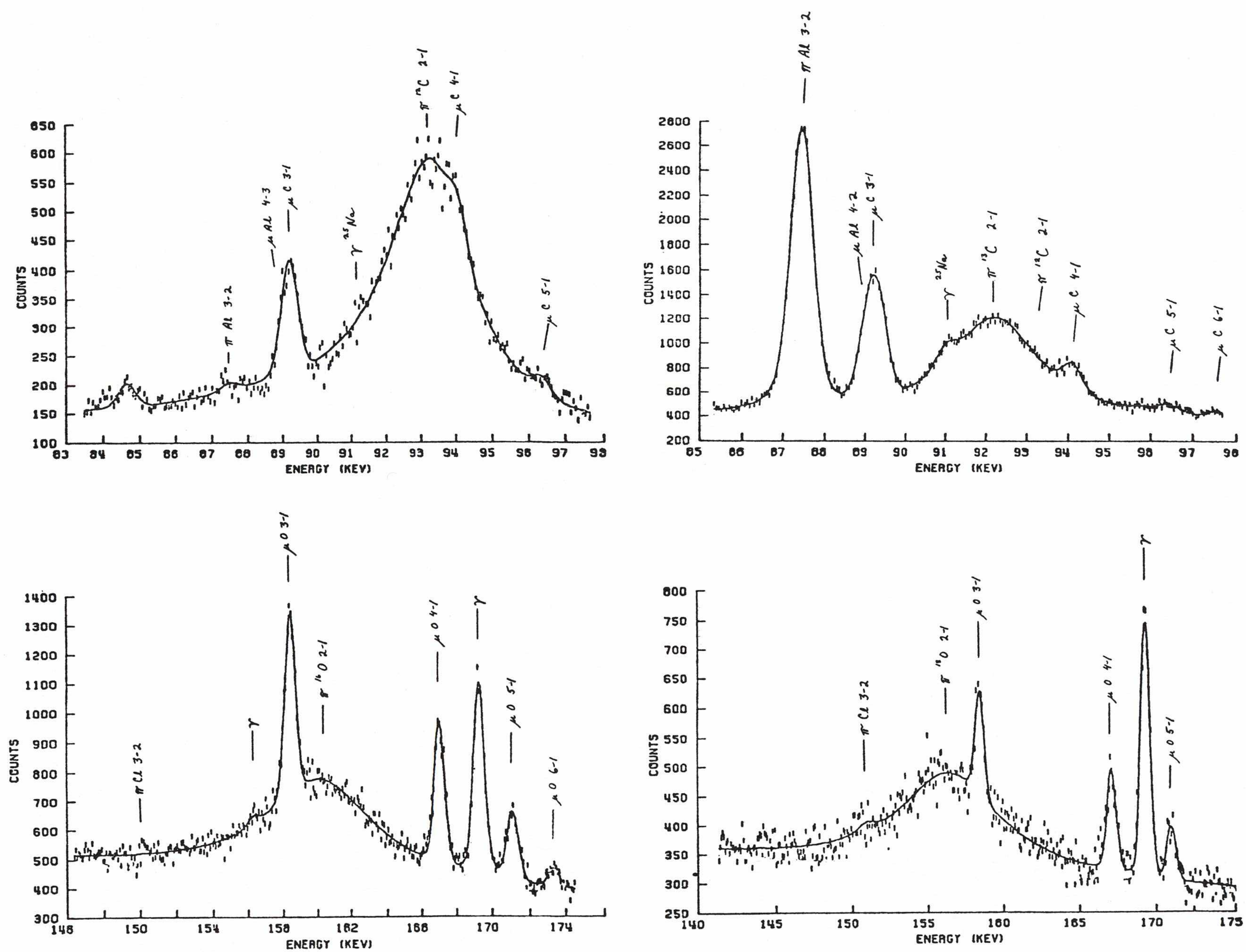

Fig. 58. Pionic X-ray spectra from carbon and oxygen isotopes.

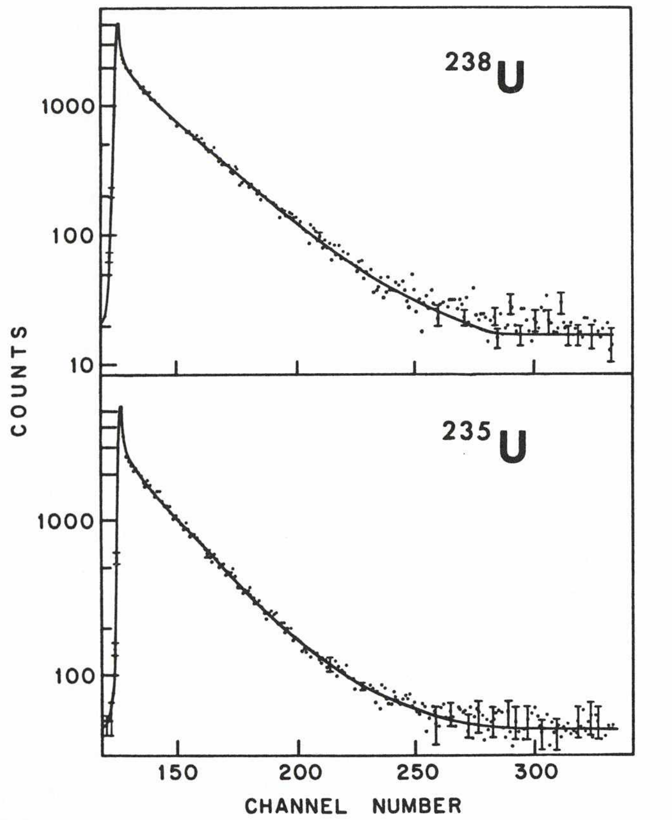

Fig. 59. Time distributions of fission events relative to time of muon stopping in ^{238}U and ^{235}U. The solid curve is the least squares fit to the data. (One channel corresponds to 2.926 nsec.)

prompt-to-delayed fission ratios for both the targets are shown in Table VIII; the fission time distributions from which they were deduced are shown in Fig. 59.

Recently both ^{235}U and ^{238}U X-ray data were obtained from approximately 2 g/cm^2 targets using the separator on the M9 channel to obtain a clean μ beam. These data will be analysed in a search for back decay gammas and to deduce the γ lifetimes.

Experiment 99
Studies of (p,d) reactions in nuclei

Experiment 99 completed its program of data acquisition in 1979 with an impressive body of usable data on the (p,d) reaction. All data were acquired using the TRIUMF medium resolution spectrometer. The use of polarized proton beams to measure analysing powers has proven to be particularly interesting and informative for this reaction.

Differential cross section and analysing power angular distributions were measured for the ground state and 4.4 MeV 2^+ state of the reaction $^{13}C(\vec{p},d)^{12}C$ at 200 MeV and 400 MeV incident proton energy over the angular range 4-47.5° (200 MeV) and 4-34° (400 MeV). Preliminary analyses and distorted wave Born approximation fits to the ^{13}C data were presented by several speakers at the EICOHEPANS and at the Los Alamos Future Options Workshop in August. The ^{13}C analysing power data appear to be sensitive to the spin-orbit term in the deuteron optical potential. Figure 60 shows preliminary fits to the 200 MeV data.

Angular cross section and analysing power measurements were made at 200 MeV on the

Table VIII. Present results.

	$\frac{\text{Fissions} \cdot K_\alpha \text{ X-ray}}{K_\alpha \text{ X-ray}}$	$\frac{\text{Prompt fissions}}{\text{Delayed fissions}}$	Mean life (nsec)	$\frac{\text{Total fissions}}{\mu^- \text{ stopping}}$
^{235}U	0.125 ± 0.023	0.138 ± 0.009	71.5 ± 0.9	0.142 ± 0.023
^{238}U	0.062 ± 0.013	0.089 ± 0.017	76.0 ± 1.3 (92 ± 2%)	0.068 ± 0.013[a]
			18 ± 5 (8 ± 2%)	0.074 0.013[b]

[a] Assumes both delayed components follow K X-ray emission.
[b] Assumes only longest lifetime component follows K X-ray emission.
The counting statistics in the K X-ray associated, fission-time spectrum were insufficient to distinguish between possibilities a) and b)

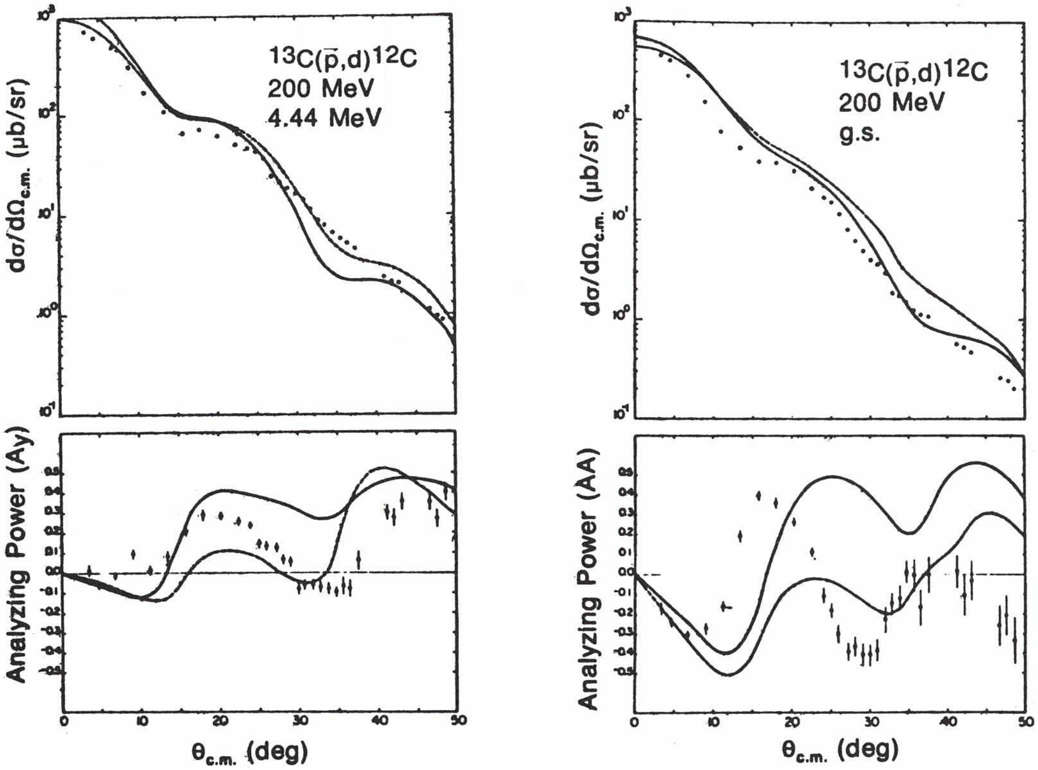

Fig. 60. The $^{13}C(\vec{p},d)^{12}C$ cross sections and analysing powers for T_p = 200 MeV measured at TRIUMF. Curves are EFR (——) and zero-range (ZR) (---) DWBA calculations.

$^{16}O(\vec{p},d)^{15}O$ reaction using a water target. Final analysis of the data requires careful background subtraction corrections for the target cell; off-line analysis of these data has not yet begun.

Differential cross-section data were also taken on $^{7}Li(p,d)^{6}Li$ at 200 MeV (8-46°) and at 400 MeV (8-34°) with a resolution of about 1.5 MeV at 200 MeV incident energy. The data have been replayed off line, and spectra are presently being processed by the University of Colorado collaboration using a computer peak-fitting routine. Interest in this reaction centres on the change in relative cross sections of the ground state and first excited state of the residual nucleus as a function of incident proton energy.

Finally, small amounts of $^{40}Ca(p,d)^{39}Ca$ data were taken at 200 MeV from 8-20°. These data have since been greatly improved by measurements taken during Expt. 144 using polarized beam with better resolution and a cleaner target. The Expt. 144 data, taken in December, cover $^{40}Ca(\vec{p},d)^{39}Ca$ from 4-20° at 200 and 400 MeV.

Experiment 103
Spin dependence

The experiment to measure the spin dependence of $^{9}Be(p,p)$ elastic scattering had a preliminary run in August. The experiment is a measurement of the depolarization parameter. The focal plane double scattering polarimeter was built at the University of Alberta and installed on support rods between two multiwire proportional chambers at the focal plane of the MRS. Installation is such that the polarimeter can be moved out of the way to allow the MRS to operate in its normal mode. The BASQUE superconducting solenoid was located in the normal position of the MRS quadrupole. It was required to rotate the polarization of the scattered protons into the horizontal plane so that the magnetic field of the MRS would not precess the polarization direction.

Figure 61 is a schematic of the apparatus. The first detector S1 is located in front of the solenoid and serves to define the solid angle of the MRS. The next detector is the lower focal plane MWPC, PL1. S2 consists of

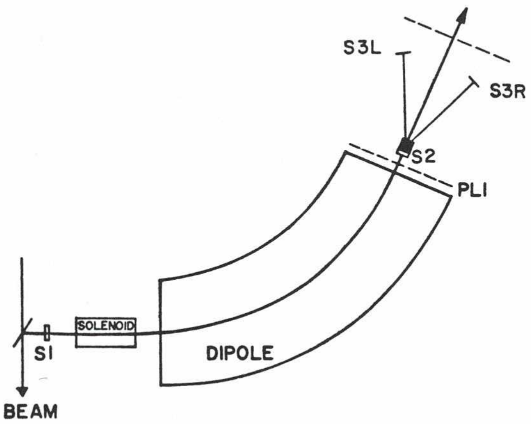

Fig. 61. Schematic of the MRS set up to measure the depolarization parameter (D) in elastic proton-beryllium scattering.

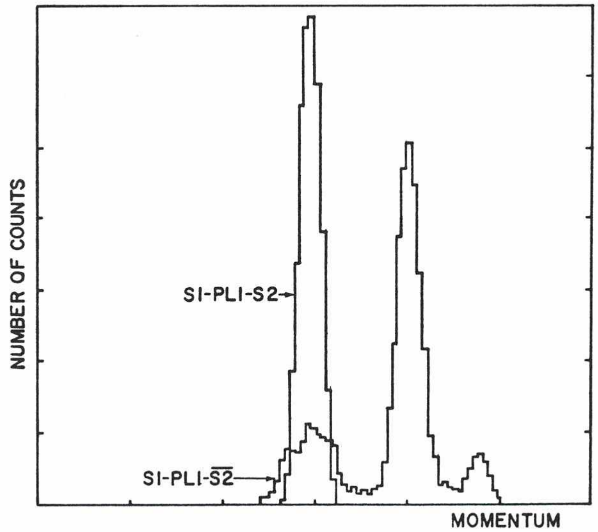

Fig. 62. Momentum spectra of scattered protons in the reaction $^9Be(p,p')X$.

a sandwich of a thin plastic scintillator and a thick carbon second scatterer. S3R and S3L are the right and left scintillation paddles. Finally there occurs the upper MWPC which is not in the detection logic. The MRS is operated in such a way that the focus of the particles of interest occurs as closely as possible to the lower wire plane. Data are collected by requiring the coincidence of either S1•PL1•S2•S3R or S1•PL1•S2•S3L. At the same time, data are collected on coincidences of S1•PL1•$\overline{S2}$. These latter data yield a MWPC spectrum with a hole in it corresponding to particles striking S2. This spectrum serves to monitor the experiment to check that the MRS is indeed focusing the scattered particles of interest onto S2, the second scatterer. Figure 62 shows superimposed spectra of the MWPC spectrum S1•PL1•$\overline{S2}$ and S1•PL1•S2.

Preliminary results show that the double scattering efficiency of the focal plane polarimeter is about 1 part in 200 and that the analysing power agrees reasonably well with the carbon analysing power at these energies. We hope to obtain final data in our next experimental run.

Experiment 104
The time projection chamber

The limits of lepton number conservation are being further pursued in an experimental search for the muon-electron (μ→e) conversion reaction in the field of a nucleus μ^-+Z → e^-+Z. The apparatus, which was constructed and assembled during 1979, is the TRIUMF time projection chamber (TPC). The TPC (Fig. 63) is a large acceptance drift chamber located in a uniform magnetic field. The magnetic field parallel to the drift electric field ($\overline{E}\times\overline{B}$ = 0) serves to bend charged particles for momentum analysis and also to reduce diffusion of the drifting ionization electrons.

Preparations for the μ → e conversion experiment continued during the year with the construction and acquisition of electronic and detection hardware, magnetic field shimming and measuring and software development.

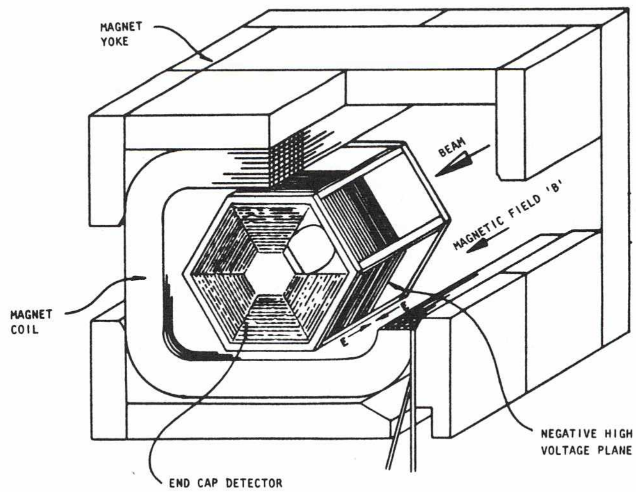

Fig. 63. TRIUMF time projection chamber.

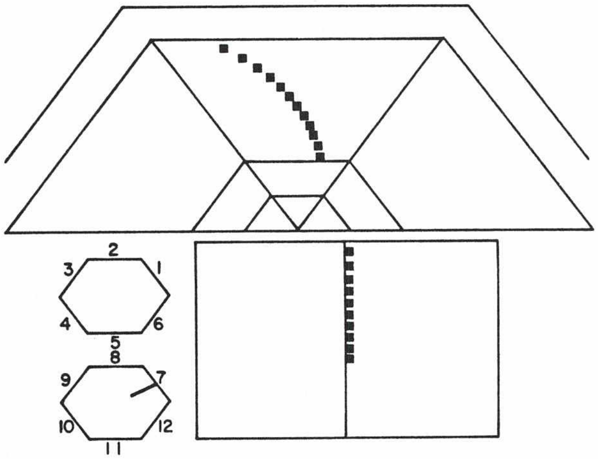

Fig. 64. Shown here is an on-line computer reconstruction of an electron track in the TPC. The top display gives a projection of the track at the TPC end-cap. The stars are the calculated positions of the track segments and the boxes are a fit to the trajectory (wire #8 is not instrumented here). The line in lower left hexagon indicates that the event occurred in sector #7, and the lower right display shows the track projection in the plane perpendicular to the end-caps.

The work culminated in a year-end run during which electrons from the decays $\mu^+ \rightarrow e^+\nu_e\bar{\nu}_\mu$ and $\pi^+ \rightarrow e^+\nu_e$ were detected and used to study the operating characteristics of the TPC system. An on-line computer reconstruction of a $\pi^+ \rightarrow e^+\nu_e$ event is shown in Fig. 64.

Earlier in the year a small TPC prototype chamber was tested extensively in zero magnetic field using 100 MeV/c positrons in the M9 beam. Signals from the segmented cathode strips of four active anode drift wires were amplified and recorded using charge-sensitive CAMAC analogue-to-digital converters. For the gas mixture argon 50%/methane 50% it was found that the position resolution along an anode wire was approximately 550 μ (FWHM) over a drift distance of approximately 10 cm. The resolution was limited by diffusion of drifting ionization electrons, variances of the avalanche process and electronic noise. The results of the prototype tests can be extrapolated to the case of the large TPC (32 cm drift, 9 kG magnetic field) to estimate that the resolution to be expected is ⩽225 μ.

Experiment 105
Inclusive scattering

Data analysis has been completed on the p-^{4}He inclusive scattering experiment. Results of the cross sections at angles of 65°, 90°, 120° and 160° are shown in Fig. 65, as are cross sections (arbitrarily normalized) for the dummy target, which is predominantly nickel. Analysing power measurements are shown in Figs. 66 and 67. Preliminary calculations by D. Boal are shown in Fig. 68.

The cross-section data show the standard inclusive scattering shape—basically an exponential drop-off with energy. The p-^{4}He analysing powers are significantly different from the results of Frankel *et al.* [Phys. Rev. Lett. 41, 148 (1978)]. We only observe small negative analysing powers at 65° and 90°, whereas they observed substantial positive analysing powers. We do observe small positive analysing powers in the p-nickel case. It is not clear whether these differences are

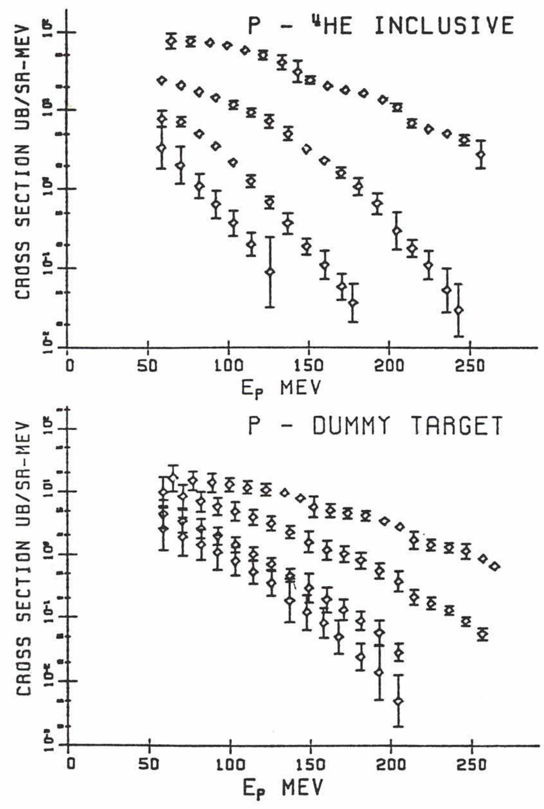

Fig. 65. Cross-section results for the reaction ^{4}He(p,p')X at 65°, 90°, 120° and 160° for the helium and dummy targets.

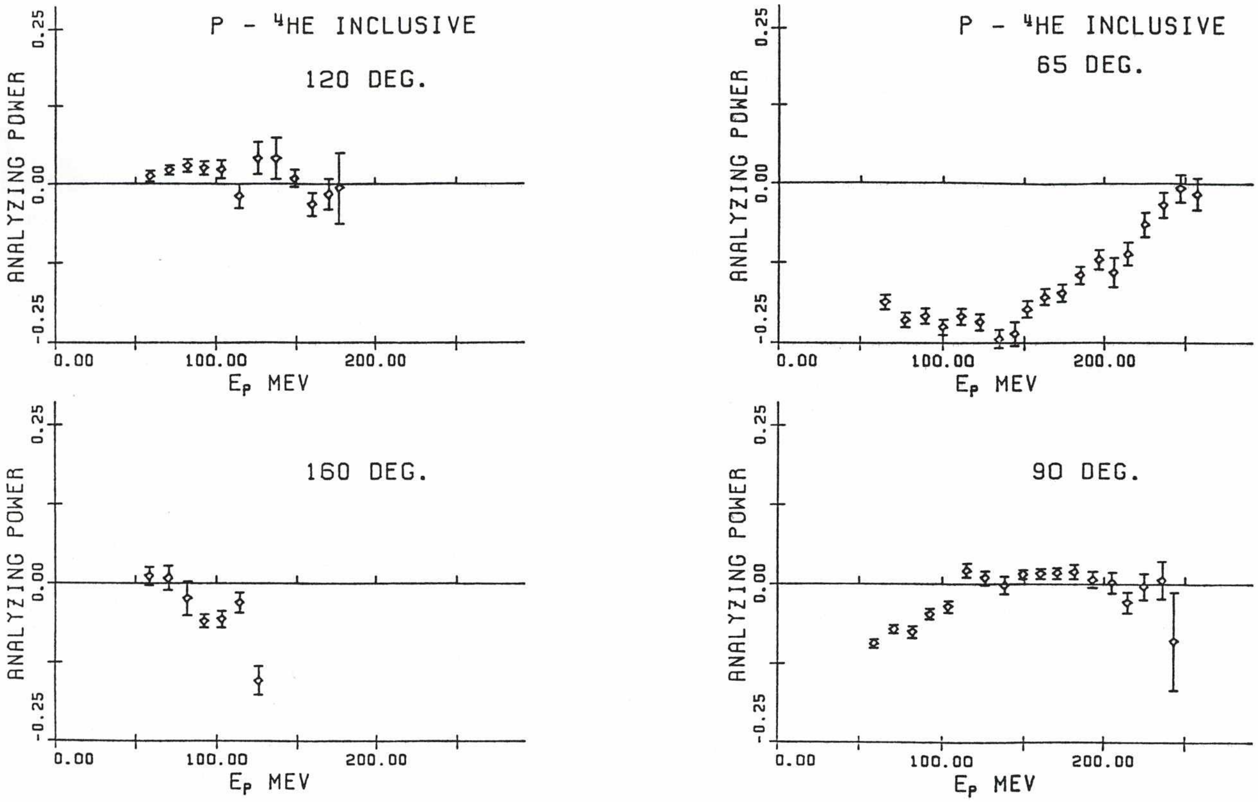

Fig. 66. Analysing power measurements for $^{4}He(p,p')X$ at four scattering angles.

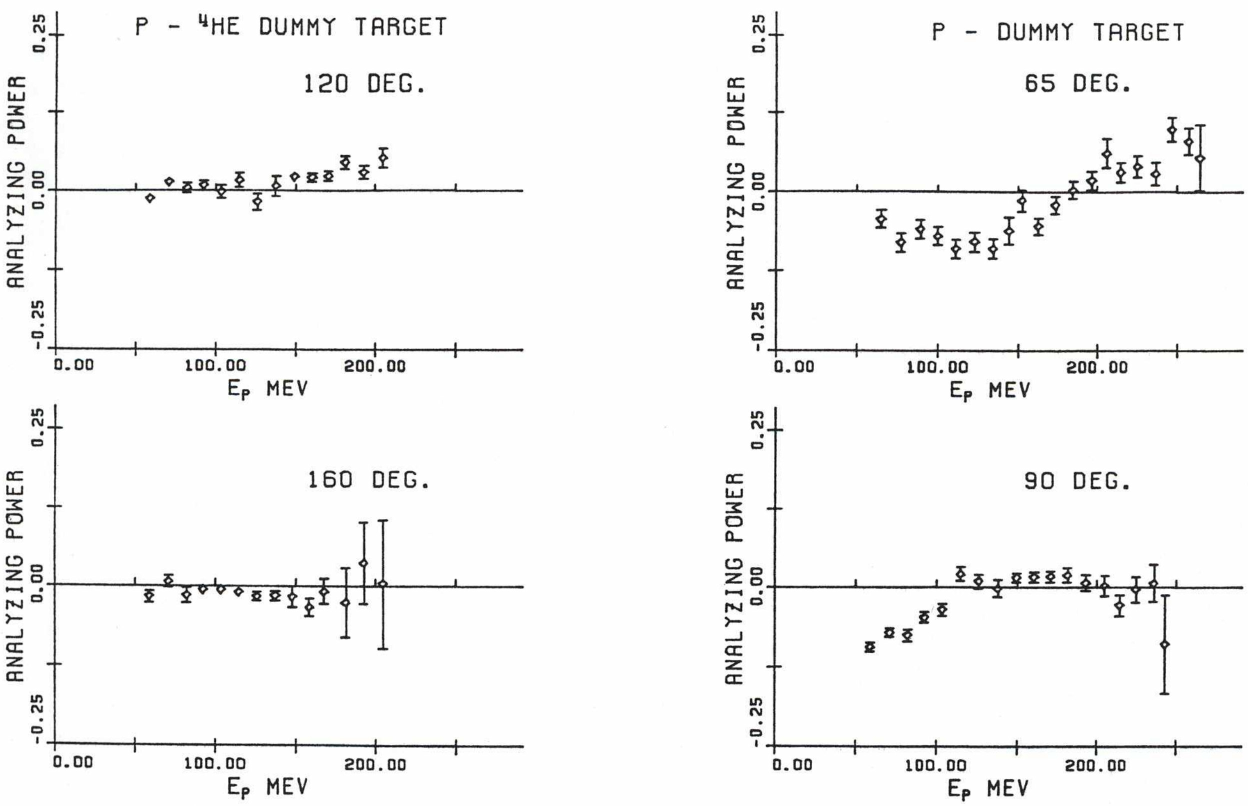

Fig. 67. Analysing power measurements for inclusive proton scattering off nickel at four scattering angles.

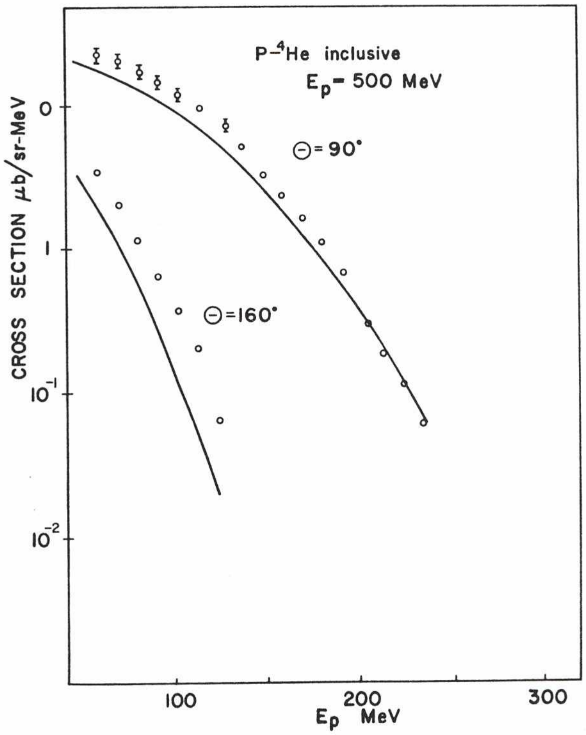

Fig. 68. Comparison of the measured inclusive proton scattering cross section for ^4He with preliminary calculations.

due to the lower bombarding energy in our case, or due to the light target nucleus.

Experiment 111
Pion absorption

During 1979 several tests have been performed using the M13 channel at TRIUMF, since this channel provides low momentum pion beams. After several tests it was decided to work at the momentum of 113 MeV/c as a good compromise between intensity and stopping rate in thin targets.

At $\Delta P/P$ of about 4%, more than $5 \times 10^3/\mu A/$sec negative pions were brought to rest in a 2 mm thick graphite target. A production target of carbon 1 cm thick was used. According to a method which has been described [Cernigoi *et al.*, Nucl. Instrum. Methods 165, 401 (1979)], the electrons present in the beam (10%) were selected for carrying out pulse height calibration and timing of the neutron counters and the range telescope counter used for detecting charged particles and neutrons. These measurements showed that all these counters have intrinsic time resolution of less than 400 psec when used in time-of-flight systems.

Finally, measurements performed with a 2 mm ^{12}C target and using the counters in a geometrical set-up compatible with the size of the experimental area gave 14 events/min of (n n), (n p), (n d) correlated pairs. It has to be noted that this figure will be lowered at about 6 events/min in the final geometrical set-up.

Experiment 108
Variation of pionic X-ray intensity with atomic number

We have observed the intensity of pionic X-rays per pion stop to vary with the atomic number of the stopping material. One of the largest variations occurs in the case of the 4-3 transition where the intensity has a maximum at Z = 32 which is twice the value of the minimum at Z = 24 [Annual Report 1978, p.46]. Results are also available [Pearce *et al.*, Can. J. Phys. 57, 2084 (1979)] for 3-2, 5-4, 6-5, 7-6, 4-2, 5-3, 6-4, 7-5, 5-2, 6-3 and 7-4 transitions.

As an example, Fig. 69 shows the observed percentage of n = 6 to n = 4 pionic X-rays per pion stop as a function of atomic

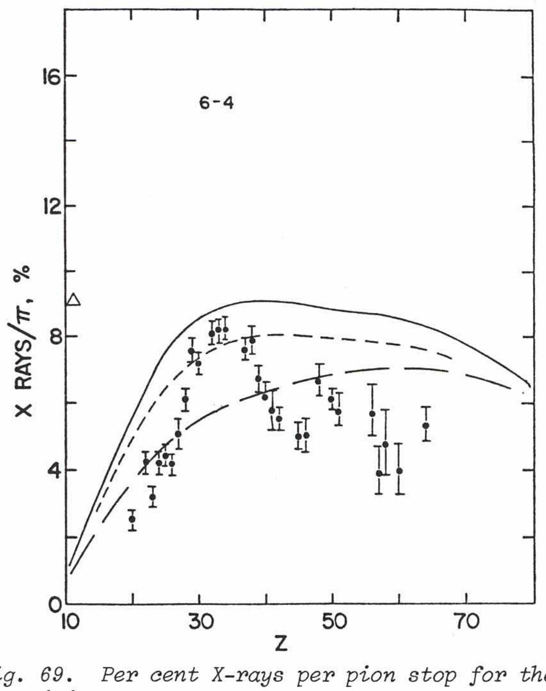

Fig. 69. Per cent X-rays per pion stop for the 6-4 transition.

number for elemental materials. The curves are the predictions from a standard cascade code which includes the following processes in the atomic cascade of the pion: electric dipole radiation pion decay, nuclear absorption, and $\Delta\ell = \pm 1$ K- and L-Auger processes, assuming that 2 K electrons are always present. In this model the initial atomic states were assumed to occur only at n = 17 with a distribution in angular moment of $(2\ell+1)\exp(-a\ell)$. The solid line corresponds to a = 0, the short dashes to a = 0.1, and the long dashes to a = 0.2.

The general trend of the experimental intensity variations as a function of Z is to some extent reproduced by the predictions of the cascade model. The decreased intensity at high Z and low n is caused by the relatively large overlap of the meson wave function with the nucleus and the consequent absorption of the meson. The decreased X-ray intensity at low Z and large n is caused directly by competition from the Auger effect. The Auger process also depletes the low Z X-ray intensity in an indirect manner: Auger transitions are favoured at low Z and tend to produce lower angular momentum states than do radiative transitions. This is because radiative transitions prefer $\Delta\ell = -1$ with large $|\Delta n|$, while Auger transitions prefer $\Delta\ell = -1$ with a minimum $|\Delta n|$ consistent with energy considerations. Thus the Auger processes at low Z indirectly cause more mesons to be lost by the strong interaction during the cascade.

In addition to the broad maxima caused by the strong interaction and the Auger effect, there are sharper peaks whose origin may lie in a combination of the strong interaction and some atomic effects. Since the dominant initial atomic capture process is an Auger process, the electronic configuration of the host material Z may affect the probability $P(Z,n,\ell)$ of a meson being captured into an atomic state with quantum numbers, n, ℓ, and affect the nuclear absorption probability.

The intensities of the $|\Delta n| = 1$ X-rays are found to be relatively insensitive to the initial distribution of angular momentum states for the following reasons: In the early part of the cascade there are many large Δn transitions which tend to populate preferentially the circular orbits $\ell = n - 1$. Once in a circular orbit a meson descends by a series of $\Delta n = \Delta\ell = -1$ steps through more circular orbits. The population of a circular orbit n,ℓ is therefore approximately proportional to the sum of the initial distribution over most angular momentum states higher than this ℓ. Since the transitions between circular orbits dominate the $|\Delta n| = 1$ X-rays, the latter tend to be insensitive to the initial distribution.

$|\Delta n| = 2$ transitions, on the other hand, have only a small contribution from the circular orbits (since these would have to be relatively weak quadrupole transitions) and therefore have larger variations with Z than $|\Delta n| = 1$ transitions.

Experiment 115
Neutral pion production

This experiment is intended to measure the total reaction (angle-integrated) cross section for the process $^{209}Bi(p,\pi^0\gamma)^{210}Po$ as a function of incident proton energy. Radiochemical separations are utilized to separate polonium from other reaction products and the yield of ^{210}Po determined from a measure of the residual alpha activity (see Annual Report 1978). The half-lives of relevant products ^{210}Po, ^{208}Po and ^{206}Po are 138.4 d, 2.898 yr and 8.8 d, respectively.

Over the past year experiments were conducted at proton energies from 183 to 480 MeV. A plot of these data along with data taken at the Indiana University Cyclotron Facility are presented in Fig. 70. The ratio of cross sections for the production of ^{210}Po to the production of ^{206}Po is displayed in the upper figure while the ratio of cross sections for the production of ^{208}Po to ^{206}Po is shown in the lower. The excitation function $[\sigma(E)]$ is expected to be similar for the latter products. The onset of the π^0 production is clearly observed around 140 MeV in the upper figure. The increase observed at higher energies ($>$350 MeV) possibly could be attributed to the onset of a different mechanism for the production of ^{210}Po. Preliminary results on absolute cross sections indicate that the excitation function for ^{208}Po and ^{206}Po exhibit a smooth decrease up to 480 MeV as expected while the production of ^{210}Po is essentially constant.

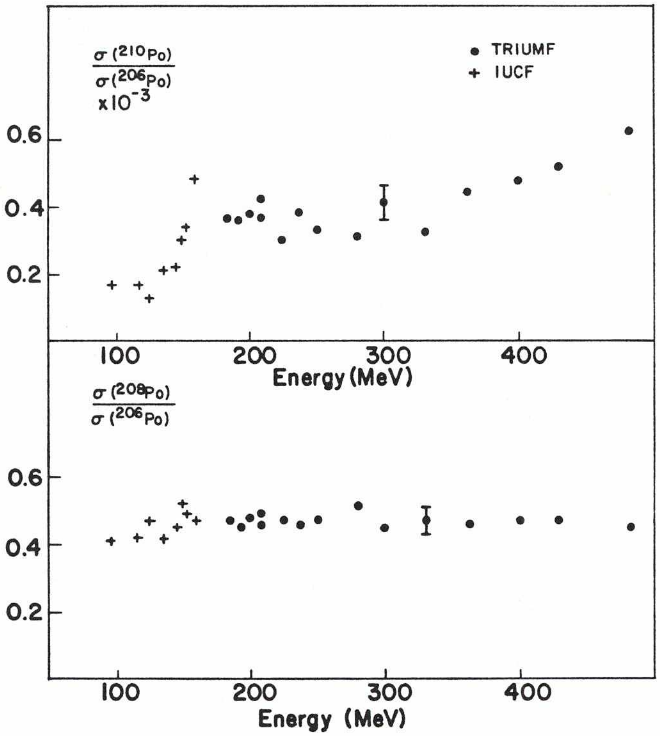

Fig. 70. Displayed here are the measured ratios of cross sections for the reactions $^{209}Bi(p,\pi^0\gamma)^{210}Po$ to $^{209}Bi(p,4n)^{206}Po$ (upper) and $^{209}Bi(p,2n)^{208}Po$ to $^{209}Bi(p,4n)^{206}Po$ (lower) as a function of proton energy.

Experiment 127
Measurement of the strong interaction shift in pionic deuterium

X-ray detectors

To provide a combined solid angle of 3.2×10^{-4} sr, two Si(Li) planars have been obtained, each with an active area of 2 cm^2 and a common cryostatic mount which would permit the addition of a third crystal when available. Both detectors have resolutions of less than 400 eV at 5900 eV and hence are capable of separating π^--D K_α X-rays from K_β. A third Si(Li), active area 0.8 mm^2, was obtained by reactivation of a massively damaged Ortec unit. Detector characteristics are:

	Energy	FWHM
115 #2	5900 eV	400 eV
	2308 eV	402 eV
115 #1	5900 eV	370 eV
	2308 eV	376 eV
	1400 eV	414 eV
Ortec	Noise	170 eV
	5900 eV	260 eV

These detectors will be tested in beam in April 1980.

Calibrated bismuth foils

Klempt has reported that new manufacturing techniques permitted the production of small absorber foils with measured uniformity of 1% (cf. 20% in the previous foils used by Bailey *et al.*), a value lower than that assumed in the calculation of the error due to foil homogeneity. Larger foils are presently in production for use with the Si(Li) detectors described above. The Bi foils will be calibrated in February 1980 by Richard Deslattes of the National Bureau of Standards, Washington, DC, and an alternative measurement will be made by Klempt at DESY following the experiment.

Target design for F2 of M9 channel

Three critical parameters of the gas target have been investigated prior to construction.

High pressure Be windows. A novel design has been evolved which, as well as permitting operation of the gas target at 10 atm pressure (an increase from an assumed 4 atm previously), also provides the ±18° collimation of low energy X-rays required to attain the error of ±0.5 eV from non-normal incidence on the Bi foil. This is accomplished by backing a 0.0005 in. Be foil with a thick stainless steel plate honeycombed with holes providing angular collimation. Transmission achieved to date is 50% at 2.5 keV.

Pion telescope and stopping fraction in thin targets. As previously established, a thin scintillator is required upstream of the gas volume to define an entering π^- without significantly increasing false stops resulting from pions stopping in the scintillator. Tests at 77 MeV/c were conducted using a 13.1 mg/cm^2 thick scintillator (cf. target gas thicknesses of $\gtrsim$15 mg/cm^2) which resulted in a measured stopping fraction of >0.6% of the π^- beam rate incident on an appropriate degrader in a 28 mg/cm^2 target of CH_2. This scales to the value assumed in the Experiments Evaluation Committee proposal for 4 atm D_2 gas.

Pion beam size at F2. An x-y wire plane was used to investigate the beam profile of the degraded π^- beam downstream of the pion telescope. With ±0.25% $\Delta p/p$ slit setting of M9 the lateral extent of the degraded π^- beam from the last upstream scintillator in the beam telescope was found to be 14.9 cm out to the <1% beam edges and the equivalent vertical distribution was 10.9 cm high.

Si(Li) background in the low-energy region

Background in the 2 keV region has been investigated using an 80 mm^2 Kevex planar detector viewing a 20 cm thickness of 1 atm He gas. The stop telescope deployed the 13.1 mg/cm^2 thick scintillator and, for convenience, the Be window of the detector, covered by the collimator, was placed within the plastic gas vessel containing He. In addition to a well-defined $\pi^- - {}^4He$ 2p-1s X-ray at 10.7 keV, a peak was seen corresponding to the L_α energy of 1.99 keV. Although statistics are poor, the peak-to-background ratios was found to be >2:1 and the background in this region was flat.

Summary

The minimum requirement of three Si(Li) detectors with ≤400 eV resolution have been obtained; bismuth foils of adequate homogeneity are presently being fabricated and will be calibrated at the National Bureau of Standards, Washington; preliminary tests of the π^- beam at F2 on M9 and of the pion telescope employing a 13 mg/cm^2 scintillator show that assumptions made in the EEC proposal are valid; and a spectrum obtained of the L_α pionic ^4He energy region shows no significant background problem. Final target design is under way with fabrication to be completed by April 1980. It is anticipated that data will be taken over the summer and fall of 1980.

Experiment 131
Asymmetries for the reactions $^2H(\vec{p},\gamma)^3He$ and $^3H(\vec{p},\gamma)^4He$

Measurements are being made for the above reactions using a technique in which the photon is detected, in a lead glass Čerenkov detector, in coincidence with the recoil nucleus. The first measurements on deuterium have been carried out using a CD_2 target and a telescope consisting of a multiwire proportional chamber (MWPC), a plastic scintillator, and a thin NaI detector. Complete separation has easily been achieved between the photons from the (p,γ) and those from the (p,π^0) reaction; background events in the kinematic region of interest are very small. The Cerenkov detectors' efficiencies for electrons between 12 and 175 MeV have been measured using the M20 channel. These results will be incorporated in a Monte Carlo program to yield the efficiency for the photons of interest.

In our first run, ostensibly to check out the technique, the cross section at $\theta_{c.m.}$ = 90°, 105° and 120° has been measured for incident protons of 300, 400 and 500 MeV. It is planned to extend these measurements and to add asymmetries in an upcoming run.

Future plans call for use of tritium-impregnated foils to allow similar measurements to be carried out for tritium. It is anticipated that these results will help clarify the somewhat disorderly state of the cross section for these processes and add the new dimension of asymmetries. It is hoped that these asymmetries will be an important constraint on theories which include such effects as a quasi-deuteron [Prats, Phys. Lett. 88B, 23 (1979)] mechanism or meson resonance effects [Finjord, Nucl. Phys. A274, 495 (1976); Bosted and Laget, Nucl. Phys. A296, 418 (1978)].

Experiment 143
Proton-induced reactions on ^9Be

The objective of Expt. 143 is the investigation of proton-induced reactions characterized by the coherent transfer of large momentum to the nucleons of a beryllium target. The magnitude and coherence of momentum transfer is determined by measurement of the angle, energy and identity of nuclei recoiling in particle-stable final states of mass 8, 9 or 10. Detection is accomplished using a semiconductor counter telescope mounted in the 1.5 m diam scattering chamber located on beam line 4A. This simple technique is naturally selective of large coherent momentum transfer and allows the study of this class of reaction to be extended to a wider range of final states in search of fresh insight into the mechanisms involved. As outlined below, the initial phase of this experiment has resulted in extensive data on four reactions. These form the basis of an ongoing program.

$^{9}Be(p,\pi^{0})^{10}B$

It is the intention that the existing data on the $^{9}Be(p,\pi^{+})^{10}Be$ and $^{9}Be(p,\pi^{-})^{10}C$ reactions be augmented with measurements of the differential cross sections and excitation function for the (p,π^{0}) reaction populating the particle-stable states of ^{10}B. By selecting ^{10}Be and ^{10}C recoils identified in the same data set a direct comparison of the yields of the (p,π^{+}), (p,π^{0}) and (p,π^{-}) reactions can be obtained as functions of both q and E(p) throughout the TRIUMF energy range. Figure 71 presents the result of preliminary analysis of the ^{10}B spectrum recorded at 10° with protons incident at 499 MeV on a 2 mg/cm^{2} Be target. The observed peak, characteristic of two-body final states, indicates

$$\frac{d\sigma}{d\Omega}(p,\pi^{0}) = 0.65\ \frac{\mu b}{sr}\ (c.m.)$$

at θ(c.m.) = 16°.

The spectrum of ^{10}Be recoils recorded concurrently with the data of Fig. 71 reveal a similar peak corresponding to the (p,π^{+}) reaction with an intensity approximately 10% greater than that of the (p,π^{0}) reaction. These and similar spectra recorded at other angles and also at lower incident energies (429 and 329 MeV) have clearly established that precise comparisons of the (p,π^{0}) and (p,π^{+}) reactions over a wide range of values of momentum transfer are feasible.

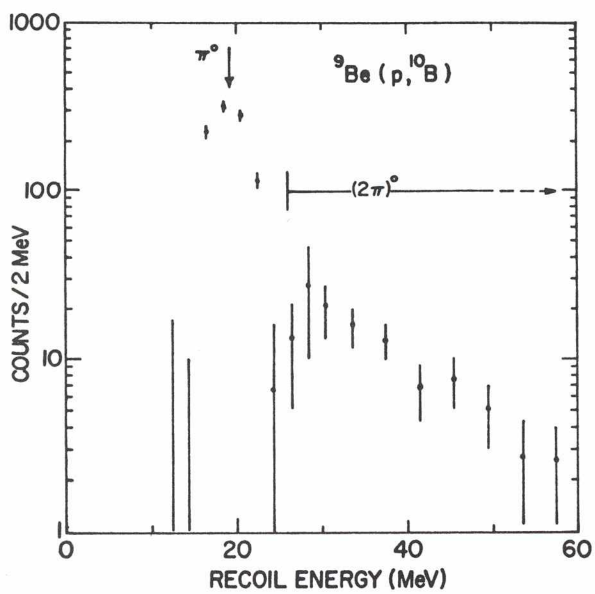

Fig. 71. The spectrum of ^{10}B nuclei recoiling at θ = 10° with protons incident at 499 MeV. The arrow marks the centroid of the peak anticipated from the $^{9}Be(p,\pi^{0})$ reaction. Also indicated is the range of energies consistent with the kinematics of the $(p,2\pi)$ reaction.

$^{9}Be(p,2\pi)^{10}B$

An additional feature of the data displayed in Fig. 71 is the continuum characteristic of at least 2 "missing" particles with a maximum intensity near 29 MeV and extending beyond 60 MeV. These data and related spectra recorded under different kinematic conditions indicate that the $(p,2\pi)$ reaction is the origin of these higher-energy recoils. There are features of these data similar to those of the "ABC effect" [Abashian, Booth and Crowe, Phys. Rev. Lett. 5, 258 (1960)] first observed in the reaction $D(p,2\pi)^{3}He$. The present data represent the first observation of this reaction on a target of A > 3.

$^{9}Be(p,N\pi)^{9}Be$

The results of initial experiments at 499 MeV reveal that, as anticipated, the ^{9}Be spectra at $55 < \theta < 80°$ are dominated by the single peak resulting from elastic scattering (the ground state is the only bound state of ^{9}Be). The prime interest in the ^{9}Be data has been focused on the angular range accessible to recoils from the $(p,N\pi)$ reaction ($\theta < 60°$).

Figure 72 shows a typical ^{9}Be spectrum spanning a range $0.5 < q < 1.0$ GeV/c. The spectra of all recoil nuclei A < 10 emitted in reactions with at least two unobserved particles exhibit similar energy dependence. The results of the measurement of the angular distribution at E(R) = 19.3 MeV are presented in Fig. 73. The smooth curve is arbitrarily normalized but represents the relative distribution that would result from a simple phase space analysis of the $(p,N\pi)$ reaction. At angles corresponding to values of the missing mass M < 1.2 GeV, the data are consistent with phase space, and the absence of any evidence of the Δ(1.23 GeV) is noteworthy. Consideration is being given to the possible origin of the observed "excess" at higher values of M as well as to an interpretation of the data at lower M in terms of pion bremsstrahlung.

$^{9}Be(p,2p)^{8}Li$

Extensive angular distribution data are available for $3.5° \leqslant \theta \leqslant 80°$ at E_p = 499 MeV. In contrast to the situation for the ^{9}Be

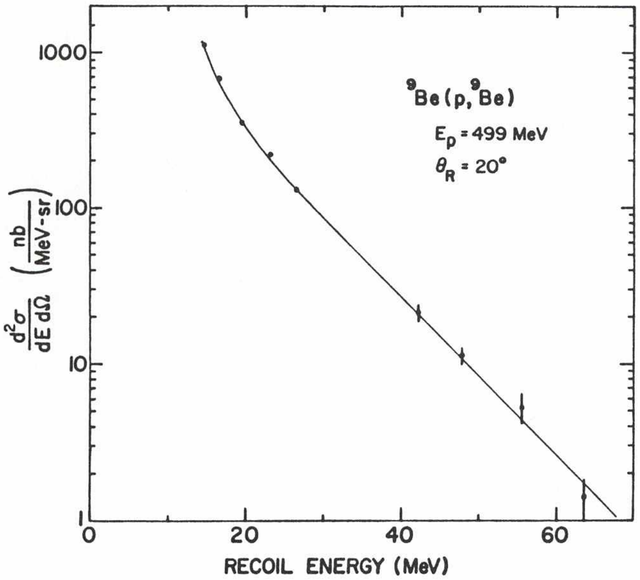

Fig. 72. A typical recoil spectrum attributed to the $^9Be(p,N\pi)^9Be$ reaction.

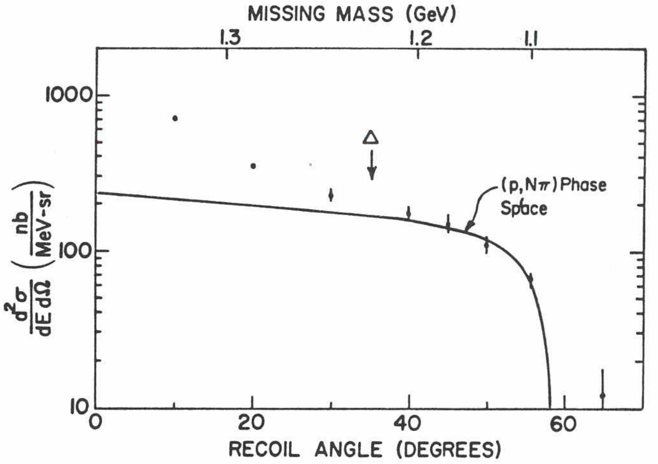

Fig. 73. The angular distribution of ^9Be recoils at fixed momentum transfer (0.57 GeV/c). The smooth curve follows (p,Nπ) phase space. Angles corresponding to specific values of the invariant missing mass are indicated.

spectra, the observed distributions for ^8Li bear little resemblance to the phase space available for the (p,2p) reaction even at the lowest values of invariant mass. Comparisons are being made of these data with several models initially developed for inclusive proton production, all of which have a contribution from a final state characterized by two protons and a residual nucleus.

Experiment 144
Asymmetries in ($\vec{p}$,d) reactions

Measurements have been made of neutron pickup from ^{13}C, ^{16}O and ^{40}Ca using the 1.4 GeV/c spectrometer and the polarized proton beam. The data for ^{13}C leading to the ground state and 4.4 MeV level of ^{12}C correspond to $p_{1/2}$ and $p_{3\ 2}$ pickup, respectively, and serve as a good test of j-dependence in the reaction at intermediate energies. These data show this dependence to be strong, even at small scattering angles and indicate that it may be a powerful spectroscopic tool to assign j-values to deep-lying hole states populated in pickup reactions at intermediate energies.

As a sample of the results we show in Fig. 74 the cross section and asymmetry for the $^{13}C(\vec{p},d)^{12}C$ reaction at 200 MeV. Comparing the asymmetries for pickup from the $p_{1/2}$ and $p_{3/2}$ shell one finds (even at small angles) the following picture. The angular distributions are somewhat structureless and show no j-dependence. In fact, by looking at data from LAMPF one also finds that $\sigma(\theta)$ is even insensitive to the ℓ-transfer. In contrast to this discouraging picture we find

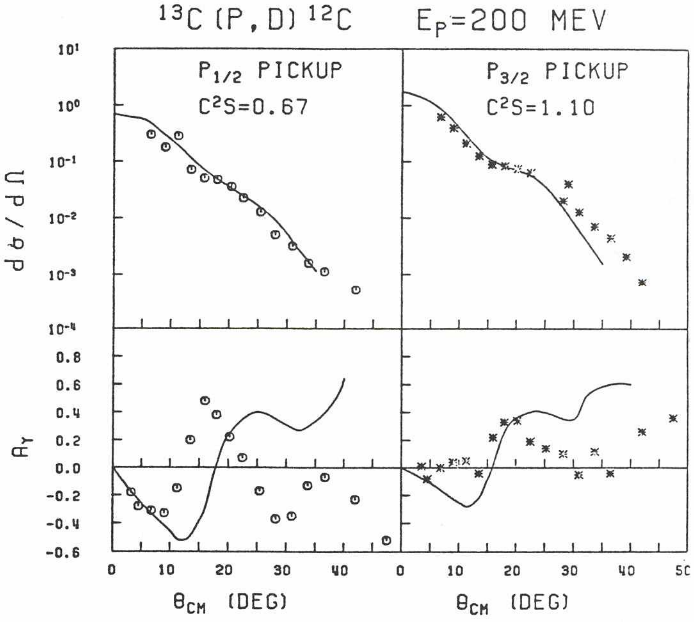

Fig. 74. Cross section and analysing power for the $^{13}C(\vec{p},d)^{12}C$ reaction at 200 MeV. Circles are for the pickup leaving ^{12}C in 0.0 MeV state and stars for 4.4 MeV state. The DWBA calculations (J.R. Shepard, University of Colorado) are shown as solid lines.

in the asymmetries a very large dependence on the nuclear structure.

Similar data taken at 400 MeV indicate that these differences may be diminishing as the energy increases and that the TRIUMF energy range is probably optimum for exploitation of this powerful tool.

Calculations in exact finite range DWBA have been carried out and are somewhat encouraging. These are shown as solid curves in the figure.

A number of areas remain to be investigated further. One area involves geometry matching between the neutron potential when it is in the bound state and when it is in scattered waves. It appears (at least for ^{4}He) that, as MEC effects play an important role in electron scattering and as they will be different in nucleon case, great care has to be taken in reorganizing single particle wave functions extracted from electron scattering.

Experiments 71, 78, 91, 122, 123
μSR in solids

New technology

Surface muon facility. In 1979 20,000 "surface muons"/sec were successfully stopped in a target consisting of a sliver of quartz 1 cm in diameter and about 0.5 mm thick—a net mass of less than 100 mg! This 4.1 MeV beam is delivered without significant scattering or other disruption to a target surrounded by counters and mounted in a helium cryostat capable of controlling its temperature down to ~2 K. The facility thus created (dubbed "Eagle") provides a qualitatively unique capability at TRIUMF for studying μSR in very small targets.

Longitudinal and zero field μSR. Many of the new results obtained in 1979 have relied upon the longitudinal- and zero-field techniques rediscovered and developed at TRIUMF in 1978 (see 1978 TRIUMF annual report, pp. 58-62). The advantage of these techniques lies mainly in their capability for measuring longitudinal relaxation rates in totally undisturbed samples—sometimes impossible with NMR methods and thus of great practical interest.

The interpretation of such data is usually in terms of the Kubo-Toyabe stochastic theory of spin relaxation by static magnetic dipoles and the extension to non-static situations. This has proved to be a very powerful phenomenological description.

Late this year a new experimental tool was added to the TRIUMF μSR arsenal which combines the advantages of surface muons (see above) with the longitudinal-relaxation techniques that have proved so fruitful. The new apparatus is nicknamed "Beaver" and can deliver a surface muon beam of 10,000/sec to a 1 cm diam target when used on M13 with 20 μA on a 2 mm C target in 1AT2. These muons stop in about 140 mg/cm^2 with a range spread of about 20 mg/cm^2 and are delivered to a target of that thickness in the same cryostat used in "Eagle". In this apparatus the field can be zeroed to less than 10 mG with long-term stability, or extremely uniform fields of up to 10 G can be applied.

Transversely polarized "clean" surface muon beam. Meanwhile, the commissioning of the crossed-field velocity spectrometer (dc separator) on M9 has solved the main disadvantage of surface muon beams: their positron contamination, which is sometimes as high as 10:1. Using "Eagle" with the dc separator of M9 has allowed background-free use of surface muons for the first time.

Another feature of the dc separator has also been successfully tested in 1979: its ability to rotate the muon spins by 90° to produce a transversely polarized beam. This allows the possibility of injecting the very low momentum muons into a strong axial magnetic field, where the muon spins will precess at high frequency; this is impossible with the normal longitudinal polarization of the muons. Thus the one remaining limitation of surface muons has been overcome.

Magnetism studies with muons
(Experiment 71)

Stochastic theory of zero-field μSR. The zero-field spin relaxation function for the static nuclear dipole system was derived theoretically by Kubo and Toyabe [*Magnetic resonance & relaxation* (North-Holland, Amsterdam, 1967) p.810]:

$$G_z^{KT}(t) = \frac{1}{3} + \frac{2}{3}\left(1-\Delta^2 t^2\right)\exp\left(-\frac{1}{2}\Delta^2 t^2\right).$$

This function is characterized by the "recovery" of the polarization of the fraction (1/3) of spins whose orientation is initially parallel to the local field.

In 1979 a stochastic theory of spin relaxation has been formulated based on the strong-collision approximation to take into account the dynamical modulation of the random local field; the following iterative formula was obtained for the modulation rate $\nu = 1/\tau_c$:

$$\begin{aligned} G_z(t,\nu) = \exp(-\nu t) \Big\{ & G_z^{KT}(t) \\ & + \nu \int_0^t G_z^{KT}(t_1) G_z^{KT}(t-t_1)\, dt_1 \\ & + \nu^2 \int_0^t \int_0^{t_2} G_z^{KT}(t_1) G_z^{KT}(t_2-t_1) \\ & \times G_z^{KT}(t-t_2)\, dt_1\, dt_2 + \ldots\ldots \Big\}. \end{aligned}$$

As shown in Fig. 75, $G_z(t,\nu)$ is sensitive even to the very slow modulation ($\tau_c \cdot \Delta \gtrsim 2$)

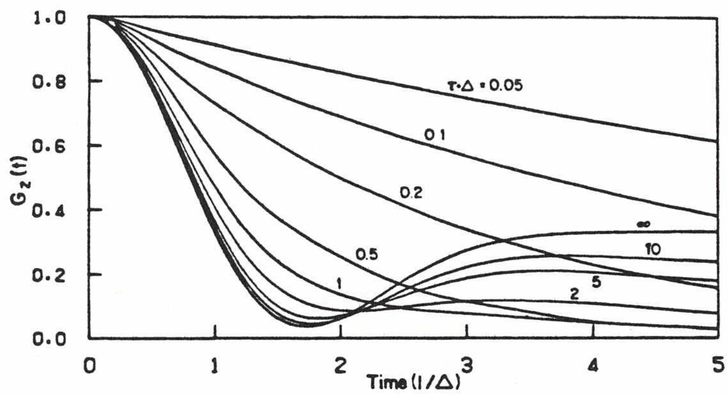

Fig. 75. Zero-field longitudinal relaxation function for muons affected by a Gaussian distribution of local dipolar magnetic fields. Effect of stochastic processes (e.g. muon 'hopping') in the strong collision limit: curves labelled by value of mean correlation time τ ($\tau = \infty$ corresponds to static Kubo-Toyabe relaxation). Time (and τ) measured in units of $1/\Delta$, where Δ = width of static field distribution ($\approx$ relaxation rate).

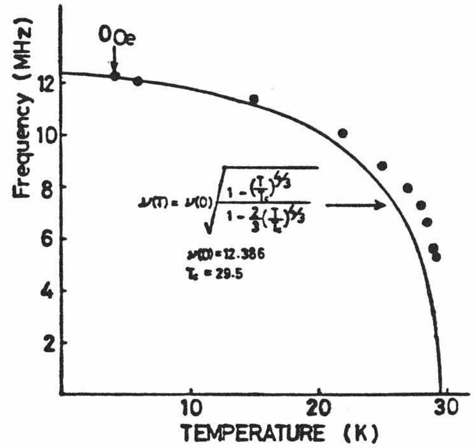

Fig. 76. Temperature dependence of μ^+ precession frequency (i.e. local field) at the muon site in MnSi in its helically ordered magnetic phase.

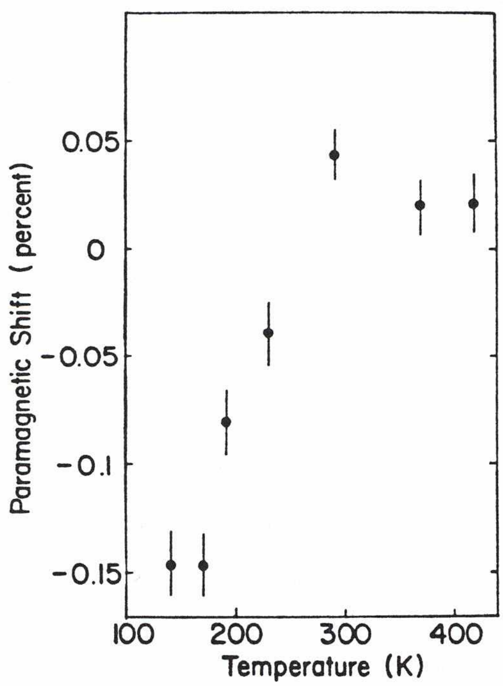

Fig. 77. Paramagnetic shift of μ^+ in MnO as a function of temperature.

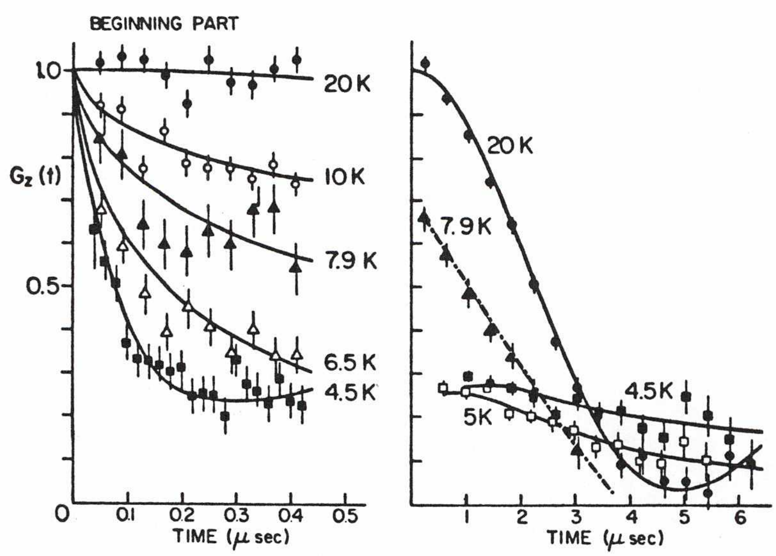

Fig. 78. Zero-field longitudinal relaxation function for μ^+ in CuMn (0.8 At.%) near the spin-glass transition temperature. Early times are shown at left; the subsequent time dependence is shown at right.

with the 1/3 component decaying as ~1/3 exp(-2νt/3). This feature makes the zero-field μSR technique a very powerful tool for the study of muon diffusion and spin glasses (see below). A stochastic theory for the random dilute spin system has also been completed for the purpose of deducing the correlation time of spin glass local fields from the observed muon relaxation functions.

Itinerant electron magnetism. The longitudinal relaxation time T_1 was measured in zero applied field in the helically ordered state of the itinerant helimagnet MnSi at temperatures below T_c. A considerable deviation from the theoretical value of T_1 was observed for the weakly ferromagnetic ordered state near T_c, which might be related to the helical spin structure of MnSi. At the same time precession of the μ^+ was observed with no applied field, giving the local magnetization as a function of temperature in a sample with no bulk magnetization and in which zero-field NMR is observable only in a limited temperature region. The staggered magnetization M_Q is shown in Fig. 76.

Near T_c the experimental values of $M_Q(T)$ are higher than predicted by theory, which is stimulating more elaborate calculations of M_Q.

Antiferromagnetic insulator. The longitudinal relaxation time T_1 was measured very precisely in MnO near the Néel temperature. The relaxation rate $1/T_1$ was found to vary smoothly with T as close as 0.1 K to T_N. On the other hand the initial asymmetry was abruptly reduced by a factor of 3 as the temperature dropped past T_N, which was thus measured to be 117.2 K. Thus the temperature dependence of T_1 observed in the paramagnetic phase must not be related to the critical behaviour of the host material but to the diffusional motion of the muon in the crystal.

The paramagnetic shift in MnO was measured in a transverse field of 5 kG as a function of T, as shown in Fig. 77. The shift changes abruptly around 230 K and is not linearly related to the susceptibility; furthermore, the shift changes with the length of time since the muon entered the crystal, in a systematic manner suggesting a slow trapping of the muon at Mn^{++} vacancies. The same picture would explain the observed temperature dependence of T_1. This experiment has provided the first measurement of the contact hyperfine field at the μ^+ in a magnetic insulator. The result is unexpectedly negative (-0.2%), presenting a challenging theoretical problem.

Spin glasses. Dilute alloys such as CuMn and AuFe show a sharp maximum in the AC susceptibility indicating an ordering below T_g into a randomly oriented but unchanging array of spins. This phenomenon, called "spin-glass ordering", is the subject of great theoretical speculation. One experimental difficulty is the sensitivity of the phenomenon to external magnetic fields, which prompted us to use the zero-field longitudinal relaxation method (developed at TRIUMF last year) to study the spin-glass transition in CuMn, AuFe and amorphous cobalt aluminosilicate glass.

Figure 78 shows the time dependence of the asymmetry for the CuMn sample at several temperatures. The apparent initial asymmetry, viewed on the long-time scale (right), drops gradually by a factor of 3 as the temperature changes from 20 K to 5 K; this is characteristic of magnetically ordered phases, confirming that some transition has taken place, but the slowness of the change with T indicates a gradual transition, in agreement with recent n-diffraction and Mossbauer results but in conflict with many theories. The early-time data (Fig. 78, left) show what has happened: the paramagnetic ions' contribution to the local field is nearly static at 4.5 K, causing a fast stochastic relaxation (and providing a measure of the first and second moments of the local field); this "line broadening" is narrowed by Mn spin fluctuations as the temperature is raised, culminating with stochastic relaxation by static nuclear dipoles alone at 20 K. The slow relaxation of the long tail at 5 K is due to slow fluctuations in the local field as the paramagnetic spins reorient slowly in the spin-glass state. This method thus allows extraction of the mean local field distribution and its average fluctuation time τ_c over a range from $\tau_c \sim 10^{-11}$ sec at $T \sim 1.5\ T_g$ to $\tau_c \sim 10^{-5}$ sec at $T \sim 0.5\ T_g$. Surprisingly, the resultant temperature dependence of τ_c is very smooth and Arrhenius-like right through T_g, showing no critical anomaly. This feature is observed in several samples of CuMn and AuFe with different impurity concentrations. The dynamical nature of the spin-glass transition is thus revealed to be quite different from that of ordinary ferro- or antiferromagnets.

Recent field-cooling experiments on the susceptibility of cobalt and manganese aluminosilicate glass samples indicate a marked difference between field-cooling in 250 mOe and 20 mOe. For this reason the new zero-field surface muon facility "Beaver" was used to study such a sample near the end of 1979. Preliminary results indicate no such field-dependent effect in the local fields at the muon.

Muon diffusion and trapping at defects in solids
(Experiment 78)

Nonstoichiometric compounds. Zero-field relaxation of positive muons was found to be different in several different samples of ZrH_2, indicating a strong dependence of the location of the muon upon the hydrogen concentration and the chemical stoichiometry. Basically, ZrH(2-x) relaxes the muon spin more slowly than ZrH(2.0), which in turn gives a slower relaxation than ZrH(2+x). This may be explained by the difference between the nuclear dipolar fields at interstitial and substitutional sites of H.

Trapping at vacancies in aluminum. Zero-field longitudinal relaxation of the μ^+ was studied in Al samples which had been quenched at several different temperatures. The relaxation rate showed a clear and consistent dependence upon the quenching temperature—i.e., upon the concentration of quenched-in vacancies. The dipolar width at the trapped site suggests trapping of the μ^+ at an interstitial site near the vacancy.

Upper limit on diffusion in aluminum. A brief measurement of μ^+ relaxation in a fine powder of pure Al showed no evidence for macroscopic diffusion (to grain surfaces), even though the extreme motional narrowing in bulk Al indicates unusually fast diffusion at low temperature. This observation establishes a crude upper limit on the muon diffusion rate in Al at room temperature. A similar result was obtained with foils of Al coated with Cu, indicating that the absence of relaxation is not simply due to some repulsive surface potential.

Muonium in semiconductors and insulators
(Experiment 91)

Silicon. High-statistics μSR spectra were taken on a Si sample 0.6 mm thick which had been strained by bending. The sample was run with and without strain at 77 K, and no difference was detectable in the spectra, even though the quality of the data was excellent (6 or 7 peaks resolved in the Fourier power spectra).

Improved techniques now allow chi squared fitting of an arbitrary number of signals in one spectrum of 10 M events taken in ~1 h. This permits extraction of quantitative details which were previously obscure. One surprising result of such studies is that Mu signals relax faster in ultra-pure Si at 10 K than at 100 K in the same sample or at 10 K in a sample with oxygen impurities. This is expected to lead to an understanding of the dynamics and chemistry of Mu atoms in Si.

III-V semiconductors. A high-statistics transverse-field spectrum for μ^+ in GaP showed no trace of Mu or Mu^* precession signals, though the free muon signal was markedly reduced. This is probably due to relaxation by nuclear moments, which are easily quenched in longitudinal-field experiments; a preliminary study of this sort indicates that paramagnetic states are indeed present in GaP, but not in InSb.

Quartz. The muonium atom has an intrinsic electric quadrupole moment in the triplet state which couples with the local charge distributions in a quartz crystal to produce a slightly anisotropic hyperfine interaction. New data at higher fields (where the "quadratic Zeeman splitting" could be compared with the constant "quadrupolar splitting") show that the absolute sign of the latter effect is definitely positive and that the isotropic part of the hyperfine interaction is (tentatively) 2(1)% lower than in vacuum, in qualitative agreement with theory.

Early in 1979 we measured the "pure quadrupole oscillation" of the Mu spin system in zero magnetic field [see Fig. 79 (top)], demonstrating that the Mu site at room temperature is symmetric about the $\hat{c}$-axis. Recently quartz was run at 77 K and zero field, and completely different "quadrupole oscillations" were observed, shown in Fig. 79 (middle and bottom). The Mu atom is

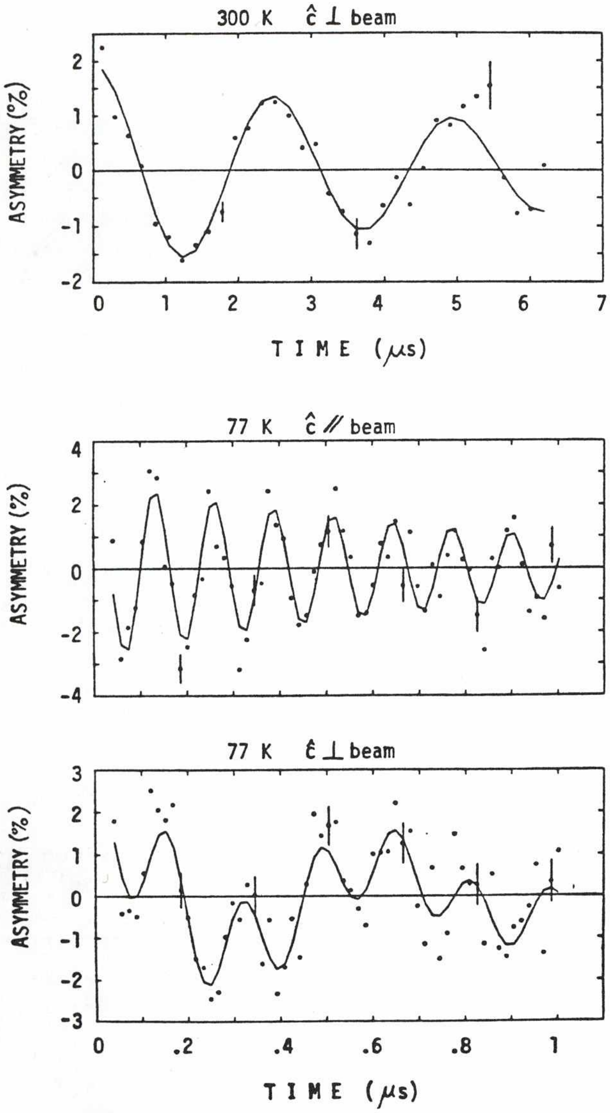

Fig. 79. Time spectra for Mu in α-SiO_2 at zero magnetic field. Top: 300 K, ĉ-axis ⊥ initial muon polarization; bottom: 77 K, ĉ ∥ and ⊥ to initial $\vec{P}_\mu$.

clearly trapped in a different site (without axial symmetry) at 77 K.

Exotic insulators. Thanks to our new experimental capabilities we were able to study muonium formation in rare crystals for the first time. We found, surprisingly, that none of the muons stopped in ZrO_2 formed Mu but that in C (diamond) 100(5)% of the stopping muons form Mu atoms or other paramagnetic centres which are for some reason depolarized subsequent to their formation.

Local field in dilute iron alloys
(Experiment 122)

Ferromagnetism in iron and iron alloys was studied by measuring the magnetic fields acting on muons in interstitial sites and the characteristic times T_1 and T_2 at temperatures up to 1200 K. At temperatures between 700 K and the curie temperature the field on the muon tracks the average magnetization yielding a coefficient that depends on the solute and its concentration. At lower temperatures there is a preferential sampling of sites reflecting the relative electronegativity of solute and solvent. Alloys with nitrogen and with vanadium were studied over the full temperature range. Preliminary work was carried out on alloys with Mu, Ci, Ti, Ta, Nb, Mo and W.

The internal field experienced by a diffusing μ^+ in dilute ferromagnetic alloys varies with concentration and type of impurity; even more interesting are the differences in temperature dependence of this local field. For FeNb (4.0%) and FeMo (4.8%) the local field changes more slowly with temperature than for pure Fe, while for FeAl (4.3%) it changes faster. This indicates an attractive interaction between the muon and the Nb or Mo impurities, contrasted with a repulsive interaction between the muon and the Al impurities; such a behaviour is consistent with positron and hydrogen work which shows that solutes to the right (left) of the host in the periodic table are repulsive (attractive) to hydrogen-like impurities.

Channeling of muon-decay positrons in silicon
(Experiment 123)

A preliminary search for evidence of channeling of positrons from μ^+ decay gave negative results; however, the principal problems (scattering of beam positrons, backgrounds, etc.) should be greatly alleviated by the availability of the "clean" surface muon beam of the dc separator on M9 and other technical improvements. A successful experiment of this sort would allow location of the muon in the Si lattice and open up a powerful methodology to μSR studies.

Experiment 141
Muonic hydrogen

Muonic hydrogen (μ^-p) is a system of great interest from the point of view of atomic and elementary particle physics, especially inasmuch as its weak capture process ($\mu^-p \rightarrow \nu_\mu n$) is the prototype of all semileptonic weak interactions involving baryons. However, both the atomic physics of μ^-p and the details of the weak capture process are obscured by the rapidity with which μ^-p forms the muonic-molecular ion $p\mu^-p$ in the liquid phase and the rapidity with which triplet $(F=1)\mu^-p$ is collisionally de-excited to singlet $(F=0)\mu^-p$ in high-pressure gases.

It is thus a particularly annoying fact that μ^- beams generally need $\gtrsim 1$ g/cm of hydrogen in which to stop and, conversely, particularly tantalizing to imagine a μ^- beam which will stop in a few inches of hydrogen gas at STP.

Preliminary measurements on M9 suggest that such a beam may exist at TRIUMF. There seem to be negative muons of 4.1 MeV in quantities about 1/15 as plentiful as the well-known "surface μ^+" beam. A later run using the dc separator failed to reproduce the "bump" in the μ^- momentum distribution at 29.8 MeV/c, but the flux of μ^- was still ~1% of the μ^+ flux, which allowed an approximate measurement of the μ^- polarization as a function of momentum. The results were somewhat discouraging, indicating only ~40% polarization.

It may still be feasible, however, to use this beam to determine whether the triplet state of μ^-p can be observed in hydrogen gas near STP. A positive result would permit a study of the rate of $(F=1) \rightarrow (F=0)$ as a function of temperature and pressure. Knowledge of this de-excitation rate is essential to any subsequent studies of (for instance) the triplet capture rate and represents a very interesting piece of atomic physics in itself.

Experiment 35
Muonium chemistry

Gas phase studies

Gas phase studies of muonium chemistry are particularly facilitated by the use of a surface μ^+ beam, with its concomitant high stopping density (see Annual Report 1978).

<u>μ^+ charge exchange and muonium formation</u>. During its slowing-down process from MeV to thermal energies the μ^+ undergoes a series of charge-exchange cycles

$$\mu^+ + e^- \underset{\sigma_{01}}{\overset{\sigma_{10}}{\rightleftarrows}} \mathrm{Mu} \ .$$

To date the fraction of μ^+ thermalizing as Mu (f_{Mu}) has been determined in pure He, Ne, N_2, CH_4, NH_3, Ar, Kr and Xe, all at ~1 atm. Recent data are given in Table IX. In addition, we have recently obtained new data on gas mixtures of Xe in He and Ne, confirming the trends previously established (Annual Report 1977) but extending to much larger Xe concentrations. As noted previously, there is apparently no relaxation of the muon signal in Xe/He mixtures, in sharp contrast to the situation in Xe/Ne mixtures (Annual Report 1978). Preliminary analysis shows that f_{Mu} is now asymptotic to close to 100% Mu formation, which is qualitatively expected on the basis of the ionization potential of Xe (12.6 eV) being lower than that of muonium (13.6 eV). This makes the result for pure Xe in Table IX of a relatively small Mu signal (accompanied by a very small μ^+ signal) all the more difficult to explain: as noted last year its lower ionization potential should result in essentially 100% Mu formation. There is clearly some additional depolarization process operative. In this regard it is interesting to note that in both CH_4 and NH_3, also gases with lower ionization potentials than Mu, f_{Mu} is indeed of order 90%.

Table IX. Muonium formation in gases.

Target Gas	Pressure (atm)	f_μ	f_{Mu}
H_2	2.6	38(5)	62(5)
	3.0	40(5)	60(5)
N_2	1.0	20(4)	80(4)
	2.5	18(3)	82(3)
Ar	0.9	37(7)	63(7)
	2.5	28(5)	72(5)
Xe	~0.5	0(5)	(100?)[a]
Kr	~0.5	5(5)	(100?)
CH_4	1.2	14(5)	86(5)
	2.9	14(3)	86(3)
NH_3	2.5	10(4)	90(4)

[a] In fact, the observed amplitude is only ~10% in both Kr and Xe at ~0.5 atm.

In order to further understand the Mu formation process we have largely completed a series of measurements on the pressure dependence of f_{Mu} in various gases. As can be seen from Table IX, and also by comparison with the earlier LAMPF data (Annual Report 1978), there is, by and large, no such pressure dependence. This result, in fact, is in accord with expectations, at least for those processes which are endothermic, i.e. the μ^+ emerges from a series of charge exchange cycles either as "free" μ^+ or as muonium, subsequently thermalizing by collision processes in the gas. In this picture changing the pressure only changes the time scale for thermalization, which is long compared with the hyperfine mixing time in muonium.

A recent interesting report from LAMPF [Bolton *et al.*, MAPS 24, 675 (1979)] on the fraction f_{Mu} in Kr gas, in which the pressure was varied between 0.1 and 0.5 atm, however, is inconsistent with the above thermalization scheme. The LAMPF people found something like a factor of five loss in polarization, which could be attributed to an enhanced time between charge-changing collisions at the lower pressures. The ionization potential of Kr is 14.0 eV. In our last run in 1979 we repeated this measurement, having measured in an earlier run the dependence of A_μ in Ne (which forms essentially no Mu) as a function of pressure. This is an important consideration in establishing any pressure dependence in f_{Mu}, since the stopping distribution at lower pressures is much broader which creates a large solid-angle effect, contributing to lower measured asymmetries. Such effects are apparent in all gases, e.g. N_2, as can be seen in Fig. 80, which compares the MSR precession amplitude for Mu in 1 and 2.5 atm N_2 pressure. In Kr we find much the same trend as reported at LAMPF but feel that a significant fraction of it is likely due to this solid-angle type of depolarization. Nevertheless, it does appear that considerable intrinsic depolarization remains, which merits further study. Rather similar results were obtained in Xe. Since these data are preliminary at this time, we will not comment on them further here but simply note that additional studies are planned for early in 1980.

Data were obtained in the last run period which will allow us to calculate the "activation energy" for the thermal relaxation process of the μ^+ spin in Xe/Ne mixtures

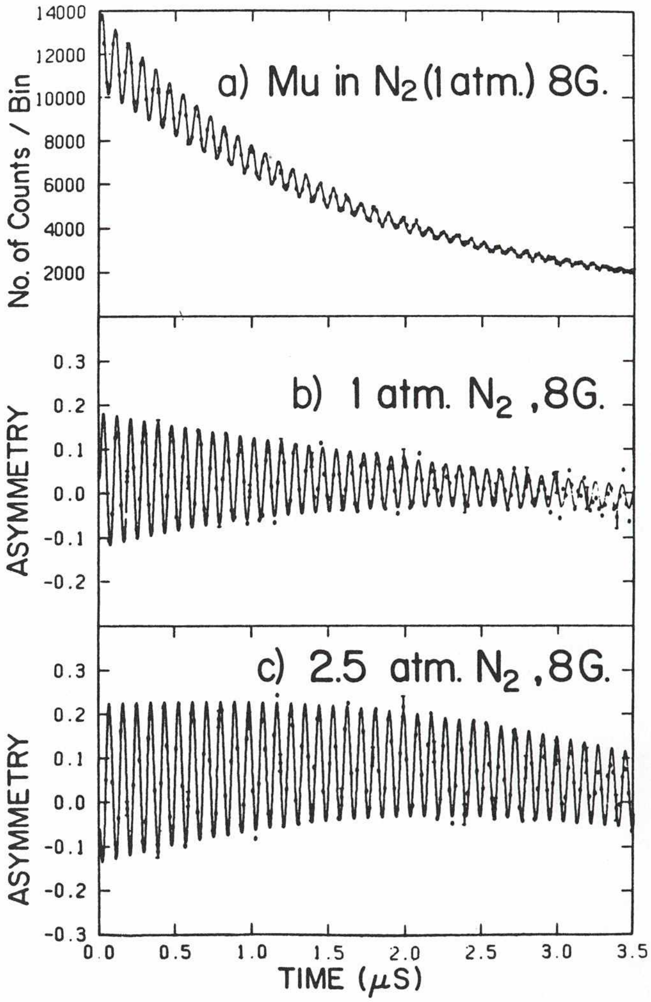

Fig. 80. Measured Mu amplitudes in N_2 gas at both 1 and 2.5 atm pressure. The larger asymmetry at the higher pressure is attributed to a smaller solid angle of acceptance for the decay positrons.

(Fig. 72, Annual Report 1978). This will be important in interpreting the physical basis for this relaxation in these mixtures. The fact that there is a relaxation in Xe/Ne but apparently not in Xe/He mixtures is not understood at this time.

This work was discussed in a poster (31F19) presented at the recent XI International Conference on the Physics of Electronic and Atomic Collisions (ICPEAC) held in Kyoto, Japan, September 1979.

<u>Muonium spin exchange</u>. In collisions with a paramagnetic molecule such as O_2 or NO, Mu may undergo a "spin-exchange" process, represented by $Mu(\uparrow) + NO(\downarrow) \rightarrow Mu(\downarrow) + NO(\uparrow)$, the effect of which is to depolarize the μ^+. This effect manifests itself in a relaxation of the MSR signal, as shown in Fig. 81.

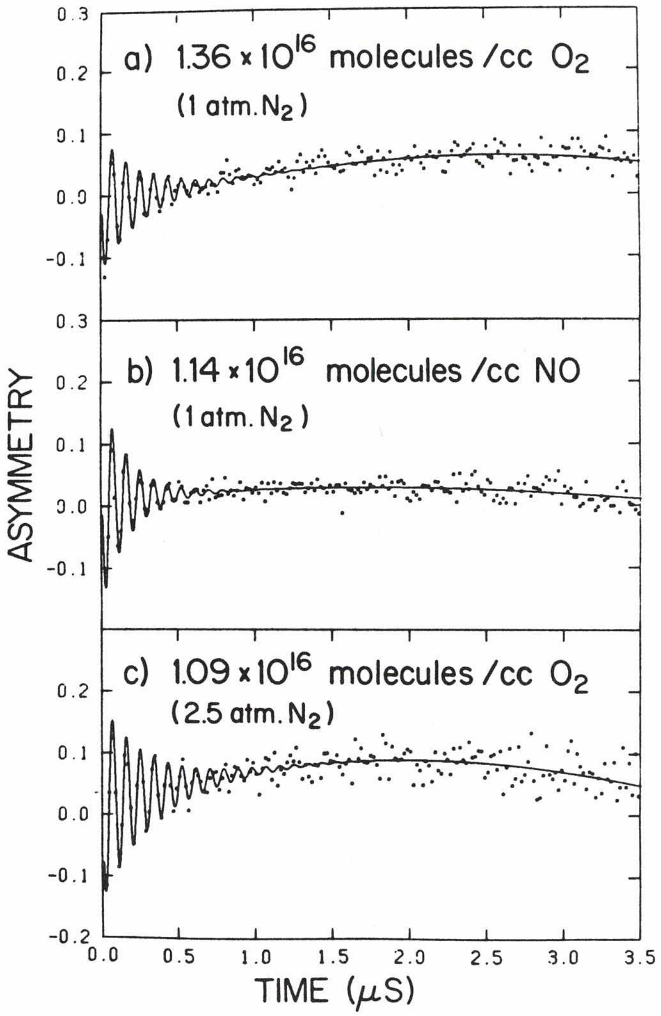

Fig. 81. Relaxation of the muonium precession signal in the presence of small amounts of paramagnetic O_2 and NO. The reaction responsible for the relaxation is believed to be electron spin exchange.

This year we completed room temperature measurements for the spin-exchange reaction Mu + O_2 and Mu + NO at both 1 and 2.5 atm N_2 moderator pressure. The results for Mu + O_2 in N_2 were exactly the same as that found previously in Ar moderator (Annual Report 1978). The bimolecular rate constants were found to be independent of pressure, as shown in Fig. 82 which plots the relaxation rate λ (for Mu + NO) as a function of NO concentration for both 1 and 2.5 atm N_2 pressure. This behaviour is exactly what one would expect for the (2-body) spin-exchange process, confirming the basic nature of the reaction mechanism. This is in sharp contrast to previous data published by Mobley *et al.* [J. Chem. Phys. 44, 4354 (1966)], obtained at ~40 atm moderator pressure. In this case one would expect significant contributions to the extracted relaxation rates from 3-body addition reactions of the type Mu + NO $\xrightarrow{Mu}$ MuNO, particularly in the case of the MuO_2 molecule, which remains paramagnetic. Nevertheless, the cross sections obtained from the relation $k = \sigma\bar{v}$, where k is the measured bimolecular rate constant, in our study and the one of Mobley *et al.*, agree rather well, as can be seen in Table X, which compares also the results for the corresponding reaction with hydrogen.

Table X. Comparison of Mu and H spin exchange cross sections, σ_{SE} ($\times 10^{16}$ cm^2) for NO and O_2.

Molecule	σ_{Mu}(~1 atm)[a]	σ_{Mu}(~2.5 atm)[a]	σ_{Mu}(~40 atm)[b]	σ_H[c]
O_2	7.9±1.2	8.4±0.8	5.9±0.6	~22
NO	10.0±0.7	12.0±1.7	7.1±1.0	~25

[a] R.J. Mikula, Ph.D. thesis in progress. This work was reported at the XI ICPEAC (poster 31F20).
[b] R.M. Mobley, Ph.D. thesis, Yale, 1967.
[c] H.C. Berg, Phys. Rev. 137A, 1621 (1965).

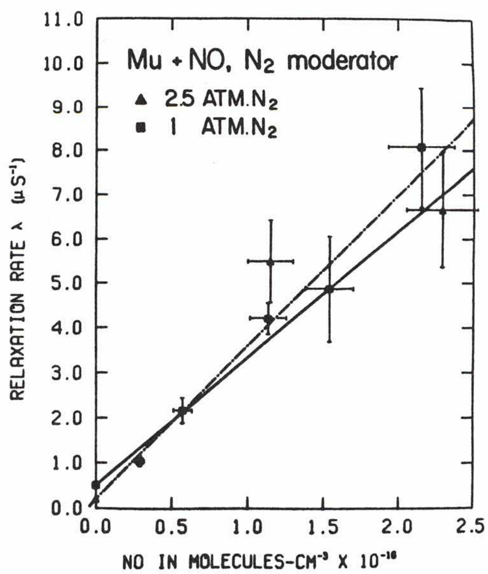

Fig. 82. The spin-exchange relaxation rate for Mu + NO as a function of NO concentration in both 1 and 2.5 atm moderator pressure. The slopes of the lines give the depolarization rate constants, which, in their errors, are pressure independent.

The most interesting thing which emerges from the comparisons in Table X is the fact that σ_{SE} for Mu is a factor of 2-3 less than the corresponding value for H, at least for the molecules O_2 and NO. This result is in marked contrast to the chemical reaction dynamics of the Mu atom where, with notable exceptions, Mu generally reacts much faster than hydrogen since it is assisted in its reaction rates by enhanced quantum-mechanical tunneling [Garner, Ph.D. thesis, Department of Chemistry, UBC, August 1979]. However, the present result is understandable within the "random-phase" approximation. In this approximation the cross section for spin exchange emerges as mass independent, which in a sense is an intuitively "obvious" result (Mu and H and the same size). However, the present experimental result of unequal spin-exchange cross sections at room temperature for Mu and H reacting with O_2 and NO is in sharp contrast to recent theoretical calculations comparing Mu-H and H-H spin exchange [and Shizgal, J. Phys. B., Atom. Molec. Phys. 12, 3611 (1979)], where it is found that, consistent with expectations, the σ_{SE} are the same. It is at low temperatures that Shizgal's calculations reveal a departure from this equality, where the number of partial waves are reduced and the reaction cross section is dominated by specific (mass-dependent) resonances; indeed, at ~50 K σ_{SE} for Mu-H is predicted to be about 5 times greater than for H-H.

These calculations are very interesting but unfortunately difficult (if not impossible) to check experimentally. However, we have embarked on measuring the temperature dependence for the Mu + O_2 and Mu + NO reactions. At higher temperatures (~300-500 K), a preliminary analysis reveals that the reaction rate scales essentially as $\sqrt{T}$, expected from the mean velocity dependence, $k = \sigma\bar{v}$, i.e. the cross sections themselves are T independent. It is at *low* T (~77-300 K) that we would like to extend these studies, looking for specific resonance behaviour. Such experiments are planned for 1980.

Chemical reaction dynamics. Since the muon mass is only 1/9 that of the proton, measurements of the chemical reaction rates of Mu provide a *unique* set of data with which to confront current theories of isotope effects in chemical reaction dynamics, particularly quantum mechanical tunneling [Garner, Ph.D. thesis, UBC, August 1979]. No new data on thermal Mu reaction rates were taken last year but we have obtained some initial studies of "hot atom" Mu chemistry in the gas phase which emerges as a byproduct of Mikula's charge exchange studies. In Table X for example based on proton charge exchange data, we expected f_{Mu} in H_2 to be comparable to N_2 (i.e. ~80%). The large μ^+ signal observed may be a manifestation of the hot atom reaction, $Mu^* + H_2 \rightarrow MuH + H$. We intend on furthering these studies in 1980 by measuring mixtures of H_2 in Ne. In like manner, the μ^+ signal in CH_4 and NH_3 may be due to hot atom reactions (forming MuH again), but in this regard it is perhaps surprising that the μ^+ fraction is as small as it is. Finally, we note that the most fundamental measurement of a thermal reaction rate is $Mu + H_2 \rightarrow MuH + H$, a measurement we plan on carrying out (at ~450 K) in 1980. Present results at room temperature give only an upper bound for a relatively slow reaction rate (as expected).

All of the material discussed above will appear in next year's annual report as Expt. 147, "Muonium formation and reaction dynamics in the gas phase".

Liquid phase studies

The application of μSR and MSR to the study of the kinetics of muonium in liquids has been continued in 1979. Some 36 shifts of M20 beam time (operating in HS surface muon mode) were assigned to the liquid phase experiments, which involve several projects, some continuing, some completed in 1979 and others just started.

Studies of muonium are of interest from three points of view: 1) the intrinsic properties and mode of formation of muonium itself, as an "exotic" chemical species; 2) as a super-light isotope of protium, deuterium and tritium, and consequently as a particularly sensitive measure of kinetic isotope effects; and 3) as a handle on the mechanism of many hydrogen-atom reactions which are not otherwise accessible to direct observation by conventional methods.

Muonium formation. The fraction of muons which emerge from intratrack processes already incorporated in diamagnetic species (P_D) varies considerably, from 1.0 in CCl_4 and 0.9 in $CHCl_3$, through 0.67-0.62 in water, alcohols and saturated hydrocarbons, to 0.2 in CS_2 and C_6H_6. In order to determine the mechanism involved and the chemical properties governing the magnitude of P_D, several mixtures of the above mentioned liquids have now been studied. The cyclohexane-benzene and benzene-CCl_4 mixture data are shown in Fig. 83. For most of the mixtures we have studied, the most pertinent trend is a nearly linear change of P_D with volume composition. This strongly suggests a direct interaction of epithermal muonic species over a small energy range. It seems to be totally inconsistent with competitive processes, as if scavenging and sacrificial protection of one type of molecule by the other is absent. This in turn leads us to believe that intraspur processes do not contribute significantly to muonium formation or reactivity (thereby corroborating our scavenger studies in aqueous solutions as in Annual Report 1978).

When present in small amounts in hydrocarbons both CCl_4 and CS_2 do show limited scavenging characteristics (as evident in Fig. 83). This may be due to reaction with muonium because very recently we measured the rate constant of muonium in CH_3OH with those two solutes. However, a full explanation for the whole variations of P_D with chemical composition has not yet emerged.

In our most recently completed series of experiments we looked for muonium in hydrocarbon media (Mu was hitherto seen only in water, alcohols and low temperature ethers—all containing oxygen) and found it, just, in only one—carefully purified tetramethylsilane (TMS). The spectrum is shown in Fig. 84. Evidently Mu reacts too rapidly with methylene hydrogens; in fact we measured k for Mu in CH_3OH with cyclohexane as a solute to be $\sim 10^6$ M^{-1} sec^{-1}, so that in pure cyclohexane the mean lifetime of Mu is calculated to be too short to observe.

Kinetic isotope effects. We have now completed a study of the temperature dependence of the reaction rate constant for a slow abstraction reaction (Mu reacting with HCO_2^-) and for three types of reaction having the largest value of k (namely, the spin-exchange reaction with Ni^{2+}, the electron-transfer reduction with MnO_4^- and the addition reaction with maleic acid). The results are most interesting and will probably enable us to distinguish the involvement of diffusion controlled encounters from quantum mechanical tunneling processes. Any kinetic isotope effects compared with H may also be revealed and could aid this distinction.

Another study of kinetic isotope effects involved measurement of the reactivity of Mu

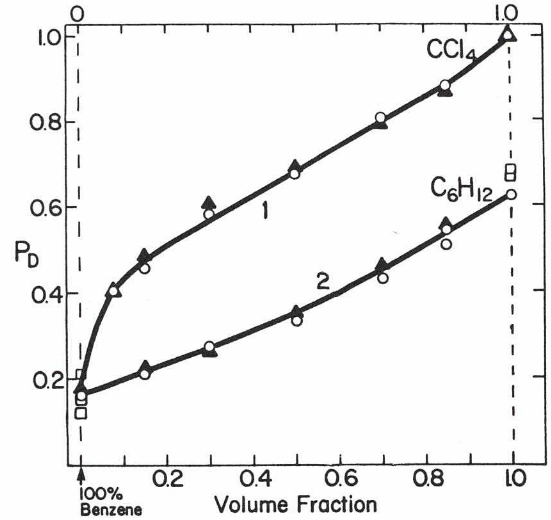

Fig. 83. Plots of the observed diamagnetic muon fraction P_D as a function of composition of solvent mixtures (benzene-CCl_4 and benzene-cyclohexane).

with O_2 in aqueous solution, and in this case a direct comparison was also made with the same reaction in the gas phase. The data are shown in Fig. 85; from the slope of the line k = (2.4±0.5) × 10^{10} M^{-1} sec^{-1} showing to what extent samples have to be deoxygenated in order to avoid interference by oxygen in typical MSR experiments.

The two types of experiment mentioned above involved our first application of the thin teflon cells to MSR measurements at different temperatures and in the presence of a controlled amount of a gas as a solute in solution.

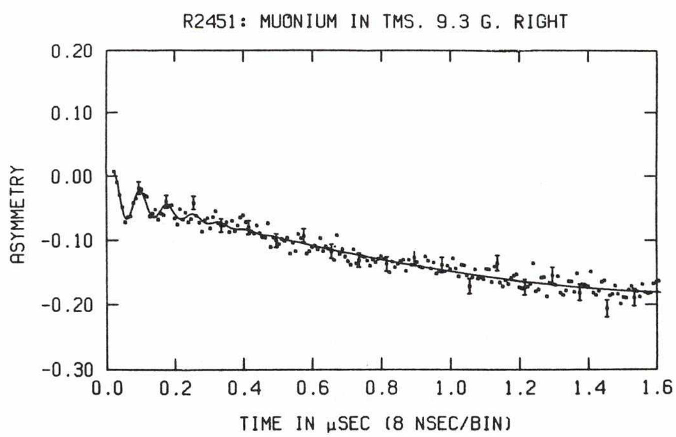

Fig. 84. MSR spectrum showing the muonium precession signal in tetramethylsilane.

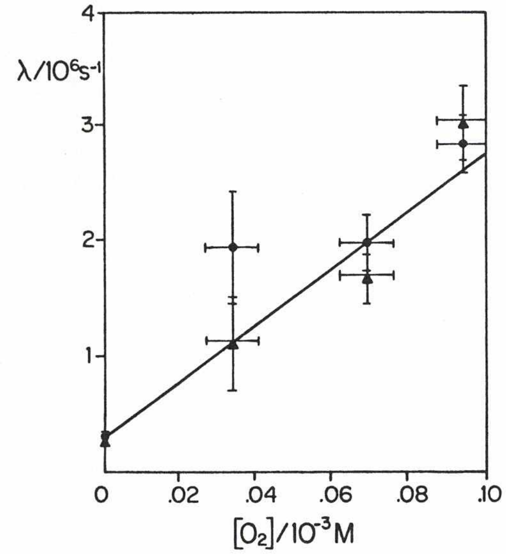

Fig. 85. Plot of the observed decay constant λ against O_2 concentration. (● left-hand side detector, ▲ right-hand side detector.) The line drawn is the least squares fit.

Muonium reactivity with biologically significant systems. Two of the incomplete projects involved chemical systems which are often regarded as simple "models" of biologically important systems. Both projects were successful and produced interesting results. First, the reactivity (specifically, the chemical reaction rate constant) of Mu with phenol as a solute was found to be almost exactly twice as large when the phenol was enclosed in a micelle (sodium decyl sulphate at >0.1 M). This could imply one of three things: either the micelle enhanced the initial encounter probability (effective reaction radius), or the presence of the enclosure enhanced the number of collisions per encounter of the reacting species, or there is a solvent effect in which the hydrocarbon medium is more favourable for reaction than the outside aqueous medium. More experiments are needed.

Second, the reaction rate for Mu with hemin ($k = 3 \times 10^9$ M^{-1} sec^{-1}) was three times that with protoporphyrin. Both these solutes are porphyrins extracted from their normal protein embellishments and differ in only one respect—the hemin contains a Fe^{3+} ion instead of two protons. These are also merely preliminary experiments of a planned series, but the implication is that the porphyrin jacket actually protects the Fe^{3+} because we have measured k for Mu with $Fe^{3+}(H_2O)_6$ and with $Fe(CN)_6^{3-}$ to be 5.5 and 20 × 10^9 M^{-1} sec^{-1}, respectively (see Annual Report 1978).

Since H atoms are formed by high-energy radiations in aqueous media (and therefore in almost all biological systems), the reactivity of H has to be understood in order to elucidate radiobiological effects. But H atom reactions cannot easily be monitored (except by comparatively slow ESR methods), which fact emphasizes the potential importance of utilizing muonium as a handle on H atom reactions.

The experiments described above will appear under Expt. 157 in future annual reports.

Residual muon polarization. The liquid chemistry program made use of the high current period at the beginning of November (10 shifts) to perform its first "production" run with backward muons on M20. The main goal was a study of residual muon polarization in aqueous solutions of K_2CrO_4. Eight different concentrations were measured at each of six different magnetic fields. A subsidiary goal was the search for muonium-substituted free radicals in systems where they have been detected at SIN. Weak signals were indeed found at the expected frequencies in a sample of benzene. The program has just begun and will appear henceforth under Expt. 150.

Solid state chemistry

Last year the search (in transverse magnetic field) for chirality-dependent Mu formation in quartz crystals was completed. The motivation for the experiment came from measurements of e^+ annihilation in various chiral media, in which a sensitivity in $3\gamma/2\gamma$ annihilation to the "D" vs. "L" nature of the stopping medium has been reported [Garay, Nature 250, 332 (1974)]. His results have not yet been corroborated, but the high polarization of the muon relative to the positron offers the possibility of more sensitive probe. Both forward and backward positive muons from the M20 channel were stopped in both L- and D-quartz in a series of runs with the initial muon momentum and hence the spin-direction both parallel and perpendicular to the principal optic axis. The sign of the optical rotation is opposite for the two orientations. The results of an analysis of several runs of the Mu amplitude (in ~10^8 total events compared to ~10^6 for a typical MSR run) yield an orientation difference of 0.6±0.7%; i.e. consistent with zero [Spencer *et al.*, Proc. Symposium on Optical Activity, Vancouver, June 1979 (North-Holland, Amsterdam, 1979), p. 87].

We have also initiated several runs on searching for Mu in various solids, such as diamond, zircon, GaP, $A\ell_2O_3$, as well as continuing our studies on the quadrupole interaction of muonium in quartz crystals. This work naturally falls under the auspices of Expt. 91 in the present report but will appear henceforth under Expt. 154.

Experiment 60
Muonium formation

Muonium and positronium formation in oxide powders

For a number of investigations it is desirable to have a dense source of Mu or Ps atoms of thermal velocity moving in vacuo. Brandt and Paulin [Phys. Rev. 21, 193 (1968)] first observed the presence of Ps in the voids in finely divided powders of MgO, $A\ell_2O_3$, SiO_2. A number of other powders have been examined as to Mu formation with results which show qualitatively similar formation of Mu and Ps. In some examples such as GeO_2 there is a large "missing fraction", i.e. one which shows no precession at the Mu frequency and only a small amplitude precession at the μ^+ frequency. This missing fraction is attributed to fast-relaxing Mu atoms since such atoms are 100 times more sensitive to random local magnetic fields and are capable of depolarizing through spin exchange and chemical reactions.

Evidence in the case of Ps in MgO and SiO_2 strongly suggests that the Ps atoms form within the grains and are expelled from the surface with an energy of ~1 eV [Gidley, Phys. Rev. Lett. 37, 729 (1976)].

In the case of SiO_2 powders investigated, the Mu fraction formed is independent of the grain size and comparable to that in bulk quartz, indicating that the surface plays no role in the formation. In a MgO single crystal also, the Mu fraction is comparable to that observed in the powder. Hence it is believed the initial formation of thermalized Mu atoms is a bulk property.

Again there is strong evidence that Mu leaves the surface and is not bound to it, just as in the case of Ps. First the rate of change of the relaxation rate with oxygen pressure in fine SiO_2 powder is the same as measured in argon gas. This rate constant is the thermal average $\overline{\sigma v}$, where σ is the spin-exchange cross section and v the Mu speed, and it seems unlikely that this average would be the same for Mu atoms on the surface of a grain as in argon. Secondly a single foil experiment has been performed in which a narrow angle positron telescope looked at a region 1 cm beyond a single collodian foil coated with SiO_2 through which a muon beam was passing. The exponential decay spectrum was found to be slightly enhanced at about 2 μsec delay incident μ/positron signal. Such an enhancement would be expected from Mu atoms formed in the foil and emerging with near thermal energies. Thirdly an experiment with MgO powder showed that the Mu relaxation rate increased as the free volume density decreased—the powder being compressed changed its density a factor of approximately 3. Relaxation occurring on the surface of grains would be expected to be independent of free volume density.

An experiment has also been performed to check the relaxation of Mu in a number of oxides just above liquid helium temperatures. With most samples there was no significant change, indicating that diffusion-controlled relaxation mechanisms such as spin-exchange or chemical reactions, which should be quenched at low temperatures, were not playing a role. However, in one sample $A\ell_2O_3$(γ form) a sharp change occurred at 12 ± 1 K.

Measurements have also been made on the temperature dependence of Ps spin conversion due to oxygen in an SiO_2 powder moderator. The quenching in this case is due to the spin conversion, oxygen being paramagnetic, ortho-Ps + O_2 → para-Ps + O_2. At room temperature this quenching is three orders of magnitude slower than the corresponding rate calculated for H [Hara and Fraser, J. Phys. B: Atom. & Molec. Phys. 8, L472 (1975)].

$M\overline{M}$ conversion experiment

Two experiments to search for the conversion of muonium to antimuonium have been completed.

In the first a beam of surface muons of high luminosity from the M13 channel was stopped in argon gas at 1 atm in an environment in which by a triple Helmholtz coil the magnetic field was kept below 2 mG. μ^- mesic X-rays from Ar were looked for using two large Ge detectors; none were seen. The sensitivity of the arrangement was checked by switching the beam line to deliver 42 MeV negative muons to the chamber, when the 2P-1S 644 keV transition and the 3P-1S 771 keV transition were observed in about 10 min running time. This experiment essentially repeated that of Amato *et al.* [Phys. Rev. Lett. 21, 1709 (1968)] with higher sensitivity.

A second experiment was performed using as a source of Mu atoms in vacuo a series of 14 thin collodian foils coated on one side with CaO and dusted on the other with SiO_2 powder. The foils, spaced by 4 mm, were at 30° to the horizontal plane and offered a total stopping power of $\sim$20 mg/cm^2. In this case again neither Ca(2P-1S) nor Si X-rays were observed after a total of 2×10^{10} muons had been stopped in the target. Rough preliminary analysis indicates a lower limit of $G_{M\overline{M}} \lesssim 80\ G_V$ from this data.

Formation of muonium in oxide powders

We have continued to study both Ps and Mu atom formation in oxides, since we have obtained general evidence that their formation is qualitatively similar, and some insight has been gained into the baffling problem of Mu formation from this comparison. Further we have established to our satisfaction that Mu atoms do diffuse out of silica grains and are not depolarized while sitting on the surface of the grains when a little oxygen is introduced into the voids.

Formation experiments. Table XI summarizes the results, and it is clear that a qualitative similarity exists between formation of ortho-Ps and Mu. Qualitative accord is hardly to be expected since the ionization potential of Mu is 13.6 and Ps 6.8 eV. Thus $A\ell_2O_3(\gamma)$ at room temperature, one of the most prolific ortho-Ps producers, shows only what appears to be an exceedingly fast relaxing Mu precession signal—so fast we were unsure initially if it was there. Whether this fast relaxation is due to the large nuclear moment of $A\ell$ is not known.

In several cases there is a large missing fraction (e.g. GeO_2) which most likely represents Mu which has been rapidly depolarized in times $\lesssim$ 2 nsec. The MSR technique detects only slow-moving polarized atoms. Relaxation of Mu is more likely than of μ^+ since such atoms are 100 times more sensitive to random local fields, and both spin-exchange and chemical reactions may depolarize.

In the case of SiO_2 powders investigated the grain size does not affect Mu fraction which is comparable to bulk quartz, indicating that the surface plays no role in the formation. In an MgO crystal (at 6 K) likewise the Mu fraction is comparable to that observed in the powder.

About the only common feature among the prolific oxide producers SiO_2, MgO, $A\ell_2O_3$, In, CeO would seem to be large holes in the lattice perhaps big enough for H atoms to move along as such (H^- ion diam 1.54 Å, H atom diam 1.06 Å).

Diffusion-related experiments. Our early experiments with very fine SiO_2 (35 and 70 Å) showed both strong ortho-Ps and Mu signals which could be quenched by adding a little oxygen. This strongly suggested—as believed for Ps—that Mu was diffusing to the grain surface drifting into the voids and relaxing there.

The relaxation rate as f^n (O_2 pressure) followed a curve closely similar to Ar + O. The rate constant is the thermal average $\overline{\sigma v}$, where σ is the spin-exchange cross section and v the Mu speed, and it seems unlikely this would be the same for Mu atoms on the grain surface as in Ar.

To confirm this hypothesis—on which our $M\overline{M}$ experiment is based—a single foil experiment has been performed in which a narrow angle e^+ telescope looked at a region 1 (and 2) cm downstream of a collodian foil dusted with SiO_2 through which a beam of μ^+ was passing. The exponential time decay spectrum was found to be enhanced a little at 2 μsec delay between incident μ^+ and e^+ signal. Such an enhancement would be expected from Mu atoms formed in the foil and emerging near thermal energies.

Further, an experiment with MgO powder showed the Mu relaxation rate increased as the free volume density decreased—compression of powder changed its density by 3 times. Relaxation of Mu on grain surface would be independent of free volume density.

Table XI. Summary of Mu formation in insulators.

Sample	Sample description	Polarized muon fraction (%)	Polarized Mu atom fraction (%)	Missing fraction (%)	Mu atom relaxation rate (μsec^{-1})	Ortho-Ps fraction (%)
SiO_2	70 Å diam powder 300 K	35 ± 5	61 ± 3	4	0.188 ± 0.010	26.4 ± 2.6
SiO_2	70 Å diam powder 6 K		49 ± 3		0.46 ± 0.03	
MgO	300 Å diam powder 300 K	71 ± 6	15 ± 3	14	4.6 ± 1.3	14.3 ± 1.4
MgO	300 Å diam powder 6 K	56 ± 6	12.6 ± 3	31	0.22 ± 0.02	
$A\ell_2O_3(\gamma)$	300 Å diam powder 300 K	72 ± 4	35 ± 14	-7 ± 15	11.3 ± 4.4	24.6 ± 2.4
$A\ell_2O_3(\gamma)$	300 Å diam powder 6 K	50 ± 5	29 ± 3	21 ± 6	0.30 ± 0.03	
GeO_2	Coarse powder 300 K	40 ± 7	nil	60 ± 7		
GeO_2	Coarse powder 6 K	28 ± 5	nil	72 ± 5		
CaO	Coarse powder 300 K	43 ± 3	35 ± 4	22 ± 5	2.5 ± 0.6	
CaO	Coarse powder 6 K	34 ± 5	27 ± 5	39 ± 7	1.7 ± 0.3	
$Ca(OH)_2$	Coarse powder 300 K		nil			
$Ca(OH)_2$	Coarse powder 6 K	41 ± 7	nil	58 ± 7		
$A\ell_2O_3(\alpha)$	5000 Å diam powder 6 K	40 ± 5	nil	60 ± 5		
$A\ell_2O_3$	Fused solid 6 K	20 ± 10	nil	80 ± 10		
ZnO	1120 Å powder 300 K		nil			
ZnS	Coarse powder 300 K		nil			
ZnS	Coarse powder 6 K	48 ± 5	nil	52 ± 5		
C	Graphite 300 K, 10,000 Å powder	101 ± 3	nil	-1 ± 3		
U_2O_8	Single crystal 6 K	<14	nil	>86		
MgO	Single crystal 6 K	<21	38 ± 10	>41	6.3 ± 1.5	
SiO_2	Silica gel 300 K		46 ± 10		1.7 ± 0.4	
SiO	Coarse powder 300 K	63 ± 1	nil	37 ± 1		
SiO	Coarse powder 6 K	38 ± 5	nil	62 ± 5		
TiO_2	Coarse powder 300 K		nil			
BeO	Coarse powder 300 K		nil			
ThO	Coarse powder 300 K		nil			
MoS_2	Coarse powder 300 K		nil			

Measurements of relaxation rates at 6 K for Mu in MgO, SiO_2, $A\ell_2O_3$ powders in a helium atmosphere are small, $\sim 0.3\ \mu sec^{-1}$ and roughly the same, in sharp contrast to observations at room temperature for powders and bulk samples. This again suggests Mu atoms diffuse into voids and relax slowly by collisions at grain surface (which might be coated with He at this temperature).

The relaxation rate in $A\ell_2O_3$ changed dramatically at 12±1 K.

Measurements on other oxides at low T to check that the absence of a Mu signal was not merely a result of diffusion-controlled relaxation (via spin exchange or chemical reaction) which should be quenched at low T, showed no significant change from room to 6 K.

Measurements have also been made on T dependence of ortho-Ps spin conversion due to O_2 in SiO_2 powders, where the quenching is known to be due to spin conversion oxygen being paramagnetic

$$\text{ortho-Ps} + O_2 \rightarrow \text{para-Ps} + O_2 \ .$$

At room temperature this quenching is 3 orders of magnitude lower than the corresponding rate calculated for H by Hara and Fraser.

Figure 86 shows on a site plan the location of Applied Program facilities. Two journal articles [Pate and Sample, Physics in Canada 35, 20 (1979); Pate, Chemistry in Canada 31, 28 (1979)] and a conference paper [Pate, Proc. Mtg. of American Nuclear Society, San Francisco, November 1979 (to be published)] were written this year on the program as a whole.

In 1979 the B.C. Cancer Foundation conducted the first pion irradiations of cancer patients, as described in detail below.

This year the 500 MeV spallation of cesium continued to be the principal source of supply of ^{123}I for the TRIM program described below. At the same time the 70 MeV beam, of which extraction from the TRIUMF cyclotron was described last year, was equipped with beam-monitoring facilities and a molten NaI target for the production of ^{123}Xe-^{123}I via the (p,5n) reaction, with greater purity from ^{125}I contaminant. In December the first ^{123}Xe was transported from this target to a trailer radioisotope laboratory installed on the north cyclotron shielding berm by AECL (see below) and equipped with trapping and purification equipment. An initial batch of 150 µCi of ^{123}I was produced.

Arrangements were completed between the British Columbia Research Council and TRIUMF through the TRIM group for development of a commercial ^{127}Xe recycling apparatus for medical applications.

In beam line 4A irradiations of solid targets were accomplished first in the 'in-air irradiation facility' and later in a more automated system accommodating nickel-sized targets, described below. Arsenic oxide and other targets produced tracer quantities of ^{67}Ga, ^{68}Ge-^{68}Ga and other nuclides for check-out of commercial-scale production chemistry by AECL personnel, while nickel targets produced ^{52}Fe for radiopharmaceutical research. The 'interim radioisotope laboratory' continued to be the site of processing these targets, and a curie-level hot cell, constructed last year, was commissioned for this work.

Preliminary experiments were conducted in the 'in-air irradiation facility' on production of ^{11}C, ^{13}N, ^{15}O and ^{18}F via 500 MeV

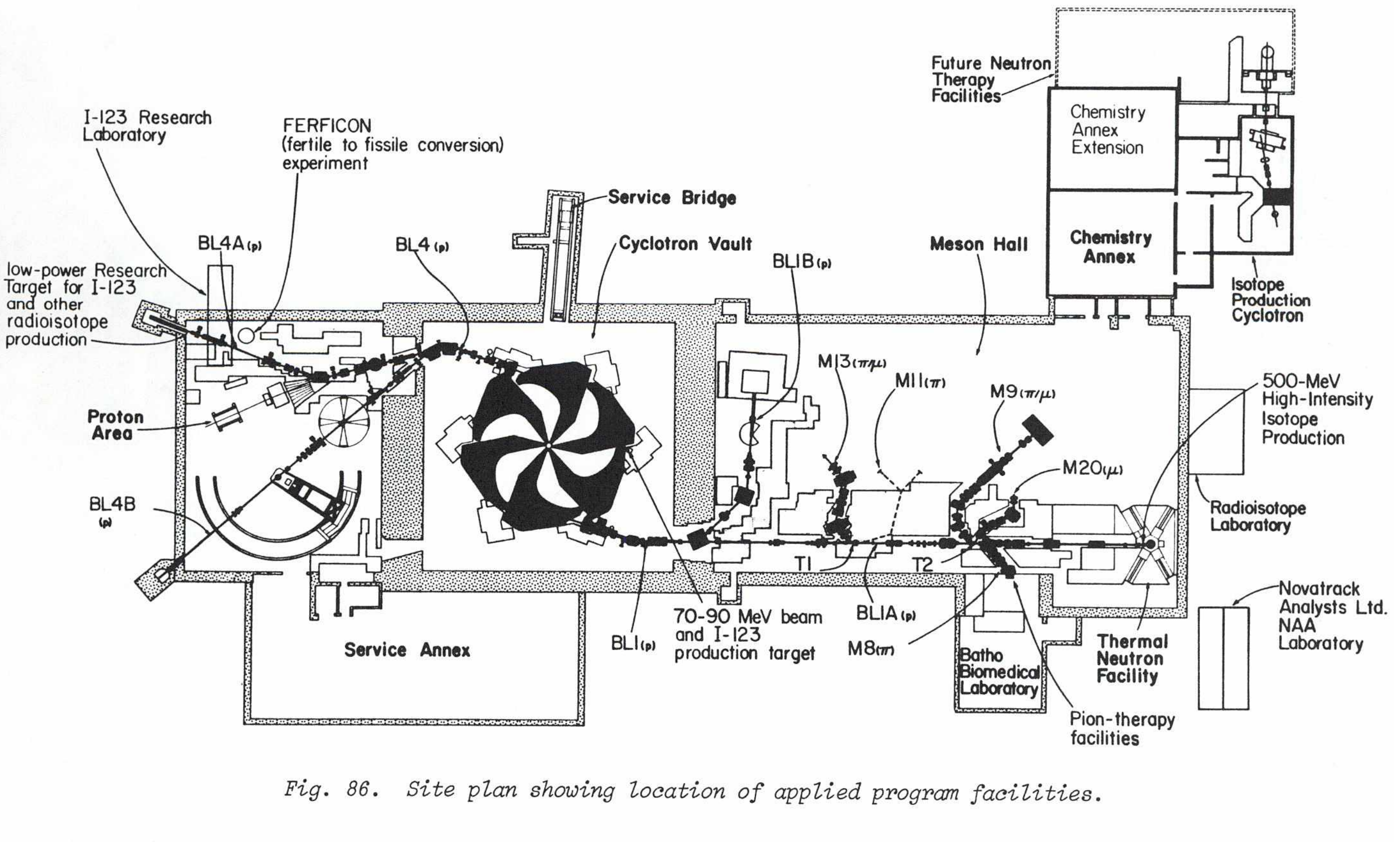

Fig. 86. Site plan showing location of applied program facilities.

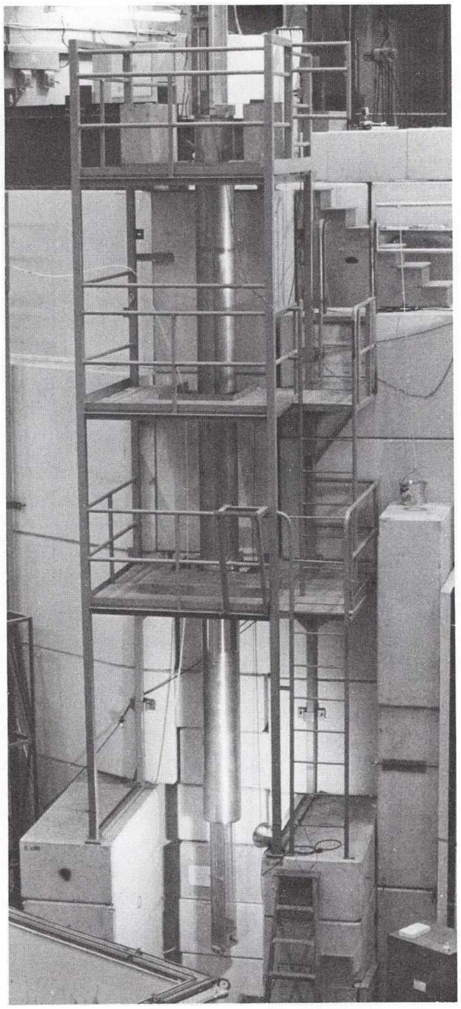

Fig. 87. 500 MeV irradiation facility assembled and under test prior to its installation in beam line 1A upstream of the TNF.

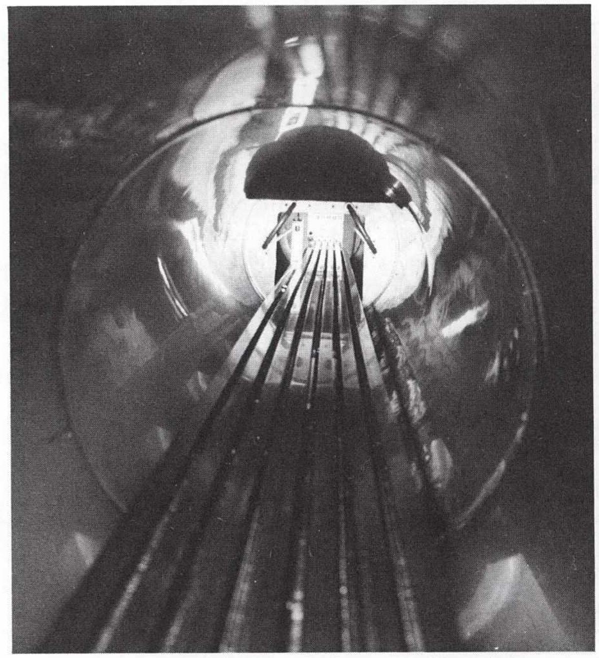

Fig. 88. Vertical view down the 500 MeV irradiation facility water tank. The 6 chain drives for insertion of targets in the proton beam are clearly seen.

spallation of gaseous targets for a program in positron emission tomography applied primarily to neurological science. A gas target for installation in beam line 1 was designed.

Progress continued in 1979 towards implementation of the agreement between TRIUMF and Atomic Energy of Canada Ltd., Commercial Products Division, on commercial distribution of TRIUMF-produced radioisotopes and radiopharmaceuticals. Construction of the extended chemistry annex and its equipment for this program and for radiopharmaceutical research continued and was almost complete at year's end.

A vault was included for installation of a CP-42 negative ion 42 MeV cyclotron from the Cyclotron Corporation. The vault walls were poured with concrete containing less than 0.25% sodium to reduce ^{24}Na gamma radiation fields from neutron activation. Construction progress on the CP-42 cyclotron continued towards a mid-year delivery in 1980. A scheme for precessional injection into the CP-42 was investigated.

AECL commenced construction of 100-Ci-level hot cells in the chemistry annex with completion expected in February 1980.

Development and construction of the 500 MeV irradiation facility (for irradiation of targets for the TRIUMF-AECL production program) was almost complete at the end of the year, and installation in beam line 1A was under way. The facility was described in detail in a paper presented at the American Nuclear Society meeting in San Francisco [Burgerjon *et al.*, in Proc. (to be published)]. Figure 87 shows the facility in a test stand prior to installation, and Fig. 88 is a view vertically down the track carrying targets into the proton beam.

Exploitation of the TNF neutron fluxes continued this year under the agreement between TRIUMF and Novatrack Analysts Limited. Commercial geological exploration samples were analysed by Novatrack for gold, uranium and other metals, and environmental samples were analysed for natural radioisotope content. Neutron irradiations and neutron activation analysis of samples were conducted for researchers from UBC, SFU and UVic under the terms of the TRIUMF-Novatrack agreement.

A study was pursued of means to exploit the available neutron fluxes in the TNF more effectively for the simultaneous irradiation of larger numbers of samples.

Studies of fertile-to-fissile conversion continued this year under contract between SFU and AECL and are described below.

Progress in the area of proton radiography continued this year, as described below.

Experiment 61
Biomedical program

During 1979 we have had, for the first time, significant amounts of 100 μA operation. This has allowed most of the remaining preclinical studies contained in proposal 61 to get under way, and it has also been possible to launch the first patient treatments with the M8 pion beam at TRIUMF.

Mouse skin experiments, which were begun in 1978, have been extended to a variety of different dose fractionation regimes including 1, 2, 10, 16 and 20 dose fractions, analogous to the different dose fractionation regimes which will be used in radiation therapy. The results of one 10-fraction experiment are shown in Fig. 89. Identical experiments were carried out using two groups of mice, one group receiving 10 equal doses of X-rays over a period of 3 days, while the other group received 10 equal but lower doses of peak pions. Only 1 hind foot of each mouse was irradiated, and the skin reaction was scored daily when it reached a maximum, two-three weeks later. Figure 89 shows the resulting skin reactions, averaged over seven days centred about the peak reaction. The ordinate scale is a standard scoring scale which assigns numerical values to different qualitative features of the skin reaction. It is evident that for a given dose per fraction, say 4 Grays, the pion reaction is much more severe. In fact, the relative biological effectiveness (RBE) of pions for this normal tissue effect can be evaluated from the ratio of the X-ray and pion doses which produce equivalent skin reactions. The RBE

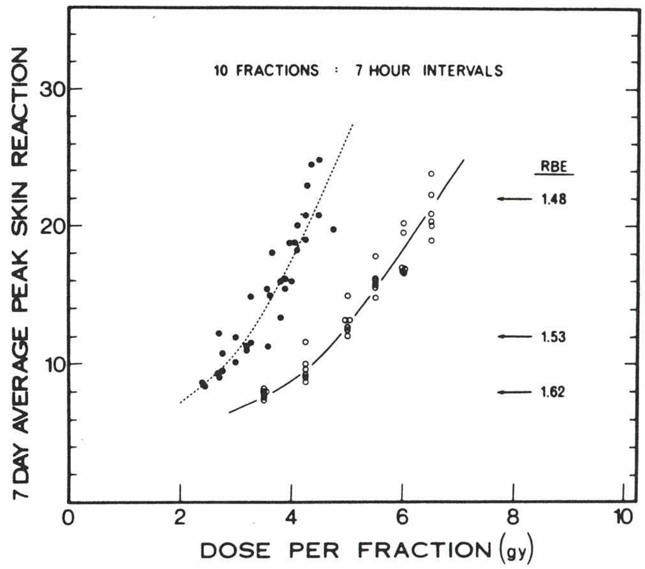

Fig. 89. Dose response curves for mouse foot skin reactions obtained after irradiation with 10 equal dose fractions of pions (closed circles) or 270 kVp X-rays (open circles). The interval between dose fractions was approximately 7 h. Each point represents one mouse foot.

values determined in this way for various skin reaction levels are shown in the figure, and they vary from 1.48 to 1.62, depending on the reaction level. The results of the first four mouse skin experiments are summarized in Table XII. It can be seen that the RBE values increase with increasing fraction number, probably indicating that there is less repair between successive dose fractions with peak pions than with X-rays.

In May a comparable experiment was carried out with pigs. This was noteworthy, among other reasons, by virtue of the fact that it was the world's first intentional pion irradiation of pigs. Selected areas (4 cm diam) of

Table XII. RBE values for peak π^- relative to 270 kVp X-rays obtained at TRIUMF using the mouse foot system.

Experiment number	Number of fractions	Hours between fractions	RBE
1	1	-	1.1
2	2	24	1.2
3	10	7	1.5
4	10	9	1.4

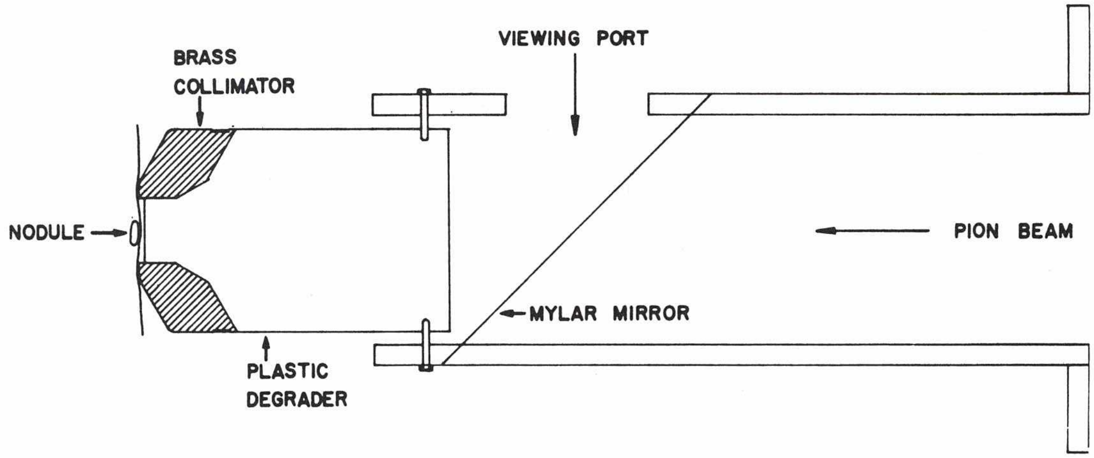

Fig. 90. The pion beam collimator used to deliver a beam of circular cross section, 4 cm diam. This was used for the human skin nodule irradiations as well as for the pig skin experiment. The 45° mirror allows continuous viewing of the treatment area, for accurate positioning. The Perspex degrader is of sufficient thickness to place the pion stopping peak at the skin surface.

the skin of each pig received either X-ray or pion treatment in 10 daily fractions, a regime which exactly duplicated the one to be used for the first patient irradiations in November. Aside from occasional housekeeping problems, this experiment, too, was successfully executed, providing further evidence that the cyclotron is indeed able to deliver 100 μA on demand with a good degree of reliability. The RBE for the early skin reaction was 1.4-1.5, in good agreement with the mouse skin experiment. The results for late effects on pig skin (>4 mo) are still being evaluated, though there are indications that the RBE may be somewhat larger in this case.

With the successful completion of the series of mouse skin studies and the 10-fraction pig skin study, it was possible, in November, to initiate the first patient treatment protocol at TRIUMF, the human skin tumour nodule. In the period November 1 to December 9 four patients with multiple subcutaneous tumour nodules (which generally arose from primary disease elsewhere) received 10 dose fractions of peak pion irradiation in 12 days to one of the tumour nodules while the remaining nodules received conventional X-ray treatment using exactly the same fractionation regime. The pion doses used were chosen according to the RBE values derived from the mouse and pig skin studies. Figure 90 shows the pion beam collimator which was used for the patient treatments on beam line M8. It delivers a horizontal beam of circular cross section, 4 cm in diameter, as defined by a brass collimator which is in contact with the patient's skin. A 45° inclined mirror and closed circuit TV permits continuous monitoring of the position of the tumour nodule during each treatment, which requires approximately 15 min.

Preliminary indications from the first four patients suggest that the RBE of peak pions for early reactions in human skin is approximately 1.4, as predicted by the mouse and pig experiments. This protocol will be continued in 1980.

Progress towards other patient treatment protocols (bladder, advanced cervix, etc.) requires large beam sizes and pion stopping volumes and must await proton beams of 200 μA (500 MeV) or equivalent.

Continuing preclinical studies with cultured cells have concentrated on providing the necessary RBE information to permit the development of pion stopping profiles with uniform biological effect throughout the stopping region. This capability will be required for patient treatments involving larger tumour volume. A variable thickness degrader system is being developed to provide the necessary range modulation for this application. Other cultured cell studies have examined the effect of pions on hypoxic cells, to determine the importance of the oxygen effect for pion beams; we have also investigated cellular recovery between dose fractions of pions.

Experiments 77, 93
Isotope production

Highlights of the medical isotope research project this year have been operation of the cesium spallation facility at full power for the ^{123}I pilot distribution program and the first clinical use of a locally produced radiopharmaceutical for research. In addition, new facilities have been commissioned for solid target bombardment and chemical separations.

At the close of 1978 the TRIM group had produced the first few millicuries of ^{123}I from the spallation target for distribution to clinics across Canada. Progress during the year is evident in Fig. 91 which shows the millicuries shipped per run. The quality of this product has been established as inferior to iodine produced by the (p,5n) reaction but is acceptable for use within 24 h from production. The principal contaminants at that time are ^{125}I, <2.0% and ^{121}Te, <0.2%. Distribution of the material by air over distances as great as 4000 km posed little problem once the logistics had been established. TRIM ^{123}I has been used in the remote clinics for thyroid studies and the development of iodinated pharmaceuticals. Toward the end of the year continued funding was sought and acquired from Vancouver Foundation.

The TRIM group has commenced clinical trials of ^{123}I-labelled fatty acids for the assessment of myocardial disease. Patients with coronary disease and healthy volunteers have received iodinated fatty acid preparations at Vancouver General Hospital. Heart scans can reveal the anatomical location of ischemic or infarcted tissue. The general metabolism (catabolism) of fatty acids has been studied in a kinetic analysis of the scans. Several distinct types of metabolic patterns have been discovered in diseased hearts.

In another project ^{123}I-labelled iodo-deoxyuridine (IUDR) has been produced. IUDR can be incorporated by cells into DNA in place of thymidine. Using IUDR we hope to visualize the overall distribution of DNA synthesis in humans.

The ^{52}Fe program has continued on two fronts. Firstly, the new target system and hot cell noted in the 1978 annual report have been commissioned. Up to 100 mCi of spallation products can now be safely generated and processed. Work has started on the study of the porphyrin family (related to the oxygen-carrying component of hemoglobin) as a carrier for ^{52}Fe. These agents are known to localize in certain human tumours and have previously been detected in skin and esophageal sites using an ultraviolet fluorescence technique. Measurements of tissue culture uptake of tagged porphyrins are under way and will be followed by animal distribution studies using gamma-ray scintigraphy in the coming year.

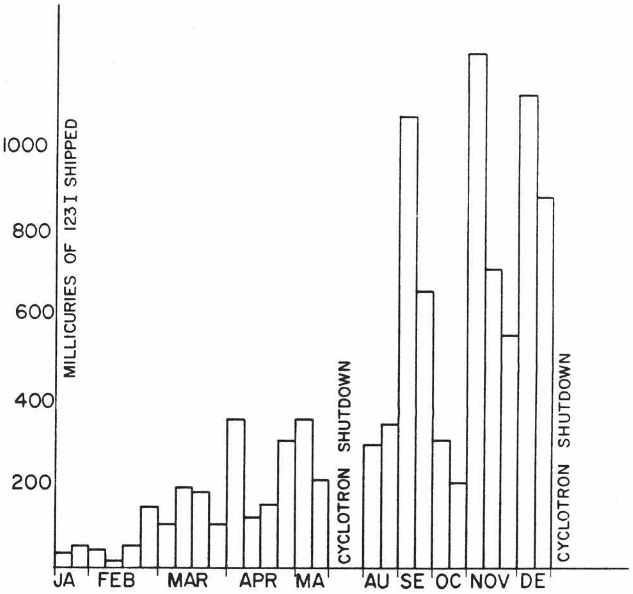

Fig. 91. ^{123}I shipped during 1979 to clinics in Toronto, Winnipeg, Edmonton and Vancouver by TRIM.

Experiment 48
Fertile-to-fissile conversion (FERFICON)

Analysis of the experimental data taken on the source strengths of neutrons leaking from thick targets of lead, thorium and depleted uranium during bombardment, with 480 MeV protons, was completed during the year. The thermalized neutron capture rate in the water bath surrounding the target was deduced from measurements of the activation induced in thin gold foils. The integral proton current for each bombardment was deduced from the ^{24}Na production in thin aluminum foils placed ahead of the targets. The targets were mostly multiple cylindrical rods, 305 mm long, assembled in hexagonal arrays to produce targets of various diameters. The dimensions of the targets studied are shown in Table XIII. Measurements were made on one target assembly of natural uranium dioxide also, as shown in Table XIII.

The deduced neutron capture rates per 480 MeV proton incident on the target are shown in Table XIV. The full primary data sets contained flux measurements from approximately 75 bare gold foil activation sites and (in an auxiliary bombardment) approximately 40 cadmium-covered gold foil activation sites. The latter were required to establish the effective thermal neutron capture cross section for the bare gold foils. The partial primary data sets contained only ~40 bare foil points and were used only as reproducibility checks on the full data sets. The composite targets of lead-thorium and lead-uranium contained lead central elements with thorium and uranium surrounding blankets. The calculated results were produced by P. Garvey of Chalk River Nuclear Laboratories and will be reported in a forthcoming publication of the experimental and calculation results.

Table XIII. Target dimensions (target rod lengths all 305 mm unless otherwise noted).

Material	Rod diameter (mm)	Number of elements in arrays studied
Lead	101.6	1
	38.4	1, 7
	32.4	1,7 (as central cores of composite Pb-U targets)
	41.9	1,7 (as central cores of composite Pb-Th targets)
Depleted uranium (0.26% ^{235}U)	32.4	1, 7, 19, 37, 37i[a]
Thorium	41.9	1, 7, 19
UO_2 (0.71% ^{235}U)	23.8	37 (inside 0.5 mm thick aluminum sheaths) length = 248 mm

[a]Central element taking incident proton beam was 152 mm long covering back half of target only. Outer 36 elements were all normal 305 mm length.

Novatrack

In February Novatrack Analysts Ltd. entered into an agreement with the Department of Supply and Services to develop and operate a neutron activation analysis (NAA) laboratory at the thermal neutron facility (TNF) of TRIUMF. In the first years of operation four irradiation tubes were installed in the TNF. This provided access to a neutron flux which averaged 2×10^{11} neutrons/cm^2/sec during the cyclotron operating periods in 1979. An ionization-type flux monitor was installed, which measures the flux on a continuous basis. Two pneumatic rabbit systems were installed to move samples from the Novatrack trailers to and from the TNF. A storage facility was also constructed, which is large enough to accommodate a year's

Table XIV. FERFICON water bath results. Neutron captures in water per 480 MeV proton incident.

Target	Full primary data set	Partial primary data set	Preferred value	Calculated
U-1	10.0		10.0 ± 0.7	9.4
U-7	14.9	14.7	14.8 ± 0.9	10.4
U-19	15.6,17.3	16.5	16.5 ± 1.0	12.0
U-37	18.9,16.2,17.9		17.9 ± 1.0	12.0
U-37i	17.9		17.9 ± 1.0	11.4
Th-1	8.5		8.5 ± 0.6	9.1
Th-7	9.6		9.6 ± 0.6	8.7
Th-19	10.5,9.6	9.2	9.9 ± 0.7	8.3
UO_2	10.5	11.3,10.8,9.8	10.5 ± 0.6	
Pb1-U6	10.6		10.6 ± 0.7	
Pb1-U36	13.3		13.3 ± 0.7	
Pb7-U30	11.5		11.5 ± 0.7	
Pb1-Th6	7.7		7.7 ± 0.9	
Pb1-Th18	6.6		6.9 ± 0.8	
Pb7-Th12	8.4		8.4 ± 0.6	
Pb-1 (d=3.84 cm)	6.3		6.3 ± 0.5	
Pb-7	7.7,8.6,8.5		8.3 ± 0.4	
Pb-1 (d=10.6 cm)	8.7		8.7 ± 0.5	8.8

supply of irradiated samples.

During the course of the year a computer system was installed and interfaced to analysis equipment. Presently the system can measure neutrons, gamma rays and alpha particles emitted by samples. Most of the early part of the year was used to automate as much of the equipment as possible. This involved the construction of sample changers, automated rabbit systems and computer software development.

From July through November approximately 10,000 samples were analysed for such elements as Au, As, Sb, Re, U and Th. Most of the work was per cent value determinations rather than trace element concentrations. A low neutron flux in the TNF made trace element analysis very difficult as well as economically impossible.

The greatest problem with operating this facility lies with the TRIUMF operating schedule. In 1979 the total amount of beam production suitable for NAA was about 39 weeks. The proposed schedule for 1980 indicates only 27 weeks of suitable beam.

The combination of very irregular and usually unpredictable beam performance with the low flux presents a grave predicament for Novatrack in 1980.

Experiment 87
Proton radiography

During the past year the radiography equipment has been moved to the beam line 1B experimental area where it is inserted in the region immediately in front of the beam dump during running periods. A collimator with a 1 mm diam aperture is inserted into the beam line between the last two dipoles to reduce the beam intensity by 10^2-10^4 and to reduce the beam emittance for pencil beam operation.

Two techniques are being studied. The first technique involves using a pencil beam of 180-250 MeV protons which is scanned over the sample in a raster fashion by means of a pair of horizontal and vertical steering magnets. The protons are detected with two scintillators before the sample, for normalization to the incident beam intensity, and with a range telescope consisting of four thin scintillators placed at the sensitive region of the proton range curve. The second technique uses a brass absorber/scatterer placed 4 m upstream of the sample to provide a broad beam, uniform in intensity to better than 1%, over an 8 in. diam aperture. The range telescope is replaced with X-ray film as detector, and normalization is by means of an integrating ionization chamber. The samples are usually placed in a rectangular water box to maintain uniformity of material thickness in front of the film. Two types of X-ray film have been selected for use, Kodak X-OMAT M and Ilford Ilfex 90. Typical proton exposures for these films are in the range $10^7/cm^2$-$10^8/cm^2$. The main disadvantage of using protons for radiography, that of poor spatial resolution due to multiple scattering, has been studied quantitatively by radiographing a series of 0.25 in. thick perspex rods placed in a water box at various distances from the film. The rods represent a density change of 0.5% and are clearly visible on the film.

Several running periods have been used to study the optics of beam line 1B and to make measurements on the beam parameters relevant to the radiography work. The location of the beam-defining collimator is an improvement over the previous configuration in beam line 4A as the second dipole removes slit-degraded beam. The smallest beam spot achieved, which determines the spatial sensitivity of this technique is about a factor two larger than calculated, and more work on the optics is required. The measured beam stability is equivalent to an energy stability of ±65 keV but appears to be due to intensity effects in the range counters rather than true energy fluctuations.

A fast-scanning magnet capable of ±20 mrad deflection has been built from a power supply transformer and tested successfully. Further work with the scanning beam technique is awaiting improvements in the data-handling rate which could be solved using the PDP-11/34 in the 1B counting room.

Two potential applications of proton radiography techniques are being studied: investigation of voids in high voltage cable insulation and alignment of the TRIUMF polarized target. A common failure of high voltage cables used in power distribution is a process called 'treeing' where breakdown first takes place in a small void in the insulation and then spreads through the insulation. Samples of

25 kV cable have been radiographed with a sensitivity which could detect voids of 0.50 mm diam. Further systematic work is required before the viability of this technique could be determined. The TRIUMF polarized target is in a cryostat in a superconducting solenoid, so it is not simple to use conventional alignment techniques. A variation of proton radiography called 'scatter' radiography has been tried with the target cell in the water box and appears promising for providing alignment information.

THEORETICAL PROGRAM

Introduction

The Theory group at TRIUMF exists to provide a focus for theoretical research and a group of active researchers who are interested in the kinds of medium-energy nuclear and particle physics problems which are under experimental investigation here. Another aim is to make possible the interchange of ideas between experimentalists and theorists which benefits both the experimental and theoretical research programs.

The group is currently quite small, especially considering the large variety and number of experiments under way at TRIUMF, though there has been some expansion in the past year. There are now three permanent staff: H.W. Fearing, A.W. Thomas and R. Woloshyn. Research associates in the group, who are supported jointly with UBC, include J. Greben, J. Ng, A. Saharia and M. Betz (from December). Graduate students G. Brookfield, J. Johnstone, N. Shrimpton, R. Sloboda (Ph.D. 1979) and S. Théberge, long-term TRIUMF visitors A. Fujii and J.M. Laget, visitor to SFU H. von Baeyer and visitor to UBC A. Gersten have been involved in group activities and in some of the projects listed below. A number of theoretical faculty at member universities have also been active participants including D. Beder, M. McMillan, E. Vogt (UBC), A. Kamal, H. Sherif (Univ. of Alberta), C. Picciotto, C. Wu (Univ. of Victoria) and D. Boal (SFU).

Members of the group have been involved in a number of special activities during the year. Particularly successful was a summer workshop on pion-nucleus interactions which attracted a sizable group of physicists and generated lively discussion of this important area. Various individuals also contributed to the organization and planning of a workshop on kaon physics to discuss possibilities of developing TRIUMF into a kaon factory and to a workshop to discuss physics possible with an improved high resolution spectrometer at TRIUMF. Theory group members helped with the planning of the Eighth International Conference on High-Energy Physics and Nuclear Structure held in Vancouver in August and participated in the sessions. Others represented TRIUMF at a variety of external meetings and workshops including II International Conference on Meson-Nuclear Physics at Houston; LAMPF Workshop on Program Options in Intermediate-Energy Physics; LBL Medium-Energy Physics Review Committee; LAMPF Workshop on Pion Single Charge Exchange; International Conference on Nuclear Physics with Electromagnetic Interaction; Neutrino '79, International Conference on Neutrino Interactions.

Weekly theory meetings have provided opportunities for members of the group to discuss work in progress. Some have been responsible for the TRIUMF seminar series, which together with the theoretical visitors program has made possible visits to TRIUMF of a number of theorists, including:

I. Aitchison	B. Holstein	G. Miller
L. Arnold	M. Huber	M. Moravcsik
B. Bhakar	N. Isgur	J. Niskanen
J. Blair	D. Jackson	J. Noble
B. Day	B. Kayser	H. Pilkuhn
N. Deshpande	B. Keister	A. Popova
J. Dubach	F. Khanna	M. Rho
G. Epstein	L. Kisslinger	E. Rost
D. Ernst	K. Klingenbeck	F. Scheck
E. Ferreira	M. Krell	L. Schroeder
R. Freedman	R. Landau	P. Singer
W. Haxton	H.C. Lee	J. Vergados
L. Heller	M. Locher	R. Vinh Mau
P. Herczeg	T. Londergan	

and many others passing through.

Specific areas and topics of research which have been of interest in the past year include the following:

Muon capture

Ordinary muon capture $\mu+(Z)\rightarrow(Z-1)+\nu$ and radiative muon capture $\mu+(Z)\rightarrow(Z-1)+\nu+\gamma$ (RMC) both provide the opportunity to investigate the weak coupling constants at non-zero momentum transfer. RMC in particular is quite sensitive to the induced pseudoscalar coupling g_P and so can be used as a way of measuring this coupling and checking the Goldberger-Treiman prediction. Certain aspects of muon capture also give information on nuclear structure. Several different problems in ordinary and radiative capture have been investigated in the past year.

($1/m^2$) and nuclear structure effects in radiative muon capture in nuclei

In all previous calculations of RMC an effective Hamiltonian good only to order 1/m in the nucleon mass m has been used. However, for the photon asymmetry at least, it is known that the order $1/m^2$ terms are quite important [Fearing, Phys. Rev. Lett. 35, 79 (1975)]. Thus motivated, we have derived a Hamiltonian consistent through $O(1/m^2)$ and used it to calculate both photon spectrum and asymmetry. The $O(1/m^2)$ terms give a non-negligible (20-25%) increase in the spectrum, but most of this contribution is from the square of the $O(1/m)$ parts of the usual Hamiltonian. They do, however, affect the value of g_P extracted from a given set of data at the level of a few times g_A.

We have also tried several different nuclear models in order to test the sensitivity to nuclear structure effects. These include a harmonic oscillator shell model, a model using Hartree-Fock wave functions and an improved giant dipole resonance model. In general the ratio of radiative-to-ordinary rates is quite independent of the model, although the absolute rates vary significantly.

The results have been fitted to the data of the SREL group [Hart *et al.*, Phys. Rev. Lett. 39, 399 (1977)], as shown in Fig. 92. The fit is good, but the value of g_P extracted is too low, indicating that the theoretical results are higher than the data for a given g_P. This effect has been observed before [e.g. Rood and Yano, Phys. Lett. 35B, 59 (1971)] but is more pronounced in our calculations because of the additional $1/m^2$ terms included. Preliminary data of a new experiment [Adler *et al.*, EICOHEPANS, Vancouver, (1979)] may possibly indicate a somewhat larger cross section than that of the SREL group, which would increase the value of g_P obtained. Our calculation is now complete, and described in detail in a preprint [Sloboda and Fearing, TRI-PP-79-36, Nucl. Phys. (in press)].

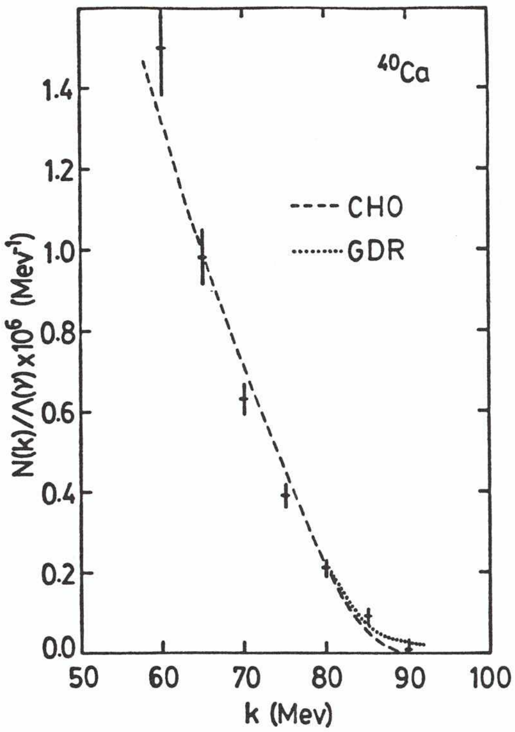

Fig. 92. $O(1/m^2)$ and two-parameter fit to the relative photon spectrum of Hart et al. with k_m/ν fixed at 1.06. Results for the fitted parameters are (i) closure harmonic oscillator model; $k_m = 89.1 \pm 0.9$ MeV, $g_P = (-2.8 \pm 4.8)g_A$, $\Lambda_{ord} = 5.3 \times 10^6$/sec, and (ii) giant dipole resonance model; $k_m = 87.0 \pm 3.0$ MeV, $g_P = (-0.3 \pm 2.0)g_A$, $\Lambda_{ord} = 3.9 \times 10^6$/sec.

Radioactive muon capture in hydrogen and helium

A separate calculation of RMC in ^1H and ^3He, this for the first time completely relativistic, has also been completed [Fearing, TRI-PP-79-37, Phys. Rev. C (in press)]. One major motivation here was to understand why a new calculation [Hwang and Primakoff, Phys. Rev. C 18, 414 (1979)] which supposedly was based on the general principles of conserved vector current, gauge invariance and PCAC differed so much from the (somewhat fragmentary) existing calculations. Another motivation was to avoid the non-relativistic expansions in powers of 1/m which are conventionally used for heavier nuclei. Finally, by emphasizing the very light nuclei one avoids possible problems with nuclear structure effects.

It was found that the standard approach, based on a set of Feynman diagrams, satisfies the same general constraints used by Hwang and Primakoff. The different numerical results were caused by a number of their approximations, but most important was an assumption, which they called the linearity hypothesis, which led to an amplitude which was made gauge invariant in a way that violates the analyticity conditions of the Low soft photon theorem. Relativistic effects turned out also be be non-negligible, and so our results gave for the first time accurate numbers for capture in these very light nuclei. An example of the photon spectrum following capture in ^3He is shown in Fig. 93. The main effect is an increase of a factor of two over results of Hwang and Primakoff.

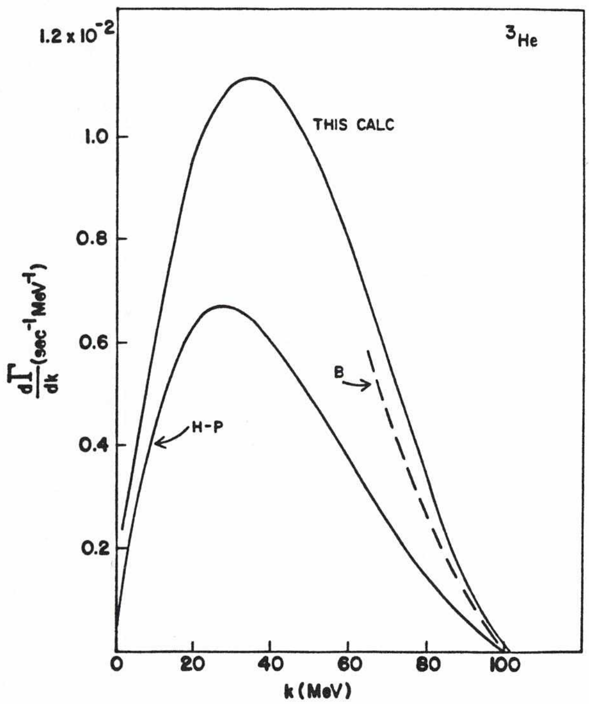

Fig. 93. Photon spectrum for radiative muon capture on ^{3}He in the standard theory of this calculation and from Hwang and Primakoff. Beder's result (perhaps with the wrong sign for g_P) is also shown. Reversing the sign of g_P would increase his result to be about 10% above the result of this calculation.

Quark model calculation of radiative muon capture

Radiative muon capture by the proton has been re-examined from the point of view of the Weinberg-Salam gauge theory of electroweak interactions of quarks and leptons. A dynamic model has been constructed wherein both electromagnetic and weak interactions take place along one of the valence quark lines for the proton. The resulting photon spectrum has an infrared singularity which can be cancelled by photon emission from the spectator quarks. Further work using more realistic quark wave functions in a proton is now in progress.

Systematics of nuclear muon capture

The experimental strength of the total muon capture as a function of Z (atomic number) shows some remarkable general trends. It rises almost linearly up to Z ~ 25 and becomes approximately constant for higher Z. To explain this gross behaviour a statistical approach and a giant multipole resonance model have been combined.

For heavier nuclei and higher excitations the density of states increases rapidly; hence the sum over final states can be replaced by an appropriate integral (statistical approximation).

In a simple model the strength as a function of excitation energy is assumed to have a broad resonance peaked at the position of the giant dipole resonance (GDR). This position is shifted linearly with Z by Coulomb force. The characteristic Z-dependence for the strength clearly emerges from this crude model.

In an improved model several elaborations are made: relativistic corrections terms, parity selection rules, and blocking due to the Pauli exclusion principle are included, and the strength as a function of excitation energy is constrained by energy-weighted sum rules. The computation is performed assuming a resonance at the position of GDR and another at the position twice as high as GDR. The calculated capture rates for natural elements reproduce the experimental rates mostly within 10%.

Pion-nucleus and pion few-body interactions

One of the most challenging problems in medium-energy physics is to understand the interaction of a pion with the nuclear many-body system. The questions answered by investigations in this area should lead to a better understanding of both the nucleon-nucleon force and the nucleus itself. In addition, the results obtained with real pions will have important implications for the behaviour of virtual pions, and hence the structure of dense nuclear matter (e.g. the possible existence of pion condensation).

During the past year the Theory group has continued to attack this problem from a number of points of view. One of the reasons for the Workshop on the Future of Pion-Nucleus Physics [TRI-79-2] was to encourage discussion between proponents of the many available theories (particularly the multiple scattering and isobar doorway models). A comprehensive review of the current status of the microscopic optical model, derived from multiple scattering theory, and the related pion few-nucleon problem was completed during the year [Thomas and Landau, Phys. Reports, in press]. We describe in more detail below some of the investigations for specific energy regions and reactions, but it should be borne in mind that these are parts of a more comprehensive picture which is slowly being developed. There is as well a great deal of interest in the πD and $NN\pi$ systems which have been investigated from several points of view during the past year.

Nuclear sizes from low-energy pion scattering

One of the outstanding questions in pion-nucleus physics is whether the obvious qualitative differences between the $\pi^+p(\pi^-n)$ and $\pi^-p(\pi^+n)$ scattering amplitudes can be used to deduce quantitative information about nuclear densities (ground state, or transition densities). At present the extraction of neutron and proton radius differences based on the comparison of π^+ and π^- scattering in the (3,3) resonance region is extremely model dependent. Indeed, the *only* paper which has demonstrated a significant model-independent radius determination from pion scattering is the work of Johnson *et al.* [Phys. Rev. Lett. 43, 844 (1979)] at TRIUMF. The experimental work involved the measurement of the ratio of the differential cross sections for π^- elastic scattering from neighbouring isotopes ($^{13}C/^{12}C$ and $^{18}O/^{16}O$, see Fig. 94) at low energy (30-50 MeV)—see the discussion of Expt. 1 for more detail (p. 37).

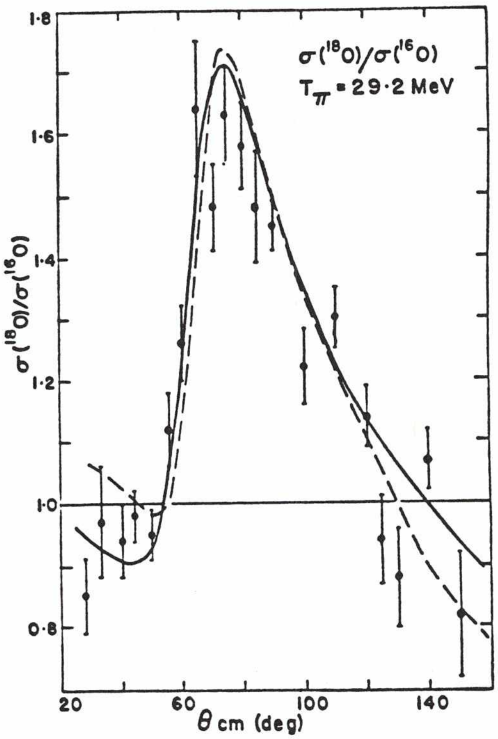

Fig. 94. Ratio of the π^--elastic differential cross sections on ^{18}O and ^{16}O together with best fit theoretical curves. The fit is very sensitive to the difference in the neutron rms radii of the two isotopes.

At low energies the nucleus is quite transparent to the pion, which therefore probes the whole nuclear distribution, not just the surface as in the resonance region. In addition the ratio of the free p-wave $\pi^-n:\pi^-p$ scattering amplitudes is ~13:1. Our task as theorists was to test all known features of the low energy π-nucleus interaction which could alter the apparent nuclear size—e.g. true absorption, Lorentz-Lorenz effect, Pauli effects, non-locality. The final number quoted, namely an rms neutron radius of 2.81 ± 0.03 fm for ^{18}O (relative to 2.60 fm for ^{16}O) and 2.35 ± 0.03 for ^{13}C (relative to 2.31 fm for ^{12}C), include all known theoretical and experimental uncertainties. At the time of publication the models which had been tested were those of the Michigan State group [Phys. Rev. C 19, 929 (1979)] and the Colorado group [Phys. Lett. 66B, 421 (1977)]. Since then we have shown that the momentum space potential developed at TRIUMF over the past few years [e.g. Landau and Thomas, Nucl. Phys. A302, 461 (1978)] is also in agreement ($r_n^{13} = 2.36$ fm, $r_n^{18} = 2.81$ fm). With this calculation complete, the last known theoretical loophole—namely a possible dependence on the range of the pion-nucleon interaction (see 1978 Annual Report)—has been closed.

This work is being continued in two important directions:

1) Using π^+ on isotones it should be possible to check predicted proton rms radius differences against electron scattering, thereby justifying the technique in an essentially experimental way.

2) Once established by 1) the π^- technique can be used to extract n-radii for light isotopes which may be of theoretical interest(e.g. Ca isotopes).

Pion-nucleus elastic scattering in an isobar-doorway model

In the intermediate-energy region the pion-nucleon (πN) interaction is dominated by the $\Delta(1236)$ resonance in the 3-3 channel. The model for the pion nucleus (πA) interaction based on multiple scattering theories (MST), in which the Watson operator is replaced by the free π-N t-matrix neglects the additional degree of freedom provided by Δ-(A-1) interactions. The isobar-doorway model (IDM) may be used to develop the π-A optical potential in terms of phenomenological parameters which have a simple physical interpretation [Kisslinger and Saharia, TRIUMF preprint TRI-PP-79-28]. The parameters of the model are the inelastic energy shift ΔE, the inelastic width $\Gamma(=\beta\Gamma_{\Delta})$ and the non-locality λ (which takes into account the modifications to the nuclear form factor because of Δ-propagation). Two different parametrizations were considered: 1) channel-independent IDM in which ΔE and β were replaced by an average for all partial waves, 2) channel-dependent IDM in which ΔE and β were allowed to go to 0 and 1, respectively (impulse approximation limit) for impact parameters larger than the nuclear radius. The parameters of the model are extracted by fitting elastic scattering data. A typical fit in the resonance energy region is shown in Fig. 95. In this energy

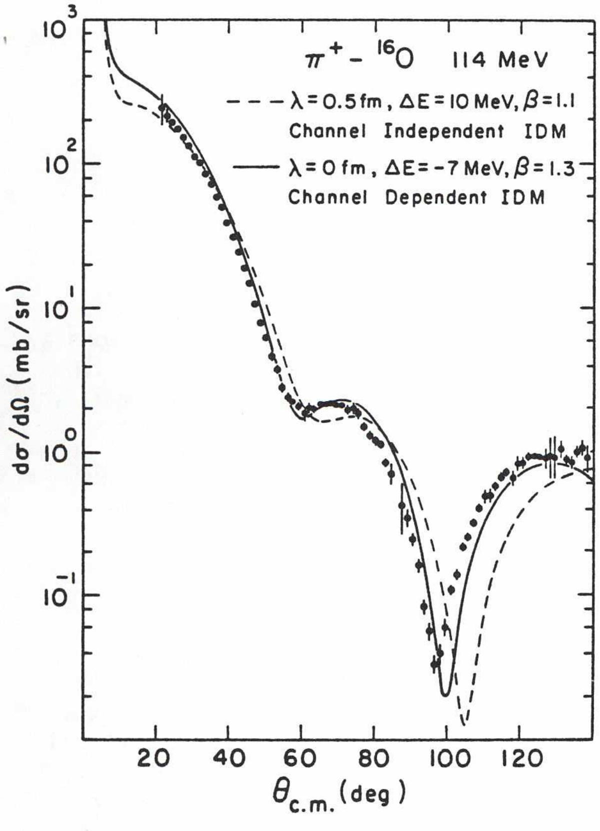

Fig. 95. π^+-^{16}O elastic scattering in the isobar-doorway model.

region it was found that a finite non-locality was required for the channel-independent IDM, whereas no non-locality is required for the channel-dependent IDM. This may suggest that the local form ($V \propto t\rho$) commonly used in models based on MST is appropriate only if allowance is made for channel-dependent modifications arising from Δ-(A-1) interactions.

Charge exchange scattering

Using charge independence it can easily be shown that the single charge exchange (SCX) scattering amplitude to the isobaric analog state is given by the difference of elastic scattering amplitudes (F_I) in definite pion-nucleus isospin channels, I. In the resonance energy region the F_I's become almost equal, leading to a small SCX cross section due to large cancellations. It is clear that small changes in the optical potentials in individual isospin channels can lead to large changes in the SCX cross section while leaving elastic scattering practically unchanged. Since many-body effects are expected to modify the optical potentials differently in different isospin channels, the SCX cross section can be reproduced by allowing w, the energy at which the pion-nucleon t-matrices are evaluated in the multiple scattering theory, to be isospin dependent [Saharia and Woloshyn, Phys. Lett. 84B, 401 (1979)]. This approach was then extended to the isobar-doorway model [Saharia and Woloshyn, Phys. Rev. (in press)]. The many-body effects will in general make all three parameters isospin dependent, which in principle can be determined by fitting elastic and SCX scatterings. A more heuristic approach was followed by allowing only the energy-shift parameter ΔE to be energy dependent. For isospin-1/2 targets, $\varepsilon = \Delta E_{1/2} - \Delta E_{3/2}$ was determined by fitting the $^{13}C(\pi^+,\pi^0)^{13}N$ total cross section, while β and λ were taken from fits to ^{12}C. Our predictions for forward angle SCX cross sections for isospin-1/2-targets are given in Fig. 96. The mass number dependence of the slope seems to be in agreement with the recent results from LAMPF [Bowman in Proc., 8th Int. Conf. on High-Energy Physics and Nuclear Structure, Nucl. Phys. (in press)].

An alternative calculation of the $^{13}C(\pi^+,\pi^0)^{13}N_{g.s.}$ reaction has been carried out using the optical potential of Landau and Thomas [Phys. Lett. 88B, 226 (1979)]. Of particular interest is the fact that a

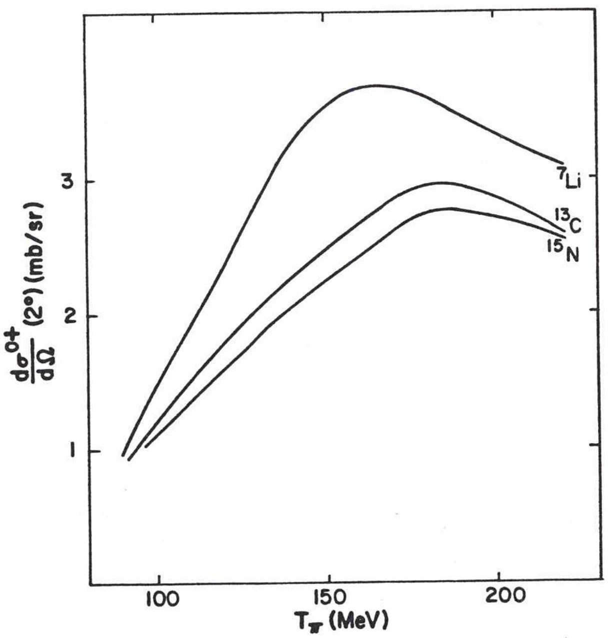

Fig. 96. Forward angle charge exchange cross section for isospin 1/2 targets.

microscopic treatment of the effect of the Pauli exclusion principle (and the three-body energy) immediately leads to an improvement in the shape of σ_{tot} (SCX) as a function of energy. The infamous dip in the region of 150 MeV, common to all simple impulse approximation optical model calculations is avoided.

In spite of this qualitative improvement σ_{tot} is still a factor of 2-3 below experiment. However, a relatively small energy shift (of a few MeV) of the type described above can easily explain this difference. The eventual microscopic explanation of this phenomenological observation in terms of a different isospin dependence of the Δ-(A-1) interaction, isospin mixing in the ^{12}C core and so on is awaited with great interest.

Pion photoproduction

Using the isobar-doorway model it can be shown that the transition operator for the reaction (γ,π) to the isobar analogue state gets modified by the Δ-(A-1) interaction in the same way as the optical potential. Using the same parametrization for the transition operator as for the optical potential, we find that cross sections for the coherent reaction $^{12}C(\gamma,\pi^0)^{12}C$ in the isobar-doorway model are substantially different from those obtained by using impulse approximation [Saharia and Woloshyn, to be published]. Also the two parametrizations of the isobar-doorway model give different (γ,π^0) cross sections, although they give a similar quality of fit to elastic scattering data. This reaction thus provides a means to discriminate between different models used to incorporate the many-body dynamics in the pion-nucleus system. The calculations are being extended to other nuclei and to the (γ,π^-) reaction to the isobaric analogue state.

Pion quasi-elastic scattering

Last year the so-called fixed condition geometry for the $(\pi,\pi N)$ reaction was briefly mentioned [Jackson *et al.*, Nucl. Phys. A322, 493 (1979)]. In particular the calculations of Jackson, Ioannides and Thomas suggested that although traditional off-shell effects would be negligibly small in this reaction the effect of the medium through the Pauli exclusion principle should be quite strong. However, for comparison with the suggested experiments, full distorted wave calculations were necessary. Such calculations have been carried out, and the first results were reported at the 8th Int. Conf. on High-Energy Physics and Nuclear Structure [Shrimpton, Miller and Thomas, abstract No. 1E26]. A detailed report will be made available during 1980.

The NNπ system

A series of relativistic three-body calculations of πD elastic scattering has been carried out over the last four years. Amongst our most recent results are predictions for vector and tensor polarizations, including the effect of virtual absorption and re-emission of the pion [Rinat *et al.*, Nucl. Phys. A329, 285 (1979)]. The most spectacular new experimental result is the determination by Holt *et al.* [EICOHEPANS contribution] of t_{20} (180°) at 142 MeV. Their value of -0.24 ± 0.15 is midway between our predictions with ($\sim$+0.20) and without ($\sim$-0.70) absorptive effects.

One of the exciting and topical issues in the nucleon system is the existence and meaning of the dibaryon resonances seen at Argonne. In collaboration with Locher and Kubodera at SIN, and Myhrer at NORDITA, the effects of a relatively small coupling of the 3^- dibaryon state to the πD channel have been investigated [J. Phys. G6, in press]. As shown in Fig. 97, the vector polarization [$it_{11}(\theta)$] undergoes a striking change when such a coupling is introduced (ε = 0 and 10^4 correspond to pure L = 2 and pure L = 4 coupling, respectively). This sensitivity is especially interesting because it_{11} is otherwise the most stable of all the predicted πD polarization parameters. (Incidentally, the effect of the 3^- dibaryon resonance on the differential cross section was also calculated by Rinat *et al.*, *op. cit.*) Experiments using a polarized deuteron target are presently under way at SIN to test these predictions.

There is also continuing interest in NN-scattering above pion production threshold [Phys. Rev. C 20, 216 (1979)] and in the production reaction itself.

The (3,3) resonance in the bag model

One of the central questions in the study of the pion-nucleus interaction is the nature of the elementary pion-nucleon interaction. This is clearly related to the structure of the nucleon and the delta. Early in the year Brown and Rho [Phys. Lett. 82B, 177 (1979)] discussed the difficulties one has reconciling the usual MIT bag model of the nucleon with our understanding of nuclear structure, and particularly the role of the one-pion-exchange potential. They suggested that a smaller bag radius (~0.3-0.4 fm) might be more appropriate. Most importantly, they showed how PCAC led to a coupling of the pion field to the nucleon bag of the usual $(f/m_\pi)\ \vec{\sigma} \cdot \vec{k}$ form (to lowest order).

By extending this argument it was realised that the Brown-Rho model would not only imply an $NN\pi$-coupling but also a non-zero $\pi N\Delta$-coupling. Thus we were led naturally to a description of πN-scattering in the (3,3)-channel [TRI-PP-79-16, Phys. Lett., in press] which involved both the usual crossed Born graphs (e.g. Chew-Low theory) *and* direct delta graphs with no question of double counting! Our first calculations used simply a sharp cut-off at the $NN\pi$ and $\Delta N\pi$ vertices at some maximum momentum $p_{max} \simeq 1/R$, but now form factors derived from the bag model wave functions were used. A complete discussion of the theoretical basis, including a proof that this model satisfies the Low equation, and numerical results, will be available in the summer of 1980.

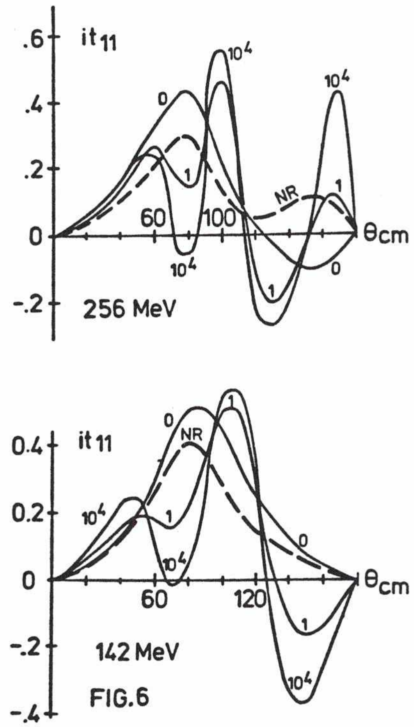

Fig. 97. The vector polarizations in $\pi\vec{D}$-elastic scattering. The dashed curve (NR) is a relativistic three-body calculation with no dibaryon resonance. The other curves show the effect of coupling to the 3^- resonance as described in the text.

Proton nucleus and proton few-body reactions

One of the major areas of experimental interest at TRIUMF deals with the interactions of protons with nuclei, and a variety of experiments are under way ranging from elastic scattering to fragmentation reactions. In parallel there have been a number of theoretical investigations including models of inclusive reactions, studies of few-body reactions such as $(p,n\pi)$, (p,d) and (p,γ) on light nuclei and work on nucleon-nucleon bremsstrahlung.

Phenomenology of inclusive reactions

The direct knockout model has been applied to $A(p,{}^4He)X$ reactions [Boal and Woloshyn, Phys. Rev. C 20, 1878 (1979)]. Using an exponential structure function with a fall-off roughly the same as obtained from (p,p') reactions we have been able to fit $(p,{}^4He)$ cross sections at 90° and 160° over the energy range 210 to 480 MeV [Korteling and Green, TRIUMF preprint TRI-79-29] with a

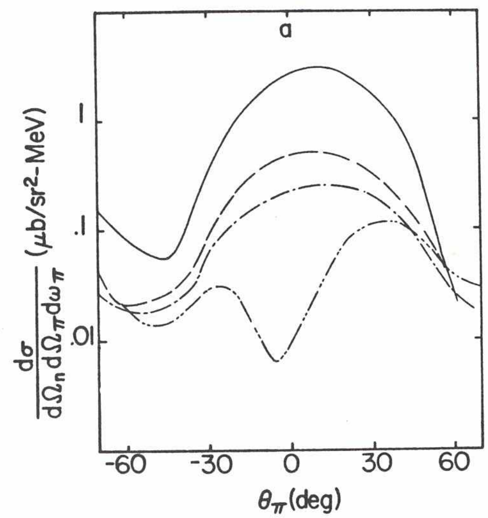

Fig. 98. Differential cross section for $^4He(p,n\pi^+)^4He$ at T_p = 750 MeV, T_π = 80 MeV, θ_n = -10. Full curve is the relativistic calculation with the pseudoscalar coupling. Broken curves are results with non-relativistic operators.

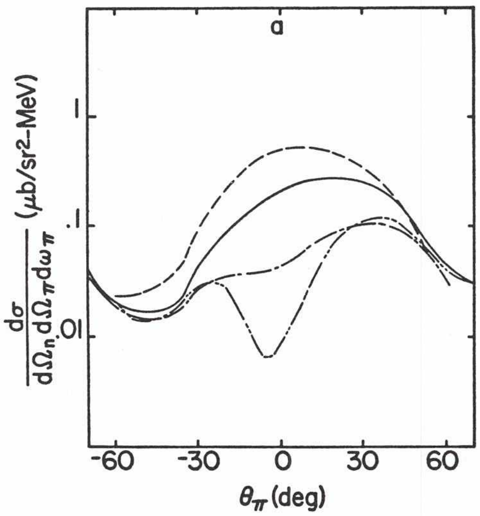

Fig. 99. Same as Fig. 98 except with pseudovector coupling.

single overall normalization constant. The effective number of target alpha clusters was found to vary from 5.6 in ^{109}Ag to 0.3 in ^{9}Be. We note that this behaviour of n_{eff} is different from that found by Dollhopf *et al.* [Nucl. Phys. A316, 350 (1979)] in the (^{4}He,2^{4}He) reaction. Cross sections for the A(e,^{4}He)X reaction [Flowers *et al.*, Phys. Rev. Lett. 43, 323 (1979)] are very similar to proton-induced knockout, and we are presently studying the extension of the direct knockout model to electromagnetic reactions.

The ^{4}He(p,nπ^+)^{4}He reaction

A relativistic model for the ^{4}He(p,nπ^+)^{4}He reaction [Greben and Woloshyn, Nucl. Phys., in press] has been constructed and used to study two aspects of pion production: 1) the validity of the non-relativistic pion production operator; and 2) the constraints of PCAC in the soft pion limit.

The relativistic pseudoscalar pion coupling results cannot be reproduced by any of the non-relativistic operators (static, static + recoil, Galilean invariant) for the given (standard) prescription of the off-mass shell behaviour of the p-^{4}He amplitude (Fig. 98). The pseudovector pion vertex operator, however, is reasonably approximated by the simple static pion-nucleon vertex. Inclusion of different recoil terms in the non-relativistic operator does not improve the agreement at all (Fig. 99).

The usefulness of the soft-pion theorem is constrained by two important considerations: 1) The pion is not massless like the photon. 2) Whereas in the electromagnetic case charge conservation gives directly an equation for the photon-emission amplitude, in the weak axial vector case PCAC only gives a self-consistency condition on the pion-emission amplitude. Nonetheless, this constraint was found to be useful as it does exclude the pseudoscalar pion-nucleon vertex in the present calculations. The soft pion theorem does not prescribe the choice of the on-shell energies, however. This leads to the range of cross sections shown in Fig. 100, which is seen to be considerably

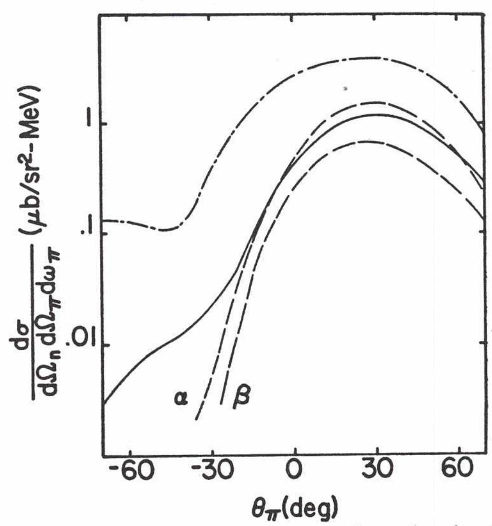

Fig. 100. Range of cross section obtained with different choices of on-shell energy (α and β).

smaller than the difference between the pseudoscalar and pseudovector calculations.

Unified theory of elastic and rearrangement scattering

At TRIUMF the (p,d) reaction has been studied experimentally for various nuclei. One of the incentives for these studies is the sensitivity of this reaction to the high momentum components in the nuclear wave functions. However, it is clear that information about these small components of the wave function can only be obtained if one understands the reaction mechanism very well. In general it will be necessary to calculate the corrections to the simple DWBA mechanism explicitly in order to obtain any quantitative information about the wave functions.

This situation has motivated us to develop a theory of elastic and rearrangement scattering which will satisfy the following requirements: 1) in lowest order it reduces to the DWBA; 2) the effects of the continuum are taken into account (which distinguishes this theory from the usual coupled reaction channel (CRC) approach); and 3) it gives a relationship between distorting and elastic optical potential.

The continuum effects can be treated by using a three-body description in which the degrees of freedom of projectile (proton), transferred particle (neutron), and residual nucleus are treated explicitly. Such a three-body description has some additional advantages: 1) no non-orthogonality problems as in the CRC approach; and 2) no diagonal terms, even if the optical potentials are non-folded. Notice, however, that the present approach is not really a three-body approach: in the latter one would use effective intercluster interactions whereas in the present approach we still have two-body interactions and treat the nucleons in the residual nucleus individually.

The resulting many-body equations are reduced using the projection techniques of Feshbach. Instead of the usual operator P which projects out the prompt components of the wave function, we now have three projection operators, each one corresponding to a specific asymptotic channel and operating on the channel component which carries the corresponding asymptotic wave. After introducing a matrix notation for the channel component wave functions one can write the resulting equations for the projected wave functions in exactly the same manner as the usual Feshbach equations for $P\psi$.

We can use these equations to derive expressions for the optical potentials and the coupling potentials in the resulting coupled channel equations. So far we have only studied the first-order terms in these expressions. These first-order terms are obtained by neglecting higher-order terms in the expansion for the many-body Green's function which operates in Q-space. In order to further simplify the resulting expressions an on-shell assumption has been made. The final expression for the optical potential is very similar to the usual expression for the first-order Kerman-McManus-Thaler (KMT) optical potential. Due to the explicit treatment of the rearrangement channels the distorting potentials are slightly reduced with respect to the elastic optical potential. This reduction manifests itself as the subtraction of the bound-state pole contributions in the folded t-matrices. The coupling potential contains the usual post or prior interaction matrix element leading to the usual DWBA. However, there exists a second contribution to the coupling potential which must be due to the continuum, as it is absent in the usual CRC formulation. The effect of this continuum contribution at intermediate energies is presently being studied for $^4He(p,d)^3He$.

In summary, the present theory extends the usual multiple scattering methods to rearrangement processes; it offers a means of calculating higher-order corrections in a distorted wave formulation without double counting; and finally can be used fairly simply within the context of the standard coupled channel computer programs.

Application of a unified theory of elastic and rearrangement scattering to $^4He(p,d)^3He$

Standard DWBA theory has met with considerable problems in explaining the various data for this stripping process. Recently it has been suggested that the neutron-^3He wave function which was deduced from elastic electron scattering data was responsible for this poor fit. Taking into account meson exchange corrections in the analysis of the electron data would reduce the high momentum components of this wave function and thereby allow for a better fit. If this suggestion would prove correct it would establish the importance of the high momentum components of the single-particle wave functions in (p,d) reactions. The importance of high momentum components is obvious in the plane wave Born approximation; however, it is less obvious in the distorted wave Born approximation where lower momentum components also do contribute.

In the present investigation we want to study corrections to the DWBA graph, as given by the new theory of rearrangement reactions described above. Obviously a good knowledge of the correction terms is indispensable for obtaining quantitative information about the high momentum components. There are two types of corrections to the DWBA: 1) due to the reduction of the optical potential when rearrangement is treated explicitly; and 2) due to the three-body continuum. The second correction has been examined and can be written as a rescattering diagram where the incoming proton first scatters from the core and subsequently combines with the neutron to form the deuteron. This diagram has been calculated in plane wave representation for forward (22.5°) and backward angles. The results are shown in Fig. 101.

Notice that the rescattering diagram is very important beyond 300 MeV at the forward angle. This shows that this correction should be included in the analysis of the data. At backward angles the rescattering diagram gives a very good fit to the data, although the fall-off with energy appears to be a little too fast. This may indicate that at these energies isobar degrees of freedom have to be treated explicitly.

Since the present results are quite encouraging it is intended to extend these calculations. At forward angles it is necessary to 1) relax the factorization approximation; 2) use a model for the ^{3}He-n scattering amplitude; and 3) combine the rescattering diagram coherently with the DWBA graph. At backward angles we should improve our model for the backward ^{3}He-n scattering amplitude. In both cases the new TRIUMF data for p-^{3}He scattering will be badly needed. The spin dependence of the elastic scattering amplitudes may also be important in reproducing the data. This dependence is certainly

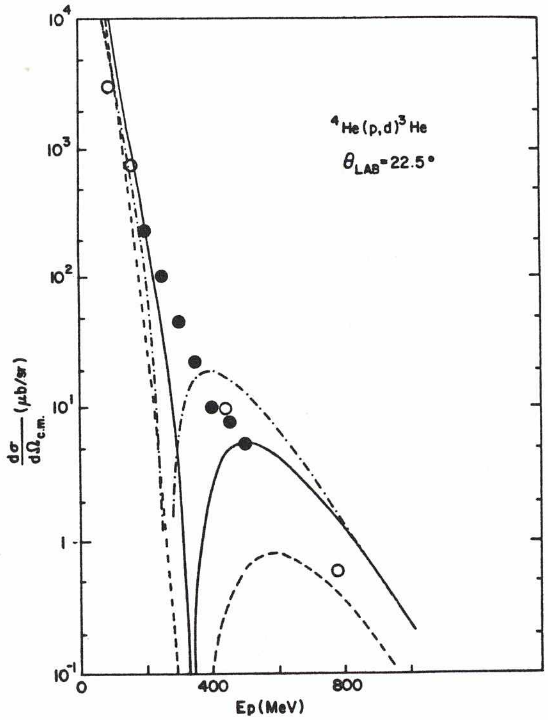

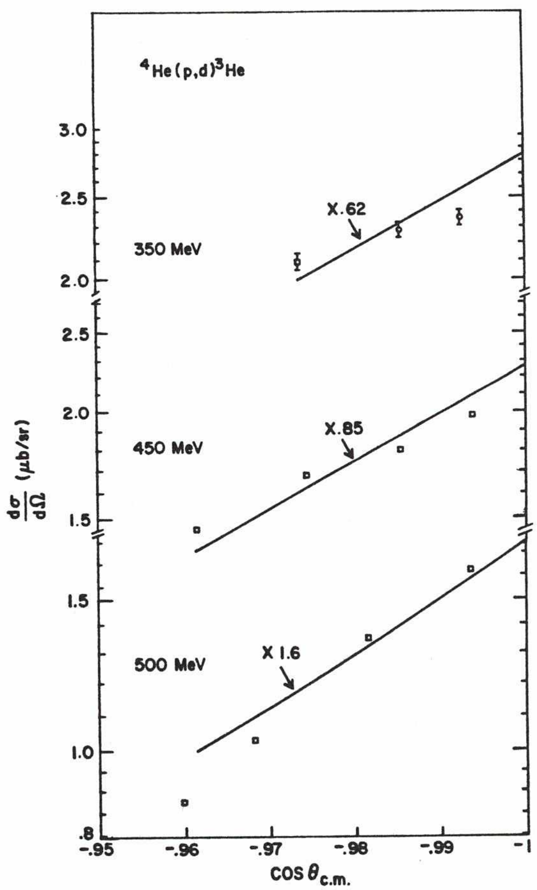

Fig. 101. —— *PWBA stripping diagram (S+D-state);* – – – *PWBA (S-state only);* —·—·— *rescattering diagram.*

essential if one wants to study asymmetries with the present formulation.

(p,γ) reaction

There has been a great deal of recent interest in (p,γ) reactions stimulated in part by new experiments at Indiana on nuclei [Kovash *et al.*, Phys. Rev. Lett. 42, 700 (1979)]. At TRIUMF an experiment is planned (#131) to measure the reaction $p+d \rightarrow {}^3He+\gamma$. Older measurements show major discrepancies which hopefully can be resolved by the TRIUMF experiment and similar new experiments at Bonn and Saclay. This reaction and others such as $p+t \rightarrow {}^4He+\gamma$ and (p,γ) on heavier nuclei are quite interesting since they involve high momentum transfers, and so have the same potential for nuclear structure information as (p,π) reactions, but the basic interaction is perhaps better understood. Many of the ingredients of (p,γ) reactions are the same as in (p,π), and so an understanding of the (p,γ) process may help isolate pionic effects in (p,π). We are exploiting the similarity of (p,γ) and (p,π) by adapting our earlier model used successfully in the TRIUMF energy range for $p+d \rightarrow t+\pi^+$ and $p+{}^3He \rightarrow {}^4He+\pi^+$ to the analogous (p,γ) reactions. The model is a distorted wave impulse approximation model using the $p+n \rightarrow d+\gamma$ cross section as input. Preliminary results give qualitative agreement with at least some of the older data. The input $p+n \rightarrow d+\gamma$ cross section is very poorly known in the resonance region, however, which introduces large uncertainties in the results in some kinematic regions.

Proton-proton bremsstrahlung (ppγ)

Bremsstrahlung is hopefully one of the most direct and least ambiguous ways of learning about the off-shell nature of the nucleon-nucleon force. It is thus a very fundamental process which, however, must be understood from an on-shell point of view first. One way of doing this is via a soft photon approximation (SPA) which is a purely on-shell approximation and which must fail if off-shell information is to be obtained. Fits to all of the modern ppγ experiments have now been completed [Fearing, TRI-PP-79-40, Phys. Rev. C, in press; Rogers *et al.*, AIPCP #41, p. 446; Nefkens *et al.*, Phys. Rev. C 19, 877 (1979)]. One example is shown in Fig. 102. From these fits and from comparison with potential model calculations interesting results have emerged. Essentially all data, except that

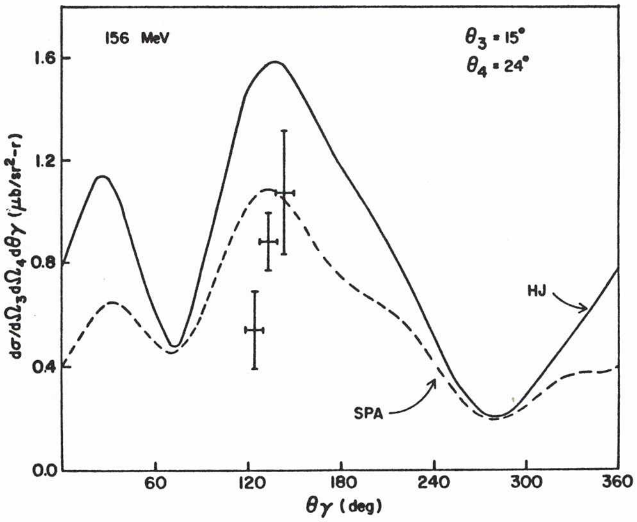

Fig. 102. Comparison of the 156 MeV Orsay data for one angle pair, $\theta_3 = 15°$ and $\theta_4 = 24°$, with SPA calculations (dotted curve) and with Hamada-Johnston non-relativistic potential model calculations (solid curve).

at 730 MeV, can be fit by SPA at least as well as by potential model calculations. Relativistic effects are very important even at 200 MeV and should be included in potential calculations. Even at 42 MeV where potential calculations should be most accurate, they seem to overestimate the cross section, by amounts apparently larger than obtainable by reasonable variations of the off-shell properties.

Asymmetries are also very interesting, and seemingly quite sensitive to off-shell effects [Moravcsik, AIPCP #41, p. 515; Fearing, Few Body Systems... vol. 1, Graz Conference (1978), p. 94] and clearly should be considered in future calculations and experiments. Finally, as a result of studies of kinematic conditions and possible expansion parameters [Fearing, Phys. Rev. Lett. 42, 1394 (1979)] it is now fairly well understood what new experiments should be done to emphasize off-shell effects.

Particle physics and miscellaneous topics

Effects of Majorana lepton in $\mu^- \rightarrow e^+$ conversion in nuclei

The branching ratio of this reaction to ordinary muon capture has been estimated to be $<10^{-13}$ for a 500 MeV/c^2 Majorana lepton. A sequential Weinberg-Salam gauge model with neutrino mixing was used. The mixings of neutral heavy leptons with ordinary neutrinos are also constrained by possible production from deep inelastic charged lepton-nucleon scattering. A detailed study of SLAC beam dump experiment limits the mixing parameter to be in the range 10^{-4} to 10^{-1} for a 500 MeV/c^2 Majorana lepton.

Bound muon decay

During the past year it has become clear that the problem of calculating the spectrum and asymmetry of the decay electron from bound muon decay sufficiently accurately is a much more challenging, and thus more interesting, problem than originally realised, touching as it does on atomic physics, field theory, and in particular on the very fundamental and as yet unsolved problems of relativistic many-body theory. Nuclear recoil allows a high-energy electron from bound decay, and such electrons will be measured in experiments such as those at TRIUMF and SIN which are looking for the muon number non-conserving reaction $\mu^- \to e^-$. In fact the bound decay spectrum at the very high energy end provides both a calibration and the major background for such experiments. The asymmetry at lower electron energies is necessary to interpret correctly any muon spin correlation experiment such as those testing T invariance or measuring second-class currents or g_P.

Previous calculations, which have included only some recoil effects, mainly those due to phase space effects and these only in crude approximation, give a large effect at the very upper tip of the spectrum. We are attempting to improve upon these calculations using the Grotch-Yennie effective potential approach [Grotch and Yennie, Rev. Mod. Phys. 41, 350 (1969)] which should make it possible to obtain both phase space and potential, i.e. wave function, effects correct to order 1/nuclear mass. Even this must be generalized for our case since, because of the neutrinos, the electron and muon are in different systems, and again the connections must be made correct to order 1/m. So far this formalism has been developed and results obtained analytically in purely Born approximation. It remains to extend the calculations to the realistic case where muon and electron wave functions are incorporated.

CYCLOTRON SYSTEMS

ION SOURCE AND INJECTION SYSTEM

Unpolarized ion source

Most of the equipment in the 300 kV source terminal performed very well during 1979. Some downtime was caused at the year's end by the main 10 in. diffusion pump which will be repaired and overhauled during next year's January shutdown. When the source had to routinely deliver high H^- beam currents, some sparking over the 300 kV accelerator stack created problems which have to be solved. The source filament often lasted for 150 h, which made it possible to exchange the source at the weekly maintenance intervals. During the June shutdown the source cabling, P.C. boards and drawings were updated.

300 keV H^- injection line

At the beginning of the year a study was completed to replace the obsolete sublimation pumps for the beam line along with its problematic and very complex control systems. During the high-current test runs the pumps would often not recover from H^- beam introduced pressure bursts, so that at the end of such a run the beam line vacuum was maintained mainly by the sublimation pumps' cold traps, and the pressure along the beam line became worrisomely high. Regeneration of the pumps had to be done via the beam line, and the system needed more than one shift to fully recover. Time was at a premium if the decision was made to improve the vacuum system, build it and make it reliable before the scheduled continuous 100 μA runs at the year's end. Therefore, we were most grateful for the advice and the support received from several groups and individuals which made it possible, on short notice, to settle on a new vacuum system, matching the beam line requirements. A break was made away from the more conventional systems and the new vacuum system was designed with cryogenic appendage pumps as the building blocks. The cryogenic pumping system offers some definite advantages over the more conventional systems.

Before the June shutdown preliminary tests with a cryogenic appendage pump were evaluated, the design frozen, pumps and systems ordered, and hardware was being manufactured in the machine shop. During the June shutdown most of the hardware was installed to receive the pumps as they arrived one by one during the last half of the year. Before the November 100 μA runs the pumping system was in place and the vacuum improved. Proper controllers will be installed during the January 1980 shutdown. During the high-current runs it was noticed that the new system handled the H^- beam pressure bursts very well and pulled the beam line vacuum back into the 10^{-7} Torr range. It was also possible to regenerate any cryogenic pump, while injecting a beam into the cyclotron, by means of a newly installed roughing line. The liquid N_2 system to the vault pumps has been eliminated, and the vault pumps replacement time was also reduced from one to two shifts to one to two hours per pump. This is important with the expected higher radiation levels at the vault pumps locations.

Polarized source

During the past year there have been no demands for intense polarized beams from experimental groups. This has been reflected in the activities within the polarized source where improvements have continued towards complete remote control.

It is now possible to remotely vary most of the parameters which are normally used in tuning the source. The only major outstanding item to be made remote is control of the cesium temperature. The lack of a proper interlocking system remains a concern but will be a high priority item during the coming year. This is especially important as the source operation will formally be handed over to operators who will not be as familiar with the source as the beam physicist.

RF SYSTEM

RF amplifiers

There was no major downtime attributed directly to the RF amplifiers or the RF control system during 1979. Approximately half of the downtime was the result of having to change the coupling loop which developed a minor vacuum leak. The remainder of the downtime was an accumulation of many short periods of normal maintenance and repair to the RF system.

RF resonators

Several tuning iterations were undertaken on the ground arm resonator tips in an attempt to reduce the RF leakage and improve the cyclotron vacuum. It was found that there were many positions of the tips which gave the same results. For example a mistuned lower resonator can be compensated for by mistuning an upper resonator in the opposite direction. The diagnostics cannot distinguish between RF leakage due to an upper or a lower resonator misalignment. However, for best fundamental operation the general trend of tuning was to increase the lower RF gap and decrease the upper RF gap, which would imply sagging of the resonator hot arm panels. A resonator straightening program was planned for the January shutdown.

In planning the resonator straightening program for the shutdown it was found that the leaf spring supports which attach the hot arm resonator panels to their strongbacks were distorted and very flexible. Any attempt to straighten the panel by brute force would only put more strain on the leaf spring supports and weaken them further. A new floating disc spring support was designed which is more rigid and adjustable to allow the resonator panels to be restrained in a controlled manner. A new resonator tip support was also designed and fabricated and will be installed in the January 1980 shutdown. This will allow twists in the resonator tips to be removed.

Third harmonic system

The 2 kW driver amplifier for the third harmonic system has been successfully tested into a resistive load. The mechanical assembly of the 100 kW output stage is almost complete. A water cooling system has been incorporated into the transmission line and the matched section of line from the vault to the RF room has been installed.

Modifications made to the resonators last year to improve the fundamental Q and reduce the RF leakage seems to have had an adverse effect on the third harmonic Q (2500 instead of a measured Q of about 6400 in December of 1976). Model work was carried out with regard to the low third harmonic Q. The results of the model work indicated that the third harmonic Q could be improved by disconnecting the ground arm flux guide top-bottom connections. This modification was performed on the resonators, but no appreciable Q improvement could be measured.

Several iterations of resonator ground arm tip adjustments were tried in order to improve the third harmonic Q, with the result of only a 10% improvement. The two major changes that have taken place since December 1976 are the addition of the upper to lower hot arm flux guide connections and the sagging of the resonator hot arm panels. The effect of these two changes will be measured in the January 1980 shutdown.

New resonator program

The central region resonators and removable quadrants first installed in the tank were considered prototypes to eventually be replaced. With the continued sagging of the standard resonators it was decided that they too should be replaced, and a design program was initiated in 1978 on the assumption that TRIUMF would replace all resonators.

The central region resonators and standard resonators will use the same basic strongback and hot arm panel design. The central region resonators and quadrants will be completely new units, but the standard resonators will use the existing ground arm panels. The existing removable quadrants become part of the lower central region resonators and now extend out the full 32 in. A plan view of the central region area and standard resonators is shown in Fig. 103.

Some of the improved design features which are common to both resonator types are:

(1) The resonator hot arm panel is supported along the full length of the resonator and has free float in the horizontal plane for improved stability and reliability.

(2) The strongbacks are more reliable and are water cooled.

(3) The new strongback design allows more clearance above the water headers for vertical alignment of the levelling arm.

(4) The new design will incorporate an improved levelling arm adjuster.

Some of the improved design features of the central region resonators and quadrants are:

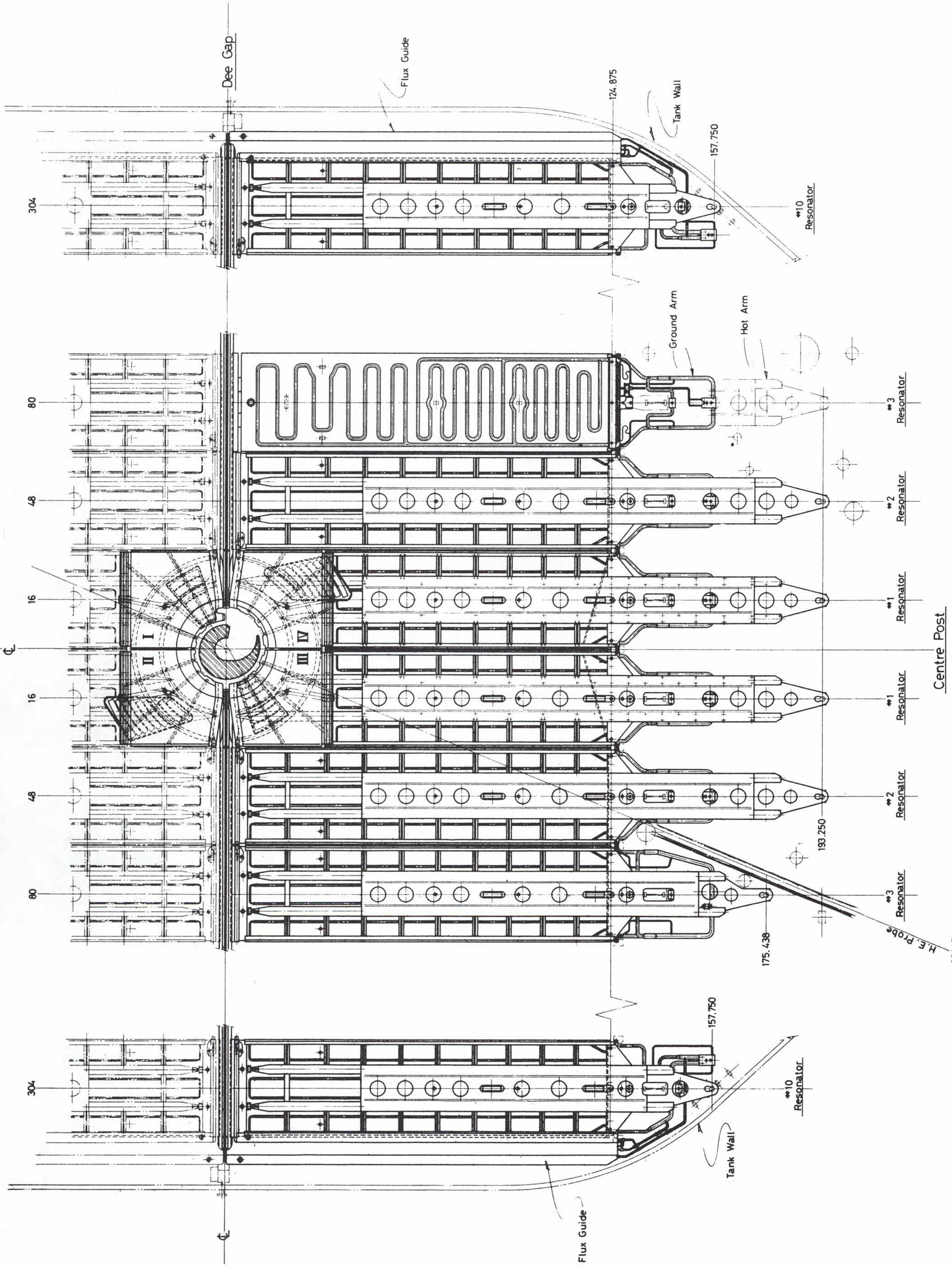

Fig. 103. Central region and standard resonators in lid-open position.

(1) The central region resonators will be in two sections for ease of alignment and remote handling.

(2) The quadrant latching will be independent of the central region geometry alignment.

(3) The central region geometry alignment will be available in three planes.

(4) Correction plates will be quick disconnect.

(5) A new vertical wall geometry will be incorporated into the quadrant design.

(6) Removable cut-outs will be available for beam dynamics studies.

(7) Wireways and most other attached components will be well shielded in the resonator strongback.

(8) The new design will include tapered root shorts for third harmonic operation.

Some improved design features of the standard resonators are:

(1) New thinner wall resonator tips fabricated from copper.

(2) New tulip design to give a better mechanical connection between adjacent resonators without the resonator tips having to overlap two resonators.

(3) A water-cooled tuning foil in the root pieces.

(4) Corrugated panels on the strongback to reduce RF leakage and make it less sensitive to resonator adjustment.

(5) Remotely handleable 'M' foils and root-root connections.

Design of the basic support structure for both resonator types, central region geometry, and beam envelope have been frozen. The conceptual designs of the latching system, alignment system, and other attachments to the central region resonators have been reviewed and accepted. Based on this information the prototype work is going ahead.

The prototype resonator program includes the fabrication and mechanical test of the following:

(1) A prototype of the centre post and the four central region quadrants.

(2) A prototype of one and one-half lower and upper central region resonator.

(3) A working prototype of a standard resonator which will be used for the model work and also tested in the tank as an installed resonator.

Long delivery items such as the aluminum extrusions, cone spinnings, various forming blocks and general machine shop materials have been ordered. Some of these items are beginning to arrive, and we are now trying to find a work area to start the prototype program.

PROBES

The cyclotron probes performed very reliably during the past year causing only 4 h of downtime. The most serious failure was a vacuum leak which occurred in a bellows on the water-cooled probe. Although the repair required raising the cyclotron lid, it was scheduled during a planned power outage and maintenance period so that beam time loss was minimized.

During the cyclotron shutdown in June the second high-energy probe was replaced with the new design which uses linear bearings and cable drive. Now both high-energy probes have been modified, and during the coming year improvements to the low-energy probes will be studied. The design of the extraction mechanism for demonstrating 70-100 MeV beam extraction, which was successfully tested last year, was reproduced on a remotely handleable bracket at radii corresponding to 68, 70, 72 and 90 MeV. The stripping foils are mounted on small coils which rotate in the cyclotron magnetic field when a current is applied. All four beams were extracted and centred on an exit halo monitor during subsequent beam tests.

The prototype design of a non-intercepting cyclotron phase probe, which had previously provided beam information only at the highest beam currents because of the very high RF pickup, was used, together with a phase detection system developed at KVI, Groningen, and showed that it was possible to detect useful phase signals at 4 μA peak current. With this demonstration it was decided to install more of these phase probes at seven radial positions from 95-460 MeV. This will occur during the shutdown in early 1980.

The major effort during the past year has been the design, fabrication and assembly of new internal slit mechanisms. These are four sets of movable jaws which can be positioned radially to provide phase and emittance selection in the central region and hence good energy resolution. Although the original sets of slits have been used with some success to provide good quality beams, it was apparent that there were several problems with the design. With the success of linear bearings and cable drive on the high-energy probes it was decided to use similar drive mechanisms on the slit assemblies. A further improvement is to have both jaws on a slit assembly move with a common radial drive. This should increase the positioning accuracy of the slits. All four sets of slits are assembled and will be installed during the next shutdown.

BEAM DIAGNOSTICS

During the last year the devices described in the 1978 annual report have been commissioned and more of them constructed to serve new beam lines and targets.

The target protect monitors at 1AT1, 1AT2 and the TNF consist of four quadrant secondary emission plates set around an aperture. These, together with a measure of the total beam current, give a warning or a trip if the position or luminosity exceeds predetermined limits. The monitors have operated at beam intensities up to 150 μA, and the continuous display of the quadrant currents has proved useful for normal operation at lower intensities, giving an indication of beam position at the production targets.

The first secondary emission wire profile monitor installed on the 1AT2 ladder about 50 cm downstream from the protect monitor foil showed a broad, beam-dependent background. This had not been observed on similar monitors placed closer to protect monitors nor in open beam lines and is thought to be due to radiation emerging at a wide angle from the protect monitor and striking the solder pads of the profile monitor. These pads present a much larger area than the carbon wires and had been shielded against particles drifting roughly parallel to the beam pipe. The background was eliminated in a second monitor by reducing the shield diameter still further and arranging for the solder pads to face downstream.

The 1AT1 production target shield vessel has a port reserved for diagnostic use at 90° to the beam line and on the opposite side of the target to the secondary channels. Target ratemeters are mounted here to give an estimate, independently from the secondary channel flux, of the number of protons striking the small cross-sectional area targets. A multi-plate ionization chamber with local air as the working gas is used, also a Čerenkov detector based on the pair production electrons from the γ-rays associated with π^0 production in the target. A counter telescope for protons, placed close to the target, had suffered from an excessive count rate, and there had been no evidence that the spatial definition provided by a telescope was necessary. The response of the air ionization chamber and Čerenkov detector are both linear with beam intensity, and Fig. 18 (see p. 17) compares their response with the relative flux of particles in channel M13 as the beam is steered horizontally across the target. Both devices have a similar response and compare with the high-energy π^+ flux in the channel. However, the surface muon flux is a maximum, and electron contamination a minimum, when the beam is steered over to the channel side of the target. This shows that it is advantageous to have a figure of merit from each channel when doing the final optimization of the beam conditions. (Note that a repeat of this experiment with a larger detector gave a π^+ distribution with a flatter top.) The air ionization chamber is a simple device, and tests are continuing of the reproducibility of the signal versus beam current response over the long term.

A visitor from Eindhoven, R.J. Vader, together with some members of the Cyclotron Development group, attached synchronous detection equipment [Vader and Schreuder, IEEE Trans. NS-26, 2205 (1979)] to a capacitive pick-up probe located in beam line 1A. This system utilizes a macropulsed beam and the modulated beam-related signals were separated from unmodulated noise to give useful beam pulse information at currents as low as a few nanoamperes.

VACUUM SYSTEM

Cyclotron

The major vacuum improvement attempted during the year was commissioning of the liquid helium cryopump. Problems associated with the length of the transfer lines slowed development and a leak in the liquid nitrogen baffle in mid-summer brought work to a virtual halt. The pump will be removed and repaired in January 1980.

The B20 cryogenerators required service at unacceptable intervals during the mid-portion of the year, and several steps were taken to try to improve the reliability of the machines. The last machine in service was operating well after 1300 h, so there is some hope the problem has been solved.

Other work during the year was aimed at improving the efficiency of the liquid nitrogen delivery system and the serviceability of the diffusion pump stacks.

Beam lines

A second turbomolecular vacuum pump was added to the beam line 1 vault section for use as an *in situ* spare or as additional pumping of temporary increases in the gas load.

A system of copper lines was installed on beam line 1 vault section to permit remote localization of leaks.

Vacuum systems for beam line 1B and M13 were installed and commissioned and have operated normally. A 'front end' valve for beam line 4C has been installed and the pumping system specified.

A prototype remotely handleable 4 in. beam line clamp has been designed by the Remote Handling group, and a bellows handling tool has been designed and built by the Vacuum group.

REMOTE HANDLING

Significant progress has been made in three areas of the operation this year.

Hot cell

Primary commissioning of the new hot cell was completed with installation of Central Research model 8-HD manipulator, a Kollmorgen periscope, the lead glass window, lighting and services. Maintenance and repair of 'hot' components is now a routine operation.

Cyclotron servicing

A total rebuild of the lift trolley, used for shadow-shield handling in the tank, has been completed. Vernier-style video positioning of the service bridge orbital location was added. A variable speed dc drive now replaces the original bridge orbit motor.

Beam line servicing

The existing transport flask for beam line servicing was 'stretched', to accommodate longer items, and commissioned on the TNF target assembly. A new design of indium seal flange was introduced to allow its passage through standard quadrupoles while still retaining the replaceable indium ring features. A shielded flask unit for the 500 MeV isotope thimble has been fabricated.

SAFETY

The Safety group was expanded to nine members during 1979 from six in the previous year. The low level-counting laboratory was re-established opposite the control room and has much improved facilities including a new counting 'cave' and a CAMAC-based microprocessor data acquisition system. The emphasis of the group is leading more towards radiation monitoring and contamination control as the beam intensity levels increase and the radiochemistry programs begin to come on stream. The safety interlock system that was implemented in 1978 functioned extremely well. The Safety group is now designing the safety interlock system for the new 42 MeV cyclotron.

The TRIUMF Safety Advisory Committee (TSAC) met twelve times during the year and reviewed experiments, facilities, interlocks and operation safety problems. A significant fraction of the TSAC effort went into study of the radiochemistry program and associated laboratories. These facilities are included in the newly complete chemistry annex, a new AECL trailer installed for commercial production of ^{123}I as well as the interim radiochemistry laboratory and the TRIM program trailer.

Operations in the chemistry annex, a portion of which will be operated by AECL, and the new 42 MeV cyclotron still require extensive scrutiny by TSAC.

Radiation protection

There were 481 individuals on the TLD and neutron badge service during 1979. The total measured man-dose was 7.4 man-rem and included only one neutron reading. This was less than half the man-dose accumulated during 1978. The decrease can be accounted for by the fact that there was only one major shutdown during the calendar year 1979. A frequency distribution of accumulated gamma/beta dose is shown in Fig. 104.

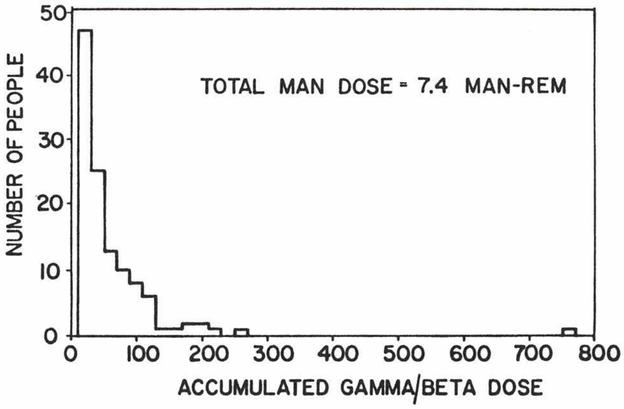

Fig. 104. Frequency distribution of accumulated gamma dose.

In 1979 the Dose Study group was formed, with members from Cyclotron Development, Planning, Remote Handling, Design Office and Safety. The purpose of the group was to estimate the future dose commitment for maintenance and development projects in light of the proposed increase in average beam intensity. By year's end first-order estimates have been made for most of the planned activities in the cyclotron vault, through to 1985.

The data acquisition system for the Health Physics lab was re-established during 1979. The system is built around an LSI-11 microprocessor housed in a CAMAC crate. Peripherals include a dual floppy disc drive, graphics terminal and decwriter. By the end of the year software development had progressed sufficiently for the system to be used routinely for collection and analysis of spectra from various detectors.

Safety interlock system

The new central safety system (CSS) installed in December 1978 is constructed around Erasable Programmable Read Only Memory (EPROM) in a CAMAC-based Kinetics 3880 microprocessor. The flexibility of this system was demonstrated by the ease with which changes were made to the CSS logic during the June shutdown. The updated logic equations were compiled and installed in an off-line simulator where they were completely tested. During the shutdown this new logic was installed in the CSS where it was again subjected to exhaustive testing. The above logic changes were necessitated by the construction of a new meson channel (M13) and alterations in the proton hall lock-up to allow free rotation of the medium resolution spectrometer (MRS). Further changes in the central logic were at year's end being tested in the simulator for installation in the CSS in the planned January 1980 shutdown. These changes will enable operation of the new beam lines 2C and 4C.

Modifications to the M9 area safety unit (ASU) logic have been made in order to provide for the several operating modes now possible in M9. These new modes became possible with the installation of the dc separator. Since this type of modification to ASU's seems to be occurring regularly, a design study is under way into the possible replacement of the relay logic in the ASU's by EPROM microprocessor-based logic.

A parallel safety system is under development for the 42 MeV cyclotron. The CSS42 logic will also be housed in a CAMAC-based EPROM system completely independent of the safety system for the TRIUMF 500 MeV cyclotron.

Industrial safety

There were 41 injuries reported and treated by TRIUMF first aid attendants, with a loss of 33.5 man-days. In addition there were eight accidents involving outside contractors working at TRIUMF. Most of these were hand injuries of a minor nature, and there was a marked decrease in the number of minor eye injuries over the previous year.

CONTROLS

Microprocessors

The extensive application of CAMAC-based microprocessors, begun in 1978 with the safety system, continued throughout 1979, and as projects started during the previous year were completed new ones were undertaken. Locally intelligent control systems for 1AT1 and 1AT2 were commissioned in 1979 including their communications protocol with the central control system. The local control station for M13 was nearly completed in 1979. Its present configuration includes no less than three microprocessors: a floppy disc-based system computer which drives the user console, a CAMAC-based processor to control slits and jaws on the secondary channel, and a similar processor which formats data passed from the central control system for local display. This last is the first example of a local processor sharing dataway access in a central control system crate using an 'A2' controller. The system has proven satisfactory, and several more such installations are planned for 1980.

Because of the large number of CAMAC-based locally intelligent systems planned, and in order to reduce costs and increase the power of such systems, a module based on an 8085 processor was designed and commissioned at TRIUMF during the year 1979. It features greater addressing capability and more versatile interrupt handling than its commercially available competitors, as well as a remote console for convenient debugging. This system, called 'TRIUMF microprocessor auxiliary controller' (TRIMAC) will be used in all future installations.

Operational improvements

As in other years, considerably more than 50% of control system work was maintaining the existing system, and implementing a large number of small additions and improvements in response to the needs of other groups. In addition, a few major projects were undertaken and completed in 1979.

One such development was to expand the REMCON system from 256 (377_8) to 512 (777_8) addressable devices or thumbwheel numbers per system. This required significant changes in both hardware and software, and its successful completion made possible a much needed expansion of the ISIS system. A byproduct of this change has been the creation of the '700 block' of thumbwheel numbers which is common to all REMCON systems.

Another, relatively minor, change to REMCON was the relocation of the 'save' tables such that they are no longer overwritten by REMCON reloads. This small change represented a considerable operational improvement.

An automatic mode for the polarized ion source 'spin flipper' was implemented during 1979. This mode permits the source to be programmed to switch automatically between 'spin-up', 'spin-down' and 'spin-off' states at operator-selected intervals. This has become the preferred mode of operating by all experimental users of polarized beam, although numerous improvements—for example, switching on the basis of integrated beam rather than time—have been suggested. These will be implemented in 1980.

In 1979 a frontal attack was made on the notorious unreliability of stepping motor controller (diagnostic probe system) software. The table structure was redesigned, and the entire module was rewritten and consolidated to run in one computer rather than two. Not unexpectedly there were some problems at first; however, the bugs were quickly exterminated, and the new system has proven quite reliable. Problems of reliability and expandability remain with the stepping motor system hardware, however, and these will be dealt with on a high priority basis in 1980.

The second display portion of the main console (the 'H' panel) was replaced with a CRT, and monitors using green phosphors were substituted for both console CRT displays. Both the new colour, and indeed the use of CRTs at all, have had mixed reviews. In addition—and after many months of harassment from the operators—a second 'TelTerm' display was incorporated into the system, greatly relieving the pressure on the use of that facility.

Reliability

Surprisingly, the control system was responsible for almost exactly the same amount of cyclotron downtime in 1979 as in 1978—both absolutely (71 h) and relatively (8.5%). Unlike 1978, however, almost none of that downtime was attributable to computer system failures: only one such failure late in the year—of an interprocessor communications board—resulted in 1.5 h of accelerator downtime.

Twenty-five per cent of cyclotron downtime due to controls problems was the result of CAMAC power supply failures—the majority of this (8 h) in one episode in late July. Another 17% of controls downtime was due to both hardware and software problems associated with the stepping motor controller system. The software problems appear to have been resolved (see above), and a redesign of the system hardware is planned for 1980. The third major offender (12%) was unreliability in the thermocouple system used for measuring temperatures in the resonators and related equipment. The entire system is scheduled for replacement in the January 1980 shutdown. Honourable mention goes to system-wide CAMAC problems (bits stuck or intermittents in branches or in the executive crate) which caused 9% of the total controls downtime. The remainder was due to a miscellany of problems including multiport memory failures, TelTerm display failures, and numerous software bugs and bombs.

It should be noted that for one three-week period in August no cyclotron downtime was attributable to control system failures. It is, of course, merely by chance that this period coincided with the vacation of the control system engineer.

Workshop

In the last week of 1979, the Controls group—engineers, technicians and programmers—met off site for a three-day workshop to identify the most serious deficiencies of the present system, decide means of dealing with those deficiencies, and prepare longer-range plans for the evolution of the system.

The first important problem is that all three control system computers are extremely busy (75-85% CPU time used), and this has resulted in observably slow response in the system as a whole. The specific reasons for the high level of activity of each computer were identified, and a detailed program, involving the off-loading of certain time-consuming repetitive tasks to local processors, was formulated.

Of equal or greater seriousness is the inadequate memory resources of the present system (see Fig. 105) which has already prevented the implementation of some desired features. A specific plan for expansion, which would involve the addition of 2-3 computers to the control system, was proposed, and the appropriate budget request was formulated. It was agreed that this plan would provide only fairly short-term (3-4 years) relief of the space problem.

Questions of longer-range philosophy were resolved much less easily. It became clear

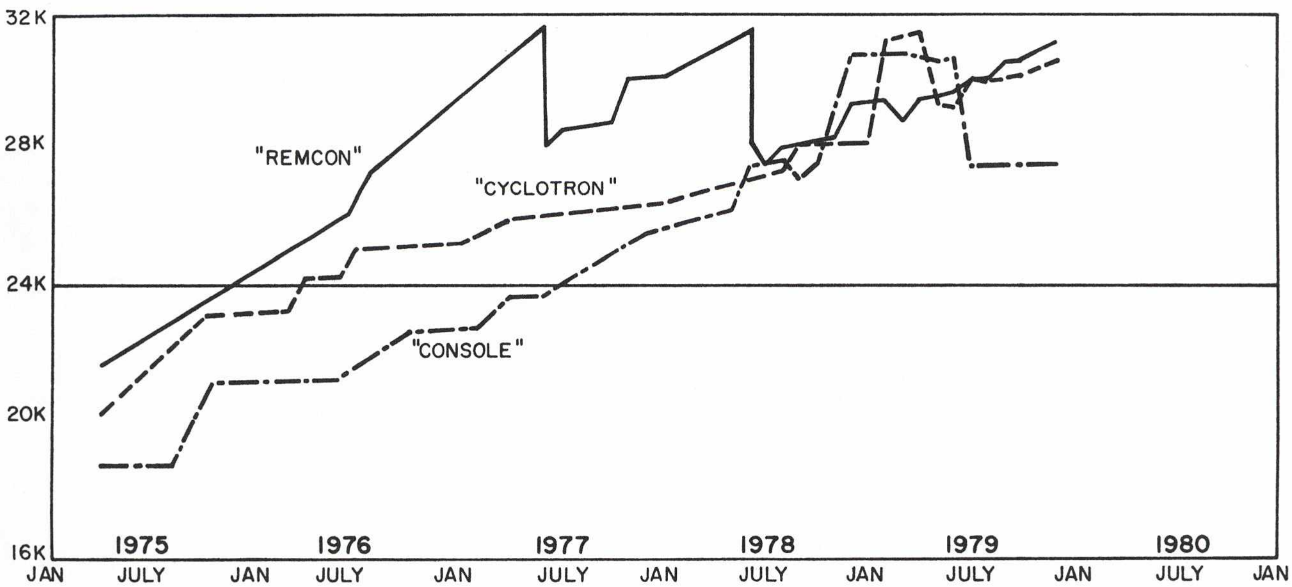

Fig. 105. Core use in three control system computers.

that two agreed design objectives, namely a minimum of interprocessor communications and a minimum number of computers sharing access to the CAMAC executive, were mutually incompatible; and that as a result some hard compromises would have to be made. Moreover, fundamental philosophical differences relating to the preferred direction of expansion emerged: some preferring continued use of still more small, dedicated computers and others suggesting more use of recent technical advances, such as large, mapped systems, microprogrammability, parallel processors, and so on.

Participants considered the workshop to have been a valuable exercise. It provided an opportunity to examine advantages and disadvantages of many alternatives, to suggest much needed specific measurements of system performance, and to provide a good basis for understanding of the compromises which must, inevitably, be made. More such workshops, dealing with quite specific questions, are planned for early 1980.

Electronics support

During 1979 the Electronics group had a staff of about 25 people, consisting of 5 electronic engineers, 15 technicians and 5 assemblers.

This year saw the introduction of the microcomputers into various control and instrumentation systems, namely the central safety system, 1AT1 and 1AT2 target controls, beam line collimator monitoring, 500 MeV irradiation facility and 70 MeV components. An initial investigation into CCD techniques for the TPC project was carried out in addition to the design and manufacture of instrumentation for this group.

A new modular microcomputer resident within CAMAC systems was designed and is known as TRIMAC. This system enables multiple CPU's to be resident within a CAMAC crate. It is described in documents referenced under TRIUMF drawing A-13471. A further instrumentation development was the 1 GHz TDC capable of measuring time intervals to an accuracy of ±1 nsec at rates of up to 10 mega measurements per second. Documents describing this system are available under TRIUMF drawing A-13736.

The group has been reconfigured in order to provide various services to cyclotron and experimental groups. Available services are:

- PDP-11 systems: service
- NOVA systems: service
- Nuclear physics instruments: service
- Commissioned facilities: service and installation
- Design services
- Manufacturing services

EXPERIMENTAL FACILITIES

INTRODUCTION

During 1979 two major projects involving secondary channels were completed and commissioned with beam. The M13 low energy π/μ channel, described in last year's report, was completed in February, commissioned first with an alpha source and then with pions and muons. Its large acceptance and good optics, together with small volume production targets of uncooled pyrolytic graphite, have resulted in excellent performance both as a low-energy pion scattering channel and as a surface muon channel. First experiments on M13 started in July, and the channel very quickly has become in great demand from experimental groups.

The extension of M9, the original low-energy π/μ channel, was installed during the late summer and received first beam in November. The channel extension was designed to provide clean muon beams at two target locations, one being the centre of the Chicago magnet which houses the time projection chamber (TPC). A 3 m long dc particle separator operating at voltages to 400 kV provides the particle separation. The 77 MeV/c μ^- beam was measured to have a flux of 5×10^5/sec for 100 μA of protons on a 10 cm Be target. More details on the commissioning results and on the development of an RF separator with greater acceptance are given later.

In addition to the secondary channels beam line 1B, a low-intensity proton line intended primarily for use with polarized beam, was completed early in the year and commissioned with beam at energies up to 350 MeV and currents up to 20 nA. The present 350 MeV limit is due to power supply limitations on the dipoles. The 65 cm magnetic spectrometer 'Resolution' has been set up at the 1B target location and has been used to detect pions from the (p,π) reaction.

In the proton hall there was further effort on improving the energy resolution of the medium resolution spectrometer (MRS) as a result of the successful demonstration of single turn extraction from the cyclotron. Multiple scattering was reduced by removing the front counters and windows during a development run and resulted in a measured resolution of 230 keV at 200 MeV compared with a previous best of 0.6 MeV. It is believed that 200 keV was contributed by the incident beam energy spread. This result shows that improvements in the front and focal plane detectors and elimination of windows are extremely worth while, and efforts in this direction have started.

In addition to the developments described above, the experimental facilities group has been involved during the year in the design of several new channels, spectrometers and related facilities. The design of M11 high-flux pion channel was completed and most of the components ordered. The magnetic septum which provides the small angle of take-off for this fast pion channel was redesigned and successfully power tested during the year. A low-intensity proton line beam line 4C was designed to provide polarized protons to a polarized target which is in the process of being commissioned. An optics design for an improved M20 channel has been completed. Further details of these projects are presented elsewhere in this report.

TARGETS

Meson production targets

A new meson production target and control system were installed at the 1AT2 position early in the year, and the old 1AT2 target was moved to the 1AT1 position while the new 1AT1 target was being built.

Services to collimators at 1AT1 and 1AT2 were re-routed through the target cooling packages and the control and surveillance of these systems were upgraded.

During the summer shutdown the new 1AT1 target and control system was installed and commissioned. The M8 channel blocker, which had become unreliable in operation, was modified and reinstalled (in collaboration with Remote Handling group) towards the end of this shutdown. The new targets have, overall, performed very reliably and have caused virtually no loss of beam time to experimenters. At the same time, one recurring problem remains with the metal bellows sections of the cooling lines inside the target vacuum vessel. Leaking bellows forced the disassembly of both targets to allow temporary replacement of the bellows connections with a shorter stroke version which was on hand. During the January 1980 shutdown three changes will be made to cure the bellows problems as follows: 1) new bellows will be fitted which are fabricated from thicker material; 2) the guide tubes on which the bellows slide will be coated with a radiation-hard solid lubricant; and 3) the control system will automatically valve off the water pressure to the target during target movement.

The problems with the bellows had the beneficial side effect of demonstrating the ability to disassemble and rebuild the target structures in the remote handling hot cell.

A new water-cooled pyrolytic graphite target has been developed for the M8 (medical) channel users and for surface muon production: the new target has been added to the 1AT2 target ladder.

Polarized targets

The principal components of a 4 cm^3 polarized proton target were received from the University of Liverpool in February. These included the cryostat, helium-3 gas-handling system, superconducting magnet and the magnet power supply. These elements were assembled and made operational, following which certain other items, including the insulating vacuum system, the helium-4 gas-handling system and the liquid nitrogen handling system, were fabricated. The magnet and power supply were then tested at the normal operating current of 53 A. After the successful completion of this test, the magnet supports and vacuum can were modified to place the superconducting coils in the horizontal plane, to meet the experimental requirement for a vertically polarized target. This last operation introduced a cold leak into the cryostat which has so far been only partially repaired.

The remaining major components of the target, primarily the microwave system, the RF system (for target polarization measurement) and the support and alignment system have all been designed and are under fabrication.

Cryogenic targets

University of Manitoba Liquid Helium-4 Target. This target was repaired for a run in January and then put into storage. In December it was removed from storage and some renovations were undertaken for a run in the spring of 1980.

Liquid Deuterium Neutron Production Target. The LD_2 has run successfully through to the completion of the present BASQUE experiment in the proton hall. At that time it had deteriorated to such a point that a complete overhaul was needed before any more extended operation could be contemplated. The repair program envisaged entails maintenance of the Phillips A20 cryogenerator, rebuilding of the vacuum system, improvement of the thermal isolation of the target, checking the target for leaks, and replacement of the control system.

Hydrogen targets

A 20 cm LH_2 target operated successfully to the completion of the BASQUE experiment and has now been moved to allow installation of beam line 4C.

The TINA group (Expt. 9) has requested that a LH_2 target be installed in M13. The storage tanks and piping have been installed and fabrication of the target and target support frame are complete, ready for installation in the January-February 1980 shutdown.

For Expt. 80 (mesic X-rays) modifications were required to the TINA target assembly, allowing it to be used as a neon target. The modifications are 90% complete.

A target support frame has been designed for the (p,π) experiment.

The BASQUE superconducting solenoid

The solenoid was set up on the horizontal arm of the MRS for two successful experimental runs.

INSTRUMENTATION/NUCLEONICS

A detailed description of the administration of the TRIUMF pool of electronics is now incorporated into the Users Handbook which is available to all members of the TRIUMF Users Group. The complete list of pool standard equipment is shown in the current handbook and will no longer be tabled in the annual report. During 1979 the Instrumentation Advisory Committee was able to provide 75% of the new rental equipment that was requested by experimental groups.

A new procedure of obtaining and returning rental items from Stores has been implemented. There are some minor problems to be sorted, but generally the new system is working well.

DATA ACQUISITION SYSTEMS

After many years of unkept promises, in 1979 a programmer was at last assigned full time to the task of assisting users of PDP-11-based data acquisition systems. Several jobs have been undertaken, including implementation of user-requested modifications to RT-11 MULTI; support of the IAC-approved Kinetics 3912 CAMAC Crate U controller under RT-11 MULTI; updating of the radioisotope production spectrum-former, with data transmission to the TRIUMF Data Interface; and implementation of MULTI operating under RSX-11-M using the BiRa MBD Branch Driver. The latter is a major task to be carried over into 1980. One programmer has also been seconded to the MRS group to assist with development of the display and event analysis parts of the MRS data acquisition systems.

RF SEPARATOR

The beam from the M9 extension installed this year suffers from the relatively poor transmission of the 3 m long dc separator (~50%, 10% $\Delta P/P$). A design study for a 1 m long RF separator was begun late in 1978 and completed this year.

The RF separator will be centred at approximately the same position as the dc separator and the beam line design has been optimized (restricted) to the 77 MeV/c μ^- beam. The beam line will use the same quadrupoles as the present M9 extension with the addition of two additional power supplies for simultaneous excitation of both doublets upstream of the separator. The location of the three experimental foci will be unchanged.

The flux of 77 MeV/c μ^- is estimated to be 9×10^5 sec^{-1} at 100 μA, with 25% of the flux outside 10% $\Delta P/P$. This is approximately an 80% increase in the flux measured on the present M9 extension. The contamination of pions is calculated to be <1% and electrons, $\lesssim$5%.

The first reference design was prepared in early 1979. Since then it has been decided that no third harmonic flat-topping would be considered and that a separate RF liner would be used in order to reduce the RF leakage being propagated down the beam line. As a result the following RF structure reference design was established:

Electrodes	Width	25 cm	
	Length	100 cm	
	Gap	15 cm	
	Gradient	24 kV/cm	
	Voltage	±180 kV	
RF liner	Width	45 cm	
	Length	115 cm	
	Height	38 cm	
Vacuum chamber	Width	58.4 cm	
	Length	123.8 cm	
	Height	51.4 cm	
Resonators		Tip	Root
	i.d.	7.6 cm	7.6 cm
	o.d.	17.8 cm	40.6 cm
	Z_0	50 Ω	100 Ω
	Length	60 cm	99 cm

The RF power will be supplied by using the 120 kW RF amplifier that was initially used for the CRC model work. The amplifier and dc power supply have been resurrected and prepared for tests into a dummy load.

A model of one-half of the RF separator was constructed, and preliminary measurements agree within 2% of the design values. The standing wave transmission line and coupling loop which connects the amplifier to the resonator have been designed, and detailed drawings are available. Mechanical design of the separator and resonator structure has been initiated. Design of the coils for a crossed magnetic field needed to enhance the separation has been begun. The overall design will be to keep the RF separator as modular as possible to facilitate future exchange between it and the dc separator on M9.

It is hoped that the RF separator will be ready for installation by September 1980.

MESON HALL

There were two major shutdown periods in the meson hall. During the shutdown which started in October 1978 and continued into January, in addition to the work on M13 and beam line 1B a new meson production target was installed at 1AT2. The old 1AT2 target was installed at 1AT1 to allow initial commissioning of the M13 channel. After some operating experience with a target at 1AT1 it was found necessary to provide additional shielding after the quadrupole doublet 1AQ10,11 downstream of the target to prevent the 1AT1 spill from reaching non-radiation-hard components. This shield was installed during the second shutdown period in June, and at the same time the meson production target 1AT1 was replaced with the new design.

The M8 blocker jammed several times during beam operation, usually during high-current runs, and was replaced with a more reliable design. The hot cell was completed by the Remote Handling group and was heavily used, as in addition to the M8 blocker work there were several repairs to the meson production targets as a result of bellows failures. The lead target at TNF was removed after 50,000 μA h of beam and replaced with an identical target having a few minor improvements.

A potentially serious problem had a happy ending when it was discovered that the middle quadrupole of the last triplet before the TNF had developed an open circuit. It turned out that the triplet which is on rails had shifted by about 1 in. causing the quick disconnect current connection to open. This was easily slid back into position with little exposure to personnel.

Three of the counting room shacks on the meson hall floor (level 264) were removed. Part of the floor space was used for the construction of the TPC counting room. The remaining space has been allocated for experimenter set-up areas and a general work shop area for experimenters. Additional storage for experimental equipment is being provided on the ground level mezzanine.

New workbenches and storage facilities are being provided for on the hall floor level (264). Also new lighting, power and services should be available by January 1980.

M9 extension

Work on the M9 extension incorporating a 3 m dc particle separator began early in the year. The final installation was realized in November and is shown schematically in Fig. 106. Some beam tuning and four experiments were run on the channel at the end of the year before the major shutdown in December.

The separator itself was tested off line in April, and high voltage of 400 kV on the plates was achieved with high vacuum (2×10^{-6} Torr). However, in later tests with beam, voltages of over 360 kV could not be reached. At values above 320 kV the stability was poor, and high fields of X-rays from the separator were found to be intolerable to some experiments. Work is going ahead to modify the vacuum system to allow the separator to be operated with a 1 Torr pressure of argon. With this change a voltage of ~600 kV should be possible with improved stability and X-ray suppression.

Beam tuning with surface μ^+ (29.8 MeV/c) showed that an electric field of 5 kV/cm (50 kV total) was sufficient to reduce positron contamination of the beam to a few per cent. The beam spot was ~4 cm diam FWHM, and calculations indicate this can be reduced by nearly a half by replacing the 25 μm windows on the separator by ⩽6 μm windows. The flux of surface muons through the separator is approximately 6.5×10^5 sec^{-1} (±20%) for a 100 μA proton beam on the 10 cm Be target at 1AT2.

The magnetic field of the separator acts to precess the spin of the surface muon beam. Measurements were made showing that the precession was close to 90° for the maximum field (~450 G) possible with the present power supply. For routine operation in this mode a larger magnet power supply and more reliable high voltage of ~400 kV will be needed. A beam of transversely polarized μ^+ will then be available for stopping in very high axial magnetic fields for μSR experiments.

The 77 MeV/c cloud μ^- beam was found to have a spot size at M9 W3 of 2×3 cm^2 FWHM and a flux of 5×10^5 sec^{-1} for 100 μA of protons on the 10 cm Be target. This is consistent with the more optimistic expectations from beam calculations. The beam spot at M9 W4 in the Chicago magnet was larger (~8 cm diam FWHM), and further beam development is planned. Beam studies at M9 W4 are complicated by the physical constraints of the Chicago magnet and TPC. A special 14-finger hodoscope has been developed to measure beam profiles at the centre of the TPC.

The beam composition of the separated 77 MeV/c beam showed ⩾50% muons with the contamination of pions and electrons depending on the high voltage of the separator. The effect of the separator is shown by the time-of-flight

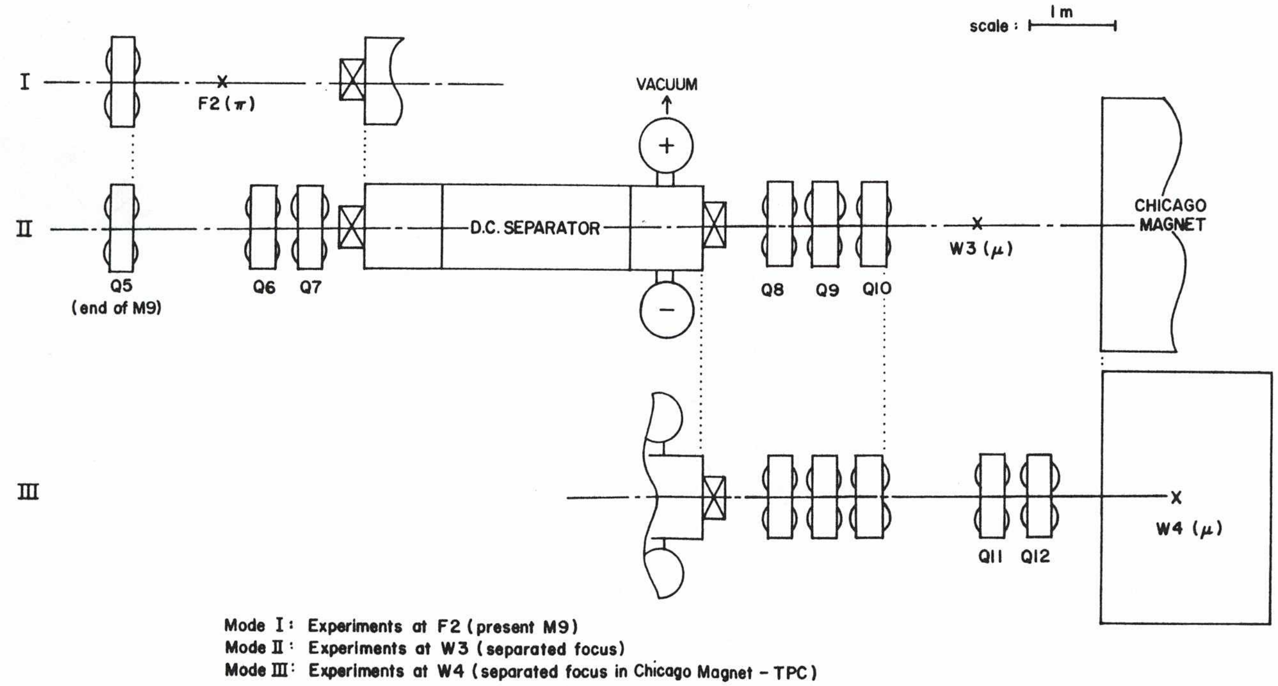

Fig. 106. Layout of M9 extension.

spectrum of the beam at M9 W3 in Fig. 107.

Improved high voltage capability (≳450 kV) should significantly reduce the contamination. The optimum location and aperture of a mass slit downstream of the separator to further reject contaminant beam will also be examined.

In beam studies thus far, it has been found that the tuning of the separator is largely independent of the tuning of the rest of the beam line.

M11 channel

Work on the M11 fast pion channel has been reactivated, and installation is scheduled for May 1980. This follows completion of an optical redesign which included second-order correction elements (TRI-DNA-78-4). The mechanical design of the channel is now complete, and a plan of the channel is given in Fig. 108. The channel centre-line length is 14.2 m. The channel will accept forward-going pions produced at the 1AT1 target and directed into the channel by 1AQ9 and the septum magnet. Three target positions are provided for in the experimental area.

Considerable effort was made on the front-end design to utilize radiation-hard materials

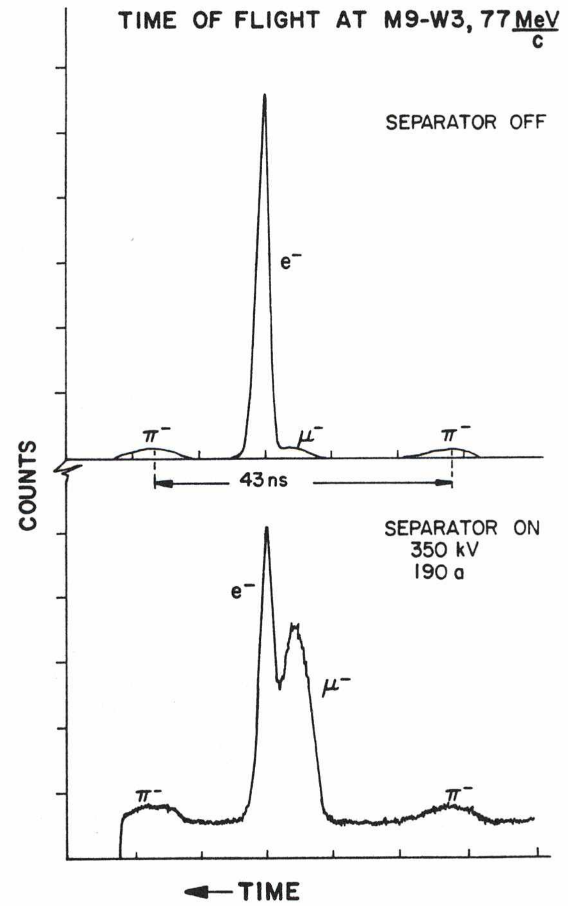

Fig. 107. Effect of the dc separator in modifying the ratios of $\pi^-:e^-:\mu^-$ reaching M9W3.

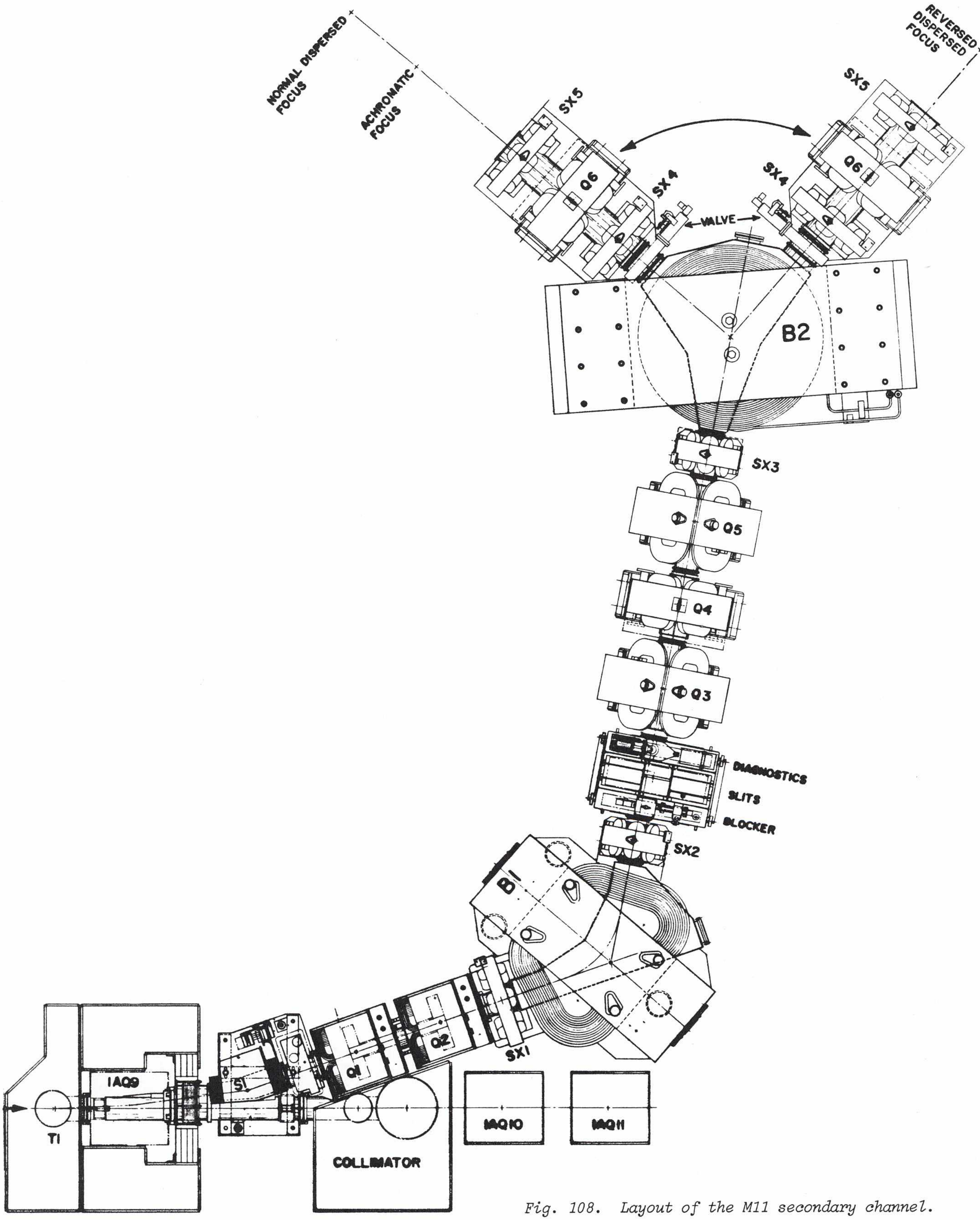

Fig. 108. Layout of the M11 secondary channel.

and provide complete remote handling capability. Each element up to the first bending magnet can be remotely removed and reinstalled. A prototype of a new remote handling flange has been built that will pass through a quadrupole and will utilize removable indium ring seals. This will allow repair of the vacuum seals without removing components.

Delivery of magnet components is critical to the installation schedule. The new M11B1 coils and yoke steel have been delivered and assembled, but the coils had to be returned to the manufacturer and could cause delay. New coils are being manufactured for M11B2 (the Corvallis magnet) while yoke and pole modifications are under way at Victoria Machinery Depot. Coils for the sextupole magnets are being made at Best Coils, a Vancouver company. However, they are having trouble with their manufacturing technique and have yet to complete a successful coil. A new septum magnet coil has been successfully completed in Victoria following failure of the brazing procedure for the first coil.

The installation of M11 will proceed in two stages. The magnet stands and bases, electrical and water services installation started in December; the final installation of the components will proceed in May 1980. The one item that may not be ready at that time is M11B2, but it is outside most of the shielding and may be installed at a later date.

Thermal neutron facility

The thermal neutron facility, which serves as the beam stop for beam line 1A, has operated throughout the year causing only 20 min of cyclotron downtime, due to hypersensitive interlocks.

A -100°C refrigerator was installed to replace the cumbersome liquid nitrogen trap in the radio-mercury storage system, eliminating the need for attention by Operations staff.

The lead target was changed for the first time during the June shutdown after having been exposed to 70,000 μAh of beam. The target has been stored in a water-filled hole, awaiting inspection at CRNL.

Four rabbit tubes were installed to use the thermal neutron flux. Two of these are in continuous use by Novatrack.

Neutron diffraction spectrometer

A vertical monochromated neutron beam has been extracted from the thermal neutron facility. The horizontal axis spectrometer has been assembled and installed over the collimator. A platform was installed at the 283 ft level for easier access to the spectrometer. The instrumentation is almost complete. Operations should start during early 1980.

PROTON HALL

General

Two 2-ton-capacity overhead cranes were installed under the roof beams to provide crane access to the target areas on beam line 4B. During the shutdown at the end of the year these cranes were modified to provide greater floor coverage.

Medium resolution spectrometer (MRS)

During beam development MRS was run with ΔE_B and the front MWPC counters removed and windowless vacuum from the target to exit of dipole horn. A 5 × 5 in. delay line readout MWPC was mounted in the focal plane between the normal focal plane detectors. The resolution measured was 230 keV FWHM at 200 MeV after correction of the T_{122} aberration. It is believed that 200 keV was contributed by the incident beam energy spread; the additional broadening might be due to vertical spot size of the beam on the target.

Resolution of 615 keV FWHM at 500 MeV was seen with the usual front-end scatterers in place. Although measured using the delay line chamber, this record resolution was also evident in the spectra of the standard amplifier-per-wire MWPC's. We believe the improvement in the raw beam resolution is due to better beam centring in the cyclotron.

Low energy tail: the giant resonance and dibaryon experiments were troubled by a tail on the elastic peak which extended down into the deep inelastic region. It was associated with an off-centre beam or extended target and is due to very-small-angle scattering from the pole faces of the dipole.

The CERN-type NMR was tested in the MRS dipole. The signal was poor, due to slightly magnetic stainless steel in the end cap of the vacuum jacket and field gradients. An all-copper, 10 cm longer vacuum tube has been made.

For the past year much of the work on MRS development has concentrated on the software system for the Data General Eclipse computer. The objective is to develop a general purpose data acquisition and analysis system which will eventually serve the three Eclipse-based computer systems currently in use by beam line 4B experiments. When the software is complete, two of these systems will replace the existing Honeywell 316 computer to acquire data from experiments at 4BT1 and 4BT2 (MRS) while the third will remain in Edmonton to analyse the resulting experimental data.

The three systems are similarly configured, each with a disc drive, one or more tape drives, display processor and CAMAC processor. The display and CAMAC processors in each system are organized around a small independent computer attached to the central Eclipse and sharing memory with it. Thus, the software development is aimed at utilizing such a three-processor system to fullest advantage. There is considerable flexibility possible in deciding whether a particular function should be performed by the central Eclipse or one of the peripheral processors.

Work has proceeded to develop simultaneously the software for the three connected processors. The first version of the software for the display processor is completed and documented. It provides the capability of driving three video monitors and receiving input from a console keyboard (attached to one of the monitors). The MRS system is presently configured with a single monitor which is used for input and output as well as graphics displays in three intensities. Another monitor will be added in the near future to display messages and tables. The display driver has separate video memory which allows graphs and text to be overlaid on the screen and instantaneous switching from one display to another.

The software for the central Eclipse utilizes Data General's Realtime Disc Operating System (RDOS), version 6.32. This multitasking system has allowed us to develop a flexible command line interpreter to handle commands from the experimenter at the console keyboard. Support routines have been developed to facilitate the implementation of commands as normal FORTRAN subroutines. When the name of the subroutine is typed at the console the named program is overlaid into memory and executed with preassigned priority. Several command routines may be simultaneously active, and their competition for core memory and I/O resources is managed to avoid conflicts as much as possible. A keyboard interrupt facility has also been developed to allow in-progress command routines to be aborted or suspended temporarily when emergency situations are discovered by the operator (such as line-printer jams, etc.).

Software development for the CAMAC processor is being done by the University of Alberta software group in collaboration with the MRS group at main site. This software will communicate with the BiRa CAMAC interface when requested by one of the command process routines in the Eclipse computer or in response to LAM interrupts from the CAMAC system. The multitasking structure of the Eclipse software is being integrated into the CAMAC processor software to allow independent access to CAMAC by several (or many) active routines in the Eclipse. A prototype version of this software is expected from Edmonton in the first quarter of 1980.

The target date for an operable acquisition system is April 1980.

VAULT

TRIUMF low-energy facility — beam line 2C

In 1979 the Cyclotron Development, Experimental Facilities and Applied Program groups worked toward the design of a multiple use, low-energy facility which will utilize a third simultaneous beam at TRIUMF.

The plan seen in Fig. 109 is for variable energy from 70-110 MeV and high currents. The magnet system will be able to deliver 2 cm beam spots to five locations on the cyclotron vault wall. Three stations will house isotope generators, a fourth is planned as a batch station, and the fifth leg will provide a collimated fast neutron beam to an external area for radiation biology experiments. The combination magnet is in construction and the quadrupoles are being designed at the year's end.

Of major concern is the man dose which will be received when this equipment is installed.

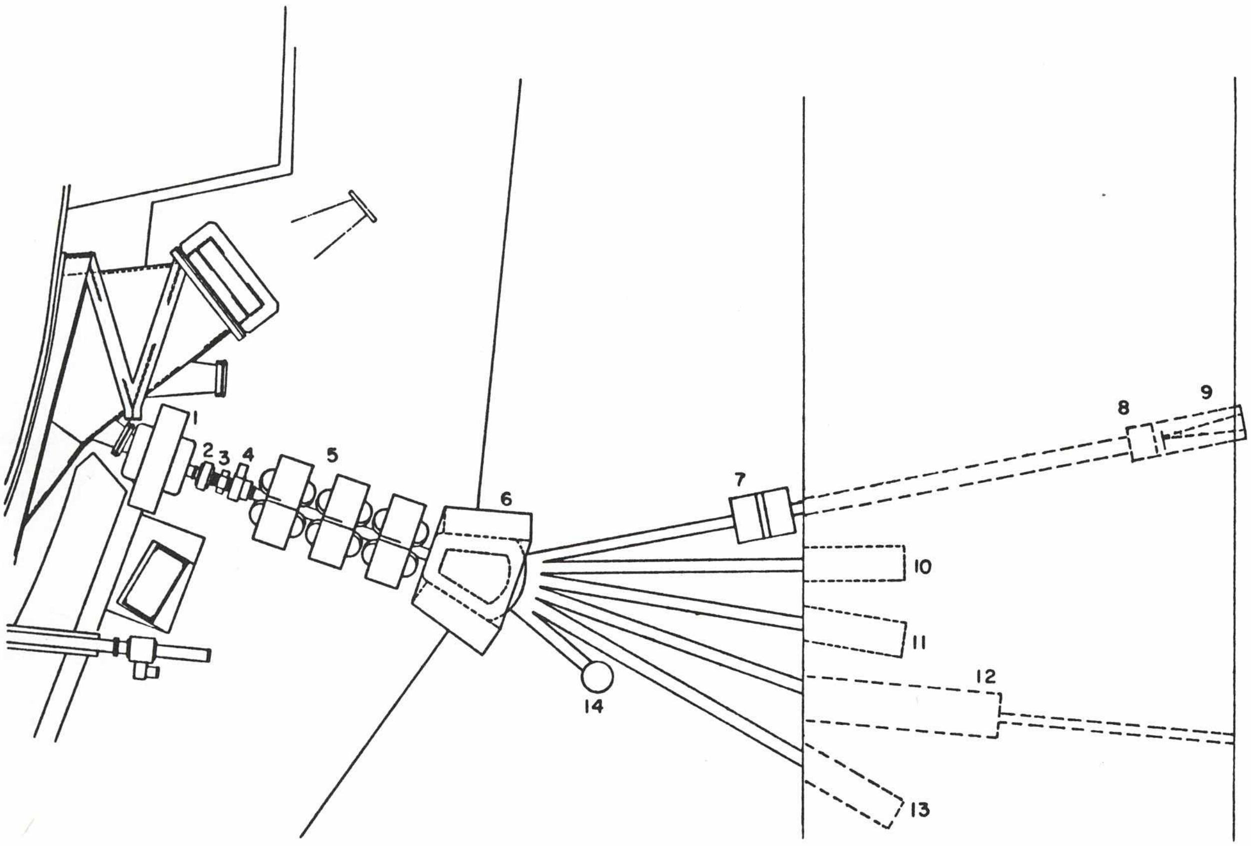

1. Combination magnet	6. Switching magnet	11. Sodium iodide target
2. Rad hard valve	7. Quadrupoles	12. Solid targets
3. Gate valve monitor	8. Quadrupole	13. Research
4. Fast valve	9. W.E.P. collimator	14. Turbo pump
5. Quadrupoles	10. Cesium target	

Fig. 109. Proposed layout of beam line 2C inside the vault.

The Cyclotron Development group has completed an extensive area dose study which allows each installation task to be assigned a man dose as a function of predicted cyclotron operation. This information is being fed back into the design to minimize personnel exposure.

During the summer it was decided to install an interim facility for the production of ^{123}I from the (p,5n) reaction. The hardware consists of a 3 g/cm^2 sodium iodide target of the generator type and a shielded receiving station located about 100 m from the cyclotron. The effort is being jointly sponsored by AECL and TRIUMF and is intended to provide operational experience with the third beam while the permanent beam line is in construction. The interim production system became operational in December and was exercised once before the winter shutdown. ^{123}Xe was collected, for a known beam flux, allowed to decay to ^{123}I, which was in turn extracted and analysed. The yield of activity was consistent with the physical parameters of the system and published cross sections. Nuclidic purity, while much improved over that achieved with ^{123}I from 500 MeV spallation of cesium, was somewhat lower than expected but should be improved with some adjustments in the beam and target system. A regular production schedule is envisioned for 1980 at beam fluxes consistent with the overall plans for the permanent beam line.

CONFERENCES, WORKSHOPS AND MEETINGS

8-ICOHEPANS

The Eighth International Conference on High Energy Physics and Nuclear Structure, organized jointly by TRIUMF and UBC, was held August 13-17 with 540 delegates from 24 countries. This conference series, which was initiated at CERN in 1963 by V.F. Weisskopf and A. De Shalit, has become the natural home for reporting research at the meson factories. These machines were constructed expressly to apply the techniques and the particle beams of the then 'high energy physics' to the study of nuclear structure. In fact the last few conferences have all been held close to meson factories, viz. 1975 Santa Fe (LAMPF), 1977 Zürich (SIN) and now 1979 Vancouver (TRIUMF). Although the title lends itself to misinterpretation, it was decided to retain it for the next conference, which will be held in France, probably Paris, in 1981.

Throughout the week it became clear that the meson factories were now 'in production' and many beautiful experiments were described and discussed. The interface of particle and nuclear physics is clearly a place for creative talent. This year's conference lacked a single high spot of interest that was the feature of the Zürich Conference (the $\mu \rightarrow e\gamma$ experiments), yet there were a series of important contributions on many topics including baryonium, nucleon-nucleon resonances, lepton conservation laws, matter radii of nuclei, isospin mixing in nuclei, and finally a cluster of exotic ideas about the properties of nuclei including pion condensation and the quark soup model.

The social highlight of the conference was undoubtedly the cruise to the small town of Nanaimo on Vancouver Island. Someone had spread the rumour that the boat contained nuclear scientists who were looking for a site to build a 'nuclear structure' (i.e. reactor) to produce 'high energy'. We were

(Photo: Nanaimo Daily Free Press)

greeted by a fair-sized but peaceful demonstration, including small boats bearing occasionally obscene slogans! Needless to say, the overseas delegates delighted in snapping photos of banners such as 'No nukes', or 'I'm too young to die''. It must be added that after discussions with delegates on the dock many of the youngsters demonstrating went away wiser than they came, and several delegates acquired placards as a memento of a short but intense discussion. In attempting to explain the delegates' essential harmlessness to the local press, Karl Erdman, Associate Director of TRIUMF, was memorably quoted to the effect that 'Most of these physicists wouldn't know one end of a screwdriver from the other'.

KAON FACTORY WORKSHOP

This workshop, sponsored by TRIUMF and attended by 230 delegates from 18 countries, was held at UBC in August in parallel with the Eighth International Conference on High Energy Physics and Nuclear Structure. Its purpose was to consider both the physics potential and the practical design of machines to produce intense beams of kaons and antiprotons—typically 100-1000 times more intense than those available from present proton accelerators in the 8-30 GeV range. Table XV lists the program of invited papers. In addition 35 contributed papers were presented either orally or in poster sessions. All the papers appear in the Proceedings of the Workshop, which has been published as a TRIUMF report.

There are two strong thrusts for the experimental program. One is the study of resonance and particle properties, particularly the K^- nucleon system, and the rare decays of the kaons and hyperons. The other (emphasized perhaps by current activity and the nuclear leanings of the main conference) is to explore nuclear physics problems from a fresh angle, using the very different properties of the K^-, K^+ and Λ as probes, the first rich in its capacity to excite resonances, the second poor, a feebly interacting hadron, the third a 'strange' tagged neutron, the seed for the rapidly blossoming field of hypernuclear physics. All in all it appears that the kaon factories would open up an exciting new realm of physics just as the pion factories are doing now.

Particle physics

Here discussion centred around a number of important fundamental questions which can only be tackled with the help of more intense beams. Searches for possible muon number non-conserving kaon decays such as $K \to \mu e$ in the strangeness non-conserving sector would complement the current searches for reactions such as $\mu \to e\gamma$ and set limits for this violation within modern gauge theories. Precision measurements of usual kaon and hyperon decays would be useful as would detailed studies of the various rare decay modes which test our understanding of effects of higher-order weak and electromagnetic interactions. CP violation is not yet understood and investigations of CP-violating correlations in K decays might elucidate the mechanism responsible for the violation. In a slightly different area, detailed studies of the spectrum and decay properties of hyperon resonances (particularly the K^--nucleon system, rich in resonances of all degrees of reliability) could test crucial ingredients of current theories of quantum chromodynamics.

Consideration was also given to possibilities of experiments with antiprotons. Here the new LEAR project at CERN will give orders of magnitude improvement over existing facilities. The spectroscopy of baryonium and protonium, searches for $qq\overline{qq}$ quark states, quasi-nuclear $N\overline{N}$ bound states, $p\overline{p}$ annihilation reactions, and exotic channels such as $\overline{p}\Lambda$ are just a sampling of the rich field of antiproton physics dependent on higher intensities.

Hypernuclear physics

In the area of hypernuclear physics the (K^-,π^-) reaction allows one to produce a Λ essentially at rest in a nucleus. Already a good start has been made on a periodic table of such hypernuclei, and some excited states have been observed, with the best resolution being achieved by the Strasbourg/Saclay/Heidelberg group at CERN. Such information opens new areas of nuclear spectroscopy. Does the Λ behave simply as a 'strange neutron' forming Λ-particle-neutron hole excitations? Do the strangeness analogue resonances, generalizations of the usual isobaric analogue states, exist? A whole host of interesting questions can be explored. To obtain detailed excitation spectra, however, coincidence experiments detecting the decay γ will be needed, as will

Table XV. Kaon Factory Workshop.

	Speaker
Physics I (Chairman: D.V. Bugg)	
Opening remarks	J.R. Richardson
Nuclear physics with kaons	C.B. Dover
Physics for a new kaon facility at the AGS	M. May
Report on Los Alamos Kaon Factory Workshop: Physics	R.R. Silbar
Kaon elastic and inelastic scattering at 800 MeV/c	R.A. Eisenstein
Kaon-nucleus interactions	F. Tabakin
Contributed papers	
Accelerators and Beams (Chairman: J.R. Richardson)	
An improved kaon beam and spectrometer for the AGS	E.V. Hungerford III
The Fermilab booster as a kaon factory	B. Brown
Possible kaon and antiproton factory designs for TRIUMF	M.K. Craddock
A LAMPF kaon factory	D.E. Nagle
Contributed papers	
Physics II (Chairman: E. Boschitz)	
Symmetry-violating kaon decays	P. Herczeg
Hyperon physics and chromodynamics	N. Isgur
Physics possibilities with LEAR, a low-energy anti-proton facility at CERN	U. Gastaldi
Contributed papers	
Poster session	
Joint session with 8-ICOHEPANS	
Summary of Kaon Factory Workshop	E.M. Henley
Related invited papers at 8-ICOHEPANS	
Hypernuclei	B. Povh
Baryonium	H.-M. Chan
Exotic atoms and hypernuclei	C.B. Dover

(K^-,π^-) experiments at larger momentum transfers so as to allow higher angular momentum transfer. For both of these more intense beams are essential.

Hypernuclei also provide information on the basic Λ-nucleon force, and already indications are that the spin-orbit component is much weaker than the NN case. Clearly a basic understanding of Λ-N (and Σ-N) interactions is extremely important, and may enhance our understanding of the more familiar NN force.

Kaon-nucleus interactions

Another area of discussion dealt with the elastic and inelastic scattering of kaons from nuclei and the kinds of nuclear information which can be obtained. K^-'s are strongly absorbed on nuclei, leading to the production of a large variety of relatively narrow Y^* resonances whose spectra and decay properties can be studied. One can also investigate the propagation of such strange resonances in the nuclear medium in analogy with, and using similar formalisms as, for example, the isobar-doorway formalism, used to study Δ's in nuclei.

On the other hand, K^+'s are very weakly absorbed, with a long mean free path and no 'true' absorption, and are potentially simpler than the pion and very useful for exploring nuclear densities via elastic and inelastic scattering. Some beautiful new data for both K^+ and K^- scattering from the Carnegie-Mellon/Houston/Brookhaven collaboration were shown at the workshop together with relatively successful analyses in terms of kaon-nucleus optical models. More information is needed on the K-nucleon amplitudes which serve as input for the calculations but clearly the first steps have been taken towards making the kaon, like the pion, a very useful nuclear probe.

Improved beams

Studies for improved low momentum kaon beams were reported from BNL and KEK, in the former case integrated with a high resolution spectrometer. Both designs are aiming at short channel lengths (8-10 m) to reduce the decay losses (at KEK by the help of superconducting combined function current sheet magnets). At Brookhaven, the hope is to gain a factor 10 in kaon flux over existing lines on the AGS while maintaining a π/K ratio $\leqslant 10$. The beam line itself will probably provide the dispersing system for the energy loss spectrometer; the aim is for an energy resolution of 200 keV at 800 MeV/c, with a momentum bite of 6% and angular coverage 0-140°. (It now seems that this project may be funded in the early 1980's.)

For slow antiproton physics it seems that the immediate future will be dominated by the recently funded LEAR project at CERN. This 0.1-2 GeV/c storage ring, fed by beam decelerated from the antiproton accumulator, will increase low-energy antiproton beam intensities by 10^3 to 10^6 over those now available, and will eliminate beam contamination.

Kaon and antiproton factories

Although (with one exception) present-day multi-GeV accelerators provide proton beams of no more than a fraction of a microampere, it appears to be technically feasible to construct accelerators capable of giving (see Fig. 110) 30 μA at 30 GeV, or even 400 μA at 8 GeV (energies suitable for production of antiproton and kaon beams, respectively). At Fermilab the 8 GeV fast-cycling booster synchrotron (the exception noted above) has already reached 7 μA and could eventually produce 12 μA at 10 GeV. It was pointed out that although the present duty factor is too small for coincidence experiments, it could be lengthened either by slow resonant extraction or by the use of a 'stretcher' ring. So apparently a potential kaon factory already exists—if the users to whom it was previously committed can be squared!

The virtues of fast-cycling synchrotrons were also recognized by LAMPF and TRIUMF in their after-burner proposals, the former based on a machine for 50 μA at 16 GeV, the latter on one for 80 μA at 10 GeV. In TRIUMF's case a second stage slow-cycling synchrotron with superconducting magnets was proposed to accelerate 30 μA to 30 GeV for

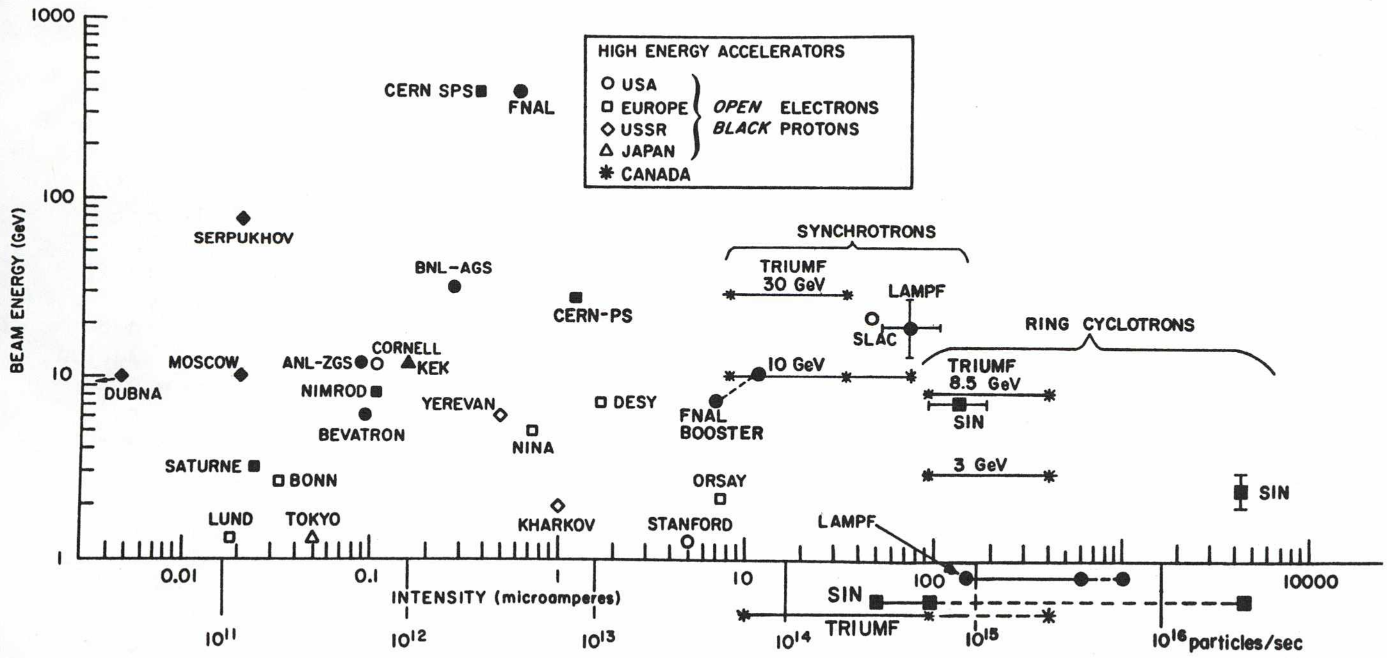

Fig. 110. Distribution of high-energy accelerators in energy and intensity (adapted from Panofsky, Proc. IX Int. Conf. on High-Energy Accelerators, Stanford, 1974, p. xi).

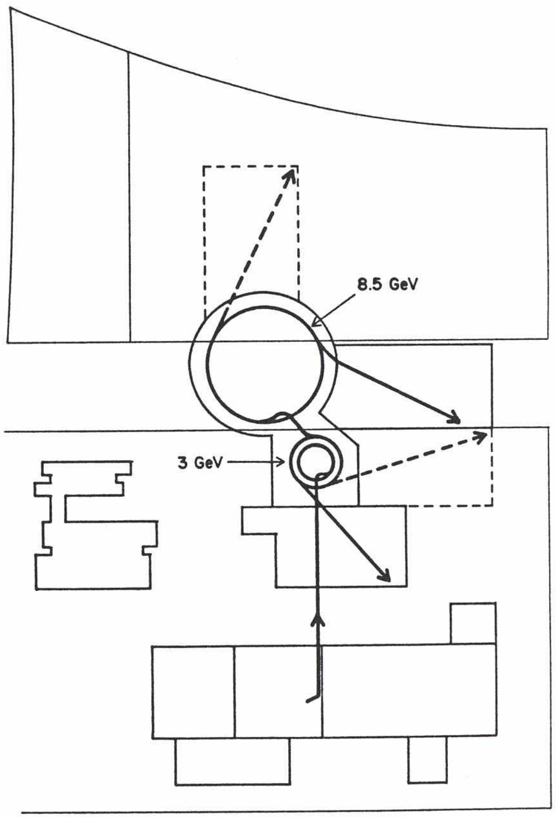

Fig. 111. 'CANUCK' superconducting ring cyclotrons.

antiproton production. An alternative proposal, which would not compete directly with the strong effort going into antiproton physics at CERN and Fermilab, was for a two-stage isochronous ring cyclotron ('CANUCK'—Canadian University Cyclotron for Kaons—see Fig. 111) to accelerate 100-400 µA protons first to 3 GeV and then to 8 GeV for kaon production. SIN also reported starting a design study for a 4-5 mA 2-3 GeV ring cyclotron as a high flux spallation neutron source, with the possibility of this feeding into a 100-200 µA 8 GeV cyclotron kaon factory.

From this workshop and similar ones held elsewhere, it is clear that orders of magnitude more intense kaon and antiproton beams would open up exciting possibilities in both particle and nuclear physics; and moreover that the machines to produce them are technically feasible. The question remaining is who has the will and can command the resources needed to build these facilities and reap the consequent rewards?

WORKSHOP ON THE FUTURE OF PION-NUCLEUS PHYSICS

The workshop on the future of pion-nucleus interactions was held at TRIUMF from July 22 to August 3. Financial support was provided by NSERC, AECL and TRIUMF. We would like to thank all of these organizations for their assistance and support. The overwhelming feeling of all present was that the funds were well spent.

The format of the workshop was very simple. Each speaker had a morning to develop his topic in an atmosphere where discussion was encouraged. The afternoons and evenings were free for spontaneous small group discussions and collaborations. With little exception the speakers were willing to explain not only the advantages of their pet approaches but also the problems. Thus we were all led to a better understanding of the future theoretical developments, and also of the possible experimental tests of existing theory.

The topics covered ranged all the way from quantum chromodynamics and bag models to meson exchange current corrections in Gamow-Teller transitions, and to pion-nucleus elastic scattering and reactions. During the two weeks of the workshop it was appreciated just how closely related were these apparently different areas of nuclear and particle physics. Since it is impossible to do justice to any of the presentations here, the interested reader is referred to TRIUMF report TRI-79-2 for more details and references.

WORKSHOP ON HIGH RESOLUTION SPECTROSCOPY WITH INTERMEDIATE ENERGY PROBES

Of the eight panels making recommendations for the direction of intermediate-energy physics over the next decade at LAMPF, not less than three recommended a high resolution spectrometer for TRIUMF. A workshop was therefore held at TRIUMF on October 5 and 6 to examine the role of a high-energy spectrometer three years hence.

TRIUMF occupies a unique position, having an energy continuously variable from 185 to 515 MeV, multiple extracted beams, the highest intensity polarized proton beam of all meson factories and excellent prospects for achieving 0.1 MeV resolution in the extracted beam. Spin effects have a clear, large signature in the intermediate-energy region, and it is hoped to use these effects in unravelling underlying nuclear structure and reaction dynamics.

Attendees listened to presentations on inelastic scattering, elastic scattering, giant resonances, pick-up reactions and (p,π). The proceedings will be published as a TRIUMF report in 1980.

TRIUMF USERS GROUP ANNUAL GENERAL MEETING

In keeping with tradition, the annual general meeting was organized by the TRIUMF Users Executive Committee (TUEC) to immediately precede the November meeting of the Experiments Evaluation Committee. The program was divided into six sequential (as opposed to parallel) sessions, five held in the BCRC Auditorium and one evening session in the Graduate Student Centre of UBC. For a change in format from previous years, many of the shorter facility reports were written and distributed at the meeting, thereby concentrating the discussion on specific items of interest and avoiding the need for parallel sessions. Emphasis was placed on more extensive presentations of general interest to the TRIUMF users.

Session A consisted of talks by P. Percival on muonium chemistry in liquids and A. Astbury on the proposal to build a low-energy antiproton ring (LEAR) at CERN.

Session B was devoted to discussions of two new facilities at TRIUMF and the TUEC Chairman's report. As outlined by G. Ludgate, beam line 4C and a polarized proton target have been constructed to facilitate $\Delta\sigma_L$ and $\Delta\sigma_T$ measurements for pp scattering. J. Macdonald summarized the features of the M9 extension including operation of the dc separator. In his summary of TUEC's activities for the year, G. Beer drew special attention to its role in response to the Fyfe Report.

The applied program with emphasis on the biomedical aspects was the subject of Session C. J. Sample's survey of the general program at TRIUMF was followed by details of the latest achievements in the pion therapy experiments from L. Skarsgard. Perspective was added with a review of C. Tobias of the biomedical program at Berkeley using heavy ions.

T.R. Ingraham from NSERC initiated Session D with an outline of that agency's plans for major increases in funding anticipated over the next five years. G. Dutto followed with highlights of the year's activities in the area of cyclotron development at TRIUMF. Finally, this session was concluded by brief discussion of the written facility reports distributed at the meeting.

The evening session was intended to promote thought and discussion of future plans. R. Liljestrand reviewed the findings of a LAMPF summer workshop and D. Measday focused on aspects of the present status and possible future directions of the TRIUMF program. M. Craddock's summary of the findings of the recent kaon factory workshop urged serious consideration of such a facility for TRIUMF. Insight into the aspirations of the IPP community was obtained by an outline by J. Prentice of their proposal to build an electron storage ring and detector for the study of very high energy e-p collisions at Fermilab.

In the closing session (shared with the EEC) J. Sample, K. Erdman and W. Bryan summarized recent achievements at TRIUMF and discussed plans for the immediate future. J. Cameron reviewed the outcome of the HRS workshop held at TRIUMF in October. The final presentation was a report by J. Prentice on experiments in progress at Fermilab to determine the lifetime of charmed hadrons.

ORGANIZATION

Board of Management

The Board of Management of TRIUMF manages the business of the facility and has equal representation from each of the four universities. At the end of 1979 the Board comprised:

University of Alberta	Dr. H.E. Gunning	
	Dr. G.C. Neilson	
	Dean K.B. Newbound	*Hon. Secretary*
Simon Fraser University	Dr. B.P. Clayman	
	Dr. W. DeVries	
	Dean J.M. Webster	
University of Victoria	Dean J.M. Dewey	
	Dr. R.M. Pearce	
	President H.E. Petch	
University of British Columbia	Dean P.A. Larkin	
	Mr. D. Sinclair	
	Dr. E.W. Vogt	*Chairman*

Non-voting members:	Dr. R. Pottie, National Research Council	
	Dr. J.T. Sample, Director, TRIUMF	
	Dr. G.A. Ludgate, TRIUMF	*Secretary*

Changes in board membership were: Dr. G.A. Ludgate, Documentation Officer at TRIUMF, assumed the duties of the secretary; Dean K.B. Newbound was appointed the Honorary Secretary. Dr. G.C. Neilson, Director, Nuclear Research Centre at the University of Alberta, replaced Mr. W.A.B. Saunders.

The board met three times during the year.

Operating Committee

The Operating Committee of TRIUMF is responsible for the operation of the facility. It reports to the Board of Management through its chairman, Dr. J.T. Sample. It has four voting members, one from each of the four universities. The Associate Directors are non-voting members. The members of the committee (alternate members in parentheses) at the end of 1979 were:

Dr. J.T. Sample	*Chairman*	Director	
Dr. K.L. Erdman		Associate Director, Facilities	
Dr. B.D. Pate		Associate Director, Applied Program	
Dr. G. Roy		University of Alberta	(Dr. J.M. Cameron)
Dr. R.G. Korteling		Simon Fraser University	(Dr. J.M. D'Auria)
Dr. L.P. Robertson		University of Victoria	(Dr. G.R. Mason)
Dr. G. Jones		University of British Columbia	(Dr. M.K. Craddock)
Dr. G.A. Ludgate	*Secretary*	TRIUMF	

Changes in 1979 were: Dr. G.A. Ludgate, Documentation Officer, TRIUMF, assumed the duties of the secretary from Dr. K.L. Erdman.

TRIUMF Safety Advisory Committee

Mr. I.M. Thorson	*Chairman*	
Dr. E.W. Blackmore		
Mr. J.J. Burgerjon		
Mr. J.W. Carey		
Mr. S.C. Fraser		attends meetings as a WCB observer
Dr. D.R. Gill		
Dr. M.W. Greene		Ministry of Health
Dr. G.A. Ludgate	*Secretary*	
Mr. L.E. Moritz		
Mr. A.J. Otter		
Dr. B.D. Pate		
Mr. W. Rachuk		Radiation Protection and Pollution Control Officer, UBC
Mr. P.C. Taylor		
Dr. G.D. Wait		

Experiments Evaluation Committee

Dr. F. Khanna	*Chairman* (since October)	Chalk River Nuclear Laboratories
Dr. A.E. Litherland	*Chairman* (until October)	University of Toronto
Dr. A. Astbury		Rutherford Laboratory
Dr. A.D. Bacher		Indiana University
Dr. G.A. Beer		University of Victoria
Dr. R.L. Burman		Los Alamos Scientific Laboratory
Dr. J. Domingo		SIN
Dr. E.M. Henley		University of Washington
Dr. J-M Poutissou		TRIUMF
Dr. J.T. Sample		TRIUMF
Dr. L.D. Skarsgard		B.C. Cancer Foundation
Dr. A.W. Thomas	*Secretary*	TRIUMF
Dr. A. Turkevich		Enrico Fermi Institute
Dr. M. Walker		University of Toronto
Dr. L. Yaffe		McGill University

Biomedical Experiments Evaluation Committee

Dr. L.D. Skarsgard	*Chairman*	B.C. Cancer Foundation
Dr. M.J. Ashwood-Smith		University of Victoria
Dr. H.C. Johns		Ontario Cancer Institute
Dr. R.R. Johnson		University of British Columbia
Dr. A.E. Litherland		University of Toronto
Dr. T.R. Overton		University of Alberta
Dr. J.T. Sample		TRIUMF
Dr. A.W. Thomas		TRIUMF
Dr. D.C. Walker		University of British Columbia
Dr. G.F. Whitmore		University of Toronto

Appendix A

PUBLICATIONS

Conference proceedings:

A.S. Rinat and A.W. Thomas, NN scattering above the pion threshold, in *Meson-Nuclear Physics—1979*, Houston, March, AIPCP#54 (AIP, New York, 1979), p. 75.

G. Jones, $\vec{p}\pi$ reaction on light nuclei, *ibid.*, 116.

J.M. Greben and R.M. Woloshyn, A study of non-relativistic approximations to the pion production operator in $^4He(p,n\pi^+)^4He$, *ibid.*, 182.

A.N. Saharia and L.S. Kisslinger, Pion true absorption in the isobar-doorway model, *ibid.*, 366.

E. Mazzucato, B. Bassalleck, M.D. Hasinoff, T. Marks, M. Salomon and J-M Poutissou, Observations of 2γ and 2e emission in nuclear pion capture, *ibid.*, 418.

W. Gyles, R.R. Johnson, T. Masterson, B. Bassalleck, T. Marks, K.L. Erdman, A.W. Thomas, D.R. Gill, C. Sabev, J. Arvieux, E. Rost, J.J. Kraushaar, J. Alster, M. Krell, π^- elastic scattering on $^{12,13}C$ and $^{16,18}O$ at low energies, *ibid.*, 522.

Y. Alexander and R.H. Landau, A calculation of intermediate-energy proton-^{4}He elastic scattering with a microscopic optical potential, *ibid.*, 620.

M.K. Craddock, New facilities and kaon factory designs for TRIUMF, *ibid.*, 750. [TRI-PP-79-3]

J.J. Burgerjon, A.S. Arrott, I.M. Thorson, T.L. Templeton, T.A. Hodges, R.E. Blaby, R.R. Langstaff, The TRIUMF thermal neutron facility, Proc. 1979 Particle Accelerator Conf., San Francisco, March, IEEE Trans. NS-26, 3061 (1979). [TRI-PP-79-4]

D.E. Lobb, A high flux muon channel incorporating a high quality spectrometer field, *ibid.*, 3194.

J.L. Beveridge, M.K. Craddock, G. Dutto, G.H. Mackenzie, C. Oram, L.W. Root, G. Roy, P.W. Schmor, The variable energy polarized proton beam at TRIUMF, *ibid.*, 3215. [TRI-PP-79-6]

E.W. Blackmore, M.K. Craddock, G. Dutto, D.A. Hutcheon, C.J. Kost, R. Liljestrand, G.H. Mackenzie, C.A. Miller, J.G. Rogers, P.W. Schmor, Improved beam quality at TRIUMF, *ibid.*, 3218. [TRI-PP-79-7]

R.L. Poirier, RF impedance of the accelerating beam gap and its significance to the TRIUMF RF system, *ibid.*, 3947. [TRI-PP-79-5]

N. Nishida, R.S. Hayano, Y.J. Uemura, J. Imazato, K. Nagamine, T. Yamazaki, H. Miyajima, W.S. Chan, S. Chikazumi, Muon diffusion and location in iron alloys, Proc. 5th Int. Conf. on Positron Annihilation, Tokyo, April (Japan Inst. of Metals, Sendai, 1979), p.759.

M. Doyama, R. Nakai, H. Fukushima, N. Nishida, Y.J. Uemura, T. Yamazaki, Trapping of positive muons by vacancies in Cu-Al and Al-Ni non-stoichiometric compounds, *ibid.*, 763.

T. Yamazaki, Interplays between magnetic interaction and diffusional motion of positive muon, *ibid.*, 795.

L.D. Skarsgard, The biological properties of pions, in Proc. Int. Congress of Radiation Research, 6th, Tokyo, May (Japanese Assn. for Radiation Research, Tokyo, 1979), p.788.

L.D. Skarsgard, R.M. Henkelman, G.K.Y. Lam, B. Palcic, C.J. Eaves, A. Ito, Preclinical studies of negative pi-mesons at TRIUMF, in Proc. Int. Symp. on Prospects for Treatment of Radioresistant Cancers, Kyoto, May (Elsevier-North Holland, New York, 1979), p.127.

D.P. Spencer, D.G. Fleming, J.H. Brewer, R.J. Mikula, A search for chirality-dependent muonium formation in quartz crystals, Proc. Symp. on the Origins of Optical Activity in Nature, Vancouver, June (in press).

A.N. Kamal and J.N. Ng, Majorana lepton mediated μ^- to e^- conversion in nuclei, Proc. Neutrino 79, Bergen, June (to be published). [TRI-PP-79-21]

L.D. Skarsgard, R.M. Henkelman, C.J. Eaves, Pions for radiotherapy at TRIUMF, Proc. of 42nd CAR Annual Meetings, Vancouver, June, J. Can. Assoc. of Radiologists (in press)

P.H. Depommier, Rare decays of the pion and muon, Proc. 8th Int. Conf. on High-Energy Physics and Nuclear Structure, Vancouver, August, eds. D.F. Measday and A.W. Thomas, Nucl. Phys. (in press).

D.V. Bugg, The nucleon-nucleon interaction, *ibid.*

J.M. Laget, Pion photoproduction, *ibid.* [TRI-PP-79-27]

J.M. Cameron, Proton nucleus interactions, *ibid.* [TRI-UAE-5025]

W.J. McDonald, The (p,2n) and (p,pn) reactions, *ibid.* [TRI-UAE-5024]

T. Yamazaki, Basic physics aspects of muon spin research, *ibid.*

K. Kubodera, M.P. Locher, F. Myhrer, A.W. Thomas, Interference of dibaryon resonances with Faddeev amplitudes for πd elastic scattering, in Abstracts of Contributed Papers, 8-ICOHEPANS, Vancouver, p.4.

A.S. Rinat, Y. Starkand, E. Hammel, A.W. Thomas, A relativistic description of πd scattering, *ibid.*, 6.

A.W. Thomas, S. Théberge, G.A. Miller, Pion-nucleon scattering in the cloudy bag model, *ibid.*, 7.

G.R. Mason, G.A. Beer, M.S. Dixit, S.K. Kim, J.A. Macdonald, A. Olin, R.M. Pearce, W.C. Sperry, J.S. Vincent, Precise measurement of pionic K X-rays in liquid ^{3}He, *ibid.*, 20.

G.A. Beer, M.S. Dixit, A. Fry, J.A. Macdonald, G.R. Mason, A. Olin, R.M. Pearce, P.R. Poffenberger, W.C. Sperry, Strong interaction shifts and widths in pionic ^{10,11}B and ^{12,13}C, *ibid.*, 21.

R.H. Landau and A.W. Thomas, ^{13}C(π^+,π^0)^{13}N reaction calculated with an improved theoretical optical potential, *ibid.*, 23.

A.N. Saharia and R.M. Woloshyn, Pion charge exchange and double charge exchange in the isobar-doorway model, *ibid.*, 29.

W. Gyles, R.R. Johnson, T. Masterson, B. Bassalleck, T. Marks, K.L. Erdman, A.W. Thomas, D.R. Gill, C. Sabev, J. Arvieux, E. Rost, J.J. Kraushaar, J. Alster, M. Krell, π^- elastic scattering on ^{12,13}C and ^{16,18}O at 30 and 50 MeV, *ibid.*, 30.

A.N. Saharia and L.S. Kisslinger, Pion elastic scattering in the phenomenological isobar-doorway model, *ibid.*, 33.

N. Shrimpton, C.A. Miller, A.W. Thomas, A study of pion quasi-elastic scattering, *ibid.*, 54.

B. Bassalleck, F. Corriveau, M.D. Hasinoff, T. Marks, D.F. Measday, M. Salomon, J-M Poutissou, Charge exchange of stopped π^- in nuclei, *ibid.*, 55.

B.D. Patterson, A.S. Arrott, Th. Wichert, Channeling of positrons from μ^+ decay, *ibid.*, 56.

D.G. Fleming, R.J. Mikula, D.M. Garner, J.H. Brewer, J.B. Warren, Gas phase studies in atomic physics using positive muons, *ibid.*, 56.

C.E. Stronach, B.D. Patterson, A.S. Arrott, A.T. Fiory, Muon spin precession in Fe alloyed with Mo and Nb, *ibid.*, 57.

H.W. Fearing, Comparison of soft photon calculations with the Manitoba and Orsay proton-proton bremsstrahlung data, *ibid.*, 62.

E.G. Auld, D. Axen, D.V. Bugg, A.S. Clough, M. Comyn, R. Dubois, J.A. Edgington, W.R. Gibson, R. Keeler, G.A. Ludgate, J.R. Richardson, L.P. Robertson, N.M. Stewart, A measurement of the n-p elastic differential cross section in the energy range 210-500 MeV, *ibid.*, 63; A measurement of n-p total cross section at four energies, 216, 323, 421 and 493 MeV, *ibid.*, 63.

E.G. Auld, D. Axen, M. Comyn, R. Dubois, R. Keeler, L.P. Robertson, G.A. Ludgate, J.R. Richardson, D.V. Bugg, A.S. Clough, J.A. Edgington, W.R. Gibson, N.M. Stewart, The efficiency of a neutron detector between 140 and 390 MeV, *ibid.*, 64.

G.A. Moss, J.M. Cameron, L.G. Greeniaus, D.A. Hutcheon, C.A. Miller, G. Roy, W.T.H. van Oers, A.W. Stetz, A. Willis, N. Willis, Proton-helium-4 elastic scattering at 200, 350 and 500 MeV, *ibid.*, 72.

J. Källne, D.A. Hutcheon, W.J. McDonald, A.N. Anderson, J.L. Beveridge, J. Rogers, The ^{13}C(p,d)^{12}C reaction at T_p = 200-500 MeV, *ibid.*, 75.

J.M. Cameron, D.A. Hutcheon, R. Liljestrand, C.A. Miller, R. MacDonald, W.J. McDonald, W.C. Olsen, C.E. Stronach, J.G. Rogers, J.J. Kraushaar, J.R. Shephard, T. Tinsley, ^{13}C, ^{16}O($\vec{p}$,d) analyzing powers at 200 and 400 MeV, *ibid.*, 76.

K.P. Jackson, G. Bischoff, D.H. Boal, J.M. D'Auria, R.E.L. Green, R.G. Korteling, The inclusive reactions ^{9}Be(p,X)^{8}Li,^{9}Li,^{9}Be,^{10}Be, ^{10}B, *ibid.*, 77.

H.S. Sherif and R.S. Sloboda, Triton pick-up contribution to backward p + ^{4}He elastic scattering, *ibid.*, 99.

N.S. Chant, P.G. Roos, P. Kitching, Spin orbit effects in (p,2p) reactions, *ibid.*, 101.

E. Mazzucato, B. Bassalleck, M.D. Hasinoff, T. Marks, J-M Poutissou, M. Salomon, Two-photon emission after pion capture in ^{12}C, *ibid.*, 121.

H.W. Fearing, Radiative muon capture in hydrogen and helium, *ibid.*, 126.

R.S. Sloboda and H.W. Fearing, O(1/m^2) and nuclear effects in radiative muon capture in ^{40}Ca, *ibid.*, 126.

S. Ahmad, G.A. Beer, M.S. Dixit, J.A. Macdonald, G.R. Mason, A. Olin, R.M. Pearce, O. Häusser, S.N. Kaplan, Absolute fission yields per muon capture in ^{238}U and ^{235}U, *ibid.*, 129.

J.H. Brewer and C.J. Oram, How to measure the triplet/singlet ratio of $\mu^- p \rightarrow n\nu_\mu$ using μSR, *ibid.*, 129.

P. Depommier, J.P. Martin, R. Poutissou, G. Cormier, C. Leroy, J-M Poutissou, D.A. Bryman, M.D. Hasinoff, W. Dey, E. Mazzucato, J.A. Macdonald, M. Dixit, A study of the $\pi^+ \rightarrow e^+\nu_e\gamma$ decay, *ibid.*, 143; An upper limit on the $\mu^+ \rightarrow e^+\gamma$ decay, *ibid.*, 144.

E.G. Auld, K. Erdman, B.L. White, J.B. Warren, J.M. Bailey, G.A. Beer, B. Dreher, H. Kalinowsky, R. Landua, E. Klempt, K. Merle, K. Neubecker, W.R. Wodrich, H. Drumm, U. Gastaldi, R.D. Wendling, C. Sabev, X-rays from antiprotons stopped in gaseous H_2 and D_2 targets, *ibid.*, 151.

G.A. Beer, M.S. Dixit, S.K. Kim, J.A. Macdonald, G.R. Mason, A. Olin, R.M. Pearce, C. Sabev, W.C. Sperry, C. Wiegand, Variation of pionic X-ray intensity with atomic number, *ibid.*, 184.

M.K. Craddock, C.J. Kost, J.R. Richardson, Possible kaon and antiproton factory designs for TRIUMF, Proc. Kaon Factory Workshop, Vancouver, August, TRIUMF report TRI-79-1, p.185. [TRI-PP-79-43]

T. Yamazaki, Y.J. Uemura, M. Takigawa, C.Y. Huang, Time correlation of random moments in spin glass CuMn observed by zero-field muon spin relaxation, Proc. Int. Conf. on Magnetism, Munich, September (J. Magnetism & Magnetic Materials, to be published).

M.K. Craddock, Kaon and antiproton factories (Report on Vancouver Kaon Factory Workshop), 13th LAMPF Users Group Meeting, October (to be published in LAMPF Users Group Newsletter). [TRI-PP-79-44]

B.D. Pate, Medical radioisotope production at TRIUMF, Proc. 27th Conf. on Remote Systems Technology, San Francisco, November (in press) [TRI-PP-79-38]

J.J. Burgerjon, B.D. Pate, R.E. Blaby, E.G. Page, J. Lenz, B.T. Trevitt, A.D. Wilson, The TRIUMF 500 MeV, 100 μA isotope production facility, *ibid.* [TRI-PP-79-39]

Proceedings of 1978 conferences published in 1979 included the following papers:

P. Depommier, The mysterious muon, in *Common Problems in Low- and Medium-Energy Nuclear Physics*, Proc. Banff Summer Inst. on Nuclear Theory (Plenum, New York, 1979), p.79.

C.A. Miller, Current topics in quasi-elastic scattering, *ibid.*, 513.

K.L. Erdman, Recent developments at TRIUMF, Proc. 8th Int. Conf. on Cyclotrons and Their Applications, Bloomington, IEEE Trans. NS-26, 1958 (1979).

D.E. Lobb, An axi-symmetric high flux muon channel, *ibid.*, 2020.

M.K. Craddock, C.J. Kost, J.R. Richardson, A ring cyclotron kaon factory, *ibid.*, 2065.

G.H. Mackenzie, Beam diagnostic techniques for cyclotrons and beam lines, *ibid.*, 2312.

E.W. Blackmore, P. Bosman, R. Burge, G. Dutto, D. Gill, G.H. Mackenzie, P.W. Schmor, Achievement and control of the 100 μA beam at TRIUMF, *ibid.* 2320.

E.W. Blackmore, M.K. Craddock, G. Dutto, C.J. Kost, G.H. Mackenzie, P.W. Schmor, Measurements and corrections to the beam properties in the TRIUMF cyclotron, *ibid.*, 2371.

J.R. Richardson, Future directions for isochronous cyclotrons, *ibid.*, 2436.

N. Nishida, K. Nagamine, R.S. Hayano, Y.J. Uemura, J. Imazato, T. Yamazaki, H. Miyajima, S. Chikazumi, D.G. Fleming, J.H. Brewer, Hyperfine fields on the μ^+ in NiCr and FeSi alloys, Proc. 1st Int. Topical Mtg. on Muon Spin Rotation, Rorschach, Hyperfine Interactions 6, 87 (1979).

T. Yamazaki, Muon spin relaxation in magnetic materials, *ibid.*, 115.

Y.J. Uemura, R.S. Hayano, J. Imazato, N. Nishida, K. Nagamine, T. Yamazaki, H. Yasuoka, Spin relaxation of positive muon in paramagnetic MnO, *ibid.*, 127.

R.S. Hayano, Y.J. Uemura, J. Imazato, N. Nishida, T. Yamazaki, H. Yasuoka, Zero- and low-field μ^+ spin relaxation behaviour in MnSi, *ibid.*, 133.

R.S. Hayano, Y.J. Uemura, J. Imazato, N. Nishida, K. Nagamine, T. Yamazaki, H. Yasuoka, Y. Ishikawa, Spin fluctuation of itinerant electrons in MnSi probed by μ^+, *ibid.*, 137.

J.H. Brewer and D.P. Spencer, Quadrupole splitting of muonium precession in single crystal quartz, *ibid.*, 181.

R.F. Kiefl, J.B. Warren, G.M. Marshall, C.J. Oram, J.H. Brewer, D.J. Judd, L.D. Spires, Muonium and positronium production in oxide powders, *ibid.*, 185.

N. Nishida, K. Nagamine, R.S. Hayano, T. Yamazaki, R.I. Grynszpan, A.T. Stewart, J.H. Brewer, D.G. Fleming, S. Talbot-Besnard, Diffusion of positive muons in α-iron crystals, *ibid.*, 241.

M. Doyama, R. Nakai, H. Fukushima, N. Nishida, Y.J. Uemura, T. Yamazaki, Trapping of positive muons by vacancies in non-stoichiometric compounds, *ibid.*, 341.

K. Nagamine, Negative muon spin rotation in solids, *ibid.*, 347.

R.J. Mikula, D.M. Garner, D.G. Fleming, J.H. Brewer, Muonium formation in gases, *ibid.*, 379.

D.G. Fleming, D.M. Garner, J.H. Brewer, R.J. Mikula, Reaction dynamics of the Mu atoms using surface muons in the gas phase, *ibid.*, 405.

Y.C. Jean, J.H. Brewer, D.G. Fleming, D.M. Garner, D.C. Walker, Determination of the effective charge on muonium during its reaction in aqueous solution, *ibid.*, 409.

Journal publications:

H.W. Fearing, Forbidden asymmetries and choices of geometry in proton-proton bremsstrahlung, Phys. Rev. Lett. 42, 1394 (1979). [TRI-PP-78-28]

B.M.K. Nefkens, O.R. Sander, D.I. Sober, H.W. Fearing, The differential cross section for proton-proton bremsstrahlung at 1.38 GeV/c, Phys. Rev. C 19, 877 (1979).

A.W. Thomas and A.S. Rinat, Nucleon-nucleon scattering above the pion production threshold, Phys. Rev. C 20, 216 (1979).

F. Myhrer and A.W. Thomas, An important correction to πD scattering in the resonance region, Nucl. Phys. A326, 497 (1979).

D.F. Jackson, A.A. Ioannides, A.W. Thomas, The case for studying the $(\pi,\pi N)$ reaction in coincidence under optimum conditions, Nucl. Phys. A322, 493 (1979). [TRI-PP-78-29]

H.S. Sherif, S.W. Leung, A.W. Thomas, G. Brookfield, The $(p,n\pi^+)$ reaction and the NNπ vertex, Phys. Lett. 83B, 293 (1979). [TRI-UAE-5013]

A.S. Rinat, Y. Starkand, E. Hammel, A.W. Thomas, The effect of genuine absorption and emission on pion deuteron scattering, Phys. Lett. 80B, 166 (1979).

R.H. Landau and A.W. Thomas, Elements of the theory of the $^{13}C(\pi^+,\pi^o)^{13}N$ reaction, Phys. Lett. 88B, 226 (1979). [TRI-PP-79-24]

R.M. Woloshyn, Weak interaction effects in low energy pion photoproduction, Can. J. Phys. 57, 809 (1979). [TRI-PP-79-25]

A.N. Saharia and R.M. Woloshyn, Energy dependence of the $^{13}C(\pi^+,\pi^o)^{13}N$ cross section, Phys. Lett. 84B, 401 (1979). [TRI-PP-79-8]

D.H. Boal and R.M. Woloshyn, A direct knockout model for nuclear fragmentation, Phys. Rev. C 20, 1878 (1979). [TRI-PP-79-20]

G.A. Miller and J.N. Ng, Effects of odd-parity components of the deuteron on inelastic polarized eD scattering, Phys. Rev. D 19, 3236 (1979).

A.N. Kamal and J.N. Ng, Majorana-lepton-mediated μ^- to e^+ conversion in nuclei, Phys. Rev. D 20, 2269 (1979).

J.M. Greben and F.S. Levin, A test of bound-state approximation in a three-body model of rearrangement collisions, Phys. Rev. C 20, 437 (1979). [TRI-PP-79-10]

J.M. Laget and P. Bosted, Threshold effects in neutral pion photoproduction reactions on few-body targets, Phys. Lett. 88B, 18 (1979). [TRI-PP-79-22]

H. Pilkuhn, Off-shell πN scattering near the Δ resonance, Phys. Lett. 87B, 177 (1979). [TRI-PP-79-25]

L.G. Greeniaus, D.A. Hutcheon, C.A. Miller, G.A. Moss, G. Roy, R. Dubois, C. Amsler, B.K.S. Koene, B.T. Murdoch, Measurement of p-p and p-^{4}He analysing powers at medium energies, Nucl. Phys. A322, 308 (1979). [TRI-UAE-5012]

A.N. James, W.J. McDonald, J.M. Cameron, C.A. Miller, D.A. Hutcheon, P. Kitching, G.C. Neilson, G.M. Stinson, E.D. Earle, Quasi-free collisions of 400 MeV protons in deuterium and carbon, Nucl. Phys. A324, 253 (1979). [TRI-UAE-5015]

W.J. McDonald, A. Anderson, L. Antonuk, W.K. Dawson, D.A. Hutcheon, P. Kitching, C.A. Miller, D.M. Sheppard, E.D. Earle, The efficiency of a pilot U scintillator for neutrons in the energy range 55-225 MeV, Nucl. Instrum. Methods 166, 187 (1979). [TRI-UAE-5018]

N.S. Chant, P. Kitching, P.G. Roos, L. Antonuk, Spin-orbit effects in medium-energy (p,2p) reactions, Phys. Rev. Lett. 43, 495 (1979). [TRI-UAE-5023]

R.M. Pearce, Reduction of multiple scattering by a magnetic field parallel to the beam, Nucl. Instrum. Methods 164, 11 (1979). [TRI-PP-79-2]

W.C. Sperry, G.A. Beer, M.S. Dixit, S.K. Kim, J.A. Macdonald, G.R. Mason, A. Olin, R.M. Pearce, C. Sabev, C. Wiegand, Z-dependence of the intensity of $|\Delta n| = 2$ pionic X-rays, Phys. Lett. 86B, 29 (1979). [TRI-PP-79-15]

R.M. Pearce, G.A. Beer, M.S. Dixit, S.K. Kim, J.A. Macdonald, G.R. Mason, A. Olin, C. Sabev, W.C. Sperry, C. Wiegand, The variation of pionic X-ray intensity with atomic number, Can. J. Phys. 57, 2084 (1979). [TRI-PP-79-18]

P. Walden, D. Ottewell, E.L. Mathie, T. Masterson, G. Jones, R.R. Johnson, A. Haynes, E.G. Auld, The $\vec{p}+p \rightarrow d+\pi^+$ reaction with a polarized proton beam, Phys. Lett. 81B, 156 (1979).

B. Bassalleck, M.D. Hasinoff, M. Salomon, Test results from a position-sensitive NaI detector, Nucl. Instrum. Methods 163, 389 (1979). [TRI-PP-79-1]

R.R. Johnson, T. Masterson, B. Bassalleck, W. Gyles, T. Marks, K.L. Erdman, A.W. Thomas, D.R. Gill, E. Rost, J.J. Kraushaar, J. Alster, C. Sabev, J. Arvieux, Neutron radii determinations from the ratio of π^- elastic scattering from $^{12,13}C$ and $^{16,18}O$, Phys. Rev. Lett. 43, 844 (1979). [TRI-PP-79-14]

R. Feenstra, R.R. Johnson, C. Winter, Rapid CAMAC data handling in FORTRAN real time programs, Nucl. Instrum. Methods 160, 511 (1979).

C. Cernigoi, N. Grion, G. Pauli, B. Saitta, On an experimental method for the discrimination and the absolute counting of the pions absorbed in a target in experiments regarding the π^- capture at rest in nuclei, Nucl. Instrum. Methods 165, 401 (1979).

Y.C. Jean, D.G. Fleming, B.W. Ng, D.C. Walker, Reaction of muonium with O_2 in aqueous solution, Chem. Phys. Lett. 66, 187 (1979).

D.G. Fleming, D.M. Garner, J.H. Brewer, D.C. Walker, L. Vaz, K.M. Crowe, Muonium chemistry, a review, in *Positronium and Muonium Chemistry*, ACS Adv. in Chem. Series 175, 279 (1979).

D.C. Walker, Y.C. Jean, D.G. Fleming, Muonium atoms and intra spur processes in water, J. Chem. Phys. 70, 4534 (1979).

R.S. Hayano, Y.J. Uemura, J. Imazato, N. Nishida, T. Yamazaki, R. Kubo, Zero- and low field spin relaxation studied by positive muon, Phys. Rev. B 20, 850 (1979).

Y.J. Uemura, R.S. Hayano, J. Imazato, N. Nishida, T. Yamazaki, Non-secular part of nuclear dipolar broadening detected by zero-field spin relaxation of μ^+, Solid State Commun. 31, 731 (1979).

R.I. Grynszpan, N. Nishida, K. Nagamine, R.S. Hayano, T. Yamazaki, J.H. Brewer, D.G. Fleming, Diffusion of positive muons in zone-refined iron below room temperature, Solid State Commun. 29, 143 (1979).

J.H. Brewer, D.S. Beder, D.P. Spencer, Quadrupole splitting of muonium precession in α-quartz, Phys. Rev. Lett. 42, 808 (1979).

T. Yamazaki, R. Hayano, Y. Kuno, J. Imazato, K. Nagamine, S.E. Kohn, C.Y. Huang, Giant hyperfine anomaly between bound negative muon and Rh nucleus in Pd metal, Phys. Rev. Lett. 42, 1241 (1979).

B.G. Douglas, R.M. Henkelman, G.K.Y. Lam, J.F. Fowler, C.J. Eaves, Practical and theoretical considerations in the use of the mouse foot system to derive epithelial stem cell survival parameters, Radiat. Res. 77, 453 (1979).

G.K.Y. Lam, R.M. Henkelman, B.G. Douglas, C.J. Eaves, Method of analysis to derive cell survival from observation of tissue damage following fractionated radiation, *ibid.*, 440.

G.K.Y. Lam, R.M. Henkelman, R.W. Harrison, L.D. Skarsgard, B. Palcic, Uniform depth dose distribution for biological irradiation using negative pions, Phys. Med. Biol. 24, 1243 (1979).

J.A. Nordin and R.M. Henkelman, Measurement of stopping power ratios for 60 MeV positive or negative pions, *ibid.*, 781.

L.D. Skarsgard, R.M. Henkelman, G.K.Y. Lam, M.N. Poon, Preclinical studies of the negative pi-meson beam at TRIUMF, Radiat. Environ. Biophys. 16, 193 (1979).

K. Sakamoto, S. Okada, G.K.Y. Lam, R.M. Henkelman, L.D. Skarsgard, The comparative survival of clonogenic cells of a murine epithelioma irradiated *in vivo* with 250 kVp X-rays, ^{60}Co gamma rays or negative pions produced by the cyclotron at TRIUMF, Radiology 133, 501 (1979).

Preprints and in press:

H.W. Fearing, A relativistic calculation of radiative muon capture in hydrogen and ^{3}He (Phys. Rev. C, to be published). [TRI-PP-79-37]

R.S. Sloboda and H.W. Fearing, $O(1/m^2)$ and nuclear effects in radiative muon capture in ^{40}Ca (Nucl. Phys. A, to be published). [TRI-PP-79-36]

H.W. Fearing, Comparison of proton-proton bremsstrahlung data at 42 MeV and 156 MeV with soft photon calculations (Phys. Rev. C, to be published). [TRI-PP-79-40]

A.W. Thomas and R.H. Landau, Pion-deuteron and pion-nucleus scattering: A review (Phys. Reports, in press). [TRI-PP-79-23]

G.A. Miller, A.W. Thomas, S. Théberge, Pion-nucleon scattering in the cloudy bag model (submitted to Phys. Rev. Lett.). [TRI-PP-79-16]

A.S. Rinat, E. Hammel, Y. Starkand, A.W. Thomas, A relativistic description of πD scattering II (Nucl. Phys., in press).

K. Kubodera, M.P. Locher, F. Myhrer, A.W. Thomas, Interference of dibaryon resonances with Faddeev amplitudes for elastic πD scattering (J. Phys. G, in press).

R.M. Woloshyn, PCAC and the non-relativistic pion-nucleon vertex (Nucl. Phys. A, in press). [TRI-PP-79-19]

J.M. Greben and R.M. Woloshyn, Non-relativistic approximations to the pion production operator in ^{4}He(p,nπ^+)^{4}He (Nucl. Phys. A, in press). [TRI-PP-79-9]

A.N. Saharia and R.M. Woloshyn, Application of the isobar-doorway model to pion charge exchange reactions (Phys. Rev. C, in press). [TRI-PP-79-31]

L.S. Kisslinger and A.N. Saharia, The pion-nucleus optical potential in the isobar-doorway model (submitted to Phys. Rev. C). [TRI-PP-79-28]

A.N. Kamal and J.N. Ng, Constraints on heavy lepton mixings from deep inelastic charged lepton scattering (Phys. Rev. D, to be published). [TRI-PP-79-32]

D.H. Boal, Probing inclusive production mechanisms with the (p,2p) reaction (Phys. Rev. C, to be published). [TRI-PP-79-33]

A. Fujii and Y. Kohyama, Systematics of nuclear muon capture (submitted to Nucl. Phys. A). [TRI-PP-79-41]

A.S. Clough, W.R. Gibson, D.A. Axen, R. Dubois, L. Felawka, R. Keeler, G.A. Ludgate, C.J. Oram, C. Amsler, D.V. Bugg, J.A. Edgington, L.P. Robertson, N.M. Stewart, J.L. Beveridge, Neutron-proton elastic scattering between 200 and 500 MeV. I. Experimental details and measurements of the D_t and P parameters (submitted to Phys. Rev. C). [TRI-PP-79-11]

D. Axen, R. Dubois, R. Keeler, G.A. Ludgate, C.J. Oram, L.P. Robertson, N.M. Stewart, C. Amsler, D.V. Bugg, J.A. Edgington, W.R. Gibson, N. Wright, A.S. Clough, Neutron-proton elastic scattering between 200 and 500 MeV. II. Measurement of R_t and A_t (submitted to Phys. Rev. C). [TRI-PP-79-12]

D.V. Bugg, J.A. Edgington, W.R. Gibson, N. Wright, N.M. Stewart, A.S. Clough, D. Axen, G.A. Ludgate, C.J. Oram, L.P. Robertson, J.R. Richardson, C. Amsler, Neutron-proton elastic scattering between 200 and 500 MeV. III. Phase shift analysis (submitted to Phys. Rev. C). [TRI-PP-79-13]

P. Kitching, C.A. Miller, W.C. Olsen, D.A. Hutcheon, W.J. McDonald, A.W. Stetz, Quasi-free scattering of polarized protons (Nucl. Phys. A, in press). [TRI-PP-79-34]

G.A. Moss, L.G. Greeniaus, J.M. Cameron, D.A. Hutcheon, R.L. Liljestrand, C.A. Miller, G. Roy, B.K.S. Koene, W.T.H. van Oers, A.W. Stetz, A. Willis, N. Willis, Proton-^{4}He elastic scattering at intermediate energies (Phys. Rev. C, to be published). [TRI-PP-79-35]

E.G. Auld, R.R. Johnson, G. Jones, E.L. Mathie, P. Walden, D. Hutcheon, P. Kitching, W.C. Olsen, C.F. Perdrisat, B. Tatischeff, Differential cross section and analyzing power for backward pions in ^{2}H(p,π^+)^{3}H (Phys. Lett. B, in press). [TRI-UAE-5022]

J. Källne, A.N. Anderson, J.L. Beveridge, J. Rogers, D.A. Hutcheon, W.J. McDonald, Some dynamical aspects of pickup reactions studied in ^{13}C(p,d)^{12}C at 200-500 MeV (Phys. Rev. C, in press). [TRI-UAE-5027]

G.R. Mason, G.A. Beer, M.S. Dixit, S.K. Kim, J.A. Macdonald, A. Olin, R.M. Pearce, W.C. Sperry, J.S. Vincent, Pionic K X-rays in liquid ^{3}He (Nucl. Phys. A, to be published). [TRI-PP-79-17]

R.E.L. Green and R.G. Korteling, Fragment production from p + Ag interactions at intermediate energies (submitted to Phys. Rev. C). [TRI-PP-79-29]

R.E.L. Green and R.G. Korteling, A description of the evaporation component in heavy fragment emission following p + Ag interactions at intermediate energies (submitted to Phys. Rev. C). [TRI-PP-79-30]

H. Dautet, G. Bischoff, J.M. D'Auria, B.D. Pate, Yield of deep spallation products of medium to heavy mass targets bombarded with 480 MeV protons (Can. J. Phys., in press). [TRI-PP-79-42]

B.D. Patterson, Simplified channeling and the rule of reversibility (submitted to Am. J. Phys.). [TRI-PP-79-26]

Reports:

TRI-79-1 Proceedings of the Kaon Factory Workshop, Vancouver, August 13-14, ed. M.K. Craddock

TR1-79-2 Proceedings of Workshop on the Future of Pion-Nucleus Interactions, Vancouver, July 22-August 3, eds. H.C. Lee, A.N. Saharia, A.W. Thomas

USERS GROUP

University of Alberta:

L. Antonuk*
E.B. Cairns
J.M. Cameron
W.K. Dawson
J.B. Elliott
G.R. Freeman
L.G. Greeniaus
H.E. Gunning
A.N. Kamal
P. Kitching
R. Liljestrand*
W.J. McDonald
G.A. Moss
G.C. Neilson
A.A. Noujaim
W.C. Olsen
T.R. Overton
G. Roy
D.M. Sheppard
H. Sherif
R. Sloboda
R.E. Snyder
J. Soukup
L.G. Stephens-Newsham
G.M. Stinson
J. Thekkumthala*
R.C. Urtasun
H. Wilson*

University of British Columbia:

N. Auersperg
E.G. Auld
D.A. Axen
B. Barnett
D.S. Beder
J.H. Brewer
M. Comyn
D.H. Copp
M.K. Craddock
R. Dubois
A. Duncan
K.L. Erdman*
D.G. Fleming
D. Garner
M.D. Hasinoff
R.R. Johnson
J. Johnstone
G. Jones
R. Keeler
R. Kiefl
B. Larkin
K.C. Mann
G. Marshall
P.W. Martin
E.L. Mathie
C.A. McDowell
J.M. McMillan
D.F. Measday
R. Nodwell
C. Oram
B.D. Pate*
M. Salomon
J. Sams
N. Shrimpton
H. Stich
T. Suzuki
S. Théberge
J. Trotter
E.W. Vogt
D.C. Walker
J.B. Warren
B.L. White

*at main site Vancouver

B.C. Cancer Foundation:

C.J. Eaves
J.M.W. Gibson
R.O. Kornelsen†
K.Y. Lam
B. Palcic
L.D. Skarsgard
D.M. Whitelaw
M.E.J. Young†

†*B.C. Cancer Control Agency*

University of Victoria:

G.A. Beer [Chairman 1979]
G.R. Branton
T.W. Dingle
G.B. Friedmann
T.A. Hodges
A.D. Kirk
D.E. Lobb
G.R. Mason
T. Numao*
D. Olaniyi*
A. Olin
R.M. Pearce
C.E. Picciotto
P.A. Reeve*
L.P. Robertson
C.S. Wu

Simon Fraser University:

A.S. Arrott
D. Boal
J.M. D'Auria
B.L. Funt
R. Green
C.H.W. Jones
F.M. Kiely
R.G. Korteling
P.W. Percival
I.M. Thorson
W.J. Wiesehahn

TRIUMF:

K.P. Jackson [Chairman 1980]
R. Baartman
M. Betz
J.L. Beveridge
E.W. Blackmore
C.W. Bordeaux
W.J. Bryan
D.A. Bryman
J. Doornbos
G. Dutto
H.W. Fearing
D.R. Gill
J. Greben
D.P. Gurd
D.A. Hutcheon
C.J. Kost
G.A. Ludgate
J.A. Macdonald
G.H. Mackenzie
C.A. Miller
J.N. Ng
D. Ottewell
J-M Poutissou
J.G. Rogers
A. Saharia
J.T. Sample
P. Schmor
J.E. Spuller
A.W. Thomas
V.K. Verma
J.S. Vincent
G.D. Wait
P. Walden
G. Waters
R. Woloshyn
M. Zach

Visting experimentalists based at main site:

G. Azuelos, R. Poutissou, *Université de Montréal*
R. Abegg, *University of Manitoba*
B. Robertson, *Queen's University*
N. Stevenson, *Queen Mary College*
Y. Uemura, *University of Tokyo*
J. Tinsley, *University of Oregon*

Other institutions:

Canada

C.Y. Kim, S. Rowlands, *University of Calgary*
T. Walton, *Cariboo College*
A.L. Carter, E.P. Hincks, *Carleton University*
G.A. Bartholomew, E.D. Earle, J.S. Fraser, O.F. Hausser, F.C. Khanna, H.C. Lee, A. McDonald, *Chalk River Nuclear Laboratories*
J.W. Scrimger, S.R. Usiskin, *Dr. W.W. Cross Cancer Institute, Edmonton*
P.A. Egelstaff, *University of Guelph*
B.S. Bhakar, N.E. Davison, M.S. de Jong, W. Falk, J. Jovanovich, R. McCamis, A.M. Sourkes, K.G. Standing, W.T.H. van Oers, *University of Manitoba*
J.K.P. Lee, B. Margolis, S.K. Mark, L. Yaffe, *McGill University*
J. McAndrew, *Memorial University of Newfoundland*
P. Depommier, J-P Martin, *Université de Montréal*
M.S. Dixit, C. Hargrove, *National Research Council*
H. Blok, *Novatrack Analysts Limited*
G.T. Ewan, H.B. Mak, A.T. Stewart, *Queen's University*
A. Szyjewicz, *University of Saskatchewan*
M. Krell, *Université de Sherbrooke*
J.M. Daniels, T.E. Drake, A.E. Litherland, *University of Toronto*
A. Cone, *Vancouver City College, Langara Campus*
R.T. Morrison, *Vancouver General Hospital*
W.P. Alford, *University of Western Ontario*

Overseas

D.V. Bugg, J.A. Edgington, R. Gibson, *Queen Mary College, London*
N.M. Stewart, *Bedford College, London*
A.S. Clough, *University of Surrey*
A. Astbury, *Rutherford Laboratory*
D. Wilkinson, *University of Sussex*
A.N. James, *University of Liverpool*
R. Engfer, B. Patterson, *Universität Zürich*
J.P. Blaser, J. Domingo, *Schweizerisches Institut für Nuklearforschung*
S. Jaccard, *Université de Neuchâtel*
C. Amsler, C. Sabev, *CERN*
R. Frascaria, B. Tatischeff, *Institut de Physique Nucléaire, Orsay*
J.M. Laget, *CEN Saclay*
R. Grynszpan, *CNRS Vitry*
R. van Dantzig, *IKO Amsterdam*
J. Alster, D. Ashery, *Tel-Aviv University*
Y. Alexander, *Hebrew University*
B.K. Jain, *Bhabha Atomic Centre*
R. Hayano, J. Imazato, K. Nagamine, N. Nishida, K. Sakamoto, T. Yamazaki, *University of Tokyo*
G.E. Coote, *INS, Dept. of Science & Industrial Research, New Zealand*
I.R. Afnan, *Flinders University of South Australia*

United States

K.W. Jones, *Brookhaven National Laboratory*
F.P. Brady, *University of California, Davis*
B.M.K. Nefkens, J.R. Richardson, *University of California, Los Angeles*
M.P. Epstein, D.J. Margaziotis, *California State University*
B. Bassalleck, L. Wolfenstein, *Carnegie-Mellon University*
H.L. Anderson, *University of Chicago*
J.J. Kraushaar, T. Masterson, *University of Colorado*
C.A. Goulding, *Florida A&M University*
H.S. Plendl, *Florida State University*
G.T. Emery, M.E. Rickey, T. Ward, *Indiana University*
Y.K. Lee, *Johns Hopkins University*
P. Tandy, *Kent State University*
C. Clawson, K.M. Crowe, F.S. Goulding, S. Kaplan, R. Lombard, C. Martoff, R.H. Pehl, V. Perez-Mendez, S. Rosenblum, *Lawrence Berkeley Laboratory*
J.W. Blue, *Lewis Research Center, NASA*
L.E. Agnew, R.J. Macek, L. Rosen, *Los Alamos Scientific Laboratory*
H.G. Pugh, *National Science Foundation*
B. Dieterle, *University of New Mexico*
J.K. Chen, *State University of N.Y. Geneseo*
K.K. Seth, *Northwestern University*
F.E. Bertrand, *Oak Ridge National Laboratory*
B.C. Clark, *Ohio State University*
D.K. McDaniels, *University of Oregon*
K.S. Krane, R. Landau, A.W. Stetz, L.W. Swenson, *Oregon State University*
H. Primakoff, *University of Pennsylvania*
R.F. Carlson, A.J. Cox, *University of Redlands*
L. Church, *Reed College*
M. Furić, G.S. Mutchler, *Rice University*
V.L. Highland, *Temple University*
R. Bryan, R.B. Clark, *Texas A&M University*
W. Denig, V.G. Lind, R.E. McAdams, O.H. Otteson, *Utah State University*
J. Källne, K. Ziock, *University of Virginia*
M. Blecher, K. Gotow, D. Jenkins, *Virginia Polytechnic Institute and State University*
H. Bichsel, J.S. Blair, I. Halpern, E.M. Henley, J.E. Rothberg, K.A. Snover, P. Wooton, *University of Washington*
H.B. Knowles, *Washington State University*
A.S. Rupaal, *Western Washington University*
W.C. Sperry, *Central Washington University*
C.F. Perdrisat, R.T. Siegel, *College of William and Mary*

EXPERIMENT PROPOSALS

The following lists experiment proposals received up to the end of 1979 (missing numbers cover proposals that have been withdrawn, replaced by later versions, or combined with another proposal). Page numbers are given for those experiments which are included in this annual report.

			Page
1.	Low-energy pi nuclear scattering R.R. Johnson, University of British Columbia	[Active]	37
3.	The study of fragments emitted in nuclear reactions R.G. Korteling, Simon Fraser University	[Completed]	40
6.	Studies of the proton- and pion-induced fission of light to medium mass nuclides B.D. Pate, University of British Columbia	[Completed]	40
9.	A study of the reaction $\pi^- + p \rightarrow \gamma + n$ at pion kinetic energies from 20-200 MeV D.F. Measday, University of British Columbia	[Active]	
10.	Positive pion production in proton-proton and proton-nucleus reactions G. Jones, University of British Columbia	[Active]	42
11.	Nuclear spectroscopic studies of short-lived radioactive products of high energy reactions J.M. D'Auria, Simon Fraser University	[Active]	
14.	The interaction of protons with very light nuclei in the energy range 200-500 MeV G.A. Moss, University of Alberta	[Completed]	43
15.	A proposal to study quasi-free scattering in nuclei W.J. McDonald, University of Alberta	[Active]	
18.	Influence of chemical environment on atomic muon capture rates R.M. Pearce, University of Victoria	[Inactive]	
19.	Nuclear decays following muon capture R.M. Pearce, University of Victoria E.D. Earle, Chalk River Nuclear Laboratories	[Inactive]	
20.	Isotope effect in μ capture R.M. Pearce, University of Victoria	[Inactive]	
21.	Optical activity induced by polarized elementary particles D.C. Walker, University of British Columbia	[Active]	
22.	Negative pion capture and absorption on carbon, nitrogen and oxygen H.B. Knowles, Washington State University)	[Passed to Biomedical EEC]	
23.	Study of decay modes a) $\pi^o \rightarrow 3\gamma$, b) $\pi^+ \rightarrow e^+ + \nu_e + \gamma$, c) $\pi^+ \rightarrow \pi^o + e^+ + \nu_e$ P. Depommier, Université de Montréal	[Completed]	
24.	Elastic scattering of polarized protons on ^{12}C G. Roy, University of Alberta	[Completed]	
26.	Measurement of the differential cross-section for free neutron-proton scattering and for the reaction D(n,p)2n L.P. Robertson, University of Victoria	[Completed]	29
27.	Measurement of the polarization in free neutron-proton scattering D.A. Axen, University of British Columbia	[Completed]	
35.	A study of positive muon depolarization phenomena in chemical systems D.G. Fleming, University of British Columbia	[Active]	66
40.	A proposal for neutron experiments at TRIUMF D.A. Axen, University of British Columbia	[Completed]	
41a.	Radiative capture of pions in light nuclei M. Salomon, University of British Columbia	[Active]	44

154. Muonium in solids
J.H. Brewer and D.G. Fleming, University of British Columbia [Active]

155. Study of deep hole states in ^{40}Ca with ($\vec{p}$,2p) reaction
P. Kitching, University of Alberta [Active]

156. Deuteron production in proton-nucleus collisions
J.M. Cameron, University of Alberta
J. Källne, University of Virginia [Deferred]

157. The chemistry of muonium atoms in condensed media
D.C. Walker, University of British Columbia [Active]

158. Study of the reactions $p^2H \rightarrow d\pi^+n$ and $n^3He \rightarrow t\pi^+p$
J.M. Cameron, University of Alberta
C.F. Perdrisat, College of William and Mary [Active]

159. $\bar{p}p$ and $\bar{p}d$ interactions at threshold
B.L. White, University of British Columbia [Active]